SIMULATION OF VEHICLE-PEDESTRIAN INTERACTION

A thesis submitted in partial fulfilment of the

requirements for the Degree

of Doctor of Philosophy in Engineering

in the University of Canterbury

by T. J. Stevenson

University of Canterbury

2006

Table of Contents

List of Figures

Figure

List of Tables

Acknowledgements

The author wishes to express sincere appreciation and thanks to the following people and organisations:

- Professor John Raine for offering the research
- Land Transport New Zealand for their support including a Road Safety Trust Research Scholarship
- New Zealand Vice Chancellor's Committee for admininistering the LTNZ scholarship
- University of Canterbury for a Canterbury Doctoral Scholarship
- Department of Mechanical Engineering for a Departmental scholarship
- Dr Shayne Gooch for taking on the senior supervisor role very late into the research
- Professor Harry McCallion for overseeing the examination process and subsequent revisions
- Paul Southward for providing advice and support
- The New Zealand Police for involving me in their accident reconstruction work and providing the material for the thesis case studies
- Joe Tomas at Advea Engineering for providing MADYMO and MADYMO support
- Tony Gray for providing and supporting HyperMesh
- My brothers John and Kim for their help in the final stages
- Special thanks to my Father for his support and advice
- My Mum!

Abbreviations

m	……metre
G	……acceleration due to gravity (taken to be $9.81ms^{-2}$)
km/h	……kilometre per hour
MHz	……megahertz
MIPS	……millions of instructions per second
Nmm^{-1}	……Newtons per millimetre
kN	……kilonewton
ms	……millisecond (10^{-3})
µs	……microsecond (10^{-6})
Nm	……Newton-metre
ms^{-1}	……metres per second
ms^{-2}	……metres per second squared
kg	……kilogram
$kgmm^{-1}$	……kilogram per millimetre
mm	……millimetre
SUV	……Sport Utility Vehicle
LTV	……Light Trucks and Vans

Abstract

The literature on vehicle crash reconstruction provides a number of empirical or classical theoretical models for the distance pedestrians are thrown in impacts with various types of vehicles and impact speeds. The aim of this research was to compare the predictions offered by computer simulation to those obtained using the empirical and classical theoretical models traditionally utilised in vehicle-pedestrian accident reconstruction. Particular attention was paid to the pedestrian throw distance versus vehicle impact speed relationship and the determination of pedestrian injury patterns and associated severity.

It was discovered that computer simulation offered improved pedestrian kinematic prediction in comparison to traditional vehicle-pedestrian accident reconstruction techniques. The superior kinematic prediction was found to result in a more reliable pedestrian throw distance versus vehicle impact speed relationship, particularly in regard to varying vehicle and pedestrian parameters such as shape, size and orientation.

The pedestrian injury prediction capability of computer simulation was found to be very good for head and lower extremity injury determination. Such injury prediction capabilities were noted to be useful in providing additional correlation of vehicle impact speed predictions, whether these predictions were made using computer simulation, traditional vehicle-pedestrian accident reconstruction methods or a combination of both.

A generalised approach to the use of computer simulation for the reconstruction of vehicle-pedestrian accidents was also offered. It is hoped that this approach is developed and improved by other researchers so that over time guidelines for a standardised approach to the simulation of vehicle-pedestrian accidents might evolve.

Thoracic injury prediction, particularly for frontal impacts, was found to be less than ideal. It is suspected that the relatively poor thoracic biofidelity stems from the development of pedestrian mathematical models from occupant mathematical models, which were in turn developed from cadaver and dummy tests. It is hoped that future research will result in improved thoracic biofidelity in human mathematical models.

Chapter 1

Foreword

1.0 Introduction

This foreword details the research aims, the rationale behind the approach taken to accomplish the research and provides some background to the research findings discussed in this thesis.

It is hoped that the material in this section provides the reader with a better understanding of the methodology, time and effort required to conduct this research.

1.1 Research Aims

The aim of this research was to examine the validity of the prediction offered by the mathematical modelling of vehicle-pedestrian interaction resulting from a collision. More specifically, could the software program MADYMO (MAthemtical DYnamic MOdelling) accurately predict the following:

I. The pedestrian throw distance versus vehicle impact speed relationship commonly used as a forensic tool. Existing methods typically rely on simple models derived from the equations of motion and are usually associated with a fairly restrictive set of assumptions and limitations resulting from the deceptively complex kinematics of an impacted pedestrian.

II. The resulting pedestrian injury pattern from a simulated vehicle-pedestrian collision. When the vehicle-pedestrian impact point or final rest point is unknown, the proportion of airborne versus sliding pedestrian travel is uncertain or if unusual pedestrian kinematics are suspected (such a pre-impact pedestrian movement, short pedestrian versus tall vehicle or similar) then an additional basis for validating a simulation scenario is needed. Injury patterns are suspected to form such basis.

Additionally, if MADYMO can be shown to be capable of accurately predicting pedestrian injury patterns, can the injury prediction capacity be utilised to analyse

potential methods of pedestrian injury reduction. In particular, can MADYMO evaluate the potential of wearable apparel designed for injury reduction for use by high-risk pedestrian road users such as Police Officers directing traffic and road workers. The results of this research may be found in Appendix I.

1.2 Research Preparation

An important part of the background work required for this research was the identification of simulation software appropriate for the task. A literature review was conducted and the tools available for the computer simulation of accident analysis were surveyed. The vehicle manufacturers were found to favour finite element analysis for their crash analysis, due in no small part to the large amount of virtual, computer-based automotive design and optimisation modern vehicle manufacturers use to create better product more quickly. However, the computing facilities available to the automotive manufacturers exceeded by no small margin the computing facilities available for this research, hence more computationally efficient methods of simulation were sought.

The combination of multibody analysis and finite element analysis, as used in the occupant safety software package MADYMO, attracted the attention of the author with the promise of fast multibody analysis coupled with finite element analysis for the areas of critical interest.

1.3 Resources

To obtain a good performance-to-cost ratio it was decided to run MADYMO in a Microsoft Windows environment. The rationale behind this decision related to the pricing scheme which meant that MADYMO, when run on dual-processor UNIX workstations, attracted an increased licensing cost over uniprocessor systems. In comparison, MADYMO licensing costs for dual processor workstations running Windows were the same as for uniprocessor systems. The downside to running MADYMO on Windows was the need for third-party pre-and-post processing software. Based on the advice of the MADYMO agency, Altair's HyperMesh was chosen.

Initial MADYMO simulations were conducted by the author on a single processor Intel PC operating at 800MHz whilst familiarity with the software was gained. MADYMO training was provided by the Australasian MADYMO agency, Advea.

As user proficiency with MADYMO increased more complex models were created and the limited computational power made its presence felt. The computer hardware was upgraded to a dual-processor Intel PC operating at 1GHz with 1GB of memory and running Windows 2000.

1.4 MADYMO Usage

Shortly after the acquisition of this hardware a series of simulations were conducted to analyse the mechanisms that resulted in a pedestrian dying from massive head injuries. The vehicle impact speed was in question and MADYMO was utilised to solve it. Excellent injury correlation with the pedestrian injury pattern and severity was obtained and the origin of an inexplicable 'black-eye' on the pedestrian was unexpectedly located.

Based on the success of this simulation series a second vehicle-pedestrian accident was analysed but in this instance the 'accident' was in reality a homicide. Several different impacts had occurred between the vehicle and the pedestrian and with the driver deliberately concealing their actions a methodical approach was needed to evaluate the wide range of potential scenarios.

With very little evidence available on which to base the reconstruction it was deemed crucial to obtain excellent pedestrian injury pattern correlation. Accordingly, it was decided to model the vehicle using a finite element model to obtain as realistic as possible collection of surfaces for the pedestrian model to interact with. The vehicle used was carefully measured using a three-dimensional measurement rig designed and built by the author and, with the inclusion of manufacturer data, a finite element vehicle model was created (See Appendix III for information on the creation of the vehicle model). Most MADYMO vehicle-pedestrian simulations run at this time used multibody vehicle models (Yang, 1997; Mizuno and Kajzer, 2000; Linder et 2005).

A multibody vehicle model was considered unsuitable by the author for accurate pedestrian injury correlation because of the inability associated with such models to accurately represent vehicle details and characteristics. The need for accurate vehicle representation was recognised by researchers. As stated by Linder et al:

> *"It has previously been highlighted by among others van Rooij et al. (2003) that generating a vehicle model with the correct geometry largely determines where on the vehicle various parts of body impact. In addition, localized contact stiffness characteristics have a great influence on the injury outcome. Therefore great care was taken to ensure that for each case vehicle, profiles and appropriate stiffnesses were used in the simulations."*

The vehicle models used by van Rooij were in fact modelled using facet element meshes (see Chapter 3, Section 3.4.2 for a description of facet modelling in MADYMO) with the mesh generated using a public-domain finite element car model. Nonetheless, Linder et al (and most other researchers) conducted their vehicle-pedestrian simulations using multibody vehicle models, presumably due to computational restraints and the long timeframe associated with both finite element (or even facet element) model creation and simulation runtime. Whilst the compromises associated with multibody modelling of vehicles may well be appropriate for many vehicle-pedestrian simulations the author of this thesis did not consider it the best method for pedestrian injury correlation, instead preferring the more accurate representation afforded by finite-element vehicle models. However, it should be noted that multibody pedestrian models are less then ideal for injury correlation, as there is little doubt that a better representation of the human body can be achieved by using a finite-element human model. Unfortunately, at the time the simulations for this thesis were conducted validated finite-element pedestrian models were not readily available.

Some problems were identified with the finite element implementation in the version of MADYMO (version 5.4) resulting in unstable and time-consuming simulations. Other researchers experienced similar issues, including Troutbeck et al (2001) who found MADYMO to have excessive computation times, 'noisy' finite element models and the use of non-SI units for some inputs. The finite element implementation in

MADYMO prior to version 6 may well have dissuaded some researchers from using it.

In total over 290 simulations were run for the analysis of the second vehicle-pedestrian 'accident' with the longest simulations, simulating 3.5 seconds of event and high vehicle speeds (and correspondingly long pedestrian slide to rest), taking over 20 hours to complete (See Figure 1.1 for a section of the MADYMO log showing run time). This long simulation time resulted from the combination of relatively modest computational power and the need for an accurate finite element vehicle model.

```
Number of CPU's  :      2
Number of cycles  :     150002 (multi body part)
Max. nr. of cycles  :   450002 (model    2 )
Begin time          : 14:15:16
End   time          : 11:40:16
Total CPU time      :  153203.9 sec (   42 hours 33 minutes 23 seconds)
Total elapsed time :    77100.4 sec (   21 hours 25 minutes  0 seconds)

MADYMO TERMINATED NORMALLY
```

Figure 1.1 Section of MADYMO Log File

Data analysis was also time-consuming, an issue experienced by other researchers including Hulme et at (2003): *"However, fully understanding and correctly interpreting the results generated by complex crash simulations is often an inherently difficult task… "*

Although the use of powerful and versatile software such as MADYMO can create some problems for the researcher, the author considers such issues a fair price given the capability to model such extremely complicated events as a vehicle-pedestrian collision, the resulting kinematics and even the pedestrian's injuries.

1.5 Thesis Organisation

The thesis begins with an introduction to traditional vehicle-pedestrian reconstruction methods and then compares these methods to the predictions offered by computer

simulation. The functionality of MADYMO as an accident investigation tool is investigated as well as its injury prediction capabilities. A generalised approach to the computer simulation of vehicle-pedestrian accidents is offered.

The thesis concludes with a summary of the research findings, a discussion of these findings and the author's conclusions.

An evaluation of a proposed method of reducing pedestrian thoracic injury is included in Appendix I.

Chapter 2

Overview of Traditional Vehicle-Pedestrian Accident Reconstruction Methods

2.1 Introduction

In this chapter the traditional vehicle-pedestrian accident reconstruction methods are discussed, compared and analysed. The need for accident reconstruction is discussed and the appropriateness of the different techniques used in traditional vehicle-pedestrian accident reconstruction is examined in comparison to these needs. Where appropriate, the derivation of the different methods is examined and compared to traditional projectile motion equations more obviously derived from simple physics. The results indicated by the various equations are also compared to actual vehicle-pedestrian accident data.

2.2 The Need for Accident Reconstruction

Anything that moves has the potential to collide with another object. The existing human culture is heavily reliant on the transportation of both people and goods over a wide range of distances at a wide range of speeds. Whether from human error, mechanical failure or the forces of nature transportation collisions occur on a frequent basis. Approximately 1.2 million people are killed and up to 50 million are injured in traffic collisions worldwide (Cameron et al, 2004).

Accident reconstruction is the science of determining the cause of transportation related accidents. Ideally, the aim of accident reconstruction is to understand the cause of a vehicle accident so that, if necessary, steps can be taken to reduce the likelihood of similar accidents occurring in the future. In reality, the most common usage of vehicle-pedestrian accident reconstruction is in litigation. In such circumstances a conservative estimate of vehicle speed is required from the reconstructionist.

2.3 Traditional Methods of Accident Reconstruction

Accident reconstruction typically involves the application of physics to determine the dynamics of the transport vehicle(s) in question prior, during and following the incident(s) that is being studied. The methodology employed is usually based upon

research conducted using the actual or sufficiently representative vehicles, whether they are cars, trucks, motorcycles, planes or any other vehicle.

Transport vehicles that are produced in high volume, such as passenger cars, are now required to have several exemplar vehicles crash-tested in a variety of tests prior to the model being made available for public sale. This crash testing provides a significant amount of information that is available to accident investigators to assist in accident reconstruction.

With accidents involving one or more vehicles in which the crush stiffness of the vehicle is known from crash testing, it is possible to determine the energy expended during the collision that resulted in the given accident damage (Campbell, 1974). Using conservation of momentum the vehicle(s) speed loss during the collision can then be quantified. Combining this information with calculations of vehicle speed loss prior and post accident as well as the corresponding directions of travel it is possible to reconstruct the accident.

Low volume and high-cost transport vehicles, such as trucks and commercial airliners, are not subject to crash-test requirements (National Highway Traffic Safety Administration (NHTSA) Federal Motor Vehicle Safety Standard, 2005; European Road Safety Observatory (2006) Vehicles, 2007). In accident cases involving low volume/high cost transport vehicles various assumptions must be made with a corresponding loss of accuracy. Potential sources of reconstruction error include:

(i) Limited understanding of the handling and performance of the vehicle(s) in question.
(ii) Limited understanding of the structure of the vehicle(s) involved, particularly in regard to failure and energy dissipation.
(iii) Frequently large disparities in mass between the impacting vehicle(s).

These potential sources of error also affect vehicle-pedestrian collisions. Aside from the large mass-disparity that exists in this scenario, the dynamic response range of the human body following a vehicle impact is not well understood and proves difficult to model (Brands et al, 2001). There are many factors that influence the dynamic

response of the human body during and following an impact from a vehicle including (but not limited to):

- the stiffness and damping properties of the many different types of tissue in the human body
- mass distribution throughout the human body
- muscle tension and response
- joint stiffness in various directions of travel
- the coefficient of friction that exists between the person and contacting surfaces, including between different body parts
- the different failure strengths of different human bones, ligaments and cartilage
- the variability in properties that occur within individuals and across populations

The variability and lack of knowledge of these factors create many problems for the accident reconstructionist when analysing a vehicle-pedestrian collision. Factors such as muscular response are known to influence pedestrian kinematics and injury patterns but are very difficult to account for (Vezin and Verriest, 2005).

Aside from the influence of the variability and lack of knowledge of the properties of the human body, other pedestrian factors also influence post-vehicle impact kinematics, including:

- pedestrian orientation with respect to vehicle
- pedestrian speed (eg walking, running, stationary)
- pedestrian posture (eg standing upright, bending over, crawling)

These factors will create rather obvious differences in trajectory following a vehicle impact but the exact influence is difficult to quantify.

Despite the inherent difficulties in modelling the interaction of the human body with a impacting vehicle there is a large number of practitioners in the field of vehicle-pedestrian accidents who consider that the response of the human body following a vehicle impact can be reconstructed using fairly simple mathematical models.

2.4 Overview and Theory of Mathematical Methods of Pedestrian Accident Analysis

Pedestrian accident reconstruction has typically utilised pedestrian throw distance to obtain the speed of the impacting vehicle at the time of impact. Whilst there is debate over the validity of this approach, as some authors contend that due to variation in initial pedestrian orientation and vehicle attitude it is not possible to reliably determine vehicle speed from pedestrian throw distance (Ademec and Schonpflug, 2003), there are many instances where mathematical models have been demonstrated to provide close correlation to dummy and cadaver testing. In research conducted by Wood (1991) using cadavers and dummy tests good correlation was obtained between the predicted and actual test results of vehicle impact speed versus throw distance even when the vehicles were decelerating with a corresponding downwards pitch.

When a pedestrian is struck by a moving vehicle the resulting trajectory of the pedestrian can vary considerably, depending on the height of the pedestrian with respect to the height of the part of the vehicle that strikes the pedestrian, the speed of the vehicle and the orientation of the pedestrian with respect to the vehicle. According to American research, 80% of pedestrian impacts result in a post-impact pedestrian trajectory that falls within one of the following five categories (Ravini, 1981; Eubanks, 1994):

1. Wrap trajectory
2. Fender vault
3. Roof vault
4. Somersault
5. Forward projection

In a wrap trajectory the pedestrian has typically been struck by a decelerating vehicle where the contact point of the vehicle is below the pedestrian's centre of mass. This relatively low contact results in the pedestrian toppling onto the vehicle and often results in the pedestrian's head contacting either the bonnet or windscreen of the vehicle. The pedestrian is accelerated to a speed close to that of the vehicle and as the vehicle brakes the pedestrian moves forward, relative to the vehicle, and falls to the ground. This is the most common of the post-impact pedestrian trajectories.

A fender vault occurs when rotation about an axis approximately perpendicular to the ground is imparted to the pedestrian in a collision that would otherwise result in a wrap trajectory. This rotation causes the pedestrian to topple over one of the vehicle's front fenders. In this type of impact the contact between the vehicle and pedestrian occurs over a shorter period of time and there is less likelihood of the pedestrian attaining a similar velocity to the impacting vehicle.

A roof vault occurs when the impacting vehicle is travelling too fast for a wrap trajectory to occur. It can also happen at lower speeds when the vehicle is not braking at the time of impact. In this type of trajectory the vehicle passes underneath the pedestrian after impact.

The somersault trajectory is the least common of the post-impact pedestrian trajectories. It occurs when there is considerably more rotation imparted to the pedestrian about an axis approximately parallel to the ground than in the other trajectories. This rotation causes the pedestrian to somersault. It would appear most likely to occur when the impacting vehicle is travelling at moderately high speed and is braking heavily at the time of impact. The heavy braking results in a nose-down attitude for the vehicle, lowering the point of contact with the pedestrian.

For a forward projection to occur the contact point of the impacting vehicle must be above the centre of mass of the pedestrian (Wood et al, 2005). This occurs when a passenger car strikes a small child or an adult that is not standing upright. It can also occur with larger vehicles, such as a truck, van or bus striking a standing adult. The impact results in the pedestrian's centre of mass being accelerated in the direction that the vehicle was travelling and also downward. This is the second most common of the post-impact pedestrian trajectories (Ravini et al, 1981).

In the somersault and forward projection trajectories there are two stages:

1. The pedestrian is impacted by the vehicle and is launched in the direction of vehicle travel. The launch angle is affected by the relative heights of the point of impact and the pedestrian's centre of mass.
2. The pedestrian contacts the ground and tumbles and/or slides to rest.

If the point of impact is known (as it often is due to debris and/or fluid splatter) and the point where the pedestrian came to rest is noted then the horizontal distance that the pedestrian travelled post-impact is a known quantity. The height of the pedestrian's centre of mass is also determinable. What is not so easily determined is the launch angle. Whilst a launch angle of zero degrees could be assumed for a vehicle that strikes a pedestrian with a vertical front that is at least as high as the pedestrian is tall (such as a bus) with no possibility of the pedestrian's legs or feet partially going under the vehicle such a scenario seems unlikely. What can be stated is that a vehicle-pedestrian collision where the point of contact is below the centre of mass of the pedestrian is likely to result in a positive launch angle of between 0 and 90 degrees whilst an impact where the point of contact is above the centre of mass of the pedestrian is liable to result in a negative launch angle.

2.5 Pedestrian Motion Post-Impact Modelled as Projectile Motion

Before examining the traditional vehicle-pedestrian accident reconstruction equations it is useful to examine the motion of an object launched at a known velocity and angle and consider the influence of gravity on the object's path. The resultant trajectory is universally referred to as 'projectile motion'.

The majority of traditional vehicle-pedestrian accident reconstruction equations are derived from equations describing projectile motion. In this section a basic analysis of pedestrian motion post impact is performed by considering the pedestrian as a point mass undergoing projectile motion.

The equations for projectile motion can be derived from the equations for uniformly accelerated linear motion, namely:

$$x = t\frac{(v_1 + v_2)}{2} \tag{2.1}$$

$$v_2 = v_1 + at \tag{2.2}$$

$$x = v_1 t + \frac{at^2}{2} \tag{2.3}$$

$$v_2^2 = v_1^2 + 2ax \tag{2.4}$$

where x = displacement(m)

a = acceleration (ms^{-2})

v_1 = initial velocity (ms^{-1})

v_2 = final velocity (ms^{-1})

t = time (s)

Galileo deduced that the horizontal and vertical motion of a projectile can be described separately (Hill, 1988). In terms of the equations of linear motion, the horizontal displacement of a projectile may be described using equation (2.1). In this instance the velocity is taken to describe the horizontal velocity only and v_1 is taken to be equal to v_2, i.e. the initial horizontal velocity equals the final horizontal velocity (therefore ignoring air resistance), giving the expression:

$$x = v_x t \tag{2.5}$$

The vertical displacement can be described using:

$$y = v_1 t + \frac{at^2}{2}$$

In this expression y refers to vertical displacement or height and the velocity is taken to be the vertical component of the velocity. Therefore the expression can be rewritten:

$$y = v_y t - \frac{at^2}{2} \tag{2.6}$$

Rearranging equation (2.5) to solve for time and substituting into equation (2.6) yields:

$$y = \frac{v_y x}{v_x} - \frac{ax^2}{2v_x^2} \tag{2.7}$$

In a typical vehicle-pedestrian collision the pedestrian is initially standing prior to impact but lies prone post-impact. If it is assumed that the trajectory of the pedestrian is best modelled using the centre of mass of the pedestrian, then the change in pedestrian attitude needs to be accounted for by using a launch point higher than the landing point. The designations of the initial launch height h, launch angle θ, initial velocity v and the distance travelled whilst airborne d_a are as shown in Figure 2.1.

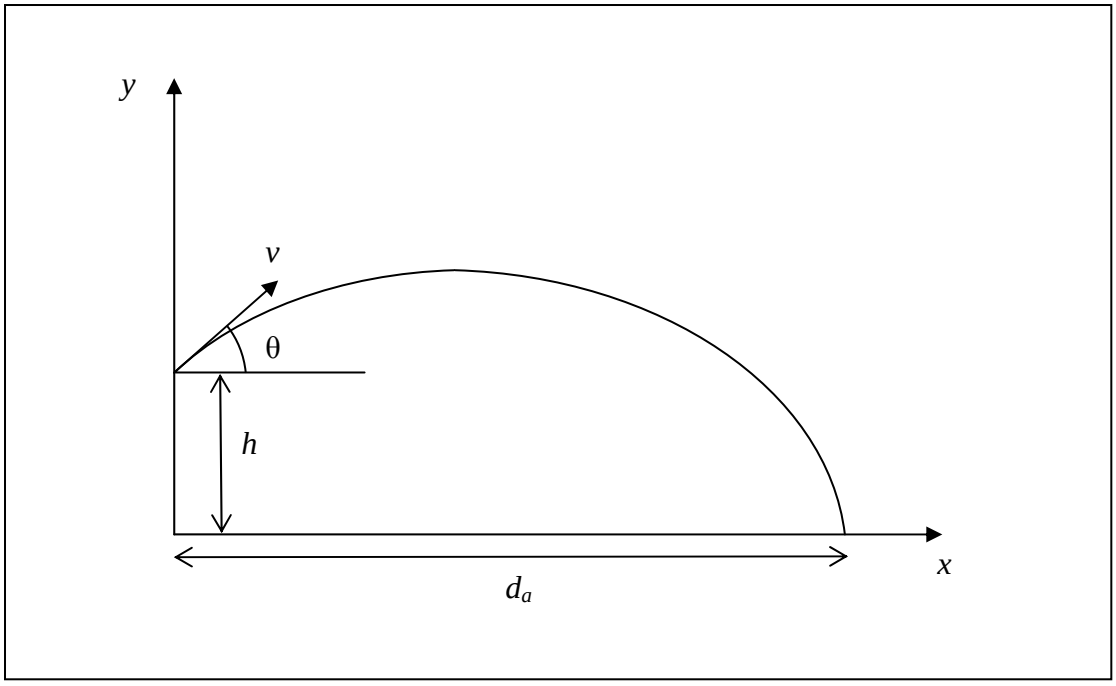

Figure 2.1 Definition of Launch Angle *θ*, Initial Velocity *v*, Initial Launch Height *h* and the Distance Travelled *d*

From Figure 2.1 it is apparent that following may be defined:

$$v_x = v\cos\theta$$

$$v_y = v\sin\theta$$

Furthermore, at $x = 0$, and at $x_{(max)} = d$ and $y = 0$. Substitution of these expressions into Equation 2.7 yields:

$$0 = h + \frac{d_a v\sin\theta}{v\cos\theta} + \frac{a{d_a}^2}{2v^2\cos^2\theta}$$

Simplifying and rearranging into a standard quadratic gives:

$${d_a}^2\left[\frac{a}{2(v\cos\theta)^2}\right] + d_a\frac{\sin\theta}{\cos\theta} + h = 0 \qquad (2.8)$$

Using the general quadratic solution of:

$$x = \frac{-b \pm \sqrt{b^2 - 4ac}}{2a}$$

Substitution of the *a*, *b*, and *c* values from Equation 2.8 yields:

$$d_a = \frac{-\left(\frac{\sin\theta}{\cos\theta}\right) \pm \sqrt{\frac{\sin^2\theta}{\cos^2\theta} - \frac{2ah}{v^2\cos^2\theta}}}{\left(\frac{a}{v^2\cos^2\theta}\right)}$$

Simplification, discarding the negative root (which provides the negative *x* value that yields the theoretical starting point had the particle been launched at a height of $y = 0$

and substituting $-g$ for a as the acceleration acting on the projectile is gravity (which is downwards and therefore negative) gives:

$$d_a = \frac{v^2 \sin\theta \cos\theta}{g}\left[1 + \sqrt{1 + \frac{2gh}{v^2 \sin^2\theta}}\right] \qquad (2.9)$$

This describes the maximum airborne distance that a point object will travel when launched at an angle θ, at an initial launch height h and with an initial velocity v. It describes two dimensional linear motion only and ignores air resistance. It does not account for any motion post impact.

Rearranging equation (2.9) to solve for launch velocity yields:

$$v = \sqrt{\frac{g d_a^{\,2}}{2\cos^2\theta\left(h + \frac{d_a \sin\theta}{\cos\theta}\right)}} \qquad (2.10)$$

Maximum d_a is obtained for $\theta \approx 45°$ (it is obtained at $\theta = 45°$ if $h = 0$). For $\theta = 45°$ equation (2.10) simplifies to:

$$v = \sqrt{\frac{g d_a^{\,2}}{h + d_a}} \qquad (2.11)$$

If the initial launch height $h = 0$ then Equation 2.7 reduces to:

$$v = \sqrt{g d_a} \qquad (2.12)$$

2.6 Pedestrian Motion Post-Impact Modelled Using Slide to Rest Calculations

The motion of a pedestrian sliding and or tumbling to rest is often approximated using:

$$v_2^2 = v_1^2 + 2ax$$

In this instance the acceleration acting on the pedestrian is usually taken to be a proportion of the acceleration due to gravity based on the pedestrian's interaction with the ground and often referred to as the coefficient of friction, μ. The distance travelled, x, is usually taken to the rest point of the pedestrian therefore $v_2 = 0$. Using d_g is the distance travelled along the ground the equation may be expressed as:

$$v = \sqrt{2\mu g d_g} \qquad (2.13)$$

It should be noted that there is considerable debate on the coefficient of friction between a pedestrian and the ground/road, especially when the differences between sliding and tumbling are accounted for. Published values range between 0.4 and 1.1 (See Table 2.1).

2.7 Combined Projectile Motion and Slide/Tumble to Rest

Combining equations (2.11) and (2.13) yields:

$$v = \sqrt{g\left(\frac{d_a{}^2}{h + d_a} + 2\mu d_g\right)} \tag{2.14}$$

Combining equations (2.12) and (2.13) yields:

$$v = \sqrt{g\left(d_a + 2\mu d_g\right)} \tag{2.15}$$

2.8 Basic Pedestrian Accident Analysis Equations

2.8.1 Rich (1997)

Rich derives the same two equations as equations (2.10) and (2.15).

2.8.2 Searle (1983)

$$v = \frac{\sqrt{2\mu g d}}{\cos\theta + \mu \sin\theta}$$

This formula is based on an object bouncing along a level surface in a series of diminishing bounces until it stops. θ is the launch angle. Searle also establishes the following bounds:

$$v_{\min} = \sqrt{\frac{2\mu g d}{1 + \mu^2}}$$

$$v_{\max} = \sqrt{2\mu g d}$$

Searle further developed his formulae in a subsequent paper (1993):

$$v = \frac{\sqrt{2\mu g\left(d + \mu h\right)}}{\cos\theta + \mu \sin\theta}$$

$$v_{\min} = \sqrt{\frac{2\mu g\left(d + \mu h\right)}{1 + \mu^2}}$$

2.8.3 Collins (1979)

$$v = \sqrt{\frac{g}{2h}}\left(2h\sqrt{\mu^2 + \frac{\mu d}{h}} - 2h\right)$$

Collins uses the assumption that the pedestrian velocity throughout the airborne phase is the same as at the start of the sliding phase. He notes this in his book and states that this equation should only be used for vehicles with a flat impacting face, such as a large truck or bus which results in θ = 0°.

2.8.4 Wood (1988)

Wood developed an equation, published in 1988, describing the throw distance of a pedestrian which used

$$v = \sqrt{\frac{2\mu g\left(d - \mu h\right)\left(m_v + m_p\right)^2}{m_v^2}}$$

Where m_v = mass of vehicle

m_p = mass of pedestrian

2.9 Pedestrian Motion Post-Impact Modelled Using 2-Dimensional Objects

In Wood's 1988 paper also discussed the derivation and application of a two-dimensional mathematical model describing the relationship between vehicle impact speed and pedestrian throw distance. This method is commonly referred to as Wood's SSM (Single-Segment Model). As per the derivation described in Section 2.4, Wood considers the vertical and horizontal components of the pedestrian's velocity separately. Wood also breaks his analysis down to consider two separate vehicle-pedestrian impacts for each incident – a primary impact, usually involving the

pedestrian's pelvis/lower torso and the leading edge of the vehicle, and a secondary impact, usually involving the pedestrian's head/upper torso and the vehicle's bonnet and/or windscreen.

Wood describes the post-primary impact horizontal, vertical and rotational components of the pedestrian's velocity and the post-primary impact velocity of the vehicle using:

$$v_{ped\_horizontal\_post-impact1} = \frac{m_{vehicle} k^2 v_{vehicle\_pre-impact}}{k^2\left(m_{vehicle} + m_{ped}\right) + m_{vehicle} h^2}$$

$$v_{ped\_vertical\_post-impact1} = \frac{h b_w v_{ped\_horizontal\_post-impact1}}{k^2}$$

$$\omega_{ped\_post-impact1} = \frac{h v_{ped\_horzontal\_post-impact1}}{k^2}$$

$$v_{vehicle\_post-impact1} = \frac{m_{vehicle}\left(k^2 + h^2\right) v_{vehicle\_pre-impact}}{k^2\left(m_{vehicle} + m_{ped}\right) + m_{vehicle} h^2}$$

Where v = linear velocity (ms^{-1})

ω = rotational velocity (rad/s)

m = mass (kg)

b = horizontal distance between COM of pedestrian and leading edge of vehicle (m)

h = vertical distance between COM of pedestrian and leading edge of vehicle (m)

k = radius of gyration of pedestrian about horizontal axis

Following the second impact the pedestrian and vehicle velocity components are:

$$v_{ped\_horizontal\_post-impact2} = \frac{m_{vehicle}}{m_{vehicle} + m_{ped}}\left[\frac{\left(h^2 + k^2\right)\theta}{h t_{impact1-2}} - \mu_{vehicle} g t_{impact1-2} - v_{ped\_vertical\_post-impact2}\frac{\cos\left(\theta - \frac{\pi}{2}\right)}{\sin\theta}\right] + \frac{m_{ped}}{m_{vehicle} + m_{ped}}\left[\frac{k^2\theta}{h t_{impact1-2}}\right]$$

$$v_{ped\_vertical\_post-impact2} = l\omega_{ped\_post-impact2}\sin\theta$$

$$\omega_{ped\_post-impact2} = \frac{\dfrac{k^2\theta}{t_{impact1-2}} + \dfrac{m_{vehicle} l \cos\left(\theta - \dfrac{\pi}{2}\right) \dfrac{h\theta}{t_{impact1-2} - \mu_{vehicle} g t_{impact1-2}}}{m_{vehicle} + m_{ped}} + l \sin\theta \dfrac{b\theta}{t_{impact1-2} - g t_{impact1-2}}}{k^2 + l^2 \dfrac{\sin^2\theta + m_{vehicle}\cos^2\theta}{m_{vehicle} + m_{ped}}}$$

$$v_{vehicle\_post-impact2} = v_{ped\_horisontal\_post-impact2} + l\omega_{ped\_post-impact2} \cos\left(\theta - \frac{\pi}{2}\right)$$

Where l = vertical distance between COM of pedestrian and the top of the pedestrian's head (m)

$t_{impact1\text{-}2}$ = time between first and second impacts (seconds)

μ = coefficient of friction

g = acceleration due to gravity (ms^{-2})

Wood then states that for collisions with two impacts (as described above) the pedestrian throw distance is given by:

$$d = \frac{v^2_{ped\_horisontal\_post-impact2}\left(1 + \dfrac{\mu_{ped} v_{ped\_vertical\_post-impact2}}{v_{ped\_horizontal\_post\_impact2}}\right)^2}{2\mu_{ped} g} + \frac{k^2\theta}{h} + \mu_{ped}\left(y_{final} + \Delta y_{impact1-2}\right)$$

Where d = throw distance (m)

y_{final} = height of the pedestrian's COM at rest (m)

$\Delta y_{impact1\text{-}2}$ = height change of pedestrian's COM between the first and second impacts (m)

For collisions where there is only the first impact (which Wood classifies as uncommon) the throw distance is given by:

$$d = \frac{m^2_{vehicle} v^2_{vehicle\_pre-impact}}{2\mu_{ped} g\left(m_{vehicle} + m_{ped}\right)^2} + \mu_{ped} y_{final}$$

2.10 Comparison of Results Using Different Calculation Methods to Predict Throw Distance

Figures 2.2 to 2.5 display the graphical results of varying launch angle (where applied) and coefficient of friction. The results obtained for impact speed prediction using Collins, Searle, Wood (as per sections 2.8.2 – 2.8.4) and the Projectile and Sliding equation from Equation 2.9 were plotted for throw distances between 0 and 50 metres. Where applicable the launch angle was varied between 0º, 30º and 45º with the exclusion of a launch angle 0º for the Projectile + Sliding equation. Noticeably, a launch angle 0º for the Projectile + Sliding equation resulted in values that were much higher than the other equations. It is considered that the application of an equation with an airborne phase where the launch angle is 0º is inappropriate. The launch height (where used) was set to 1 metre and the airborne/sliding phases (where differentiated) were split so that each represented 50% of the total throw distance. The coefficient of friction was varied between 0.4 and 1.0.

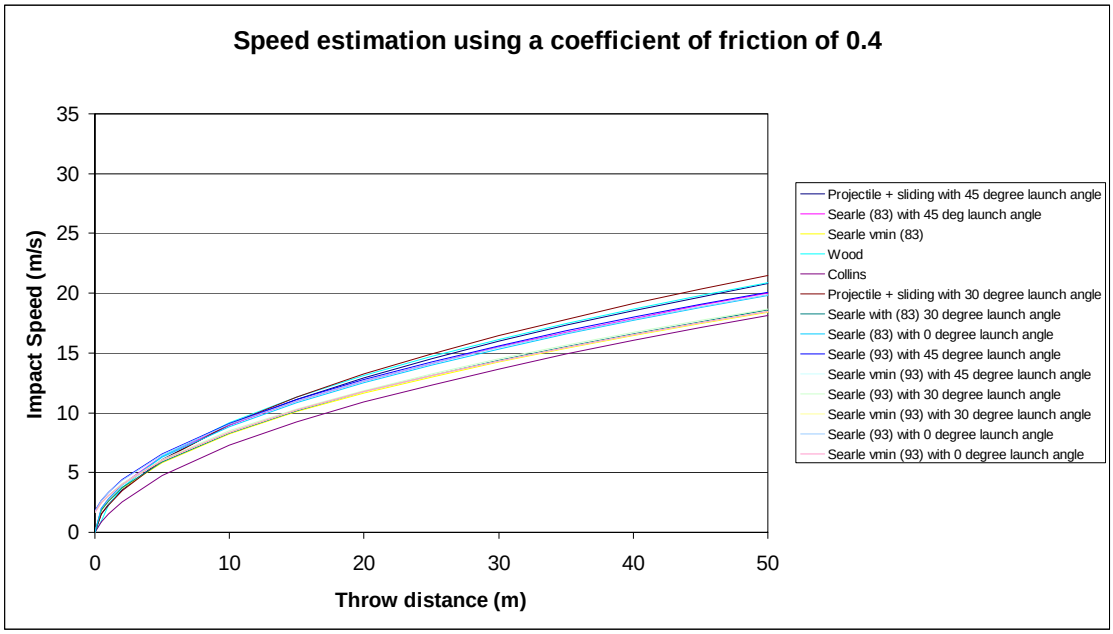

Figure 2.2 Speed Estimation Using a Coefficient of Friction of 0.4

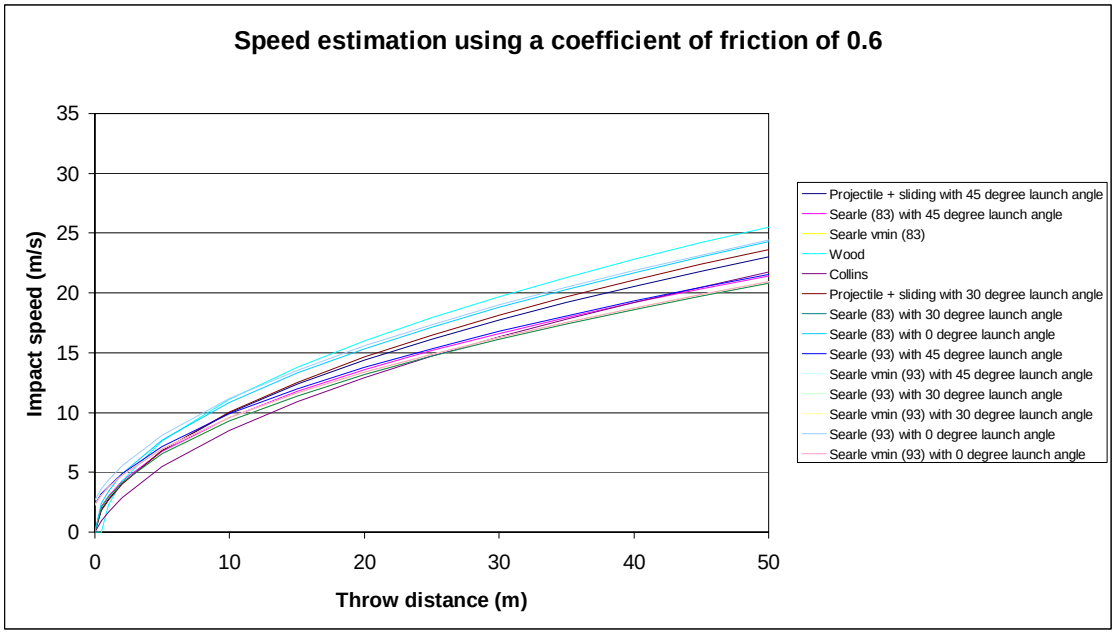

Figure 2.3 Speed Estimation Using a Coefficient of Friction of 0.6

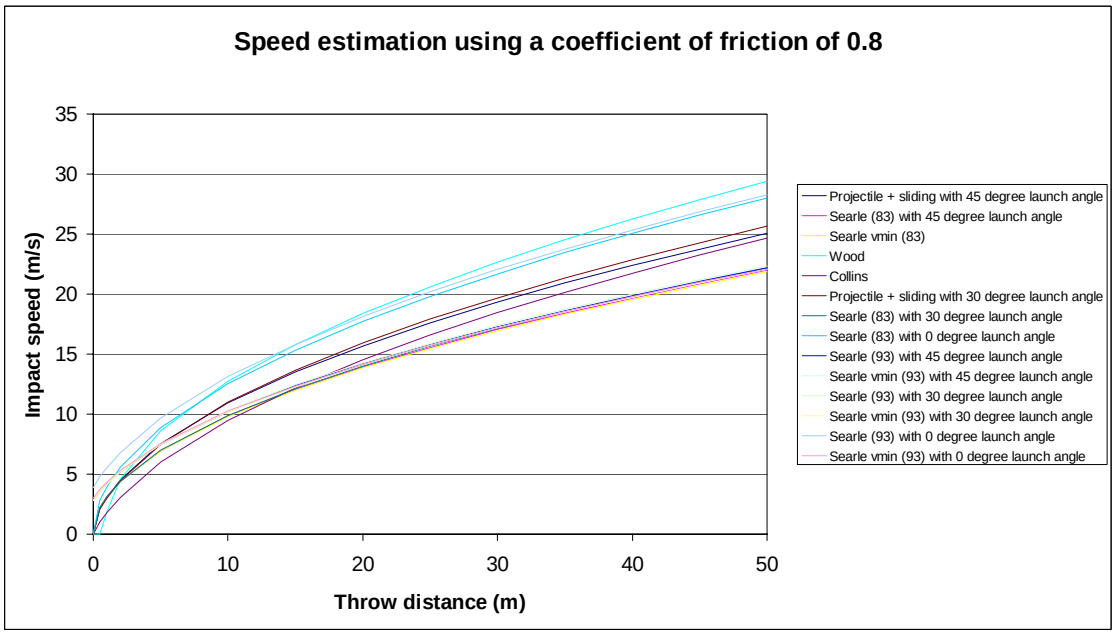

Figure 2.4 Speed Estimation Using a Coefficient of Friction of 0.8

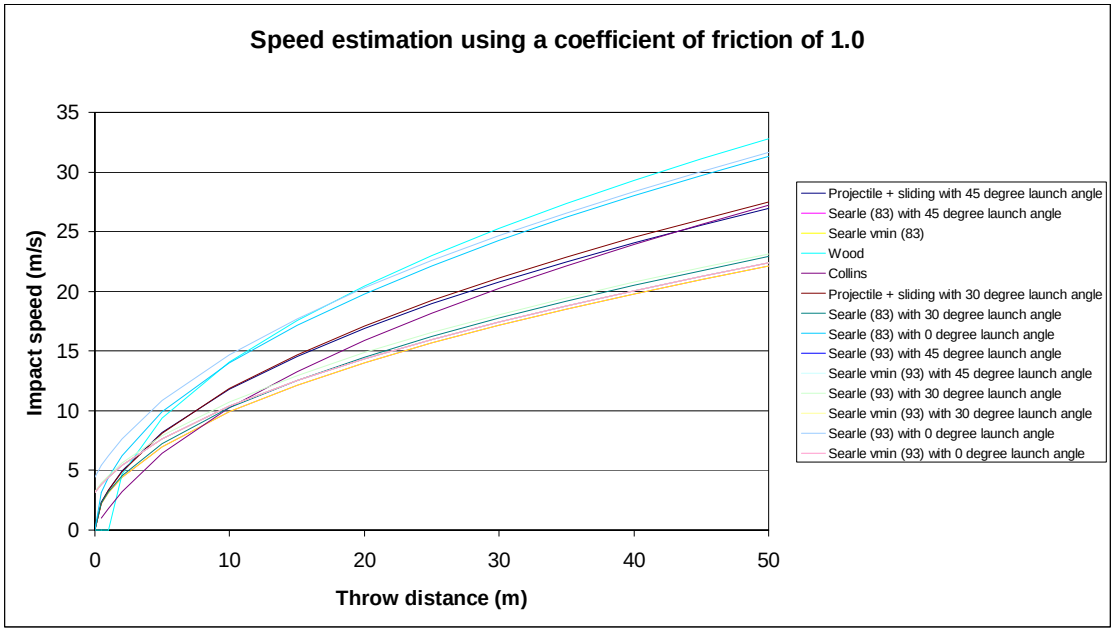

Figure 2.5 Speed Estimation Using a Coefficient of Friction of 1.0

From these graphs the following observations can be made:

(i) As expected, the application of a higher coefficient of friction to a given throw distance results in a higher calculated impact speed

(ii) With a throw distance of 50 metres and a coefficient of friction of 0.4 the predicted impact speed is between 18.1 ms^{-1} and 21.5 ms^{-1}, the results covering a range of 3.4 ms^{-1} with the highest value being 19% greater than the lowest prediction.

(iii) With a throw distance of 50 metres and a coefficient of friction of 1.0 the predicted impact speed is between 22.1 ms^{-1} and 32.8 ms^{-1}, the results covering a range of 10.7 ms^{-1} with the highest value being 48% greater than the lowest prediction.

2.11 Coefficient of Friction for a Tumbling/Sliding Pedestrian

From literature values include:

Source	Surface	Coefficient of friction
Collins (1979)		1.1
Searle (1983)	Asphalt Grass	0.66 0.79

Severy (1966)		0.40 – 0.75
Fricke (1990)	Asphalt Concrete Grass	0.45 – 0.60 0.40 – 0.65 0.45 – 0.70
Stevenson (testing by Author)	Asphalt Grass	0.57 – 0.58 0.54 – 0.60

Table 2.1 Coefficient of Friction between Pedestrian and Ground

It is uncertain how some of these values were obtained. It is suspected that in some cases an average coefficient of friction has been derived over the total throw distance which may have included an airborne portion. A pedestrian that has been accelerated to 40 km/h or less by a vehicle impact experiences negligible drag due to air resistance (Aronberg, 1990). The coefficient of friction for the airborne portion may therefore be considered to be close to zero.

The pedestrian then impacts the ground with a force between 20 – 40 times the person's weight (Severy, 1966). From the kinetic energy transferred into damage evident on the pedestrian and possibly also ground deformation (depending on the type of ground impacted) it is readily apparent how the vertical component of the pedestrian's airborne velocity is dissipated. What is not so apparent is how the dissipation of the vertical velocity component affects the continuation of the horizontal velocity component. The effect on the horizontal velocity component was noticeable in a series of tests Searle (1993) conducted by dropping a dummy from a moving bus.

At the moment of impact there is a greater amount of pedestrian-ground interaction than occurs during the subsequent slide/tumble to rest. This causes a momentarily higher effective coefficient of friction than is measured during experimental testing of a pedestrian sliding to rest. Searle performed further experimentation on the phenomenon by conducting a series of drop-tests of simply-shaped objects in a series of laboratory tests.

Wood explores this further by comparing results from Searle, Hill (1994) and Bovington (1999). Wood and Simms (2000) conclude '*There is strong evidence to show that horizontal momentum is significantly reduced by the initial vertical impact with the ground. Failure to account for this phenomenon results in a coefficient of friction that is too high.*' Wood's suggested range for the coefficient of friction is, however, entirely within the bounds displayed in Table 2.1 which seems to contradict his suggestion that the impact effect is significant.

In a previous paper Wood (1988) suggests that the coefficient of friction for a pedestrian sliding on the ground decreases as a function of the pedestrian's velocity. Wood states that the relationship is (assuming an initial, or low speed, coefficient of friction of 0.772):

$$\mu = 0.772 - 0.019v$$

Quite how this should be applied where the low-speed coefficient of friction is demonstrably different to 0.772 is unclear.

It should also be noted that most of the pedestrian accident formulae regarding throw distance are not as influenced by varying coefficient of friction as the formulae commonly used in vehicle accident reconstruction where the length of tyre mark is used to determine vehicle speed prior to braking. Indeed, Searle (1983) makes this very observation regarding the use of his formula which models a pedestrian as a bouncing object. Also, in this paper, Searle notes that the coefficient of friction that he obtained for a person on both asphalt and grass did not significantly alter regardless of whether the surface was wet or dry (see Table 2.1 for actual values). Although Searle does not note how these measurements were made, it would seem to suggest that these measurements were derived from a tumbling body, rather than one that was sliding. In vehicle accident reconstruction the reduction in coefficient of friction (and corresponding rate of deceleration) is quite marked when comparing the grip afforded by dry asphalt to that provided by the same surface when wet. The same can be said for the reduction in grip afforded by dry grass compared to wet.

In this context it is interesting to compare the rate of deceleration of a soil-tripped vehicle which subsequently rolls to the deceleration of a tumbling pedestrian. Cooperrider, Hammoud and Colwell (1998) indicate an average deceleration of 0.79 G but closer examination of their data indicates a maximum of 2.2 G over a 0.25 second interval followed by a 0.4 G deceleration over a 1 second interval. The average is not indicative of the deceleration experienced for any extended period of time during the trip and roll. It is suspected that a similar pattern occurs when a pedestrian strikes the ground and tumbles/slides to rest, i.e. a high deceleration for a relatively short period of time followed by a considerably lower rate of deceleration to rest.

The values obtained by Fricke and Stevenson in Table 2.1 for coefficient of friction were obtained by drag-testing a pedestrian or dummy over the ground and cover a range of 0.4 – 0.7. This range is not substantially different to that obtained by the other authors (0.35 -1.1) which suggests that the other values were obtained similarly. When it is considered that a tripped vehicle, as per Cooperrider's tests, which had an average deceleration of 0.79 G, actually decelerated at only 0.4 G for the majority of the test and considering that this phase of the vehicle coming to rest is comparable to the pedestrian tests conducted, would seem to indicate that the deceleration (or coefficient of friction, for that matter) that the pedestrian undergoes during impact is not only significant, but occurs for a sufficient period of time to significantly alter the effective deceleration rate (or effective coefficient of friction) experienced by the pedestrian for the entire impact-to-rest phase of the total throw distance. Whilst the structure of a vehicle is far more rigid than that of a pedestrian (and therefore prone to higher deceleration during impact with the ground), the relative softness of the human body would tend to prolong the duration of the ground impact, compared to a vehicle, and thus result in a similar deceleration over the impact phase (as the impact phase would be longer).

Therefore a third part needs to be added to the airborne and tumbling phases described by Equation 2.9, an impact phase.

In order to determine the exact effect of the impact phase more experimental work needs to be conducted. A dummy or cadaver, instrumented with accelerometers and

precisely tracked spatially, should be dropped at varying heights whilst travelling across the ground at a range of speeds appropriate for pedestrian throw. The results should then indicate the deceleration experienced by a thrown pedestrian including the impact phase.

2.12 Pedestrian Launch Angle and Apogee

Two contentious components of many traditional equations used to derive vehicle impact speed from pedestrian throw are the pedestrian launch angle θ and the apogee height (i.e. the maximum vertical displacement achieved by the centre of mass of the pedestrian during the airborne portion of the pedestrian's post-impact trajectory).

Many pedestrian accident formulae use launch angle and often it is derived from the relationship of the pedestrian's centre of mass to the leading edge height of the striking vehicle. Sometimes it is determined iteratively. For litigation purposes it is often determined to be 45º (or slightly less for an initial pedestrian centre of mass height that is higher than the centre of mass height at landing, which is usually the case) in order to obtain a minimum vehicle speed.

Searle (1993) states that a launch angle range of between 20º and 50º changes the calculated velocity by less than 4% and that for a range of 10º to 60º the computed impact velocity is changed by less than 10%. This is seen to be true in Figure 2.6 where there is a 2.0% difference between 45º and 20º (or 50º) and an 8.7% difference between 45º and 10º (or 60º) when using Seale's equation with a pedestrian to ground coefficient of friction of 0.7 or less.

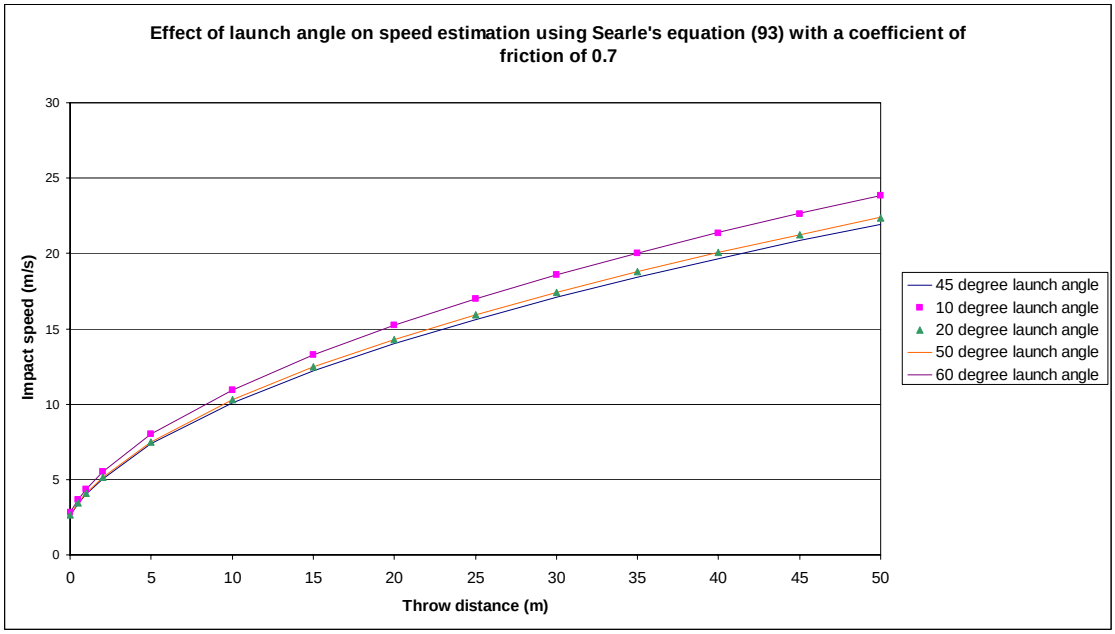

Figure 2.6 Effect of Launch Angle on Speed Estimation Using Searle's Equation (93) with a Coefficient of Friction of 0.7

When using the Projectile and Sliding equation and a coefficient of 0.7 for the pedestrian-ground contact the difference in impact speed ranges between 0.4% for the difference obtained at 45º versus 50º up to a 26.6% difference between 45º and 10º, as can be seen in Figure 2.7.

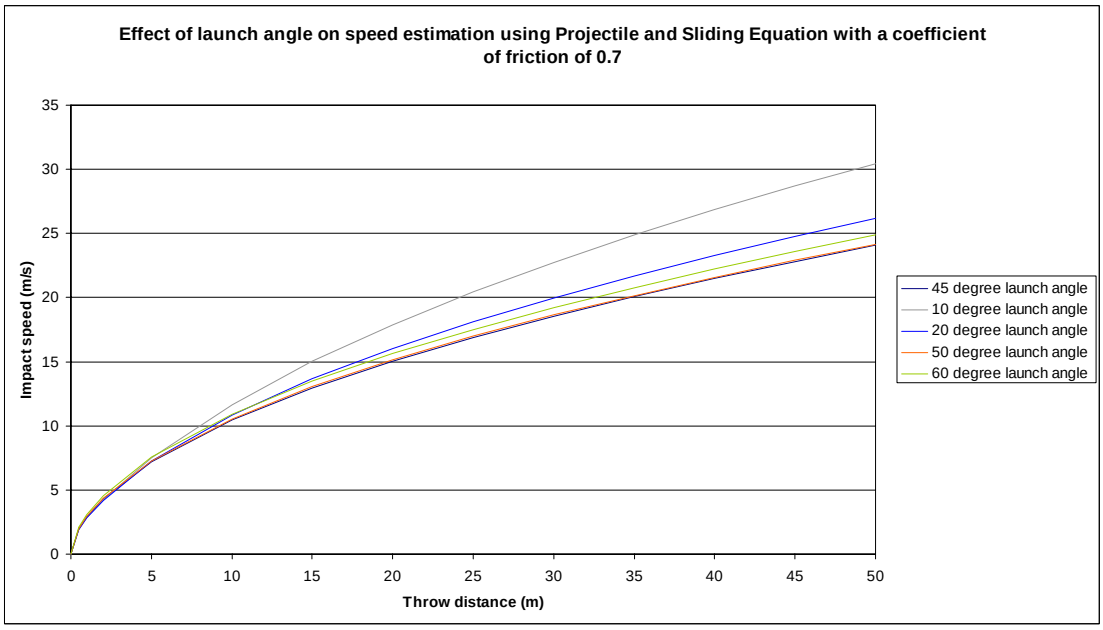

Figure 2.7 Effect of Launch Angle on Speed Estimation Using Projectile and Sliding Equation with a Coefficient of Friction of 0.7

Alternatively, using Searle's equation with a coefficient of 1.0, the calculated impact speed range has only a 0.4% spread between 45º and 50º with up to 22% difference between 45º and 10º, as is evident in Figure 2.8.

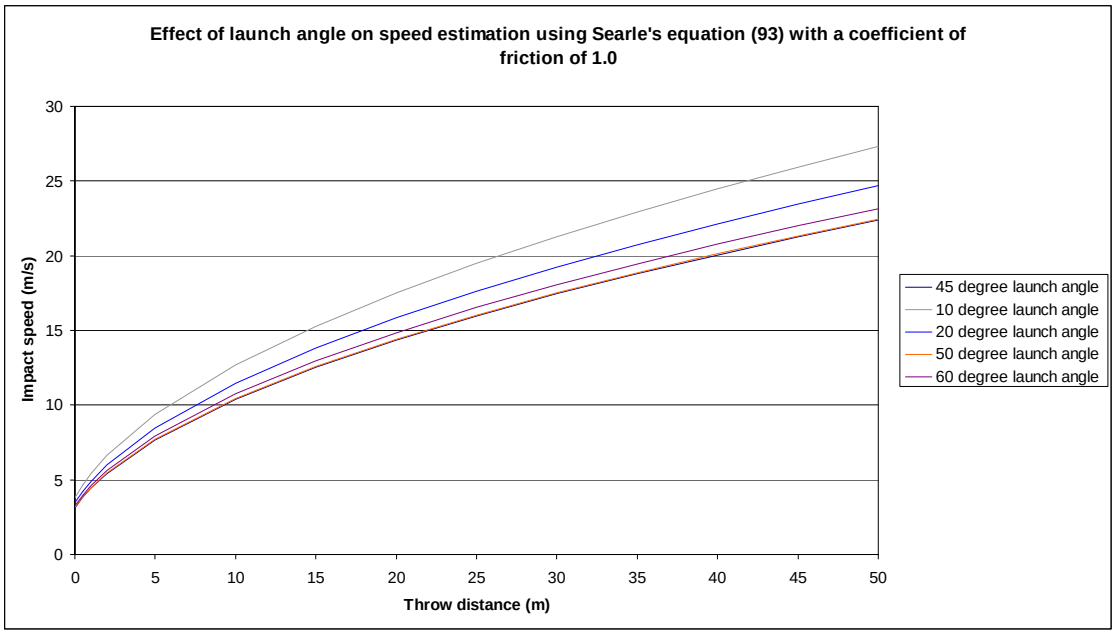

Figure 2.8 Effect of Launch Angle on Speed Estimation Using Searle's Equation (93) with a Coefficient of Friction of 1.0

Finally, when considering the Projectile and Sliding Equation with a coefficient of 1.0 the speed range has the same impact speed ranges as the previous example, i.e. 0.4% between 45º and 50º and 22% difference between 45º and 10º as can be seen in Figure 2.9.

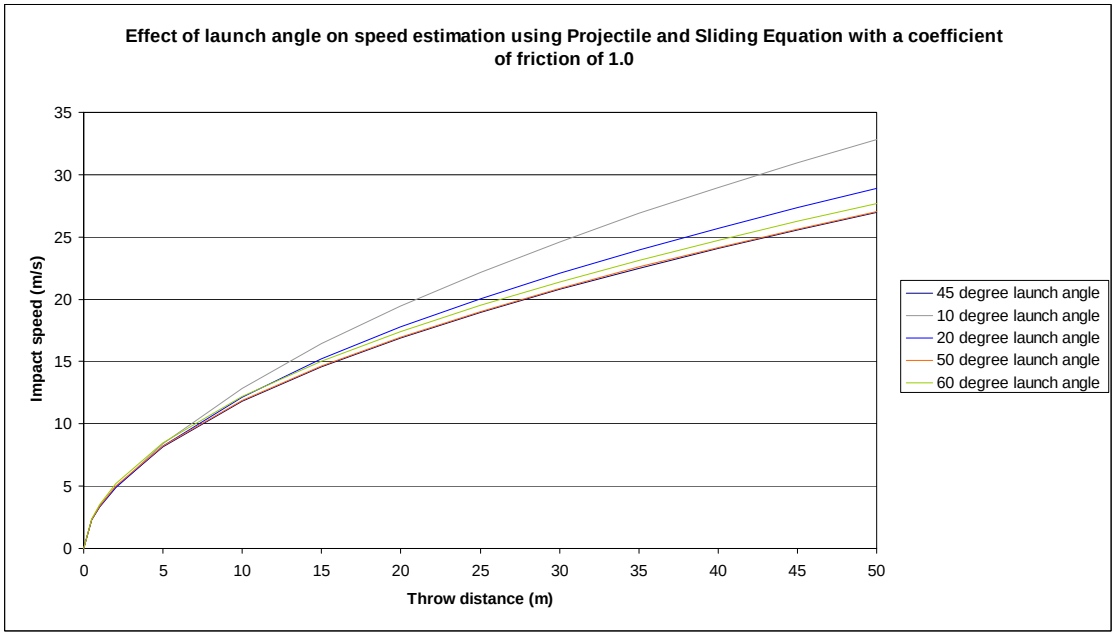

Figure 2.9 Effect of Launch Angle on Speed Estimation Using Projectile and Sliding Equation with a Coefficient of Friction of 1.0

This demonstrates an interesting issue. Searle's equation with a coefficient of friction of 0.7 is relatively unaffected by launch angle whereas, in comparison, the Projectile and Sliding Equation produces rather variable impact speeds for different launch angles when also using a 0.7 coefficient of friction. However, when using a coefficient of friction of 1.0 the dependability of the Projectile and Sliding Equation on launch angle is reduced, whereas the dependence on launch angle for Searle's equation is increased, so that both show a similar spread of results.

The use (and usefulness) of apogee height is rather controversial. As noted by Searle (1993) and others this is unreliable, usually having been determined from witness estimates. Because of this unreliable nature the author does not include any formulae based on apogee height in the analysis contained within this thesis.

2.13 Comparison to Test Data

Kühnel (1974) conducted a series of tests using a moving dummy and three different vehicles. The 50th percentile male dummy was propelled at 6 km/h (walking speed) into the path of the test vehicle. The test vehicle impact speed ranged between 35 km/h and 60 km/h. Dummy displacement was recorded at 24 millisecond intervals using high-speed photography and head, chest and pelvis acceleration were also measured. Test vehicles included a VW Beetle, a VW van and an Opel sedan. The data, as interpreted by the author of this thesis, can be seen in Table 2.2. Of note are the timed portions of the dummy's travel, including the sliding/tumbling portion along the ground. From these measurements the ratio of airborne travel to tumbling/sliding travel can be determined.

Although the data set is fairly complete only the horizontal displacement versus time of the dummy was recorded and it is not clear which of the maximum vertical displacement measurements (i.e. the maximum throw height, or apogee, of the pedestrian's trajectory, measured by Kühnel using photogrammetry) relate to which test. This is unfortunate, as it makes it difficult to ascertain the proportion of the dummy's velocity present at the moment of impact with the pavement is transferred to horizontal motion as the dummy begins its slide to rest. If 100% conservation of horizontal velocity is assumed between the airborne and sliding phases the coefficient

of friction between the dummy and the ground ranges between 1.2 and 1.6 (averaged for the impacts involving each vehicle-type and ignoring one extraneous result from the Opel tests). These values are obviously too high. For 80% conservation of horizontal velocity between the airborne and sliding phases the coefficient of friction drops to between 0.7 and 1.0. Likewise, for 60% conservation of velocity the coefficient of friction lies between 0.4 and 0.6.

Launch angle can also be approximated from Kühnel's data. If it is assumed that the pedestrian attains a launch velocity equal to the sum of the vectors of the vehicle's pre-impact velocity and the pedestrian's pre-impact velocity (which would, actually, only occur in the instance of an inelastic collision) and incorporating the pedestrian's post-impact horizontal velocity then the average launch angle was 40º for the VW Beetle tests, 46º for the Opel tests and 42º for the VW van tests. However, if the Projectile and Sliding Equation is used to solve for launch angle the results are 6.7º, 9.4º and 6.1º for the Beetle, Opel and VW van tests, respectively. This would appear to result, at least in part, from the Projectile and Sliding Equation describing an inelastic collision where the energy transfer results. In reality both the vehicle and pedestrian are likely to undergo elastic and possibly plastic deformation during the contact phase. The transfer of energy into deformation results in reduction of pedestrian launch velocity, compared to what would be expected as a result of an inelastic collision. Consequently, for the Projectile and Sliding Equation to match the correct throw distance with a launch velocity that is too high an under prediction of launch angle is required.

The centre of mass apogee height calculated using the launch angles determined from the Projectile and Sliding Equation ranged between 1.0 and 2.6 metres with an average of 1.24 metres, assuming an initial centre of mass height of 1.0 metre[1]. The eight apogee measurements quoted by Kühnel average 1.20 metres, indicating at least some agreement with the results indicated by the Projectile and Sliding Equation. However, as noted, Kühnel fails to note which apogee measurement belongs to which

[1] Note: Dummy centre of mass height estimated using the 55% of height rule, based on a height in shoes of 1.8 metres. The 55% rule gives approximately the same result as the method detailed in NASA's Man-Systems Integration Standards (MSIS) Volume 1: L (from top of head to centre of mass) = 0.486 x height (cm) – 0.014 x weight (lbs) – 4.775, using the 50th percentile male height of 177 cm and weight of 164 lb. And yes, NASA does really mix metric and imperial units, which possibly explains the moderately high failure rate of some of their designs.

test. Because the Projectile and Sliding equation represents an inelastic collision with a launch velocity that is unrealistically high (and a launch angle that is unrealistically low) it would be expected that the apogee predicted by the Projectile and Sliding equation would also be too low. Further testing or a clarification of Kühnel's measurements would be of value.

The throw distance data reported by Kühnel and comparison with the throw distance predicted by the Projectile and Sliding equation, Collins equation and Searle's equations from his 1993 paper can be seen in the three graphs in Figures 2.10, 2.11 and 2.12. Searle's equation and a coefficient of friction of 0.7 reasonably accurately predict the throw distances obtained from the VW Beetle and Opel sedan tests. Searle's v_{min} equation gives reasonable agreement with the results from the VW van tests when using a coefficient of friction between 0.7 and 1.0. These correlations can be seen in Figures 2.10 to 2.13.

Searle's 1993 equation appears to offer consistently accurate results with limited influence from the value used for pedestrian-ground coefficient of friction. Searle's v_{min} equation does indeed appear to offer a valid indication of minimum speed for a given throw distance. Collins' equation tended to underestimate and may be used in place of Searle's v_{min}.

The Projectile and Sliding equation appears to predict an impact speed that is too high when a 70:30 airborne:sliding ratio is used, despite this ratio being indicated in an average of Kühnel's data for the car (VW Beetle and Opel R3) impacts. As previously noted, the pedestrian's velocity following impact is over-predicted by the Projectile and Sliding equation and results in an over-prediction of vehicle velocity when a lower than would be expected launch angle (such as 6º) is used in conjunction with the correct airborne:sliding ratio. An increase in launch angle input, a reduction of the airborne travel proportion and/or a low pedestrian-ground coefficient of friction has to be applied for the Projectile and Sliding equation to better match the data.

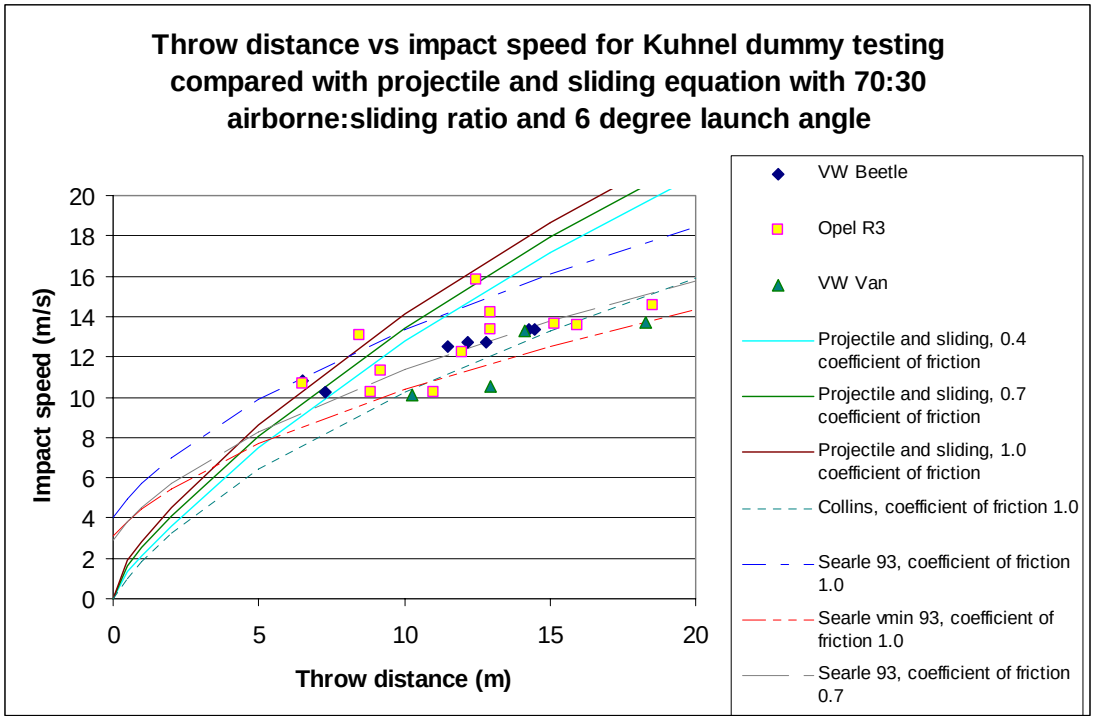

Figure 2.10 Equations matched to 70:30 airborne:sliding ratio of VW Beetle and Opel R3 assuming a 6 degree pedestrian launch angle (launch angle indication from Beetle tests)

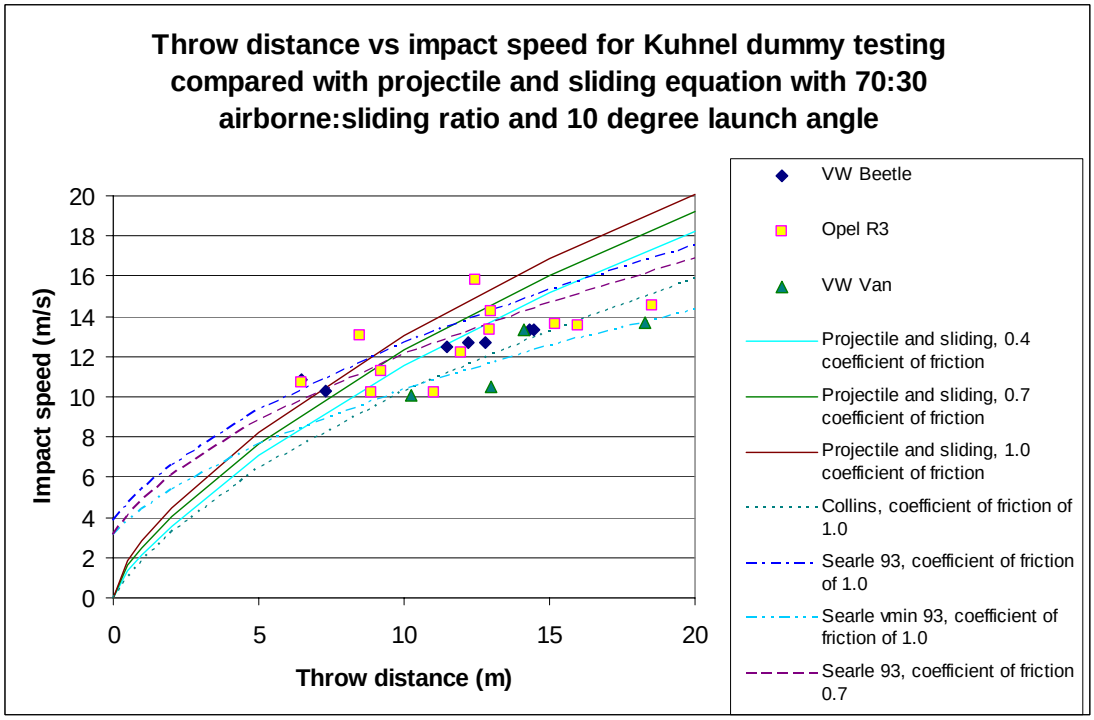

Figure 2.11 Equations matched to 70:30 airborne:sliding ratio of VW Beetle and Opel R3 assuming a 10 degree pedestrian launch angle (launch angle indication from Opel tests)

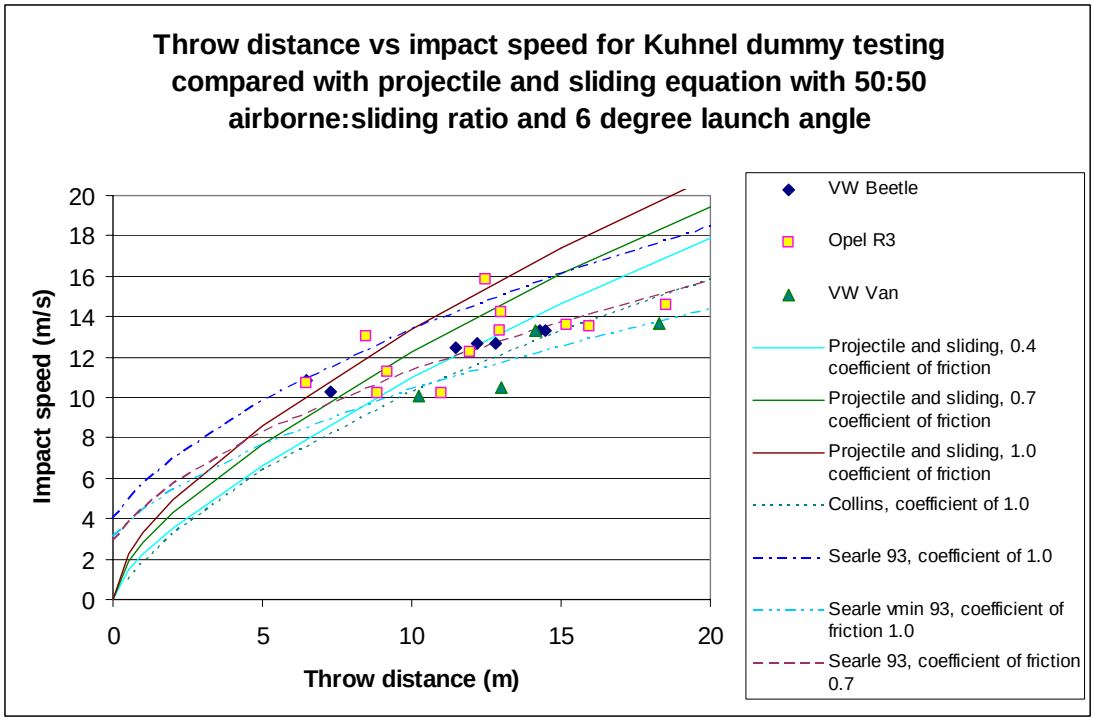

Figure 2.12 Equations matched to 50:50 airborne:sliding ratio of VW Van tests assuming a 6 degree pedestrian launch angle

Impact speed (km/h)	Impact speed (m/s)	Pedestrian walking speed (km/h)	Pedestrian walking speed (m/s)	Vehicle	Time history (seconds)							Pedestrian slide distance (m)
					Head contact on bonnet	Detachment of dummy from vehicle	Pelvis contact on ground	Head contact on ground	Avg first ground contact	Final position	Slide time	
37	10.3	6.0	1.7	VW Beetle	0.18	0.35	0.75	0.75	0.75			2.3
39	10.8	6.0	1.7	VW Beetle	0.15	0.29	0.9	0.8	0.85	1.36	0.51	1.49
45	12.5	6.0	1.7	VW Beetle	0.15	0.39	0.95	0.81	0.88	1.7	0.82	4.49
45.7	12.7	6.0	1.7	VW Beetle	0.11	0.29	0.94	1.02	0.98	2.03	1.05	2.64
45.7	12.7	6.0	1.7	VW Beetle	0.15	0.35	1.02	1.02	1.02	2.32	1.3	3.58
48	13.3	6.0	1.7	VW Beetle	0.12	0.23	0.98	1.09	1.035	2.18	1.15	4.49
48	13.3	6.0	1.7	VW Beetle	0.15	0.29	1.02	1.13	1.075	2.78	1.71	4.49
36.8	10.2	6.0	1.7	Opel R 3	0.11	0.61	0.96	1	0.98	2	1.02	1.49
36.8	10.2	6.0	1.7	Opel R 3	0.15	0.79	1	0.96	0.98	2.09	1.11	2.4
38.5	10.7	6.0	1.7	Opel R 3	0.12	0.44	0.76	0.73	0.745	1.53	0.79	0.51
40.6	11.3	6.0	1.7	Opel R 3	0.117	0.37	0.66	0.7	0.68	1.79	1.11	3.68
44	12.2	6.0	1.7	Opel R 3	0.12	0.93	1.13	1.13	1.13			3.01
47	13.1	6.0	1.7	Opel R 3	0.12							
48	13.3	6.0	1.7	Opel R 3	0.11	0.31	0.9	0.98	0.94	2	1.06	3.48
48.8	13.6	6.0	1.7	Opel R 3	0.1	0.06	1.09	1.47	1.28	2.46	1.18	4.43
49	13.6	6.0	1.7	Opel R 3	0.09	0.5	0.72	0.79	0.755	2	1.25	6.22
51.2	14.2	6.0	1.7	Opel R 3	0.15	0.44	1	0.9	0.95	2.16	1.21	3.99
52.4	14.6	6.0	1.7	Opel R 3	0.1	0.32	0.71	0.6	0.655			1.01
57	15.8	6.0	1.7	Opel R 3	0.117	0.38	0.68	0.75	0.715	1.78	1.07	4.53
36.3	10.1	6.0	1.7	VW Minitruck	0.09	0.19	0.53	0.68	0.605			4.8
37.9	10.5	6.0	1.7	VW Minitruck	0.06	0.2	0.61	0.65	0.63	1.66	1.03	5.51
47.9	13.3	6.0	1.7	VW Minitruck	0.04	0.16	0.57	0.89	0.73	1.91	1.18	7.23
49.3	13.7	6.0	1.7	VW Minitruck	0.07	0.17						8.72
Note:		= missing data where, in the instance of "Head Contact on Bonnet" the substitutions are averages, whilst for "Head Contact on ground" the substitutions are "Pelvis contact on ground"										

Table 2.2 Data from Kühnel's Experiments

2.14 Comparison to Vehicle-Pedestrian Accident Data

In 1994 the Road Accident Research Unit (RARU, now incorporated into the Centre for Automotive Safety Research, CASR) at Adelaide University, Australia, published a report on vehicle travel speeds and the relation to fatal pedestrian accidents (McLean et al, 1994]. Volume I of this work contains the analysis and findings of the study and Volume II contains the 176 case studies.

Of the 176 case studies, 102 were found to include an estimated impact speed and a measured or calculated pedestrian throw distance. The data obtained from this source can be seen in Appendix II. The results were plotted and compared to the predications indicated by the Projectile and Sliding Equation using a 50:50 ratio of airborne to sliding travel over the total throw distance and a 45 degree launch angle. The throw distance versus vehicle impact speed results from this data can be seen in Figure 2.13.

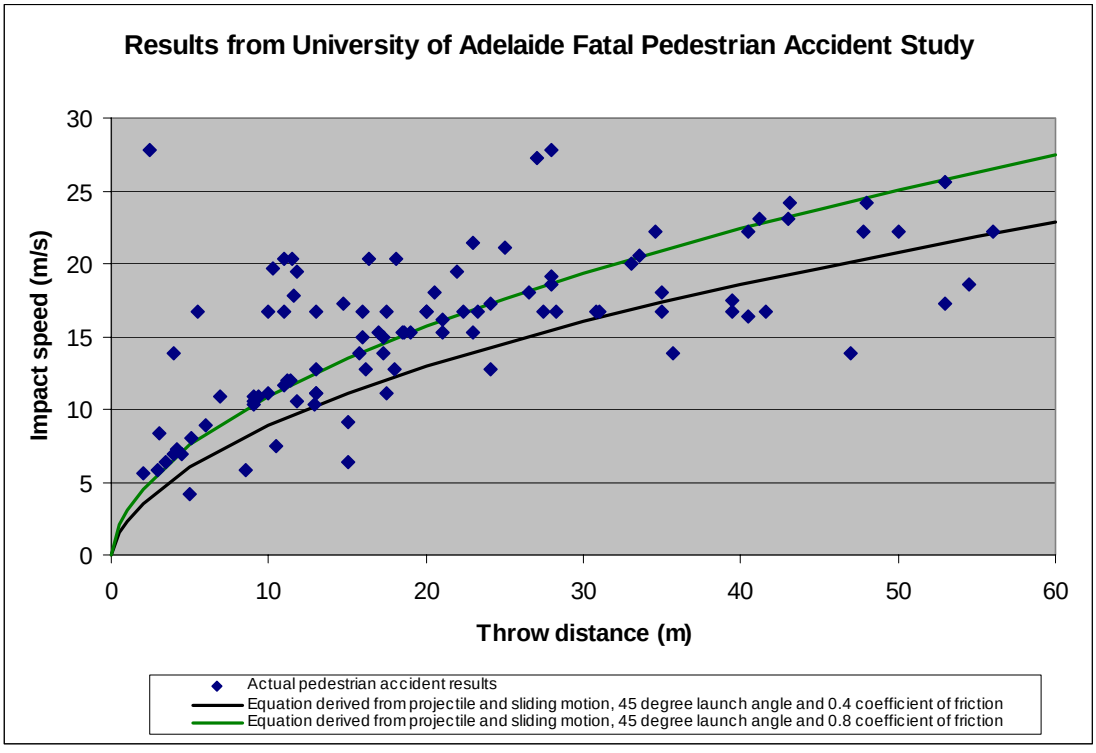

Figure 2.13 All results from University of Adelaide fatal pedestrian accident study

Some of the pedestrian throw distance data had been generated using Searle's 1983 equations for v_{min} and v_{max} and using an average value, except where there was an available estimate of travelling speed that existed between v_{min} and v_{max}, in which case that estimate was used. A coefficient of friction of 0.8 between the pedestrian and the ground was assumed for all cases, attributed to the paper by Warner (1983). Warner, however, refers to Collins work (Collins, 1979). Collins states that the coefficient of friction for a pedestrian knocked down by a car is about 1.1, with a coefficient of friction range of 0.8 to 1.2 being relevant to motorcyclists (presumably as motorcyclist leathers and helmets tend to grip the road less than the clothes worn by the average pedestrian). The use of a coefficient of friction of 0.8 does not appear to be consistent with the references given.

Data that incorporated impact speeds calculated using pedestrian projection distances is observed to agree with a line plotted using the Projectile and Sliding Equation with a 50:50 airborne:sliding ratio, a 45 degree launch angle and an 0.8 coefficient of friction. The samples based on projection-derived data were then removed from the analysis, leaving the data visible in Figure 2.14.

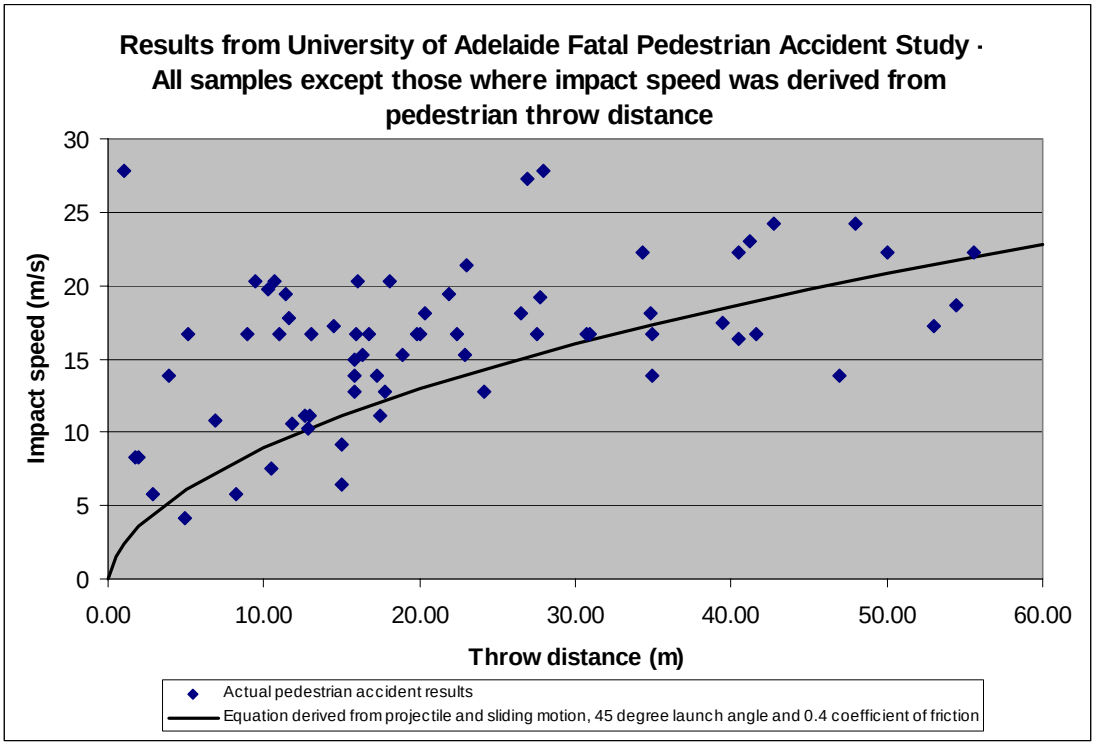

Figure 2.14 Results from University of Adelaide fatal pedestrian accident study except those where impact speed was derived from pedestrian throw distance

As can be seen a considerable degree of scatter is still visible and the following filters were applied to improve the quality of the data:

- Exclusion of accident data involving more than one pedestrian
- Inclusion of accident data based on impact speed from vehicle skid marks only
- Inclusion of accident data where vehicle deceleration was between 0.3 to 0.8g only.

The result of the above data filtering can be seen in Figure 2.15.

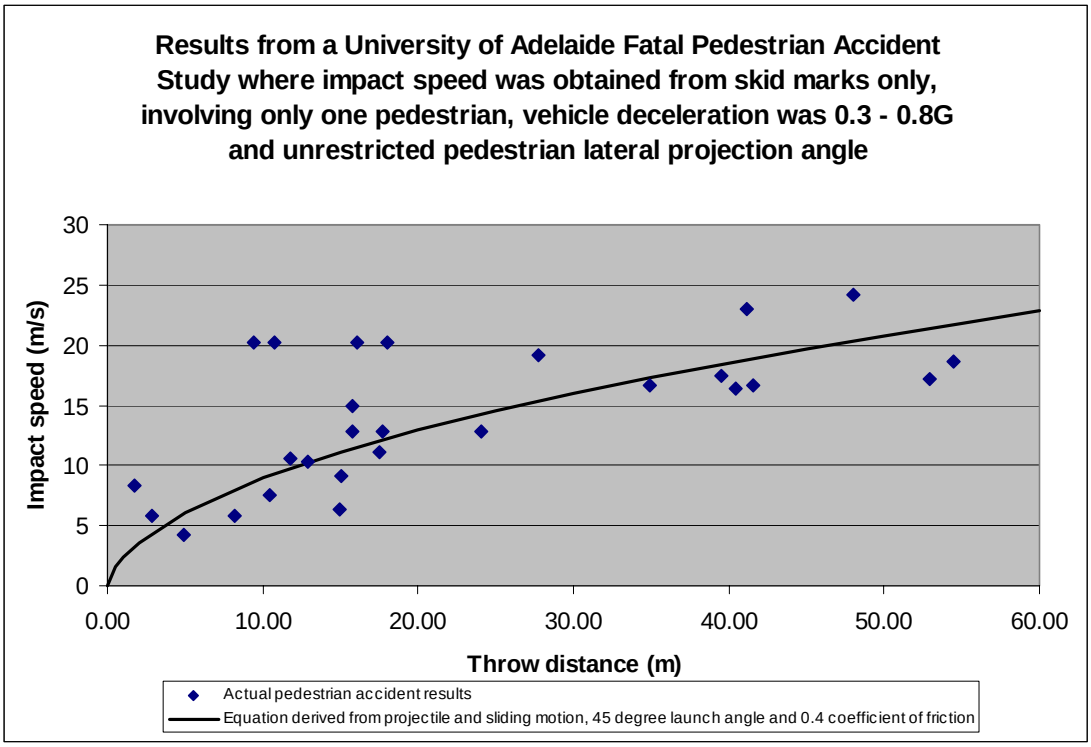

Figure 2.15 Results from University of Adelaide fatal pedestrian accident study where impact speed was obtained from skid marks only, involving only one pedestrian, vehicle deceleration was 0.3 - 0.8G and unrestricted pedestrian lateral projection angle.

The filtered data was observed to conform more closely to the prediction indicated by the Projectile and Sliding Equation with only a few diverse values evident. The non-conforming data was analysed and a relationship between lateral projection angle (i.e. the angle between the impacting vehicle's direction of travel and the pedestrian's post-impact departure angle, when viewed from above) was discovered. The results for filtering the data according to pedestrian lateral projection angle are shown in Figures 2.16 to 2.18.

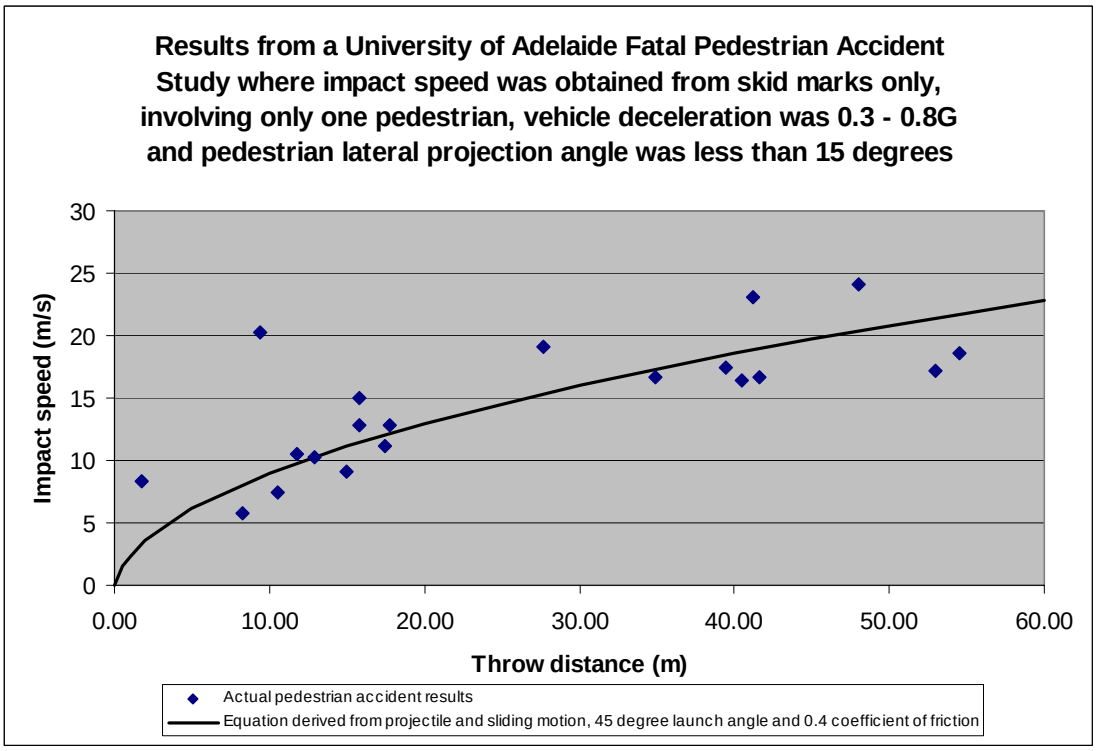

Figure 2.16 Results from University of Adelaide fatal pedestrian accident study where impact speed was obtained from skid marks only, involving only one pedestrian, vehicle deceleration was 0.3 - 0.8G and pedestrian lateral projection angle was less than 15 degrees

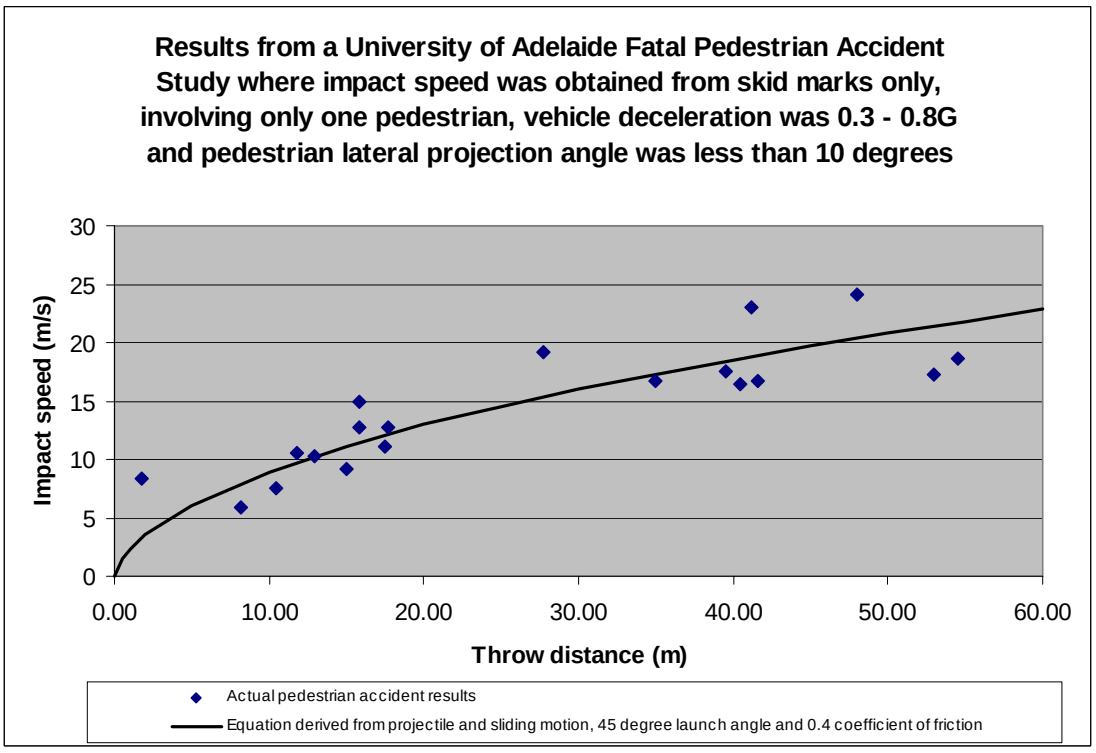

Figure 2.17 Results from University of Adelaide fatal pedestrian accident study where impact speed was obtained from skid marks only, involving only one pedestrian, vehicle deceleration was 0.3 - 0.8G and pedestrian lateral projection angle was less than 10 degrees

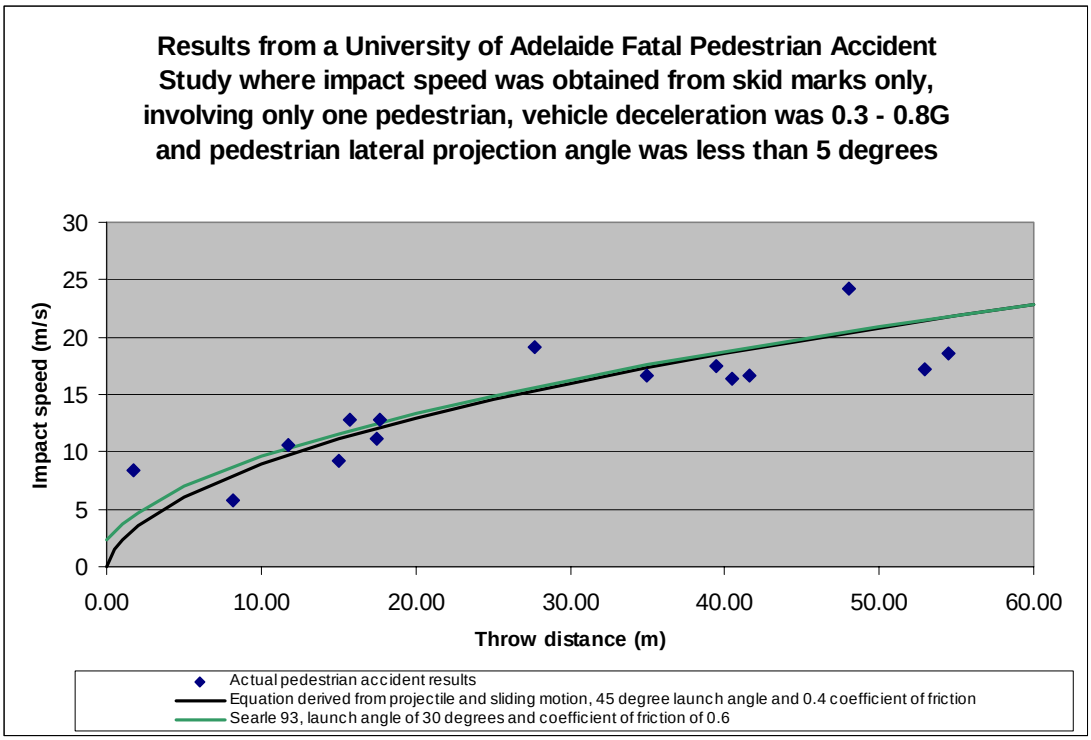

Figure 2.18 Results from University of Adelaide fatal pedestrian accident study where impact speed was obtained from skid marks only, involving only one pedestrian, vehicle deceleration was 0.3 - 0.8G and pedestrian lateral projection angle was less than 5 degrees.

In Figure 2.18 a comparison to Searle's 93 equation with a launch angle of 30 degrees and a coefficient of friction of 0.6 is also shown. It is interesting to note that the results of Searle's equation at 30 degrees and coefficient of friction of 0.6 produces similar results to the Projectile and Sliding Equation where a launch angle of 45 degrees and coefficient of friction of 0.4 was used. It is considered likely by the author that Searle's equation is more likely to be correct as a coefficient of friction of 0.4 is somewhat low for an average pedestrian-ground coefficient of friction. The author also considers the value of 0.8 used in RARU's study to be too high for an average value.

It would appear that pedestrian lateral projection angle post-impact has an affect on the impact speed predicted by throw distance. As noted by Kühnel (1974) the vehicle impact often resulted in the dummy rotating about its vertical axis. An impact that impacts rotation about a vertical axis is also likely to result in the impacted object being launched at an angle to the impacting object's original direction of travel. An analogy to this is the soccer ball that is struck off-centre.

Although much work has been conducted on the horizontal rotation imparted to pedestrians by being struck either above or below their centre of mass, there does not appear to be much work on studying pedestrian rotation about the vertical axis. Therefore, when conventional methods of calculating impact speed from pedestrian throw distance utilise the transfer of the vehicle's velocity to the pedestrian, most formulae only examine the expenditure of the linear momentum with some formulae also taking into account the angular momentum of the pedestrian about the horizontal axis. No traditional methods of vehicle-pedestrian impact analysis appear to take any account of angular momentum of the pedestrian about the vertical axis.

Further analysis of the data published by RARU (now CASR) and other vehicle-pedestrian accident studies needs to be conducted to determine the correct methodology to account for all linear and angular momentum components of the pedestrian's post-impact trajectory.

2.15 Potential Sources of Inaccuracy in Traditional Pedestrian Accident Reconstruction Calculations

In addition to the angular momentum considerations mentioned in the preceding section there are a number of factors that the author considers capable of inducing considerable inaccuracy when using traditional methods of vehicle-pedestrian reconstruction, including:

- Determining the correct coefficient of friction to use, namely:
    - Coefficient of friction for tumbling versus sliding
    - Coefficient of friction for different clothing types and accounting for the damage to clothing and/or pedestrian during the sliding phase affecting the coefficient of friction.
- Determining the ratio of airborne travel versus tumbling/sliding on the ground
- Determining the proportion of the total airborne velocity that is transferred into horizontal velocity, i.e. loss of kinetic energy due to impact, expended as damage to pedestrian and possibly ground.
- Proportion of energy that is transferred during impact to pedestrian kinetic energy versus the proportion that is expended in damage to both vehicle and pedestrian.

- Proportion of pedestrian's kinetic energy that is transferred to motion of the pedestrian's body (i.e. joint movement, fluid displacement, muscle tension) and cannot easily be accounted for.
- The effects of air drag on high-speed (over 11 ms^{-1}) pedestrian trajectories.

2.16 Further Comparison of the Different Equations Used in Traditional Vehicle-Pedestrian Accident Reconstruction

As noted in Section 2.12 the Projectile and Sliding Equation showed markedly different impact speeds for different launch angles when a coefficient of friction of 0.7 for the tumbling/sliding portion of travel was used, whereas Searle's equation (2.8.2 1993 version) was much less variable. This indicates that if the Projectile and Sliding Equation is used an accurate coefficient of friction is required which can be difficult to accurately and consistently determine (Wood and Simms, 2000). If Searle's equation is used then less importance is placed on the pedestrian-to-ground coefficient of friction. If the launch angle is unknown and the impacting vehicle tall and/or flat-fronted then Collins' equation (2.8.3) is a good candidate, as can be seen in Figure 2.19.

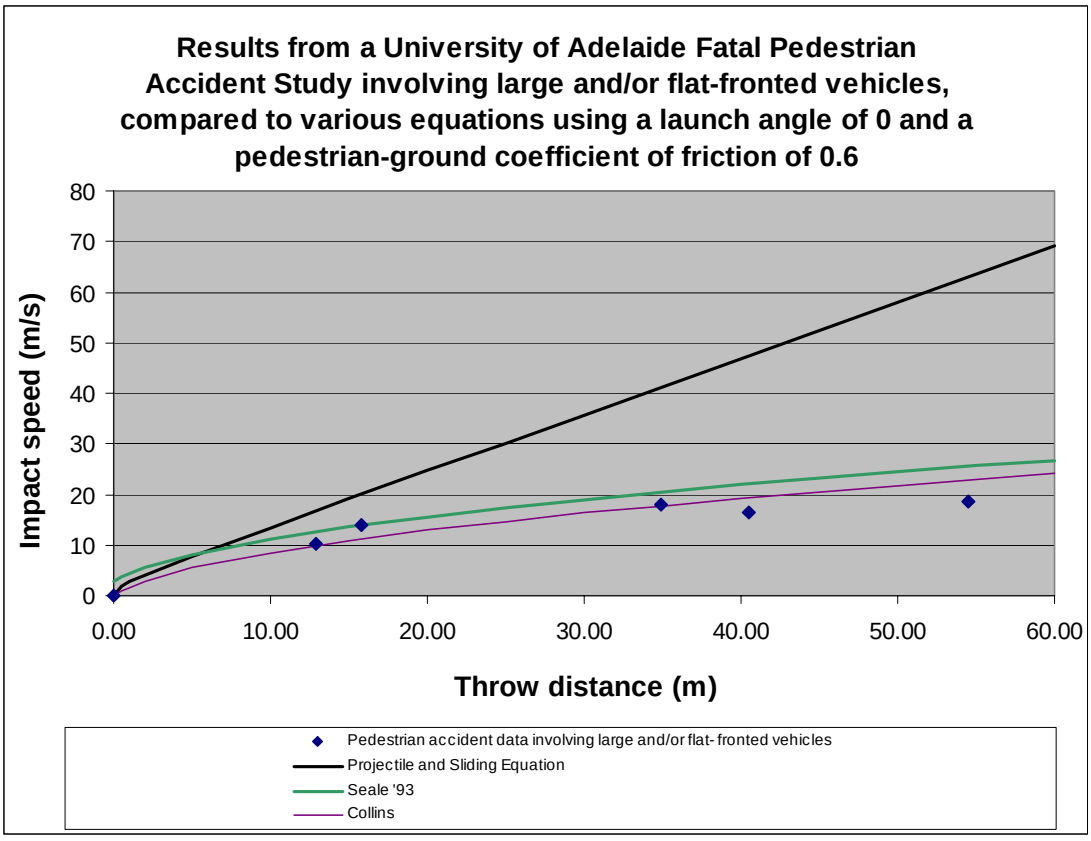

Figure 2.19 Results from University of Adelaide fatal pedestrian accident study where only impacts involving large and/or flat-fronted vehicles were considered, compared to various equations

For instances where there is considerable rotation of the pedestrian about their waist, such as can be the case in high speed collisions, Wood's SSM method (2.9) would appear to be the most appropriate as it is the only 'simple' equation to consider the pedestrian's radius of gyration.

2.17 Summary of Traditional Vehicle-Pedestrian Accident Reconstruction Methods

This chapter explored the traditional methods of vehicle-pedestrian accident reconstruction. The commonly used vehicle-pedestrian accident equations were compared to a simple projectile motion and particle slide-to-rest equation derived from the laws of physics.

A 2-dimensional method of analysing pedestrian throw post-impact was discussed.

The results of a study conducted in Germany using pedestrian dummies was analysed, as were the results of a study of actual vehicle-pedestrian accidents that occurred in Adelaide, Australia over an eight-year period.

The analysis of the German and Australian results revealed a number of deficiencies in traditional vehicle-pedestrian accident analysis.

The Projectile and Sliding equation (and Rich's 1997 equation) is based on an inelastic collision and assumes that the pedestrian attains the vehicle's velocity with no elastic or plastic deformation of either vehicle or pedestrian. Consequently, the vehicle's impact velocity is overestimated. In order to match the results of the Projectile and Sliding Equation to the test and accident data discussed in this section the following input modifications are required

- An increase in pedestrian launch angle input,
- A reduction of the airborne travel proportion, and/or
- A low pedestrian-ground coefficient of friction

Should the accident reconstruction stem from litigation, the Projectile and Sliding Equation is unsuitable due to its tendency to over-predict impact speed. In litigation conservative estimates are preferred.

The existing traditional vehicle-pedestrian accident analysis methods tend to more reliably predict vehicle impact speed from pedestrian throw than the Projectile and Sliding equation. In relation to the traditional equations the following should be noted:

- Searle's 1993 equation would appear to offer the most consistent results, especially if there is uncertainty in the pedestrian-ground coefficient of friction.
- Collins' equation is the most appropriate when large and/or flat-fronted vehicles are involved.
- Wood's SSM model is the only equation to consider the pedestrian's radius of gyration and would appear best suited to high-speed collisions resulting in considerable pedestrian rotation.

In the right circumstances traditional vehicle-pedestrian accident reconstruction methods appear to produce reasonably reliable results.

The next chapter will compare traditional vehicle-pedestrian accident analysis with the analysis afforded by computer simulation.

Chapter 3

Comparison of Computer Simulation and Traditional Methods for Prediction of Post-Impact Pedestrian Dynamics

3.1 Introduction

This chapter examines the history of computing and computer simulation and compares the computer-based mathematical simulation methods available to the traditional accident reconstruction methods discussed in the preceding chapter.

The dummy and human models available for the simulation analysis software program MADYMO are discussed and compared to models used in other mathematical models. A comparison is made between the throw distance versus impact speed relationship determined by the simulation program MADYMO and that predicted using a tradition vehicle-pedestrian accident reconstruction method.

The information in this chapter provides the necessary background information for the methods described in Chapters 4, 5 and 6.

3.2 A Brief History of Computers, Mathematical Modelling and Computer Simulation

3.2.1 Babbage's Analytical Engine

The concept of a computing machine is generally first attributed to Charles Babbage who produced a series of drawings between 1834 and 1857 describing the workings of an 'Analytical Engine' (Babbage, 1961). Babbage's machine was designed to perform calculations automatically and, unlike the automatic calculating machines of the time, could be programmed to execute sequences of instructions in different orders.

3.2.2 Analog Computers and Calculators

Analog computers first appeared in the 1920's as calculating machines designed for solving simultaneous equations (Cheng, 1987).

In the mid 1940's the Monte Carlo method was used in the Manhattan Project to assist in the analysis of neutron behaviour as it was determined that trial and error was too costly and time consuming whilst traditional mathematical analysis was too complicated (Hira, 1999). The calculations were performed using mechanical calculators operated by a large number of technicians, thus forming the basis of a distributed, hybrid computer.

3.2.3 Automotive and Aerospace Simulation

The first commercially available analog computer was built in 1948 under a US Navy contract (Piguet, 2000). Throughout the 1950's aerospace simulation, particularly missile ballistics, was a powerful driving force for the development of computer simulation with a large number of projects initiated between 1950 and 1956 by groups such as Boeing, Goodyear, English Electric, the Royal Aircraft Establishment and the US Air Force (Bissell, 2004). The need for more powerful computing machines saw the introduction of a number of new computers, both analogue (BEAC: Boeing Electronic Computer, LACE: Luton Analogue Computing Engine and TRIDAC: Three-Dimensional Analogue Computer, amongst others) and digital (UNIVAC: UNIVersal Automatic Computer). The UNIVAC was introduced in 1951 and was the first commercially available digital computer, complete with magnetic tape for data storage. Early UNIVAC customers included various US military departments, the US Census Bureau and a number of insurance companies. UNIVAC 1 weighed 13 tonnes and operated at 2.25 MHz and could perform 0.0019 MIPS (Millions of Instructions Per Second).

In the automotive arena engineers at Buick Motors developed automotive performance simulation models in the mid 1950's, initially using IBM CPC's (Card Programmed Calculators) before moving to IBM 650's and 705's (Louden, 1960). These computer models were used to optimise gearing to achieve acceptable compromises between performance and economy and to study the influence of automotive design variables (engine inertia, engine size, vehicle weight, tyre dimensions, rolling resistance - but not aerodynamic resistance, not yet). Similar work was also conducted at General Motor's Truck and Coach Division in the late 1950's and early 1960's (Noon, 1962)

In the mid 1960's NASA developed a means of discrete event mathematical modelling solved using computers. It was called NASTRAN (NAsa STRuctrual Analysis) and was the first widely used Finite Element Analysis (FEA) program. (NASA, 1996).

In the late 1960's analogue computing was still evolving but with the emphasis shifting to analogue emulators running on digital computers. In 1967 the Society for Modelling & Simulation International (SCS) published the definition of the Continuous System Simulation Language (CSSL), an analogue emulation code (Ören, 2002).

Despite the best intentions of computer manufacturers, computer users were generally limited to large corporations, government departments and well-funded academic institutions. This changed in 1977 with the introduction of the first mass produced personal computer, the Apple II. (only approximately 200 Apple I's were ever produced) (Grosse, 2004). The first IBM PC, the 5150 (earlier IBM computers were expensive and not produced in large quantities) was introduced in 1981 and heralded the beginning of the low-cost, mass-produced PC-compatible computing era. The IBM PC 5150 could perform 0.33 MIPS. In comparison, a modern, mid-range desktop computer can perform approximately 8000 MIPS (benchmark by author).

The widespread use of low-cost, high performance computers in society has created an information age where individuals can access, manipulate and analyse data with an effortlessness coveted by previous generations. This new-found ability to 'compute' has far-ranging implications and applications, not least of which is the ability to simulate reality.

3.3 The Development of Modern Automotive and Aerospace Simulation Methods

3.3.1 CRASH and SMAC: From the 1960's to Now

In the mid-1960's Raymond McHenry at the Cornell Aeronautical Laboratory was actively involved in automotive safety analysis, design and optimisation including analysis of occupant restraint systems (Cornell Aeronautical Laboratory filed a patent

for the seatbelt in 1951 (CALSPAN History, 2006)). In 1966 McHenry published a paper describing the validation of computer simulation of vehicle occupants and the effectiveness of different restraint systems (McHenry, 1966). The mathematical model developed in this research was an articulated multibody model with 10 degrees of freedom described using non-linear equations.

In 1967 McHenry and Norman DeLeys published the first of a series of papers on the simulation of single-vehicle accidents and vehicle dynamics modelling (McHenry, 1971). Meanwhile, at the University of California, Richard Emori (1968) published a paper on the mathematical modelling of either single or two-vehicle automobile collisions using vehicle masses, spring constants and the equations of motion. This is one of the first instances of vehicle crash analysis based on crush energy.

Further development of the models by McHenry, DeLeys and Emori lead to the creation of the SMAC (Simulation Model of Automobile Collisions) computer program (McHenry, 1973). By this stage the Cornell Aeronautical Laboratory had been spun off to form the corporate entity CALSPAN (Calspan History and Timeline, 2006). Funding for the SMAC computer program was provided by the National Highway Traffic Safety Authority (NHTSA), USA, indicating that the potential of computer simulation was well recognised over 30 years ago despite the relatively limited computing capabilities available at the time.

With computers being slow and expensive (by modern standards) development and execution costs for SMAC were relatively high with the software run on time-share mainframe computers. Each application run cost approximately US$25 (McHenry, 1997).

SMAC has been further developed by a number of companies (McHenry Software, Rectec, HVE by Engineering Dynamics and others) and is still in use today with a purchase price of between US$750 and US$10,000 depending on the degree of sophistication.

SMAC inputs include vehicle parameters (including but not limited to: mass, weight distribution, crush coefficients, suspension and tyre stiffness), driver inputs (steering,

brakes, acceleration) and environmental factors (coefficient of friction). Outputs include vehicle kinematics, tyre tracks and vehicle damage. An iterative approach is usually required when using SMAC; an initial guess is needed with respect to vehicle velocities and driver inputs. Modern versions can perform the iteration automatically but in the 1970's, when computing power was limited, a more basic automotive accident simulator, CRASH (Computer Reconstruction of Automobile Speeds on the Highway), was developed by McHenry to enable users to quickly evaluate a number of scenarios prior to using the SMAC program.

The CRASH program conducts a relatively simple trajectory analysis based on conservation of energy and linear and angular momentum. The user has the choice of a 'damage-only' option based on vehicle mass, deformation and principle direction of force (PDOF) and a 'trajectory' option which applies conservation of momentum using vector algebra. CRASH is based on the following assumptions and limitations (Smith, 1982; Nash, 1987):

- two-dimensional analysis only
- simplified vehicle characteristics
- simplified damage analysis
- simplified tyre-ground contact forces
- an instant of common velocity between impacting vehicles
- no driver input during post-impact trajectory
- subsequent impacts involving a previously damaged portion of a vehicle

The net effect of these assumptions and limitations varies considerably depending on the scenario analysed.

In comparison to CRASH, SMAC has a greater range of inputs and outputs and the original version was influenced by a generally more complex set of assumptions and limitations (McHenry, 1988 and 1997, Warner, 1978)

- two-dimensional analysis only
- sensitivity to integration time-step and rounding/truncation errors

- uniform linear crush stress rates do not adequately account for the vehicle structure and are incompatible with SMAC's implementation of coefficient of restitution
- poor fidelity in side-swipe and rigid-barrier collisions
- poor fidelity in vehicle side-slip motion due to calculation method of tyre-ground forces

Many of these assumptions and limitations have been corrected to some extent in subsequent versions of SMAC.

3.3.2 Multibody Analysis

McHenry (See preceding section on SMAC and CRASH) also developed a multibody model for the analysis of vehicle occupants in 1963 (Du Bois, 2004) Validation with crash test data was demonstrated for pelvis displacements, chest acceleration and restraint loadings. This work led to the development of MVMA2D (Motor Vehicle Manufacturers Association 2-Dimensional) computer simulation program. The multibody occupant model employed in MVMA2D consists of 10 segments and nine masses. The equations of motion for the linkages were derived using the explicit Langrangian technique (Prasad, 1984). Contact between the model and the vehicle interior was determined using ellipses attached to the body links. Joint stiffness was determined to be initially linear with non-linearly increasing stiffness as the limits of travel were approached.

Around 1970 CALSPAN (see section 3.3.1) developed the CAL occupant simulation model, based on the MVMA2D model (Cheng, 1987). Initially only 2-dimensional analysis was permitted, however in 1972 a 3-dimensional version was released (Prasad, 1984). Many different versions of CAL2D/3D and MVMA2D have been produced over the years and are generally referred to as CVS (Crash Victim Simulator) programs. The most current and common version CVS is the ATB (Articulated Total Body) Simulator. It is often incorporated into other software packages, such as HVE (Human Vehicle Environment) by Engineering Dynamics (Grimes, 1997) where it is used in conjunction with HVE's version of SMAC (see Section 3.3.1).

An overview of HVE's human model based on the ATB can be found in SAE 950659 (Day, 1995). Injury parameters include HIC (Head Injury Criterion), HSI (Head Severity Index), CSI (Chest Severity Index) and chest acceleration.

MADYMO (MAthematical DYnamic MOdelling) 2-D and 3-D: Both 2-dimensional and 3-dimensional versions of MADYMO were developed simultaneously by TNO (Organisatie voor **T**oegepast-**N**atuurwetenschappelijk **O**nderzoek or, in English: Organisation for Applied Scientific Research) Automotive in the Netherlands and first released in 1975. The coding for MADYMO-2D in the early 1980's (Version 3) consisted of about 1800 lines of Fortran, compared to 2200 lines of code for the 3D version (Prasad, 1984).

MADYMO multibody models consist of joint-connected bodies with the equations of motion derived using Lagrangian methods. Force models included those resulting from acceleration and contact between bodies and planes. The greatest advantage held by MADYMO over competing software was the flexibility allowed in the number of bodies permitted and the ability to use user-defined constraints and conditions (Cheng, 1987). See Section 3.4 for more information on MADYMO.

One of the first academic papers that referred to MADYMO was *Child Restraint Evaluation by Experimental and Mathematical Simulation*, SAE 791017 by Wismans, Maltha, Melvin and Stalnaker (Prasad, 1984). The authors found that the mathematical model provided better correlation with cadaver testing than the results obtained from dummy testing.

One of the first papers on the use of MADYMO for pedestrian accident reconstruction was published in 1983 by Wijk et al. 2-dimensional pedestrian models were created that consisted of either 2, 5 or 7 segments. A 3-dimensional model consisting of 15 segments was also used. The 2 and 5 segment models consisted of 5 bodies (head, thorax, pelvis, upper leg and lower leg) whilst the 7-segment model had two legs (i.e. head, thorax, pelvis and two each of upper leg and lower leg). The 15 segment model consisted of head, neck, upper thorax, abdomen, pelvis and two each of upper arm, lower arm, upper leg and lower leg. The vehicle bumper and bonnet were modelled using two hyper-ellipsoids. Accelerations of the knee, pelvis, chest and head were

measured during simulated vehicle impacts occurring at 30 and 40 km/h. The results obtained using the mathematical models were compared with experimental results from dummy testing. The 3-dimensional model was found to provide the most realistic results but required three times the computational time of the 7-segment 2-dimensional model. This time penalty was not insignificant given the limited computing power available to Wijk in the early 1980's.

Please see Section 4.2 for injury parameters in the current version of MADYMO.

Another multibody accident reconstruction program developed in the 1970's was KRASH (Lockheed-California Company). KRASH was developed in 1971 by the U.S. Army to model the impact dynamics and mechanics of airframes with support from the FAA coming in 1974 (Fleisher, 1994). It is in current use for aircraft crash analysis and uses a semi-empirical modelling method of lumped-masses, beam elements and non-linear springs (Fasanella, 2001) in order to effect fast computation on modest computational facilities. With the advent of high-performance, low-cost computing KRASH is now being superseded by programs using finite-element analysis.

3.3.3 Finite Element Analysis

Finite Element Analysis is a discrete event modelling method entailing the reduction of structures, bodies and/or fluids into discrete elements. The physical properties of these elements are governed by a relatively simple set of mathematical equations. Any state-change imposed on any given element from an external source (eg physical, gravitational or thermodynamic loading) can be easily calculated. Not only can the changes within the element be determined, but any influence on the surrounding environment including neighbouring elements and other bodies can be calculated by the application of interface properties. This method permits the analysis of complex problems by breaking the problem down into solvable pieces. (Graillet, 1999)

The solvers used in Finite Element Analysis can be either implicit or explicit. Implicit solvers use a forward difference algorithm with the assumption of constant average acceleration over the integration time step with accuracy determined by size of time step. Non-linear material properties can be used in static problems but not transient.

Explicit solvers typically use the central difference method. It is assumed displacements occur linearly and accelerations and velocities are calculated accordingly. Explicit solvers will tend to be unstable unless the time step is smaller than a value based on media stress wave velocity and smallest element dimension. Implicit solvers are quicker (by two orders of magnitude) but are not appropriate for all problems.

FEA Program	Developer	Implicit/ Explicit	Linear/ Nonlinear	Notes	References
ANSYS (**AN**alysis **SYS**tem)	Swanson Analysis Systems, 1970	Implicit	Both	In common usage, best for quasi-static problems	Chen, 2006
DYCAST (**DY**namic **C**rash **A**nalysis of **ST**ructures)	Grumman Aerospace, late 1970's, funded by NASA and FAA	Both	Nonlinear	In common usage. Quasi-static and dynamic simulations	Jackson, 2004
DYNA3D (**DYNA**mics in **3**-**D**imensions) / LS-DYNA	DYNA3D is public domain software developed at Lawrence Livermore National Laboratory by J. Hallquistin 1976.	Both	Nonlinear	LS-DYNA (commercial version by Livermore Software Technology Corp) in common usage, particularly for automotive crash testing.	Ray, 1996; Lin et a, 2000; Marzougui et al, 2000
MARC	David Hibbitt, Brown University, Rhode Island, USA. 1972	Both	Both	1st commercial non-linear FEA software. Bought by MSC Software in 1999.	MARC Datasheet, 2006
MADYMO (**MA**thematic **DY**namic **MO**dels) FEA	TNO Automotive, The Netherlands.	Both	Both	Combined multibody and FEA analysis.	MADYMO Theory Manual, Version 6.3
NASTRAN (**NA**sa **STR**uctural **AN**alysis System)	Created for aerospace research by the National Aeronautics and Space Administration in 1965	Both (depending on version)	Both (depending on version)	In common usage for structural, thermal and acoustic analysis. Commerical versions (such as MSC.NASTRAN) also available.	Kreja, 2005 Open Channel Foundation, 2006
NONSAP	Developed by K J Bathe at the University of California, 1973	?	Nonlinear	Has been superseded by ADINA (Bathe, 1997)	Bathe et al, 1974
RADIOSS	Developed by Mecalog.	Both	Nonlinear	Now licensed through Altair Engineering	Park et al, 1991

Table 3.1 Comparison of Finite Element Analysis Software

Finite element analysis advanced rapidly in the 1970's and 1980's. A comparative summary of some of the various Finite Element Software applications developed over this time can be seen in Table 3.1.

Finite element analysis requires a comprehensive understanding of the material properties being modelled. Whilst such knowledge is expected of automotive engineers it is unlikely that many accident reconstructionists have sufficient engineering knowledge to be able to obtain accurate results using finite element analysis.

3.4 Computer Simulation of the Human Body

3.4.1 Introduction

Whilst there is a great wealth of knowledge about the human body in regard to medicine and healing, there is a considerable lack of knowledge regarding the dynamics of the human body following an acceleration that has occurred as the result of an impact. Indeed, ethics dictate that this knowledge is unlikely to be advanced rapidly in the near future.

However, in order for pedestrian impacts to be accurately simulated the range of dynamic response and impact tolerance of the human body needs to be accounted for and reproduced.

3.4.2 Human Tolerances

The knowledge that exists about the dynamics and tolerances of the human body has been obtained both through research and serendipitous observation. McElhaney, Roberts & Hilyard produced an excellent text on the subject in 1976. This work was due to be updated in 2000 or shortly thereafter. However, due to changes in research ethics this update did not occur.

McElhaney et al's work is primarily a review and comparison of the data obtained by various researchers over the preceding decades with a large proportion of the work originating from the United States Air Force. The testing by the USAF usually used

live volunteers and as such the quality of the data is generally very good. A large proportion of the non-USAF research was conducted using primates and human cadavers. Because of the physical differences between humans and primates, as well as the lack of muscle tension and embalming effects present in cadavers the values obtained are best treated as indicative only. The values provided by McElhaney et al can be compared to those obtained by other researchers and in particular to the values used for the human computer model developed by TNO Automotive. TNO initially developed these models for vehicle occupant simulation for the purpose of virtual analysis of vehicle occupant safety.

3.4.3 Multibody Whole Body Human Models

Yang (2001) and Yang et al (2006) evaluated several whole-body mathematical human models in two mathematical human model reviews. As noted by Yang et al MADYMO has become the crash simulator of choice, taking the place of the previously popular CAL/CAL3D and MVMA2D (see Section 3.3.2). A three-dimensional pedestrian impact simulations conducted using CAL/CAL3D is detailed by Verma and Repa (1983). Acceleration outputs included upper and lower leg, pelvis, chest and head with peaks taken over a 3 millisecond interval. It would appear that the pedestrian model used by Verma and Repa was based on a modified occupant model consisting of 15 rigid bodies connected with 14 joints.

Ishikawa et al (1993) designed a multibody human pedestrian model for use with the Crash Victim Simulation (CVS) software (See Section 3.3.2). Their model, also consisting of 15 rigid bodies connected with 14 joints, was originally based on a Hybrid II dummy. Joint characteristics and segment stiffnesses were then modified according to the results of cadaver tests. Arm position was found to considerably influence head accelerations during validation. Leg and pelvis accelerations correlated well.

Huang et al (1994a) developed a MADYMO human model suitable for occupant injury evaluation in the event of vehicle side impact. This model was validated against sled and impact tests conducted using cadavers. It was found that the MADYMO

software at the time was too inflexible to allow both occupant and vehicle stiffnesses to be taken into account when using a multibody human model.

Between 1992 and 1997 Jikuang Yang, at Department of Injury Prevention, Chalmers University, Sweden, published a series of papers on the development of a mathematical pedestrian model for the simulation of vehicle-pedestrian impacts. Yang compiled the papers into a logical sequence to form the basis of a PhD thesis. The papers included Yang and Kajzer (1992), Yang and Kajzer (1995), Yang (1997), Yang et al (1997) and Yang and Lővsund (1997). Yang's first three papers focused on using multibody modelling of the lower extremities to predict impact loading and likelihood of injury resulting from a vehicle impact. Yang et al then developed a finite element lower extremity model in LS-DYNA to address some of the limitations inherent to multibody modelling. Yang's fifth paper discussed the extension of the model to include the rest of the human body. A multibody modelling approach was used with the physical characteristics based on a GEBOD-based (Baughman, 1983) 50^{th} percentile adult male. The model consisted of 15 ellipsoids connected using 14 joints. Mass distribution, moments of inertia and joint location were as defined by the GEBOD program. The breakable leg model from Yang's 1997 paper was also included. A series of simulations were run where bumper and hood height and stiffness, bumper lead distance and impact speed of a six-ellipsoid 'car' were varied and the resultant leg, thigh, pelvis, chest and head accelerations of the pedestrian model were measured. The impact simulations were validated by comparison with cadaver testing and lower extremity injuries were compared to those obtained using the models discussed in Yang's earlier papers.

Happee et al (1998) developed MADYMO multibody occupant models with facet surfaces that permitted more detailed environmental interaction than traditional multibody models described solely by (relatively) large ellipsoids. The impact response of the facet models was validated using human volunteer response corridors (the upper and lower limits of the results achieved from the testing of a number of subjects, usually taken to indicate the range of human response) generated from testing conducted in the 1960's and 1970's. The usefulness of the facet models, further refinement and the validation of a small female model by Happee et al (2000) warranted their inclusion in the standard MADYMO human model database as

described in Section 3.4.2. Lange et al (2005) provided objective biofidelity ratings for these models. They were found to offer good biofidelity in lateral impact and fair biofidelity in frontal impact.

Van Hoof et al (2003) describe the development of the TNO MADYMO multibody whole body pedestrian model from the work conducted by Happee and Wismans (1999). Five scaled versions of the model were produced, including a 3 year old child, a 6 year old child, a 5th percentile female, a 50th percentile male and a 95th percentile male. Validation was conducted using 18 cadaver-vehicle impact tests. Accuracy of head impact position was very good whilst acceleration pulse and timing were found to be between average and good, depending on the data set used for comparison.

3.4.4 Finite-Element Modelling of the Human Body

Huang et al (1994b), noting the issues that previous research (Huang et al, 1994a) had highlighted regarding the inappropriateness of multibody models in certain circumstances, developed a finite-element human occupant model for use in one of the CRASH (See Section 3.3.1) derivatives. Their model contained 9308 solid elements, 2384 shell elements and 514 two-node dashpot elements. It was designed to measure TTI, VC, Compression and ASA (Average Spine Acceleration). Huang et al found that the overall response of their finite-element model was no more accurate than the multibody model but noted that the finite-element model would be better suited in situations where the interaction with complex surfaces is of interest.

Lizee et al (1998) designed a 50th percentile male whole-body finite element human model for use in RADIOSS (See Table 3.1). Tests indicated good correlation was obtained when validating the model against cadaver tests. Substantial differences in response were identified between the human model and Hybrid III and Eurosid I models. This model contained 3638 solid elements, 6308 shell elements and 225 spring elements.

Howard et al (2000) created a series of human pedestrian models (6yr old child, 5th percentile female, 50th percentile male and 95th percentile male) for use in LS-DYNA (see Table 3.1). These models were validated against the cadaver testing conducted by Ishikawa et al (1993). Model trajectories and head velocities were found to correlate

well with the test results. Head and pelvis acceleration correlation was reasonable and some differences for chest acceleration were noted. It was noted that differences in arm contact may have accounted for the lack of correlation for chest acceleration.

Ruan et al (2003) also developed an LS-DYNA human model, namely a 50th percentile male finite element whole-body model. It was validated against individual cadaver tests instead of test corridors, as the authors considered the corridors too broad for meaningful validation. Ruan et al noted that validation against cadavers is less than ideal as muscle tone and circulatory systems are ignored. Their model consisted of approximately 119,000 elements.

Iwamoto et al (2002) developed a 50th percentile male occupant finite element whole body human model, designed to be used in PAM-CRASH and LS-DYNA. The base model had approximately 83,500 elements of which 30,000 were solids, 51,000 were shell/membrane and 2,500 were beam elements. More detailed sections of the head/face, shoulder and internal organs were also developed which took the element total to over 216,000, however the computational time required when using the more detailed model was found to be considerable. Cadaver test corridors were used for validation and injury prediction when reconstructing accidents was determined to be promising. Kimpara et al (2005), using the model developed by Iwamoto et al and a finite element thoracic model developed at Wayne State University, developed a new human model designed for the evaluation of thoracic injuries in 5th percentile female drivers. Reasonable model correlation with pendulum and ballistic impacts was obtained.

The MADYMO finite element human model was not available at the commencement of this research. The reader is recommended to refer to Robin (2001) for an overview of the HUMOS project and the origins of the MADYMO finite element human model. The current version of the MADYMO finite element human model is described in the MADYMO Human Models Manual Version 6.3. A summary of the models described in Sections 3.6.3 and 3.6.4 can be seen in Table 3.2.

Multibody Whole Body Human Models						Finite Element Whole Body Human Models				
Verma and Repa (1983)	Ishikawa et al (1993)	Huang et al (1994a)	Yang et al (1997)	Happee et al (1998)	Van Hoof et al (2003)	Huang et al (1994b)	Lizee et al (1998)	Howard et al (2000)	Iwamoto et al (2002)	Ruan et al (2003)
Pedestrian model with 15 rigid bodies, 14 joints	Pedestrian model with 15 rigid bodies, 14 joints	Pedestrian model, no. of bodies unknown	Pedestrian model with 15 rigid bodies, 14 joints	Occupant model with facet surfaces, 92 bodies	Pedestrian model consisting of 52 rigid bodies formed by 64 ellipsoids and two planes	Occupant model, 9308 solid elements, 2384 shell elements and 514 two-node dashpot elements	Occupant model, 3638 solid elements, 6308 shell elements and 225 spring elements	Pedestrian model, Unknown no. of elements	Occupant model, 216,000 elements maximum	Occupant model, 119,000 elements
CAL/CAL3D	CVS	MADYMO	MADYMO	MADYMO	MADYMO	CRASH	RADIOSS	LS-DYNA	PAM-CRASH and LS-DYNA	LS-DYNA
6 year old, 50^{th} percentile male	scaleable	50^{th} percentile male	50^{th} percentile male	3 yr old, 5^{th} percentile female, 50^{th} percentile male and 95^{th} percentile male	3 yr old, 6 year old, 5^{th} percentile female, 50^{th} percentile male and 95^{th} percentile male	50^{th} percentile male	50^{th} percentile male	Children from 3 – 15 years, 5^{th} to 95^{th} percentile adults	50^{th} percentile male	50^{th} percentile male

Table 3.2 Comparison of Whole Body Human Mathematical Models

3.4.5 Evaluation of the Whole Human Body Models in Terms of Suitability for this Project

As can be seen in Table 3.2, the two most popular methods of mathematically modelling the human body typically utilize either a multibody model or a predominantly finite-element model (note some 'Finite element' models, including the MADYMO finite element occupant model, do utilize multibody components to represent soft-tissue resistance around joints but are otherwise predominantly composed of finite element structures). It can also be seen that more recent models typically have higher levels of refinement and greater complexity.

At the start of this project (in 2000) finite-element human models were predominantly occupant models with little to recommend them over multibody models (Huang et al, 1994b). At the time there appeared to be no favoured choice in software for the finite element modelling of the human body (CRASH, RADIOSS, LS-DYNA). In comparison, from 1994 onwards, MADYMO appeared to be the clear choice of users of multibody software. The more modest computational requirements of multibody analysis in comparison to finite element analysis was also noted. A decision was therefore made to use MADYMO and the Van Hoof multibody pedestrian models, which were themselves a development of the models created by Happee and Wismans (1999).

3.5 Finite Element and Multibody Simulation Using MADYMO Version 6

3.5.1 Introduction to MADYMO

With increasing computing power becoming available at decreasing cost, mathematical modelling of vehicle and vehicle-pedestrian impacts is becoming increasingly practical and affordable. The use of commercial modelling software permits users to simulate numerous scenarios at a fraction of the cost and time associated with experimental testing.

There are two techniques commonly used to model human bodies mathematically in the field of crash analysis, namely multibody systems (MBS) and finite element analysis (FEA). The software program MADYMO (MAthematical DYnamic Modelling) (TNO Automotive) is a mathematical solver commonly used in the automotive and crash-safety sectors. It supports the use of both MBS and FEA.

The kinematics, accelerations and contact forces of a dynamic system can be quickly determined using an MBS model. However, given that MBS are constructed out of fairly simple geometric shapes and surfaces (ellipsoids, cylinders, planes etc) connected by a range of joint types then there are limitations as to how accurately they can be used to model many situations. For example, whilst MBS modelling may quite accurately describe the motion of a leg following an impact by a car bumper, any resultant soft-tissue damage is poorly quantified. Areas where deformation, damage or injury is of interest therefore need to be modelled using MADYMO's FEA capability. Combining FEA models of areas of interest with multibody systems results in efficient computation.

3.5.2 Multibody Analysis in MADYMO

The simplest MBS is, in fact, a single body system. It would consist of a single body in a single system. If the body was connected to another body with a kinematic joint, then there would be two bodies within one system. If there was no joint, however, then there would be two systems, each containing one body. Bodies may be joined to one another within the same system so that they may form tree structures or closed chains. Closed chains are reduced to tree structures with the removal of one kinematic joint and the subsequent insertion of a closing joint.

Simple bodies can be modelled using predefined objects such as ellipsoids, cylinders and planes. More complicated bodies can be modelled using facets: a mesh of 2-D mass-less elements.

Multibody human and dummy models available in MADYMO fall into two categories: ellipsoid and facet.

Ellipsoid models are the simpler of the two and are highly computationally efficient. A human body may be modelled via an ellipsoid model using a tree structure consisting of a parent body (for example, the torso) with a number of attached child bodies. For a very simplified model this may consist of only five child bodies organized into five branches – the head, two arms and two legs. The pedestrian model used in this study had a total of 52 bodies organized in seven branches (See MADYMO Version 6.0 Human Models Manual). The MADYMO ellipsoid model was originally designed for vehicle occupant analysis but is now primarily a pedestrian model.

Facet models allow for greater biofidelity. A typical human facet model in MADYMO has 92 bodies. The facet model is skinned with 2000 triangular elements. Internal structures include neck, spine, pelvis and shoulders. The MADYMO facet model was designed primarily for occupant analysis.

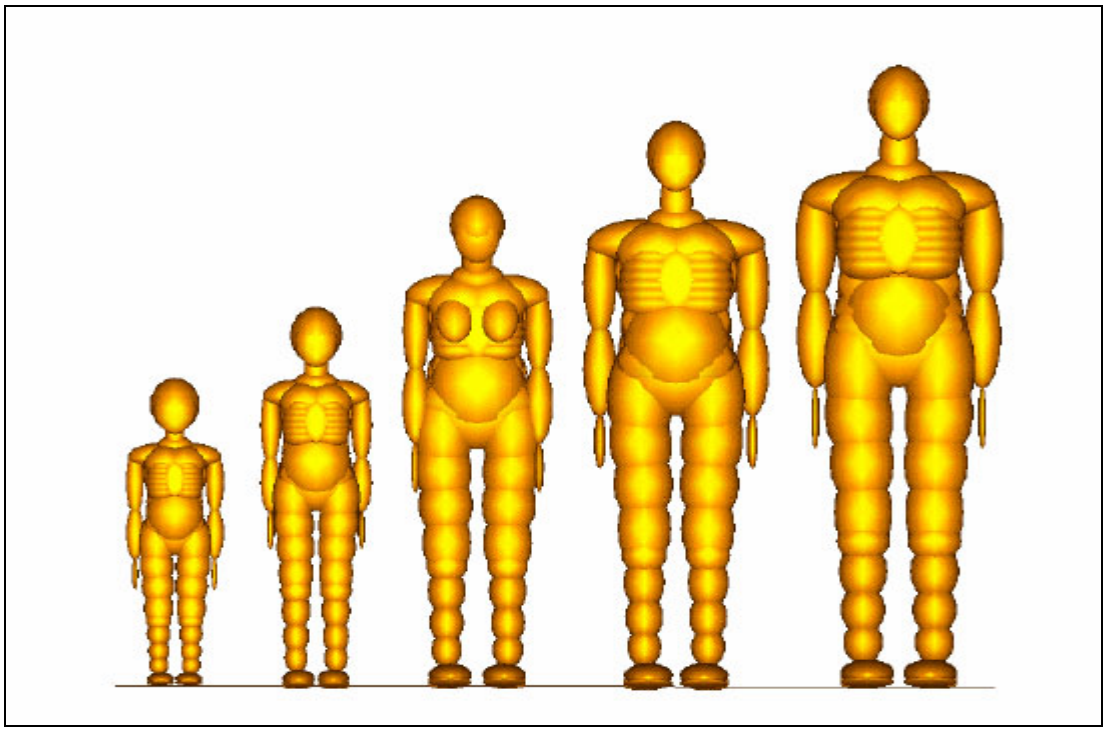

Figure 3.1 Multibody Pedestrian Models: From Left to Right - 3-yr old Child, 6-yr old Child, 5th Percentile Female, 50th Percentile Male and the 95th Percentile Male (Source: MADYMO Human Models Manual Version 6.3, TNO Automotive)

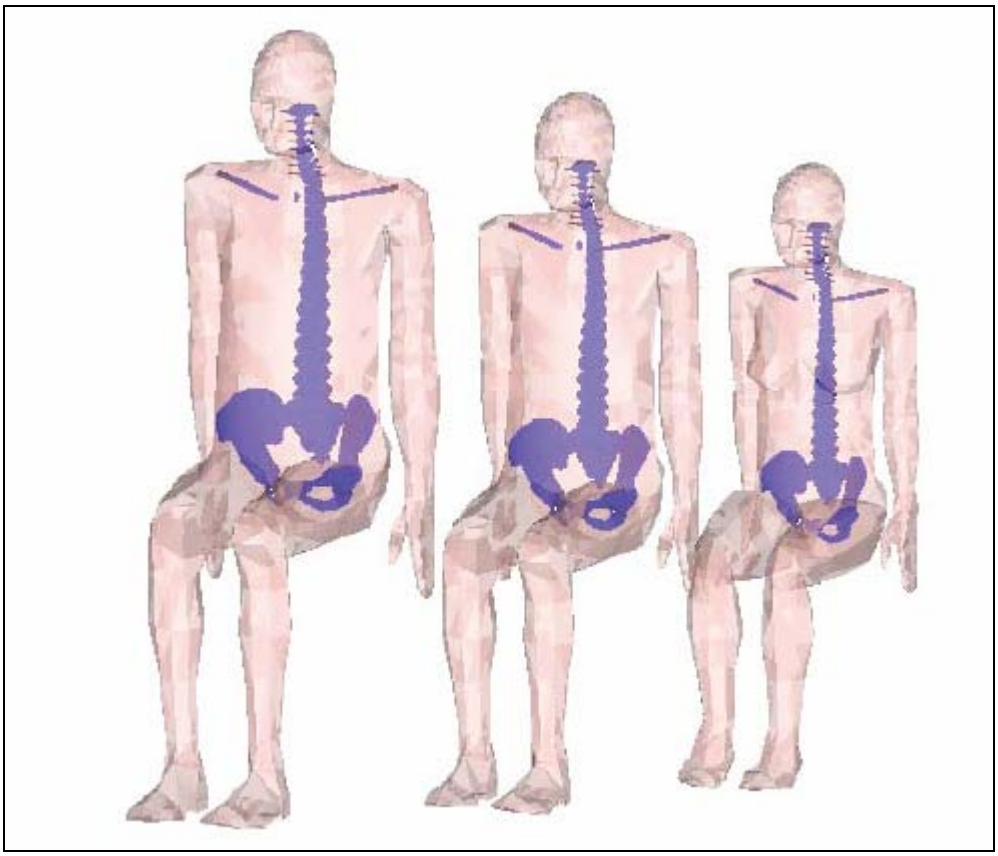

Figure 3.2 Facet Occupant Models: From Left to Right - 95th Percentile Male, 50th Percentile Male and 5th Percentile Female (Source: MADYMO Human Models Manual Version 6.3, TNO Automotive)

3.5.3 Finite Element Analysis in MADYMO

In contrast to multibody models, FEA methods use a mesh of inter-connected nodes allowing accurate geometric representation. FEA models may include well defined and context dependant material properties, as well as allowing the inclusion of complex contact and interaction expressions.

As discussed in section 3.3.3 FEA analysis in MADYMO can be conducted using either explicit Runge-Kutta or implicit/explicit Euler integration. MADYMO uses Langrangian description i.e. nodes and elements are fixed to the material and displace with the material.

Human and dummy finite element models in MADYMO are actually multibody/FEA hybrid models. A rigid body chain, the same as used in the multibody models, is used to allow consistent positioning of the FEA and multibody models. Inertial properties

of the model are determined using a combination of the inertial properties of the underlying rigid bodies and the FEA elements.

The MADYMO FEA human and dummy models provide a higher degree of biofidelity than the purely multibody models due to the ability to accurately reproduce deformation and damage of body components. The trade-off is a considerable penalty in computation time in comparison with the much simpler multibody models.

3.5.4 Combined Multibody/FEA Simulation in MADYMO

One of the most popular features of MADYMO is the ability to mix and match multibody and finite element analysis. As mentioned previously, the MADYMO FEA human model is actually a multibody/FEA hybrid.

Because of the significant computational requirements associated with FEA analysis it is recommended that as much as possible of the system under investigation is modelled using multibody representations. Conducting entirely multibody simulations in order to determine the best approach for subsequent FEA analysis is recommended.

3.5.5 Limitations of MADYMO

Aside from the general limitations applicable to any form of mathematical modelling (see Section 3.5.2) there are some limitations of MADYMO worthy of note.

Versions of MADYMO prior to Version 6 (this research project used Version 5.4 for the majority of the simulation conducted, prior to the introduction of Version 6) contained issues regarding FEA analysis including poor contact calculation and long computational time.

Other researchers appear to have had similar difficulties with pre-Version 6 MADYMO FEA implementation. Troutbeck et al (2001) noted the following:

> *"In summary, the use of the finite element capabilities of MADYMO was of limited practical application. This was due to the limited material types included within MADYMO, excessive computation times, and a lack of physical testing data with which to compare the output of the simulations."*

Indeed, many of the problems Troutbeck et al experienced, such as non-SI mass units and unlocateable 'noise' in some parts of FEA models were also encountered by this author. Despite the issues they encountered, Troutbeck et al concluded that "*MADYMO is extremely well suited to the assessment of human injury risk*", an assessment that this author agrees with.

With MADYMO Version 6 now in widespread use it is apparent that many of the issues regarding MADYMO's implementation of finite element analysis have been addressed. Nonetheless, very long computation times are still required for models with a large number of FEA elements and this remains as a large limitation to MADYMO's usefulness. MADYMO's usefulness is also reduced by the time required to gain familiarity with the software but this is by no means unique to MADYMO when compared with other FEA and accident reconstruction software packages.

3.6 Computer Simulation as an Accident Reconstruction Tool

3.6.1 Modern Computer Simulation in Accident Reconstruction

Computer simulation has now been used for a number of years to simulate vehicle behaviour. It is highly suitable for a number of applications including situations where it is not feasible to conduct testing or reconstruction using exemplar vehicles[2]; where a large number of potential scenarios need to be evaluated quickly and effectively; where there are multiple vehicles and/or impacts; where exact vehicle and/or environment features need to be replicated; or safety issues limit the possibility of on-site reconstruction. Furthermore, modern tools such as three-dimensional laser scanners can accurately measure accident sites without the need for the road to be closed or even for the equipment operators to set foot on the road being measured (Forman and Parry, 2001; Parry and Marsh, 2003).

[2] A prime example of this is the computer simulations conducted by NASA following the loss of a space shuttle in flight. It was not feasible to reconstruct the conditions that resulted in the failure of the shuttle and so computer simulation was used (Livesay, 2005).

Criticism of the use of computer simulation as an accident reconstruction tool often focuses on the myriad of inputs required by modern simulation suites and the inability of the average layperson to recognise the meaning of many of the variables. This has resulted in situations where the computer simulation has been manipulated to obtain certain, and not necessarily defensible, results in the belief that the methodology cannot be cross-checked. It is therefore prudent to clearly state all assumptions made, all variables and error tolerances used and the calculation methods employed when the results of a computer simulation are presented. The results should also be verified using traditional accident reconstruction techniques.

It should be noted that the virtual vehicle testing employed by the vehicle manufacturers prior to the mandatory crash test program provides highly accurate and physically reproducible results. Aside from monetary savings in reducing the amount of in-house crash-testing required it also provides rapid vehicle structure optimization for crash-worthiness. The vehicle models developed by the manufactures for the virtual crash testing are also ideally suited to accident reconstruction.

3.6.2 General Limitations of Computer Simulation

Any type of analysis conducted using mathematical modelling is subject to inaccuracy. These inaccuracies can stem from two types of error:

i. modelling errors, arising from the imperfect translation of reality into a set a mathematical equations.
ii. numerical errors, which arise from the need to break a linear time continuum into a series of discrete segments and the requirement that the models are broken up into manageable pieces or elements. This is particularly relevant to finite element analysis (Brands, 2002).

To address modelling errors it is necessary that (a) the physical, thermal and other material properties are fully investigated with any reproduction of such properties appropriately validated, (b) the implementation of the properties determined is consistent with the manner in which they were measured and the environment being modelled.

Any properties that are incompletely understood are unlikely to be successfully accurately modelled. With the complexity and lack of understanding surrounding

much of the human body there is a correspondingly high degree of uncertainty in modelling the human body. As the understanding of the human body increases through research the uncertainty in modelling is reduced as discussed in Section 3.4.

Numerical errors have been systematically reduced over the past decades by improved modelling techniques and increased computational power. Often it is necessary to reach a compromise between accuracy and computational cost. With Moore's Law (the hypothesis that the complexity of integrated circuits doubles every 24 months, attributed to Gordon E. Moore, founder of Intel) approaching an end (difficulties resulting from power and heat dissipation, combined with integrated circuit physical limitations) the hope of unlimited computational power in the future is now apparent to be an unfulfillable dream. Therefore computational models and numerical methods need to focus on efficiency without compromising accuracy.

Despite the inaccuracy inherent in mathematical modelling it is important to realize that often the inaccuracy is too small to significantly affect the results of the simulation. Indeed, this is being recognized by agencies responsible for transport safety. One example is the advisory circular released in 2003 by the USA Federal Aviation Authority stating the conditions in which mathematical modelling in lieu of testing is now acceptable for the purpose of seat certification (FAA Advisory Circular: 20-146, 2003). Both LS-DYNA and MADYMO were defined as acceptable modelling programs.

3.7 Application to a Typical Pedestrian Accident Reconstruction Involving a 'Forward Projection Trajectory' and Results Comparison with MADYMO

Of considerable interest are MADYMO's capabilities to predict pedestrian kinematics post-impact. In this section MADYMO's throw distance prediction is compared with that offered by several traditional vehicle-pedestrian accident reconstruction equations following a vehicle-pedestrian collision involving an SUV-type vehicle. Additionally, the airborne travel proportion of pedestrian throw and the pedestrian's launch velocity are examined.

3.7.1 Case Study Background

An investigation involving an adult female pedestrian and a slow-moving large SUV was simulated (Stevenson and Raine, 2003). It had been requested to confirm whether a pedestrian impacted by such a vehicle travelling at low speed could have been killed or was it more likely that the vehicle was travelling faster than suspected. An injury analysis will be presented in Chapter 5.

3.7.2 Methodology and Parameters

For simulating the collision, TNO's MADYMO was used as the solver, with HyperMesh from Altair as the pre-and-post processor. The simulation was based upon data obtained from the accident, with vehicle speed and pedestrian placement both before and after the collision well documented and agreed-upon. For the vehicle model, the public domain FEA model of a Ford Explorer (Figure 3.3) was used. This model was developed by Oak Ridge National Laboratory and is available in LS-DYNA 3D format at **http://www-explorer.ornl.gov/flash.html**

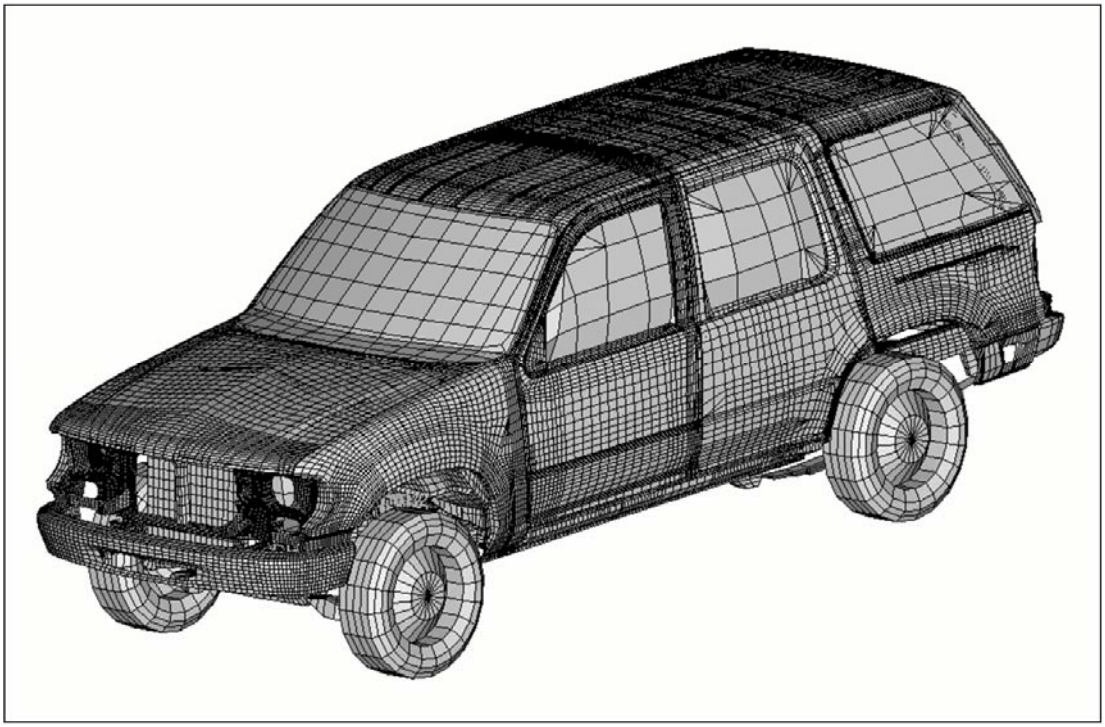

Figure 3.3 Public Domain Ford Explorer FEA Model. (Source: Oak Ridge National Laboratory)

As the complete model consists of over 136,000 elements, only the inner and outer skins of the bonnet (or hood) and front bumper were used, with these attached with rigid links to a mass equal to that of a complete vehicle. A front towing hook was

added to the vehicle model to permit any possible interaction between this hook and the pedestrian to be evaluated.

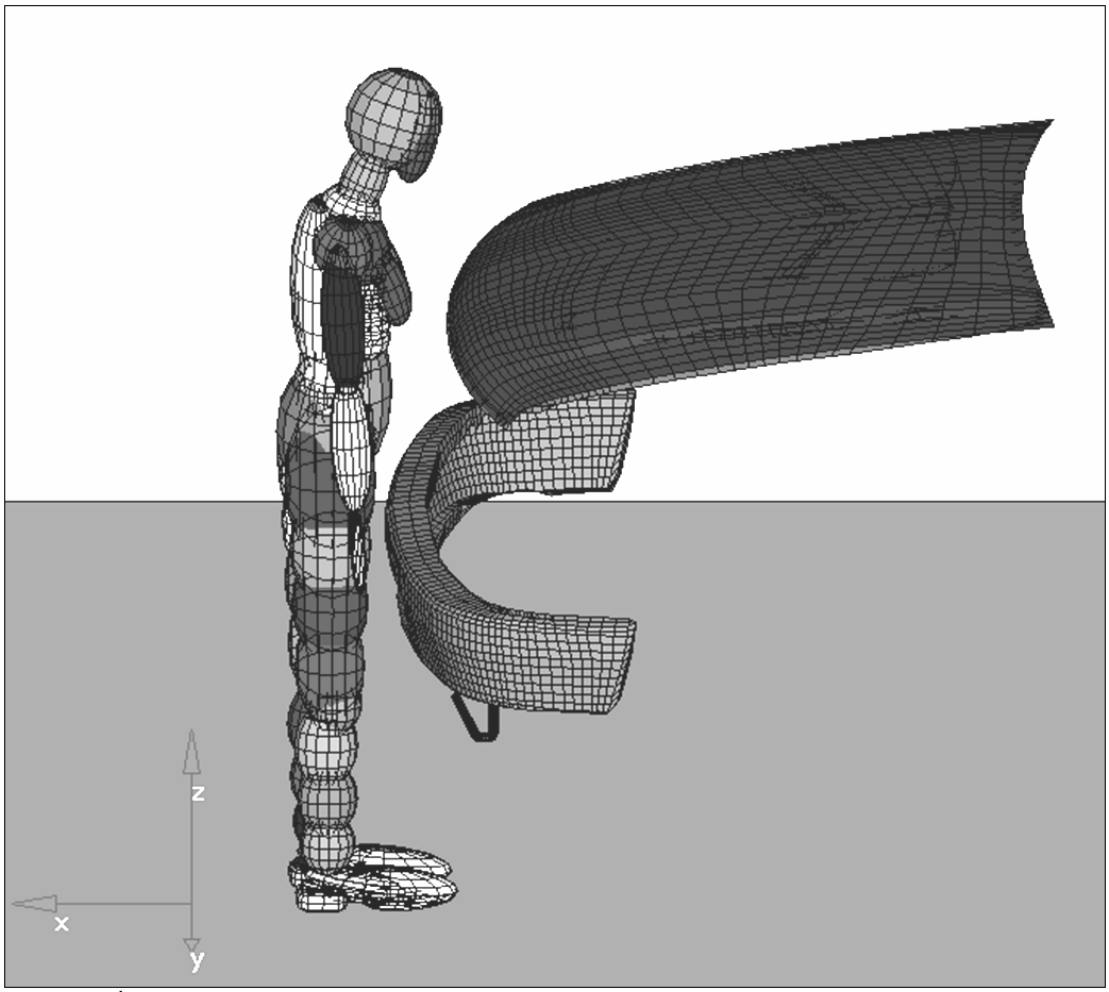

Figure 3.4. 5th Percentile Female Pedestrian Model in Front of Reduced Explorer Model. (Source: TNO Automotive)

The pedestrian model used was based on that developed for TNO Automotive by Hoof et al (2003). It is representative of a 5th percentile female. The multibody model consists of 52 rigid bodies and has been extensively validated. The multibody pedestrian model and reduced Explorer model can be seen in Figure 3.4. The pedestrian model was placed on a flat plane, representative of a road surface, and was subjected to a gravitational force of 9.81 ms^{-2}.

The contact model used for the multibody-finite element interaction was MADYMO's elastic contact model utilising a force-penetration characteristic which used the stiffness characteristics of the pedestrian. For the multibody-multibody interaction

(i.e. pedestrian versus ground) the elastic contact model utilising a force-penetration characteristic was also used, again using the stiffness characteristics of the pedestrian.

Other simulation parameters can be seen in Table 3.3. A discussion of the literature values and ranges referred to can be found in Chapter 6.

Parameter	Range	Comment
Coefficient of friction between vehicle and pedestrian	0.45	Within range of values reported in literature
Coefficient of friction between pedestrian and ground	0.55 for pedestrian on ground, 0.7 for shoe contact on ground	Value indicated to be within literature values and those determined by author
Vehicle speed at impact	2.8 to 4.8 ms^{-1}, evaluated in 0.2 ms^{-1} increments	Range determined from witness statements
Vehicle acceleration	-7.0 to 3.0 ms^{-2}, evaluated in 1 ms^{-2}	Upper and lower maximum possible values by vehicle
Stiffness of vehicle bumper	250 Nmm^{-1}	As per literature.
Stiffness of vehicle bonnet edge	1400 Nmm^{-1}	As per literature.
Stiffness of vehicle bonnet top	300 Nmm^{-1}	As per literature.
Pedestrian head stiffness	2500 Nmm^{-1}	As per literature for anterior-posterior loading.
Stiffness of road	40 $kNmm^{-1}$	Middle of range specified by Chadbourn et al (1997)

Table 3.3 Parameters for Simulation of Collision Involving an SUV-TypeVehicle

3.7.3 Simulation Results

Figure 3.5 shows the simulated pedestrian throw distances plotted against vehicle impact speed. For comparison the predictions offered by Searle's 1993 equation, the Collins equation and the Projectile and Sliding equation described in Chapter 2 are

also shown. An airborne travel proportion of 0.75 was used in the Projectile and Sliding equation and a coefficient of friction between the pedestrian and ground of 0.55 (the same as in the simulations) was used in all the equations.

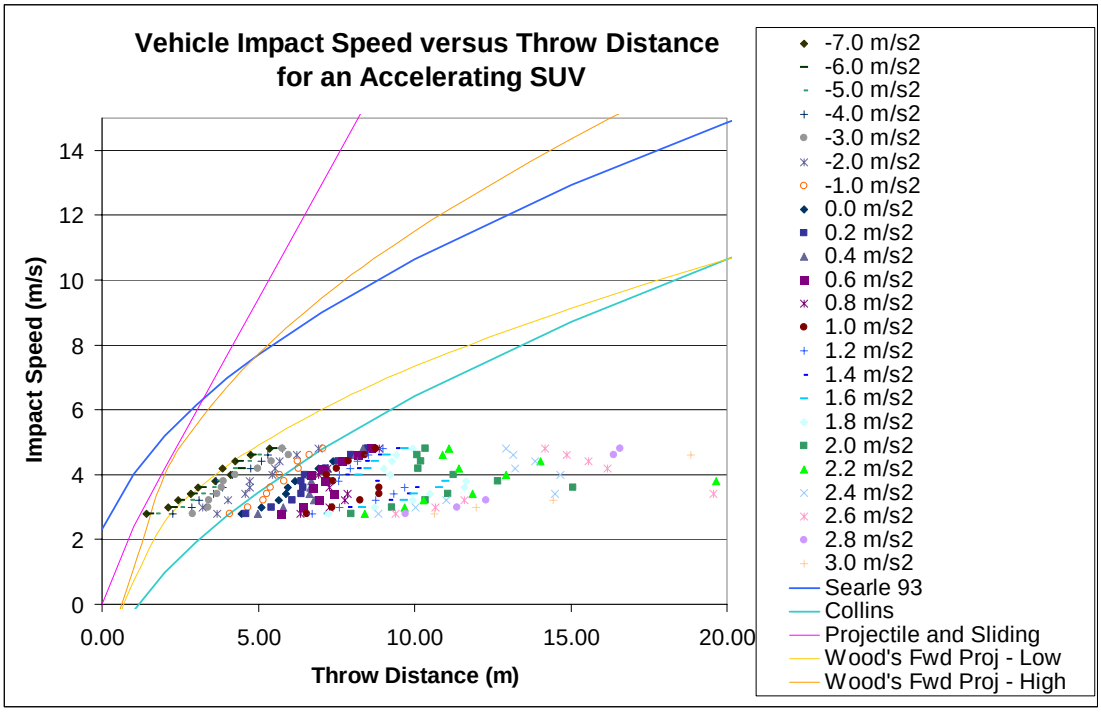

Figure 3.5 Vehicle Impact Speed versus Throw Distance for an SUV-Type Vehicle

As can be seen, Collins' equation appears to offer the most consistent prediction for an unknown level of either positive or negative acceleration and a reasonably accurate prediction for when the vehicle was decelerating at -1.0 ms^{-2}. This result is unsurprising as Collins' equation is predicted to offer the best accuracy for forward-projection trajectories resulting from tall and/or flat-fronted vehicles. Fugger et al (2002) in their paper on pedestrian throw kinematics in forward projection collisions found that two empirically-derived equations from Wood for forward projection best matched their test data.

$$V_{low} = 8.77 \times \sqrt{d} \qquad V_{high} = 13.76 \times \sqrt{d}$$

However, the author of this thesis found Wood's V_{low} equation to offer a reasonable prediction for vehicles undergoing maximum braking which may well be a reasonable assumption in many cases but definitely not all. The V_{high} only offered a reasonable prediction for heavily braking vehicles travelling at a initially low speed. Fugger et

al's testing utilized a 50th percentile male dummy facing away from the vehicle and a forward-engined van with a noticeable bonnet. No vehicle braking was conducted. It is suspected that such a test configuration may not have resulted in a true forward-projection trajectory as some potential, based on vehicle shape and pedestrian orientation relative to the vehicle, appeared to exist for the pedestrian to wrap around the vehicle front. An 18 kg breaking strain wire was used to support the dummy and this attachment may have also impeded the dummy's motion (hence reducing throw distance for a given vehicle velocity). Tests by other authors (eg Kühnel, 1974) usually ensure any attachment wire is released shortly before impact.

Happer et al (2000) initially state that there is a reduced correlation between unbraked vehicles and pedestrian throw distance. They then go on to state that: "*Review of the provided literature confirms that there is no relationship between unbraked vehicle impact speeds and pedestrian throw distance.*"

This reduced (or non-existent) correlation can be seen in the simulation results where a considerable degree of scatter is evident, much as real-life accident data and dummy test data tends to scatter (see graphs 2.10 and 2.14). Of particular note is the variation evident in the data resulting from simulations where a rate of vehicle acceleration greater than 0.8 ms^{-2} was applied. In many instances the combination of a particular initial vehicle speed and acceleration resulted in considerably longer throw distances than a higher initial vehicle speed and same acceleration level. In these instances it would appear that the pedestrian is 'caught' by the vehicle as it accelerates in a pseudo-wrap trajectory, before falling to the ground. Other authors (Happer et al, 2000) note that this can occur to some extent with a vehicle that is not braking. By extension, an accelerating vehicle appears to have a greater tendency to retain the pedestrian for longer. At higher initial impact speeds, regardless of acceleration level, a more traditional forward-projection trajectory results with reduced vehicle-pedestrian interaction duration and a shorter pedestrian throw distance.

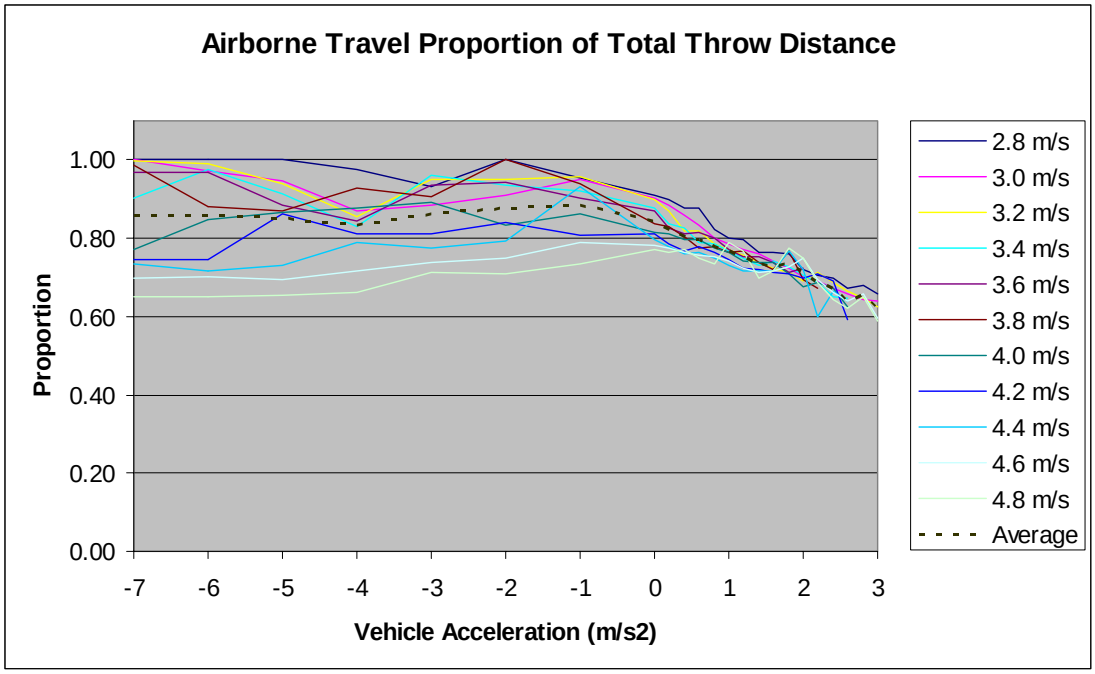

Figure 3.6 Pedestrian Airborne Travel Proportion of Total Throw Distance for SUV-Type Vehicle

Figure 3.6 shows the proportion of total pedestrian travel post-impact that is airborne. When the vehicle is braking heavily often the entire pedestrian travel distance is airborne. For impacts involving a braking vehicle the airborne proportion of pedestrian travel is highly dependent on the impacting vehicle's velocity with the higher vehicle impact speeds resulting in a reduced proportion of airborne throw distance. For vehicles that are neither braking nor accelerating at the time of impact the proportion of airborne travel is generally between 0.75 to 0.9. For vehicles that are accelerating at the time of impact the simulations indicated that the proportion of pedestrian airborne travel was less dependant of initial vehicle speed and also decreased with increasing vehicle acceleration, down to between 0.6 to 0.7 for a maximum simulated vehicle acceleration of 3.0 ms^{-2}.

The average airborne proportion for a decelerating vehicle ranged between 0.83 and 0.89. At constant vehicle speed the average airborne proportion was 0.84. For an accelerating vehicle the proportion ranged from 0.62 to 0.8. The test data from Kühnel (1974) analysed in Chapter 2 had a range of 0.49 to 1.0 of airborne travel proportion. It would therefore appear that the proportion of airborne travel predicted by the simulations is similar to these test results.

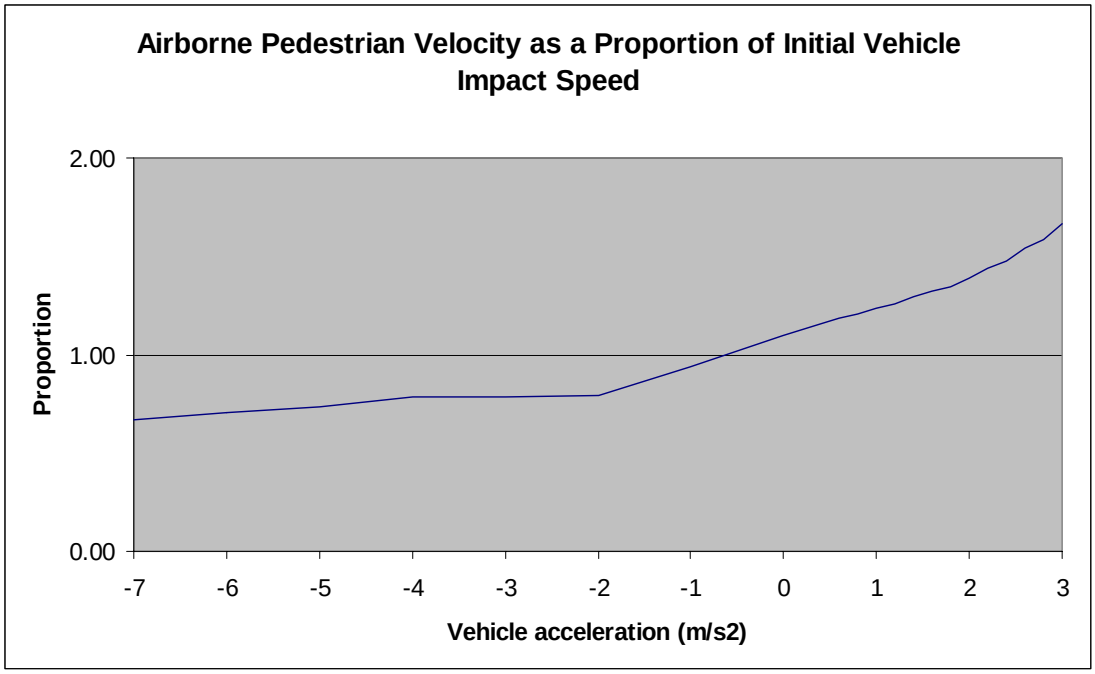

Figure 3.7 Airborne Pedestrian Velocity as a Proportion of Initial Vehicle Impact Speed for an SUV-Type Vehicle

Figure 3.7 shows how the pedestrian's horizontal velocity during the airborne stage compares to the initial vehicle impact speed. When the vehicle is braking heavily (-7.0 to -4.0 ms^{-2}) the pedestrian's airborne velocity is between 0.53 to 0.8 of the vehicle's initial impact speed. When the vehicle is accelerating during the impact the pedestrian's horizontal velocity is greater than the vehicle's initial impact speed, which is unsurprising as the vehicle's speed increases during the period of contact. What is surprising is that when the vehicle is neither braking nor accelerating, the pedestrian's horizontal velocity is approximately 10% greater than the vehicle's speed at impact. This would appear to occur due to the elasticity of the contacting surfaces resulting in an increase of the pedestrian's separation velocity relative to the vehicle's velocity. In the analysis of baseball bats this is referred to as the 'Trampoline Effect' (Russell, 2006) whereby the ball's speed upon leaving the bat is greater than the bat speed due to the bat acting like a spring.

Whether such an effect can occur in reality or is an artifact of incorrect simulation parameters is open to debate. Happer et al (2000) state: "*From the laws of physics, the vehicle impact speed (Vv) has to be greater than the pedestrian throw speed.*" On the other hand, Han and Brach (2001) when analyzing forward projection test data from Lucchini and Weissner (1980), Severy and Brink (1966) and Sturtz et al (1976) noted

that: *"A somewhat surprising and interesting result from these cases is that the fitted value of the velocity ratio, α, ranges from 1.2 to 1.3. This means that the best fit to the data is for a pedestrian forward launch velocity about 1.2 to 1.3 times greater than the forward velocity of the vehicle."* This statement would appear to lend credibility to the simulation results where the pedestrian velocity was greater than the vehicle velocity but whether such an effect only occurs for simulation models and test dummys or whether it does actually occur in forward projection pedestrian accidents is unknown but warrants further investigation. The elastic nature of 'energy absorbing' vehicle bumpers could conceivably contribute to such an effect in the real-world.

Finally, it should be noted that a vehicle accelerating during a pedestrian impact is unusual, although in this instance it is thought to be representative of the case being modelled. This unusual nature would appear to result in a pedestrian trajectory that is not accurately predicted by traditional vehicle-pedestrian accident reconstruction methods.

3.8 Application to a Typical Pedestrian Accident Reconstruction Involving a 'Wrap' Trajectory and Results Comparison with MADYMO

In the previous example the pedestrian throw distance predication as a result of vehicle impact and subsequent 'forward projection' trajectory offered by MADYMO was compared to the predictions offered by traditional vehicle-pedestrian accident reconstruction methods and the 'Projectile and Sliding' equation described in Chapter 2. In this section similar comparisons are made but in the instance of a 'wrap' pedestrian trajectory resulting from a pedestrian being impacted by a typical car.

3.8.1 Case Study Background

Using the same 5th percentile female pedestrian model as the previous case study, a series of simulations were run using a vehicle frontal profile more typical of a standard coupe or sedan. This simulation series was conducted to investigate a vehicle-pedestrian runover involving several impacts of the same vehicle and pedestrian. The case studied was identified as a homicide and not an accident. For

more information please refer to the accident report in Appendix III, Case Study 2: Lamar.

The goal of the simulation series was to determine a likely range for impacting vehicle speed and pedestrian orientation with respect to the vehicle. The pathology report detailed relatively minor head injury for the pedestrian (HIC unlikely to exceed 1000) whilst vehicle evidence indicated a head strike near the top edge of the bonnet extending onto the plastic plenum below the windscreen.

3.8.2 Methodology and Simulation Parameters

The vehicle model was an FEA representation of the bumper, bonnet and windscreen of a mid-size, 1.8 litre car. The vehicle model was created by measurement of the actual vehicle involved in the incident using a three-dimensional co-ordinate measuring rig. Profiles obtained were compared to manufacturer data.

Pedestrian orientation with respect to the vehicle were varied across three positions: facing the vehicle, side on the vehicle and facing away from the vehicle at a 45 degree angle (Refer Figure 3.8). Other orientations were determined to produce unrepresentative leg injuries. The pedestrian model used was the MADYMO 5th percentile female multibody human model, Version 6.01. Other simulation parameters can be seen in Table 3.4. A discussion of the literature values and ranges referred to can be found in Chapter 6.

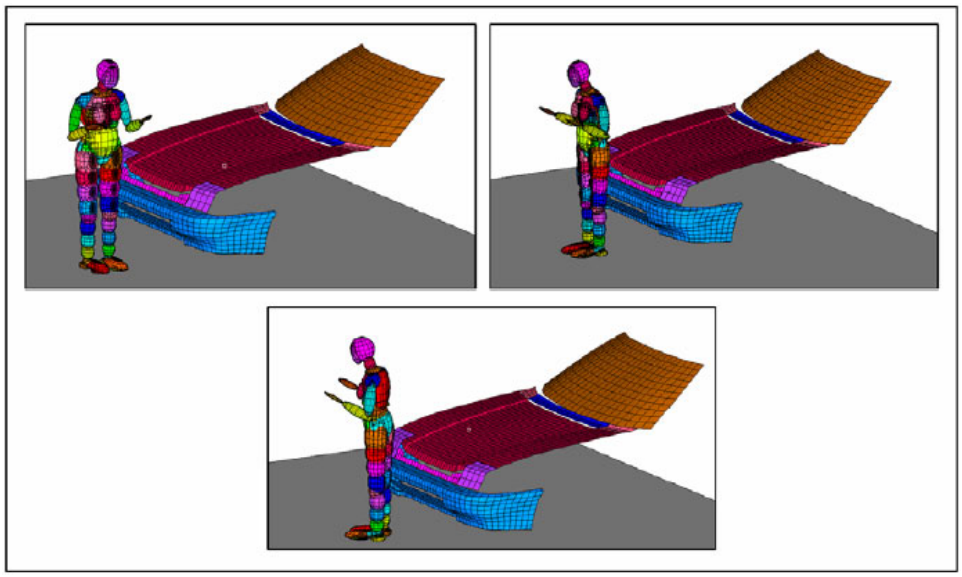

Figure 3.8 Pedestrian Pre-Impact Orientation with Respect to Vehicle

Parameter	Range	Comment
Coefficient of friction between vehicle and pedestrian	0.45	Within range of values reported in literature
Coefficient of friction between pedestrian and ground	0.55 for pedestrian on ground, 0.7 for shoe contact on ground	Value indicated to be within literature values and those determined by author
Vehicle speed at impact	5.56 to 9.72 ms^{-1} varied in 1.39 ms^{-1} increments	Range determined pedestrian injuries and damage to vehicle cowl using guidelines from Happer et al (2000)
Vehicle acceleration	-8.5, -4.0 and 0.0 ms^{-2}	Maximum vehicle deceleration (determined from on-site testing), moderate vehicle deceleration and no
Stiffness of vehicle bumper	250 Nmm^{-1}	As per literature.
Stiffness of vehicle bonnet top	300 Nmm^{-1}	As per literature.
Pedestrian head stiffness	2500 Nmm^{-1}	As per literature for anterior-posterior loading.
Stiffness of road	40 $kNmm^{-1}$	Middle of range specified by Chadbourn et al (1997)

Table 3.4 Parameters for Simulation of Collision Involving a Typical Vehicle

The contact model chosen for modelling the vehicle-pedestrian contact used a force/penetration characteristic with the contact characteristics defined within the finite element model as in this instance the only noticeable deformation was incurred by the vehicle (namely, a head-strike on the plastic cowl below windscreen). One of the limitations of the MADYMO software (especially with earlier versions, such as this model was run under) included limited potential to vary contact parameters. It

would have been better to have used a combined characteristic but this type of contact characteristic was only available for contacts between finite-element models and a stress versus penetration model. Alternatively, if a multibody vehicle model had been selected a mid-point contact and user-characteristic could have been defined, but as noted by Huang et al (1994b) such characteristics can be time-consuming to determine.

Throw distance was measured using the displacement measurement function of the model, taken from the model's sternum. Although the sternum is not at the Centre of Mass of the model, it is sufficiently close to be a convenient reference point.

The simulation matrix included the following variables:

- Pedestrian orientation varied at 45 degree increments about the vertical axis with respect to the vehicle (Refer Figure 3.8).
- Vehicle impact speed between 20 and 45 km/h at 5 km/h increments.
- Vehicle deceleration at impact taken to be either 0, 4 or 8.5 ms^{-2}, with the latter value indicating maximum achievable braking for the vehicle on that road surface.

The simulation outputs were analysed to identify test conditions that resulted in pedestrian HIC in the appropriate range and a head strike in the correct region of the vehicle.

3.8.3 Simulation Results

The throw distance results obtained and a comparison to the prediction afforded by several traditional vehicle-pedestrian accident reconstruction equations as well as the Projectile and Sliding Equation derived in Chapter 2 are shown in Figure 3.9.

The best agreement is seen for the data resulting from scenarios modelling the vehicle decelerating at -8.5ms^{-2}, which would appear to indicate that Searle's Equation assumes heavy braking (not an unreasonable assumption in the majority of cases).

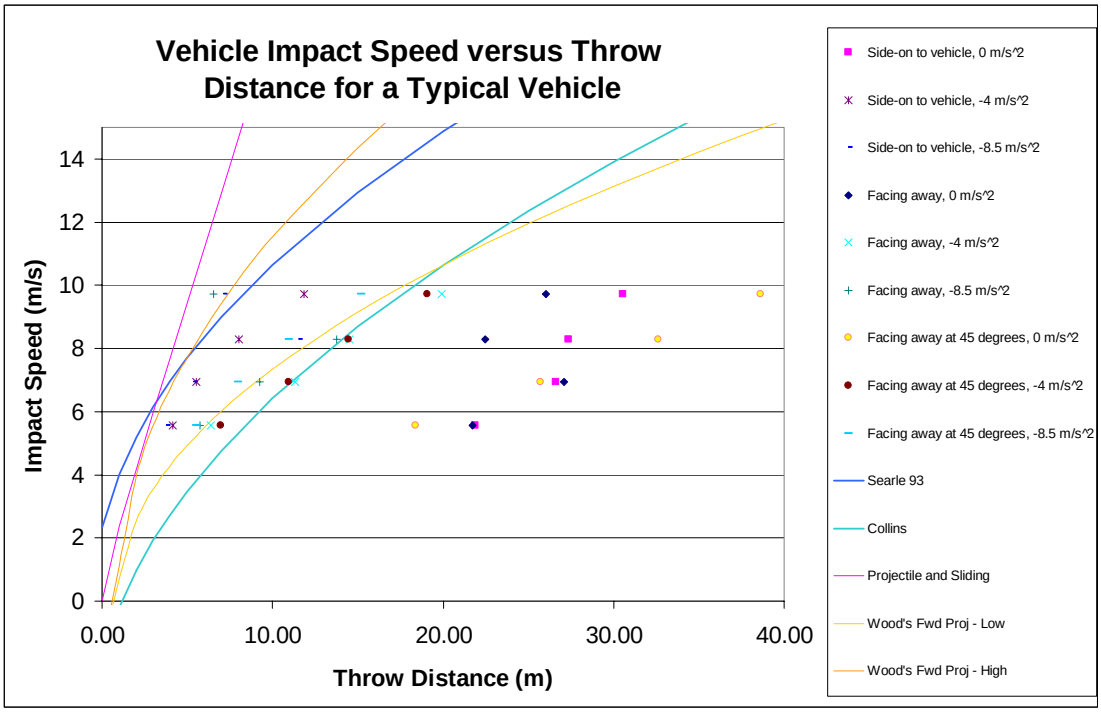

Figure 3.9 Throw Distance Comparison between MADYMO, Several Traditional Equations and the Projectile and Sliding Equation Derived in Chapter 2 versus All Results

The long throw distances apparent for the data resulting from scenarios modelling the vehicle travelling at constant speed resulted from the pedestrian being carried some distance by the vehicle before falling off, particularly at lower vehicle speeds. With the pedestrian facing away from the vehicle the collision at 6.94 ms^{-1} resulted in a longer throw distance than the impacts at 8.3 and 9.72 ms^{-1}.

In instances where the vehicle was braking moderately, reasonable agreement between the MADYMO results and Collins' and Wood's Forward Projection (Low Estimate) equations is seen.

Figure 3.10 shows the proportion of total pedestrian travel post-impact that is airborne following an impact with a typical vehicle, versus the three different pedestrian orientations analysed. In comparison to the results from the previous section, where the collision was analysed using only a single pedestrian orientation the scatter in this instance is considerable.

The results where the vehicle was braking moderately show the greatest spread, ranging from an airborne travel proportion of 0.43 to 1.0. Where the vehicle was

travelling at constant speed the range is the narrowest, covering 0.7 to 1.0. For a heavily braking vehicle the range was from 0.57 to 1.0.

In regard to pedestrian orientation the 'facing away' and 'facing away at 45º' orientations typically produced the lowest proportions of airborne travel, particularly when the vehicle was braking moderately. The 'side-on' orientations produced the highest proportions of airborne travel, particularly when the vehicle was braking moderately which resulted in 100% airborne travel regardless of vehicle speed. When the vehicle was braking heavily the 'side-on' orientation produced a range of airborne travel proportion of between 0.8 and 1.0 whilst for constant vehicle speed the range was from 0.75 to 1.0. The average airborne travel proportion was fairly consistent, ranging between 0.82 and 0.88. This is very similar to the average airborne travel proportion determined in the previous section for a decelerating SUV-type vehicle (0.83 to 0.89).

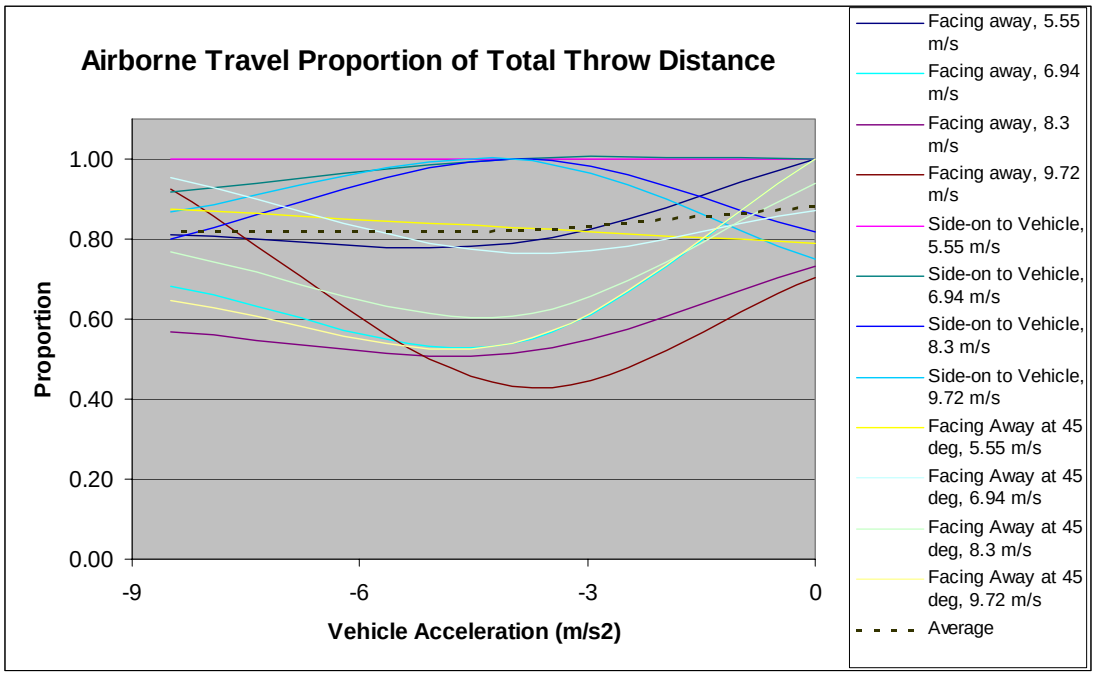

Figure 3.10 Pedestrian Airborne Travel Proportion of Total Throw Distance for a Typical Vehicle versus Three Different Pedestrian Orientations at Impact

It is apparent from the kinematics resulting from the simulations that for the side-on orientation the pedestrian, as 'it' wrapped around the front of the vehicle, travelled further up the bonnet at a given vehicle speed than for the 'facing away' and 'facing

away at 45º' orientations. As noted by Simms and Wood (2005) this appears to relate to a higher effective radius of rotation about the leading bonnet edge for the 'side-on' orientation, leading to a larger wrap-around distance. In these instances, where the pedestrian travelled further along the bonnet than for the other orientations, it would be expected that the pedestrian would take longer to contact the ground and although it is referred to here as 'airborne' travel, a good proportion would actually be 'bonnet carry'.

Generally, pedestrian orientation can be seen to influence to a considerable degree the motion resulting from a vehicle pedestrian collision.

Figure 3.11 shows the launch velocity for the pedestrian as a proportion of initial vehicle speed.

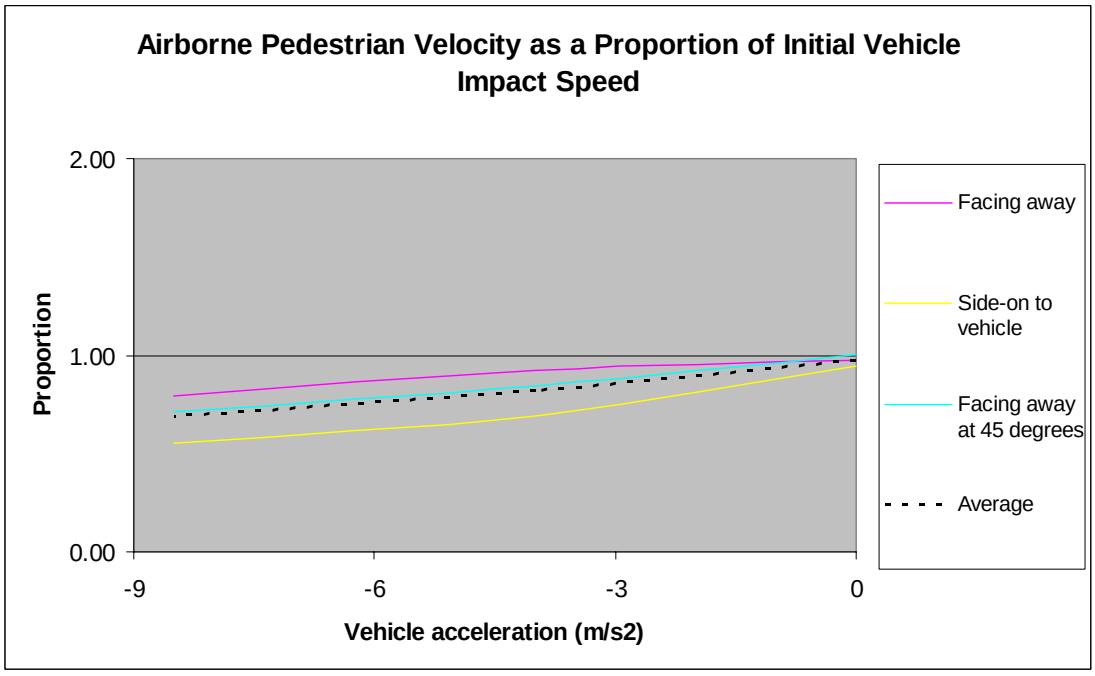

Figure 3.11 Airborne Pedestrian Velocity as a Proportion of Initial Vehicle Impact Speed for a Typical Vehicle versus Three Different Pedestrian Orientations at Impact

The velocity imparted to the pedestrian appears to increase with decreasing vehicle braking indicative of a shorter duration of contact and reduced energy transfer for collisions involving a heavily braking vehicle. For the averaged results, the pedestrian velocity as a proportion of vehicle velocity ranged between 0.69 and 0.82 for a heavily braking vehicle (more than -4.0 ms^{-2} deceleration). In comparison the same range for an SUV-type vehicle was between 0.53 to 0.8. It is thought that the major

cause of this difference would be the influence of the ‘facing away’ and ‘facing away at 45º’ orientations causing the pedestrian to obtain a greater proportion of the vehicle velocity due to greater conformity of the pedestrian’s body to the vehicle shape resulting in extended vehicle contact duration and hence greater energy transfer.

The ‘side-on’ orientation produced the lowest proportion of vehicle velocity imparted to the pedestrian whilst the ‘facing away’ orientation generally had the greatest. The ‘Facing away at 45°’ orientation generally fell in between these results except for the instance of a vehicle travelling at constant speed, where it not only indicated the greatest proportion but also exceeded 1.0 (i.e. pedestrian velocity greater than vehicle impact velocity). Although this particular result was not as high as that noted for the SUV-type vehicle-pedestrian collision analysis (1.01 in this instance, versus approximately 1.1 for the SUV-type vehicle) it can be surmised that a similar effect occurred as discussed in Section 3.7.

3.9 Discussion of the Results Obtained for an SUV-Type Vehicle and Those Resulting from a Typical Vehicle.

Pedestrian throw distance was seen to be proportional to vehicle speed and inversely proportional to vehicle deceleration. It was also apparent that the reduction in pedestrian velocity as a proportion of vehicle velocity for heavily braking vehicles was offset by lower airborne travel proportion and vice versa for lightly braking vehicles, reducing the effect on throw distance for comparable vehicle speeds and pedestrian orientations.

It would appear that the airborne travel proportion of total pedestrian throw distance is not significantly affected by vehicle shape and similar results were obtained from both the simulations involving an SUV-type vehicle and a typical car. A slight increase in airborne travel proportion with a reduction in vehicle braking intensity would appear to indicate a reduction in launch angle proportional to level of vehicle braking.

The scenarios in which a pedestrian was impacted by an SUV-type vehicle produced pedestrian launch velocities that were approximately 10% greater than the vehicle

velocity for a vehicle travelling at constant speed. In comparison, in the scenarios utilizing a typical vehicle, only a single pedestrian orientation (Facing away at 45°) produced a pedestrian velocity greater than the vehicle impact velocity and this was only 1% greater. Noting that the pedestrian models used in these simulations were essentially the same, it would appear most likely that the different vehicle shapes caused this disparity as the vehicle material properties were very similar (refer to Tables 3.3 and 3.4). In keeping with the baseball bat analogy used in Section 3.7, it would appear that an SUV-type vehicle makes a better pedestrian 'bat' than a typical vehicle.

The next section will briefly describe some examples of the vehicle-pedestrian reconstruction using MADYMO conducted by other authors.

3.10 Studies by Other Authors Using MADYMO for Vehicle-Pedestrian Accident Reconstruction

Linder et al (2005) used MADYMO and PC-Crash to reconstruct six actual pedestrian accidents that occurred in Hanover, Germany, between 1995 and 2003. The aim of the study was to assess the effectiveness of MADYMO in predicting impact severity with a particular focus on head injury. Simulated and measured throw distances were also compared. PC-Crash was used to verify impact speed range.

All simulations were initially run using Yang's 50^{th} percentile pedestrian model. This was shown to be sufficiently accurate for five of the six cases studied. For the other case, which involved two pedestrians, it was found to be necessary to use pedestrian models that more accurately represented the size of the pedestrians that were actually involved in the accident. Once this substitution was performed the kinematics and injuries were more accurately simulated.

Pedestrian velocity at the time of impact ranged between 0 and 3 ms^{-1} and vehicle impact speed ranged between 9.5 and 12.7 ms^{-1}. The authors found good correlation between simulated and actual throw distances and pedestrian injuries in all six cases.

It would be useful to see studies similar to this one conducted with a wider range of impact speeds and different vehicle types (eg SUV-type vehicles, box-fronted vans). Five of the six impacting vehicles were sedan-type vehicles (VW Golf, VW Passat, BMW 3-series touring, Ford Mondeo and Mercedes 200E). The one non-sedan-type vehicle was a VW Caravelle. The Caravelle is a front-engined, front-wheel-drive van. The leading edge of the bonnet is not significantly different to a sedan.

3.11 Case Studies by Other Authors Using MADYMO for Non-Pedestrian Accident Reconstruction

3.11.1 Study by Poland et al #1: School Bus Versus Truck

In 1997 in Minnesota, USA, a school bus carrying 13 children and an unladen tractor-trailer collided at an intersection (Poland, McCray and Barsan-Anelli, 2006). Both vehicles were travelling at approximately 22 ms^{-1}. The two vehicles contacted three times during the collision. The seat-belt restrained truck driver and three unrestrained bus passengers suffered fatal injuries.

Due to the complicated nature of the interaction between the two vehicles computer simulation, including HVE (refer Chapter 3, Section 3.3.2) and MADYMO, was used to analyse the crash and to evaluate the potential usefulness of both lap and three-point seatbelts. The authors discovered that the third impact resulted in a severe yaw acceleration at the rear of the bus. It was deemed likely that it was the third impact that resulted in the fatal injuries. It was also discovered that due to the bus seat design seatbelts did not offer the same degree of protection when compared with seatbelt usage in passenger cars.

3.11.2 Study by Poland et al #2: School Bus Versus Train

In 2000 a school bus carrying 7 children collided with a 33-car freight train at a level crossing in Georgia, USA (Poland, McCray and Barsan-Anelli, 2006). The train was travelling at approximately 23 ms^{-1} and bus was travelling at approximately 7 ms^{-1}.

The interaction between the two vehicles resulted in the ejection of the seat-belt restrained bus driver and three children and also the separation of the bus body from

the chassis. One ejected bus passenger and two non-ejected bus passengers received fatal injuries.

The accident was simulated using HVE and MADYMO. As per the previous example the highest accelerations during the impact sequence were found to occur at the rear of the bus. The authors conclude that further work is necessary to assess potential occupant protection systems and the corresponding cost/benefit ratio.

3.11.3 Study by NTSB, USA: Large Passenger Van Versus Barrier

In 2002 a 15-seat passenger van operating as day-car transport in Memphis, USA, left the road and collided with a bridge abutment. (Highway Accident Report, NTSB, 2002). Five of the seven occupants were fatally injured.

The vehicle dynamics during the accident were modelled using several software packages including HVE (Human Vehicle Environment), SIMON (SImulation MOdel Non-linear), EDSMAC4 (Engineering Dynamics Corporation Simulation of Automobile Collisions) and EDCRASH and (Engineering Dynamics Corporation Reconstruction of Accident Speeds on the Highway).

Occupant kinematics and the effect of restraint use (and non-use) was modelled using MADYMO version 6.1. It was discovered that lap/shoulder belt use significantly reduced the severity of the occupant injuries, but only if used in conjunction with a booster seat for those occupants aged 8 or less. When simulated with lap/shoulder belt restraints only, the younger occupants tended to have their upper bodies slide clear of the restraints resulting in impacts with sidewall and window structures.

The authors had difficulty in modelling the driver, as the 95^{th} percentile male occupant model of 223 lbs was considerably lighter than the actual driver mass of 380 lbs. With obesity on the increase it is possibly timely for the development of larger occupant and pedestrian models.

3.11.4 Study by Parent et al: Train Versus Train

In Placentia, USA, in 2002 a freight train consisting of 3 locomotives and 67 freight cars collided with a 3-car passenger train (Parent, Tyrell, Perlman, 2004). The

passenger train had successfully braked to a halt whereas the freight train had reduced speed to approximately 9 ms^{-1}. The leading locomotive of the freight train struck a coach car of the passenger train and shunted the passenger train some 70 – 75 metres. 161 passengers and crew were subsequently transported to local hospitals. There were two fatalities.

A one-dimensional collision dynamics model was created to generate the appropriate acceleration time-history of the leading coach-car. The acceleration output from this simple model was then used as an input to a MADYMO model to analyse occupant injuries and injury sources.

Worktables located between seats were found to be a major injury source. The report recommended strengthening the table supports and softening the table edges.

3.11.5 Discussion of Case Studies by Other Authors Using MADYMO for Non-Pedestrian Accident Reconstruction

The above case studies all analysed accidents involving large vehicles (buses, trains, large passenger vans). Two of the studies (Poland et al, 2006 and Parent et al, 2004) compared the simulated results to actual crash tests. The expense of crash-testing large, specialized low production volume vehicles would have been considerable. However, until the use of computer simulation in accident reconstruction is widely validated and accepted such crash tests will continue to be demanded.

However, it is interesting to note the large yaw accelerations present at the rear-end of the buses in two of the cases, which occurred as a result of multiple impacts with another vehicle. It is difficult to envisage how these scenarios would have been accurately predicted by mandated crash-testing. For these scenarios MADYMO was able to quickly and effectively evaluate occupant dynamics in unusual circumstances.

The analysis of the large passenger van single-vehicle accident (Highway Accident Report, NTSB, 2002) also revealed the inadequacy of standardized crash testing, this time in regard to varying occupant sizes. In this case the driver was too large and the majority of passengers were too small to be effectively restrained by lap-shoulder

restraints. In cases such as this occupant simulation software results in quick and effective analysis.

It should be noted that MADYMO was originally designed for occupant analysis for vehicle design optimization and has subsequently been adapted to the analysis of pedestrian accidents.

3.12 Conclusions Regarding the Comparison of MADYMO with Traditional Accident Analysis Methods

Computer simulation has come a long way since the Manhattan Project. In the field of accident reconstruction programs such as SMAC and CRASH have aided several generations of reconstructionists. More complex mathematical modelling methods such as those embodied in MADYMO and LS-DYNA, once used solely for design and optimization, are now being used and evaluated by accident reconstructionists thanks to the ready availability of inexpensive, high-performance computers.

A comparison between the impact speed versus throw distance relationship, as calculated by Searle's 1993 Equation and by Version 6.01 of MADYMO, shows good agreement under certain circumstances. Thus, it can be stated that under certain circumstances Searle's Equation is in close agreement with considerably more complex methods. However, the same may not be said for all circumstances thus exposing the major limitation of traditional vehicle-pedestrian accident techniques – a relatively high risk of considerable inaccuracy for collisions involving non-typical driver actions, pedestrian orientations and vehicle shapes.

Pedestrian throw distance was noted to be proportional to vehicle speed and inversely proportional to vehicle deceleration. Traditional vehicle-pedestrian reconstruction methods appear to be based on the assumption of maximum vehicle braking and do not account for different levels of vehicle deceleration or any level of vehicle acceleration.

It was apparent that pedestrian impacts involving an accelerating vehicle resulted in limited correlation between vehicle impact speed and pedestrian throw distance.

Examples such as these may prove difficult to reconstruct using either traditional vehicle-pedestrian accident reconstruction methods or by using computer simulation.

In a limited number of instances a pedestrian launch velocity between 1 to 10% greater than the vehicle velocity for a vehicle travelling at constant speed were noted. These were most apparent for impacts involving an SUV-type vehicle. It is unsure whether this would be likely in real-world situations but such observations have also been made by other authors.

An additional limitation of traditional vehicle-pedestrian accident techniques is the inability to indicate likely pedestrian injuries or vehicle damage. With such information often being available to the accident reconstructionist the ability to use such information to validate a proposed scenario is vital.

Subsequent Chapters will further explore MADYMO's injury prediction capabilities and explore the usefulness of these prediction capabilities in the context of accident reconstruction.

Chapter 4
Using Computer Simulation for Injury Prediction

4.1 Introduction

This Chapter examines the capability of simulation software regarding the successful prediction of pedestrian injuries resulting from a vehicle-pedestrian collision. Particular attention is paid to MADYMO's injury measurement approach.

Common injury parameters and pedestrian injury patterns are explored and the vehicle and pedestrian factors that influence injury are noted. The effect of injury on pedestrian kinematics is also briefly studied.

The modelling of pedestrian injuries using both traditional testing and mathematical modelling are compared and contrasted. The use of pedestrian injuries as accident reconstruction parameters is commented upon.

The effectiveness of mathematical simulation as a pedestrian injury predictor is evaluated by examining case studies by other authors. The different approaches adopted by different researchers is commented upon.

Finally, the limitations of mathematical pedestrian injury modelling and the origins of these limitations is discussed.

4.2 Injury Measurement

MADYMO is capable of recording 19 different human injury parameter measurements using a collection of virtual sensors strategically located throughout the MADYMO human model measuring linear and angular displacement, velocity, acceleration, load, force and torque.

Injury parameters available from different human and dummy multibody models in the current version of MADYMO are listed in Table 4.1 (See MADYMO Theory Manual for measurement description).

Head Injury	**GSI**: Gadd Severity Index
	HIC: Head Injury Criterion
	HCD: Head Contact Duration
	HICd: Weighted Head Injury Criterion
Neck Injury	**NIC_Forward**: Neck Injury Criterion Forward
	NIC_Rearward: Neck Injury Criterion Rearward
	N_{ij}: Neck Injury Predictor
	Nkm: Neak injury predictor
	LNL: Lower Neck Load Index
	MOC: Total Moment about Occipital Condyle
Chest and Abdominal Injury	**3ms**: Contiguous or cumulative chest acceleration over 3ms
	***x*ms**: generalisation of the above
	TTI: Thoracic Trauma Index
	VC: Viscous Injury Response
	CTI: Combined Thoracic Index
	APF: Abdominal Peak Force
Lower Extremity Injury	**FFC**: Femur Force Criterion
	TI: Tibia Index
	TCFC: Tibia Compressive Force Criterion

Table 4.1 MADYMO Injury Measurements

In comparison, other models including the Articulated Total Body (ATB) human model only measures HIC (Head Injury Criterion), HSI (Head Severity Index), CSI (Chest Severity Index) and chest acceleration (ATB Version V)(Cheng, 1998). MADYMO's injury prediction ability is one of its most important features.

Table 4.6 (in Section 4.7.5) includes a full list of MADYMO's virtual human sensors and a comparison to the sensors present in a commonly used pedestrian dummy.

In this section some of the more common measurements of head and thorax injury are discussed and how these measurements relate to the Abbreviated Injury Scale (AIS).

4.2.1 Head Injury, the Head Injury Criterion (HIC), the Abbreviated Injury Scale (AIS) and the Maximum AIS (MAIS).

Head injuries are the injury most likely to result in pedestrian fatality following a collision with a motor vehicle (Sarath, 2004; Fredriksson et al, 2001). The mechanisms of head injury are complex and are the focus of considerable research. Both linear and angular acceleration are debated as the major determinant of injury to the brain (King et al, 2003). Other factors include lateral versus frontal impact,

duration of the acceleration/deceleration phase, brain contusion versus concussion and movement of the brain relative to the skull.

The Wayne State University tolerance curve, determined from cadaver testing, describes the injury threshold with regard to the duration of a linear acceleration impulse (Gurdjian et al, 1966) based on the likelihood of skull fracture following an impact. Points above the curve are thought to indicate a high likelihood of brain injury or death.

The search for a common criterion for evaluating potential head injury during car crash testing led to the Gadd Severity Index (GSI), an integration of the Wayne State tolerance curve, with the acceleration component weighted by applying a power of 2.5. This value represents the slope of the Wayne State tolerance curve when plotted logarithmically between 2.5 and 50 milliseconds (Gadd, 1966). Thus the expression for the GSI is:

$$GSI = \int_{t_1}^{t_2} a^{2.5} dt \qquad (4.1)$$

a is the average linear acceleration and t_1 and t_2 are the beginning and end of the time interval, respectively. Gadd proposed a threshold GSI value of 1000 for concussion resulting from frontal impact.

The Head Injury Criterion (HIC) was subsequently developed by Versace (1971). This focuses the integration time interval on the most injurious part of the impulse. By defining t_1 and t_2 as the time at which equal levels of acceleration occur either side of an instant of maximum acceleration, HIC can be expressed as:

$$HIC = (t_2 - t_1)\left[\frac{1}{(t_2 - t_1)}\int_{t_1}^{t_2} a dt\right]^{2.5} \qquad (4.2)$$

t_1 and t_2 are selected so as to provide a maximum HIC value for a given time interval. For contact with hard surfaces a maximum of a 15 milliseconds interval is commonly used (Mertz, 1997) and a maximum 15 milliseconds time interval has been employed by the author.

Limitations on HIC as an injury severity criterion include:

- Angular accelerations are not taken into account

- Deals only with hard contacts
- The original data was obtained from anterior-posterior acceleration only

For the research conducted by the author, only the first limitation is a reasonably serious deficiency.

The Abbreviated Injury Scale (AIS) denotes risk of fatality for a given injury level (Garthe et al, 1998). There are six injury levels, with 1 representing minor injuries (with no resulting fatalities) through to 6 (virtually unsurvivable, often referred to as the 'Fatal' level). HIC values can be correlated with the chance of a specific AIS level and therefore assess injury risk. e.g., for an HIC of 1000, the Mertz head injury curves indicate a 17% chance of an AIS level 4 or greater. For an AIS level 4, the fatality range is 7.9 to 10.6%, i.e. a fairly small risk of fatality. For an HIC of 2000 there is a 90% risk of an AIS level 4 or greater.

AIS assigns injury severity scores by body region (head, face, chest, abdomen and extremities). Maximum AIS (MAIS) is the highest injury score across all body regions.

In order to study the pedestrian 'survivability' of vehicle-pedestrian collisions, the 3ms criterion for the upper torso should also be measured. With the exception of the brain, the organs located within the upper torso are the most likely to incur life-threatening injuries in the event of blunt trauma. The acceleration limit for the upper torso is commonly accepted to be 60 G sustained for 3 milliseconds or longer (MADYMO Theory Manual, 2001). The 3 milliseconds period may be either contiguous or cumulative.

4.3 Pedestrian Injury Patterns

Automotive designers use the bumpers on a vehicle to protect the vehicle when a collision occurs. Accordingly, the bumpers are placed at the extreme ends of the vehicle and for a vehicle travelling forwards the front bumper is usually the first part of the vehicle to strike any object in the vehicle's path. If the object is a person then

the first major interaction between a pedestrian and an impacting vehicle often involves the vehicle's bumper and the pedestrian's lower extremities. Modelling this interaction mathematically formed the basis for Yang's thesis as discussed in Chapter 3, Section 3.6.3.

Conversely, Foret-Bruno et al (1998) noted that a reasonable proportion of vehicle-pedestrian collision did not involve contact with the vehicle's front bumper, with front-guard and wing-mirror impacts making up 25% of all vehicle-pedestrian collisions. It should be noted, however, that front-guard and wing-mirror impacts constituted only 11% of fatal vehicle-pedestrian collisions. With many authors not using minor-injury cases in their statistical analysis it is possible that guard and wing-mirror impacts are under-reported in many studies.

After the initial vehicle-pedestrian contact the motion of the pedestrian will then tend to follow one of the trajectories as described in Chapter 2, Section 2.4, according to the distribution shown in Figure 4.1. In most trajectories there is a high probability of at least one more contact between the pedestrian and the vehicle.

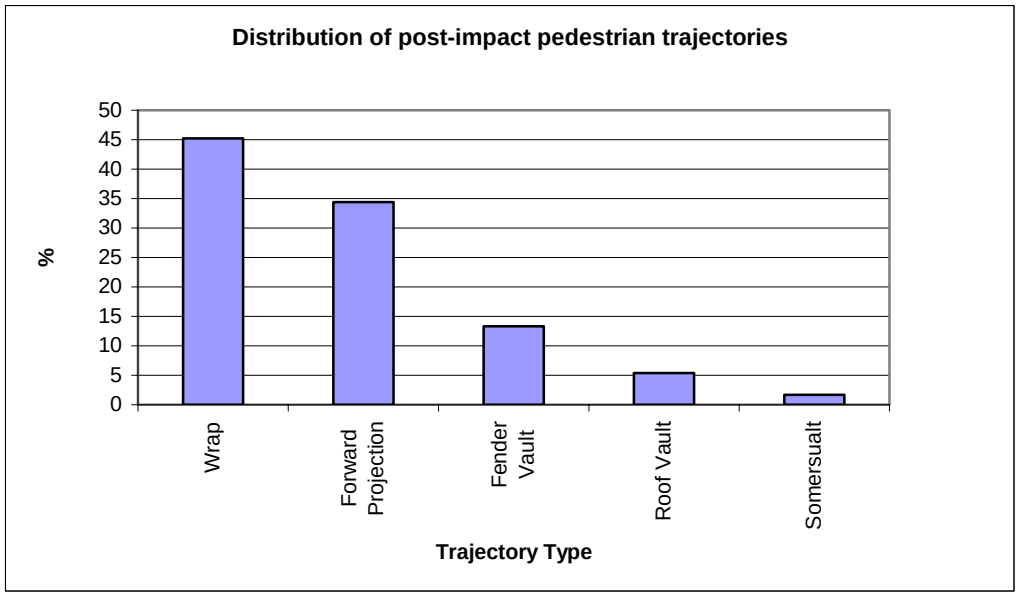

Figure 4.1. Distribution of Post-Impact Pedestrian Trajectories (Source: Ravini, 1981)

Distribution of Pedestrian Injuries, AIS 2-6, Resulting from a Vehicle Collision

Body Region	Percentage
Legs	32.6%
Head	31.4%
Chest	10.3%
Arms	8.2%
Pelvis	6.3%
Abdomen	5.4%
Face	4.2%
Neck	1.4%
Unidentified	0.2%

Table 4.2 Distribution of Pedestrian Injuries (Source: IHRA, 2001)

With pedestrian leg involvement highly likely in a vehicle collision it is unsurprising that leg injuries top the list of pedestrian injuries (Refer Table 4.2 – For AIS Scale refer to Section 4.2.1). The head is the second most likely location of pedestrian injuries, followed by the chest. Whilst leg injuries are prevalent they are rarely life-threatening. Furthermore, in order to protect the vehicle occupants, cars have been designed with a relatively soft crumple zone at the front (bumper, bonnet and guards) and a comparatively rigid occupant 'safety cell' further back (windscreen, A-pillars). Because of the relatively soft front-end of vehicles leg injuries from bumper contact are likely to be less severe than any portion of the pedestrian striking a correspondingly 'hard' portion of the vehicle.

Of interest is the relationship between pedestrian trajectory and injury pattern. Ravini et al (1981) discusses this at some length and it is useful to summarise his findings. An Injury Risk Index was used to evaluate the combined injury occurrence and injury severity to different body areas and evaluate the likelihood and location of serious injury with respect to the different post-impact trajectories. Ravini discovered that wrap and fender vault trajectories resulted in a high risk of serious head and leg injuries, whilst forward projection and fender vault trajectories had a high risk of serious head and chest injury. The statistical sample of somersault trajectories was too small to draw reliable conclusions.

Ravini notes the correlation between the different pedestrian post-impact trajectories and injury patterns but fails to identify any potential for injury from ground impact despite commenting on the high-loft of roof-vaulted pedestrians.

Problems with identifying injury from ground contact versus vehicle contact are a recurring theme in many studies. Foret-Bruno et al (1998) noted that in the dataset used for their research that only when no head impact point on the vehicle could be identified was the predominant head injury classified as occurring from ground contact. If a head impact point on the car was identified, then the pedestrian head injury was attributed to vehicle contact without any attempt to correlate the injury with the vehicle impact point. According to this methodology less than 15% of serious injuries resulted from ground contact.

Yang et al (2005) notes that if the pedestrian strikes the ground head-first following a vehicle-pedestrian collision, then the head injury from ground impact will generally be more severe than any head injury that resulted from vehicle impact. If the pedestrian does not strike the ground head-first, then head injury from vehicle impact is likely to be more severe than from any subsequent head impacts.

Ashton (1975) presented the data shown in Table 4.3. Of note are the lower injury rates for children (as compared to adults) for serious road-induced injury. This may be a consequence of adults having further to fall due to their higher centre of gravity (and hence greater road-impact velocity) or could result from children being more likely to suffer more serious injuries from vehicle contact as their head and thorax are more likely to be struck by the vehicle (as per Liu and Yang, 2001) than is the case for adults (who generally suffer leg injuries).

Otte and Pohlemann (2001) also analysed Ashton's findings but somehow arrived at the conclusion that "*secondary impacts cause 56% of all injuries*", despite the data shown in Table 4.3 indicating the percentage to be approximately 37%. Indeed, previous research by Otte (1994) indicated 37.3% of adult pedestrians suffered injuries from road impact, which is consistent with Ashton's data. Further examination of Otte and Pohlemann's research may be found in Chapter 5.

	Children		Adults	
	Percentage	n	Percentage	n
Road-induced Minor Injuries	71.8%	39	56.0%	50
Road-induced Serious Injuries	2.5%	39	18.0%	50
Average	37.2%		37.0%	
Road-induced Minor Head Injuries	70.0%	40	66.7%	42
Road-induced Serious Head Injuries	25.0%	4	40.9%	22
Average	65.9%		57.8%	

Table 4.3 Road-induced injuries from Ashton (1975)

Incidence of serious injury from ground contact can also be related to vehicle shape. Tanno et al (2000) noted that for pedestrians struck by a flat-fronted vehicle (i.e. vans, people-movers, light trucks) the incidence of serious injury from ground contact equalled the incidence of serious injury from vehicle contact. Simms and Wood (2005) used a MADYMO model to compare head versus vehicle contact and head versus ground contact. It was found that ground contact resulted in higher forces acting over a shorter duration of time than vehicle contact, results similar to those obtained by the author when studying vehicle-pedestrian collisions involving tall vehicles.

4.4 Pedestrian Factors Influencing Injury from Vehicle-Pedestrian Collision

Older adults and the elderly are the most likely pedestrian group to suffer serious injury or death following a vehicle-pedestrian collision, regardless of vehicle speed (Lee and Abdel-Aty, 2005). Children under the age of 12, whose centre of mass height is almost always below the leading edge of vehicle, show a reduced serious injury and fatality risk compared to adults for vehicle impact speeds of 45 km/h or less (Foret-Bruno et al, 1998). A medical researcher, Orsborn et al (1999), reported similar findings relating to child pedestrian injuries, noting the relatively low incidence of serious head injury compared with adults struck by cars. Orsborn et al stated that this has implications regarding the use of mechanism of injury to recognise predictable injury patterns to enhance emergency medical services, as the criteria

were established based on patterns of injury prevalent in injured adult pedestrians (i.e. high likelihood of serious head injury).

Other pedestrian factors that can influence pedestrian injury in a vehicle-pedestrian collision include drug and alcohol impairment (Miles-Doan, 1995). Miles-Doan found evidence that acute alcohol impairment increased the odds of a pedestrian receiving serious or fatal injuries as a result of a vehicle-pedestrian collision, contrary to the popular myth that "*a drunk can 'roll with the punches' and thus escape more serious injury than his sober counterpart*" (Miles-Doan, attributed to Waller et al, 1986). The effect of alcohol impairment on the chances of a vehicle-pedestrian collision were not examined in this study. The results of this study would appear to indicate that the reflexes and or muscle tension/response of an unimpaired pedestrian act to mitigate the injuries received in a vehicle-pedestrian collision in comparison to an alcohol impaired pedestrian.

Pedestrian posture, gait and orientation to the vehicle at the time of impact can all influence the post-impact pedestrian kinematics and injury severity. Anderson and McLean (2001) noted the influence of posture on head injury in a series of vehicle-pedestrian collision simulations. In a subsequent paper Anderson et al (2005) averaged the results obtained from six different gait positions using computer simulation to reconstruct four different vehicle-pedestrian accidents.

The distribution of pedestrian activities at the time of impact can be seen in Figure 4.2. Only a relatively small percentage of pedestrians are standing still at the time of collision.

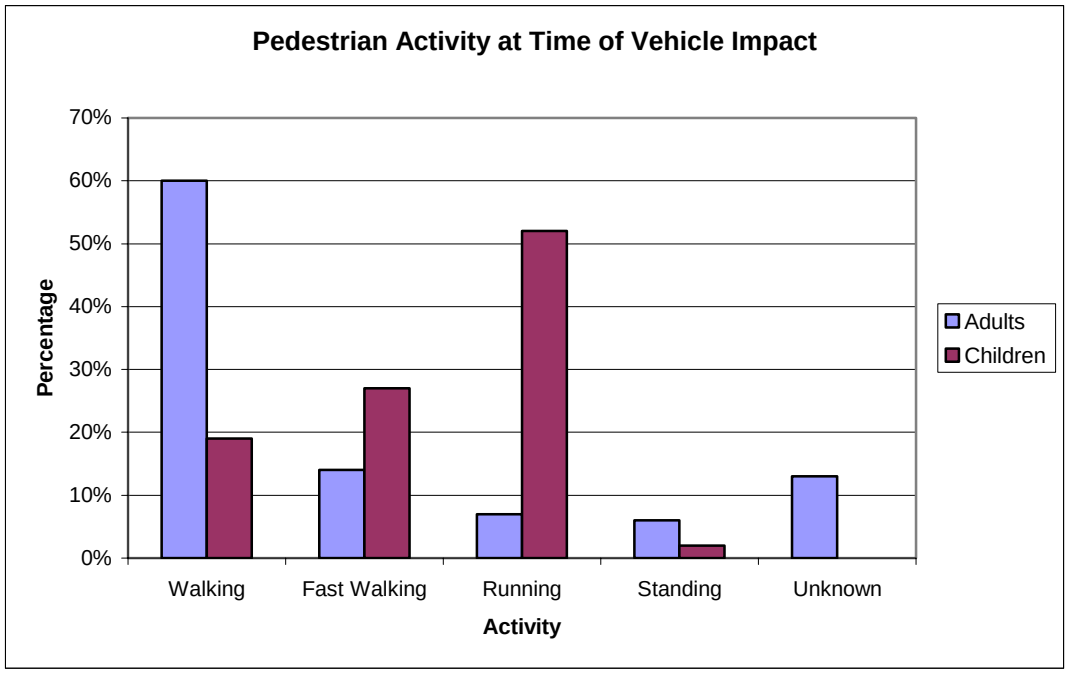

Figure 4.2 Pedestrian Activity at Time of Vehicle Impact (Source: Yang et al, 2005)

4.5 The Influence of Vehicle and Driver Factors on Pedestrian Injuries

Pedestrian injuries can also be influenced by vehicle factors with the most obvious vehicle factor being speed at time of impact (Lee and Adbel-Aty, 2005; Zajac and Ivan, 2003; McLean et al, 1994). McLean et al reviews several papers relating to the correlation of vehicle speed to severity of pedestrian injury. The consensus is that pedestrian injury severity tends to increase at least linearly with vehicle speed. Some research indicates that the relationship may be exponential.

As has been noted in several studies (Stevenson and Raine, 2002; Roudsari et al, 2004) and in Chapter 5, collisions involving large vans and utility vehicles typically result in more severe pedestrian injuries than collisions involving passenger cars. In the majority of cases this would appear to relate more to shape differences in comparison to pedestrian impacts involving passenger vehicles, as the mass difference between a pedestrian and an SUV/LTV is not markedly different to the mass difference between a pedestrian and a passenger car.

Ashton and Mackay (1983) considered the influence of relative bumper height, relative bonnet height and bumper lead angle ($= \tan^{-1}\left[\frac{BonnetHeight - BumperHeight}{BumperLead}\right]$) on pedestrian injury patterns. Unsurprisingly, the height of the bumper was found to

relate to the location of leg injuries (low bumper resulted in injury to lower leg, higher bumpers resulted in injury to upper leg). Lower bonnet heights were found to reduce the risk of pelvic injury. Bumper lead angles of less than 70° were noted to relate leg fracture to bumper contact whilst bumper lead angles of greater than 70° were noted to relate to an increased risk of leg fracture from leading edge bonnet contact.

Neal-Sturgess et al (2002) noted that vehicle impact speed would appear to have considerably more influence on pedestrian injury severity than vehicle characteristics, in particular vehicle panel stiffness.

Mizuno and Kajzer (2000) in their experimental work on vehicle shape versus the pedestrian wrap-around distance (WAD) noted that pedestrians impacted by cars with bonnets (i.e. passenger cars) tended to suffer leg injuries, whereas pedestrians impacted by mini-van type vehicles tended to suffer from head and chest injuries. Mizuno and Kajzer also noted that as the head and chest injuries tended to be more life-threatening indicating that min-van impacts were more dangerous to pedestrians than impacts with passenger cars. Mizuno and Kajzer did not, however, appear to differentiate between vehicle and ground impacts. They did note that head impacts on windscreens where the dynamic deformation of the windscreen at the point of contact was 89 mm or more resulted in only moderate (i.e. unlikely to result in serious injury) HIC values being recorded, indicating the importance of deformable impact structures in impact injury reduction.

As noted in Section 4.3, flat-fronted vehicles tend to result in a higher incidence of serious injury from ground contact. Modifying the design of such vehicles to minimise pedestrian injury from vehicle contact may not be particularly helpful, unless the redesign includes a rather fundamental shape alteration. Tanno et al (2000) also noted the increased incidence of chest, abdomen and pelvic injuries in vehicle-pedestrian collisions involving flat-fronted vehicles, resulting from the almost immediate upper-body/vehicle interaction during the collision as compared to impacts involving vehicles with bonnets. Correspondingly the incidence of pedestrian leg-fracture in vehicle-pedestrian collisions was found to be lower than for collisions involving a bonneted vehicle. Tanno et al noted that whilst the incidence of serious and fatal injuries increase markedly for vehicle-pedestrian collisions involving

bonneted vehicles travelling at 50 km/h or more, a similar collision severity increase occurs for pedestrian collisions with flat-fronted vehicles for speeds at only 30 km/h. Longhitano et al (2005) noted that 60% of collisions involving LTVs (Light Trucks and Vans, in this instance including SUVs) resulted in pedestrian chest injuries of AIS 3 or greater, compared to 24% of passenger car impacts.

SUVs have been noted to have a higher incidence of reversing collisions involving pedestrians (Takubo and Mizuno, 2000) that result in serious injury. The relatively high-mass of SUVs would appear to increase the likelihood of the SUV driver being unaware of the collision and continuing the manoeuvre after the initial collision (and aggravating the pedestrian's injuries) when compared to vehicle-pedestrian collisions involving reversing passenger-type cars. The relative lack of awareness of SUV drivers when backing over a pedestrian presumably stems from the original SUV design criteria to easily drive over objects.

Driver alcohol impairment also appears to influence pedestrian injury severity (Zajac and Ivan, 2003). This may relate to the driver's delayed response to the impending pedestrian collision and the subsequently late braking action.

Newer vehicles may also incorporate pedestrian injury reduction design features, such as pop-up bonnets (Nagatomi et al, 2005), external airbags around the base of the windscreen and A-pillars (Kuehn et al, 2005) and the use of sensors, including existing vehicle parking sensors, to deploy aforementioned pop-up bonnets and airbags (Tilp et al, 2005) as well as video-based systems for longer-range pedestrian detection.

EuroNCAP (European New Car Assessment Programme) incorporates a pedestrian testing protocol for vehicle impact which specifies a range of head and leg impactor tests (EuroNCAP, 2004). Injury parameter limits are also specified, as shown in Table 4.4. A point scoring system is used to rate the vehicles according to the injury values obtained during testing.

Body Form Impactor	Injury Criterion	Limit
Legform	Knee Bending Angle	15º
	Knee Shear Displacement	6 mm
	Upper Tibia Acceleration	150 G
Upper Legform	Sum of Impact Forces	5 kN
	Bending Moment	300 Nm
Child Headform	Head Injury Criterion	1000
Adult Headform	Head Injury Criterion	1000

Table 4.4 EuroNCAP Pedestrian Testing Protocol Limits (Source: EuroNCAP, 2004)

SARAC/SARAC II (SAfety Rating Advisory Committee) is a safety assessment system that is based on real-world crashes with SARAC II incorporating vehicle-pedestrian collisions (Langweider et al, 2003). The recent emphasis on pedestrian protection has resulted in improved pedestrian protection due to introduced EC rules and one of the aims of SARAC II is to assess the effectiveness of these new vehicle design regulations.

4.6 Pedestrian Injuries and their Influence on Kinematics

Brands et al (2001) noted in their research that pedestrian injuries such as leg fracture can influence the subsequent pedestrian kinematics during the collision sequence. Brands et al also stated the concern that finite element models of the human body may not be sufficiently accurate to model injury-influenced pedestrian kinematics with a sufficiently high degree of accuracy, presumably relating to the finite element modelling of human tissue being relatively unproven (refer Chapter 3, Section 3.6.4) compared to the more basic but well validated multibody human models (refer Chapter 3, Section 3.6.3). However, recent advances in vehicle occupant simulation using finite element models suggest that accurate, biofidelic finite element human models are not too far away (MADYMO Human Models Manual, Version 6.3 and later).

Likelihood of fracture of lower extremities in a vehicle-pedestrian collision can be related to vehicle factors including vehicle speed, vehicle deceleration (influencing vehicle attitude and duration of impact), vehicle design (including shape and materials used in construction) and pedestrian factors including height, age (especially in regard

to the elderly – 18% loss of strength for compressive loading of femur from 20 – 39 year old age bracket to 60 – 89 year old age bracket (McElhaney et al, 1976)), gender (male femur is typically 20% stronger than female under compressive loading), orientation with respect to vehicle and pedestrian movement at time of impact (standing still, walking, running).

Foret-Bruno et al (1998) compared the incidence of serious pedestrian injury between vehicle-pedestrian collisions involving older vehicles (vehicle models from 1974-1983) and newer vehicles (post 1989) and noted a generally insignificant fatality rate difference between vehicle impacts involving older and newer vehicles. What was noted, however, is a significant reduction in leg injuries: an 85% reduction in femur fractures and a 23% reduction in tibia fractures. As noted by Stevenson and Raine (2003) leg fracture may correspond to a decrease in head injury potential from ground impact. Certain newer vehicle designs which decrease the incidence of leg-fracture may well result in an increase of more serious pedestrian injury and fatality due to the designer's lack of awareness regarding pedestrian kinematics following the initial impact.

An extreme example of pedestrian injuries affecting kinematics are multiple impact collisions, where the pedestrian has been struck by one or more vehicles more than once (Karger et al, 2001). Injuries from the first impact, combined with an often prone pedestrian orientation on the road, can seriously affect the kinematics of the pedestrian during subsequent impacts. Such accidents are often very difficult to reconstruct and the injury patterns difficult to interpret. Karger et al found that upper spine fractures and neck injuries were often the best indicators of multiple vehicle-pedestrian collisions where a primary impact of an erect pedestrian was followed by a secondary impact of the then prone pedestrian, as such injuries were uncommon in pedestrians that were prone during all collisions.

4.7 Pedestrian Injury Modelling

4.7.1 Traditional Methods

Traditional methods of vehicle-pedestrian impact modelling have used impactor tests (Konosu et al, 2000), dummies (Kuhnel, 1974; Kerrigan et al, 2005), volunteers and cadavers (Kerrigan et al, 2005).

Impactor Tests	Pros:	Adaptable, relatively inexpensive, highly repeatable results (Lawrence et al, 2006).
	Cons:	Prior understanding of pedestrian kinematics necessary, interaction with and influences from rest of body unaccounted for, biofidelity questionable.
Dummy	Pros:	Readily available, ethically acceptable, instrumentable.
	Cons:	Only an approximation of human form and properties, not available in many sizes and/or shapes, full-scale testing expensive and time consuming, only validated for certain loading conditions (Brands, 2001), poor repeatability (Lawrence et al, 2006).
Volunteer	Pros:	Correct tissue properties and muscle tension, high level of feedback.
	Cons:	Only low impact, minimal injury testing, external instrumentation only.
Cadaver	Pros:	Injury experiments possible, moderately easy injury appraisal.
	Cons:	Must be examined for existing damage and or defects, difficult to instrument, questionable tissue properties, stretched spine when suspended, absence of muscle tension (head support most affected), usually older specimens, storage is difficult.

4.7.2 Impactor Testing

Examples of impactor test machines used for the evaluation of pedestrian injuries include the EEVC (European Enhanced Vehicle-safety Committee) Headform and Legform and Upper Legform impactors (Konosu et al, 2000). The Headform impactors measure the impact deceleration to derive an HIC value. In the Legform impactors shear displacement and bending angles are measured and correlated to injury parameters.

EuroNCAP (2004) specifies the following manufacturer nominated test zones when assessing the pedestrian protection potential of a vehicle, as can be seen in Table 4.5.

Manufacturer Nominated Test Zone(s)	
Impactor Type	**Notes**
Maximum of 3 Bumper Tests	To be nominated by manufacturer
Maximum of 3 Bonnet Leading Edge Tests	To be nominated by manufacturer
Maximum of 6 Child Headform Tests	To be nominated by manufacturer
Maximum of 6 Adult Headform Tests	To be nominated by manufacturer

Table 4.5 EuroNCAP Pedestrian Testing Manufacturer Nominated Test Zones (Source: EuroNCAP, 2004)

The vehicle preparation, test locations, vehicle marking, impactor design and test procedure are all specified by EuroNCAP.

4.7.3 Pedestrian Dummies

The POLAR-II (Kerrigan et al, 2005) pedestrian dummy is based on the 50th percentile adult human male, height 1.75 m and weight 75 kg. It is manufactured by GESAC, USA with the original research and development funded by Honda Motor Co. Each POLAR-II dummy costs approximately US$1 million. The POLAR-II has biofidelic knees and shoulders, flexible tibia and is highly instrumented. For a full list of instrumentation in the POLAR-II dummy please refer to Table 4.2. POLAR-II was validated using six full-scale tests: 3 tests using cadavers which were compared with 3 tests using POLAR-II. Good biofidelity was identified in the POLAR-II tests. Some issues were identified with the cadaver tests, including lack of muscle tension in the neck and a stretched spine resulting from the pre-impact support mechanism.

Other pedestrian dummy models have also been developed including dummies constructed using components from occupant dummies. A pedestrian dummy developed at Chalmers University was constructed using the head and neck of the Euro-SID (Side-impact Dummy), the thorax and spine of the US-SID, the Hybrid II standing pelvis, Hybrid III extremities (Fredriksson et al, 2001) and three drops of Dr Frankenstein's elixir. This dummy was 1.75 m high and weighed 80 kg. Information relating to the injury measurement capabilities of this dummy does not appear to be

readily available and the original design methodology employed in its construction was not stated.

4.7.4 Volunteer Testing

Research that has used data from volunteer testing for the development and validation for pedestrian mathematical modelling include Untaroiu et al (2005), Anderson et al (2001) and others.

Untaroiu et al conducted volunteer experimentation to better characterise human tissue properties for finite element modelling. Anderson et al used volunteer data obtained from the work of previous researchers to refine the neck model of the Adelaide University Pedestrian dummy.

Many injury parameters, including the Wayne State Tolerance curve have been derived using a combination of cadaver, animal and human volunteer test data (Prasad, 1999).

Because of the damaging and potentially lethal nature of pedestrian impact replication volunteer data that can be applied to pedestrian models is limited. Greater use of data obtained from inadvertent volunteers, i.e. pedestrians involved in vehicle-pedestrian collision, is extremely valuable.

4.7.5 Mathematical Models

A moderately simple mathematical model for estimating the linear and angular head accelerations that occur in a vehicle-pedestrian collision was described by Vilenius et al in their 1993 paper. The model used the stiffness of the vehicle structure impacted, the offset of the centre of mass from the force vector and the mass and moment of inertia of the human head. The accuracy of the model was compared with cadaver testing. Reasonable agreement was found with the linear acceleration values whilst a lack of data precluded an evaluation of the angular acceleration values.

Whilst determining head impact acceleration is useful, the above method requires a reasonable understanding of the kinematics of the collision being studied. Where this information is unavailable or incomplete, full-body mathematical models can be used

to iteratively derive the pedestrian kinematics. Examples of full-body mathematical pedestrian models include (Linder, 2004):

- Chalmers (Yang, 1997)
- MADYMO (TNO, 2001)
- JARI (Japan Automobile Research Institute)/JAMA (Japan Automobile Manufacturers Association) (Konosu, 2002; Neale et al, 2003; Sugimoto and Yamazaki 2005)
- Adelaide University (Anderson and McLean, 2001; Anderson et al 2005)
- Honda (Okamoto et al, 2000; Shin et al, 2006)

Partial-body mathematical human models of note (and relevant to this thesis) include:

- WSUHIM/WSUBIM (Wayne State University Head/Brain Injury Model) (Zhang et al, 2001 & 2003).
- ULP (Louis Pasteur University) Model (Willinger et al, 1999; Willinger and Baumgartner, 2003).

The benefits of mathematical human models for injury appraisal include:

- Flexibility in experimental and loading conditions
- Insight into internal dynamic mechanisms
- Flexibility in human model sizing, shape, gender and other characteristics typical of the actual human population
- Incredible range of possibility for virtual instrumentation

Table 4.6 shows the different instrumentation in the MADYMO Human Model and the POLAR-II test dummy. Both the MADYMO Pedestrian model and the POLAR-II have been validated against full scale cadaver tests (Yang, 1997; 2002; Kerrigan et al, 2005). Some differences are apparent in the instrumentation of the two models with the MADYMO model generally having a somewhat wider range of measurement capability. Exceptions to this include the ribcage and abdomen deflection measurement capability of the POLAR-II dummy. POLAR-II's T12 vertebrae and pelvis accelerometers appear to be matched by similarly located accelerometers in the MADYMO model's upper and lower torso.

Comparison of MADYMO Human Model and POLAR II Pedestrian Dummy Instrumentation			
Measurement Type	Location	MADYMO Human Model Ver 6.3 (Source: MADYMO Human Model Ver 6.3 Manual)	POLAR II Pedestrian Dummy (Source: Rangarajan, 2000)
Velocity	Head C.G.	✓	
	Sternum	✓	
Displacement	Head C.G.	✓	
	Sternum	✓	
	Pelvis	✓	
	Knee	✓	
	Foot	✓	
Acceleration	Head C.G.	✓	✓
	Sternum	✓	✓
	Upper and Lower Torso	✓	
	Upper and Lower Leg	✓	✓
	T12 Vertebrae		✓
	Pelvis		✓
Deflection	Lateral Ribcage		✓
	Lateral Abdomen		✓
Cardan Output (**R**oll, **P**itch, **Y**aw)	Hip	**R, P, Y**	
	Knee	**R, P, Y**	
	Ankle	**R, P, Y**	
Force and **T**orque	Lower Torso	**F, T**	
	Upper and Lower Neck	**F, T**	
	Upper and Lower Leg	**F, T**	
Load Cell (**R**esultant, **L**ateral, **F**orward/ **R**earward, **A**xial)	Lower Torso	**R, L, F/R, A**	
	Upper and Lower Neck	**R, L, F/R, A**	**R, L, F/R, A**
	Upper and Lower Leg	**R, L, F/R, A**	**R, L, F/R, A**

Table 4.6 Comparison of MADYMO Human Model and Polar II Instrumentation

Despite the wide range of measurement capability within the MADYMO model the validated injury parameter set for the pedestrian model is fairly limited and includes HIC, 3 millisecond and Viscous Criterion.

Other full-body mathematical models:

- The JARI model appears to be capable of displacement, velocity and acceleration measurements of the head, hand, pelvis, knees and feet (Konosu, 2002). Whilst this is sufficient to derive HIC and several other head injury parameters there appears to be limited ability to determine the potential for thorax and abdomen injury and extremity joint injuries. Neale et al (2003) compared the kinematics and head impact velocities of the TNO MADYMO pedestrian model, the JARI pedestrian model and full-scale cadaver tests. It was found that the greater biofidelity of the joints of the TNO MADYMO pedestrian model compared to the JARI model resulted in considerable differences in the predictions offered by the two models. The lack of joint biofidelity in the JARI model may have resulted in greater model accuracy in regard to head impact velocity due to the inadvertent simulation of muscle tension. Conversely, the lack of biofidelity of the lower extremities of the JARI model resulted in considerable kinematic differences from that predicted

by the TNO MADYMO model. Inspection of the impact sequence indicated right-femur fracture in the TNO MADYMO model when impacted by a simulated SUV vehicle at 40 km/h. Research by the author suggests that such a fracture is indeed highly likely at that speed in a vehicle-pedestrian collision involving an SUV. The JARI model did not appear to suffer a serious leg fracture and this changes the predicted pedestrian kinematics considerably after 270 ms. This suggests that the JARI model may not be suitable for lower extremity injury simulation. New developments have seen the development of the JAMA (Japan Association of Automobile Association) pedestrian model (Long and Anderson, 2005), a finite element model designed for LS-DYNA and PAM-CRASH solvers (See Chapter 3, Section 3.3.1 and Section 3.3.3).

- The Adelaide University model was designed with a focus on head impacts. Its neck model was based on the findings of human volunteer tests (Anderson and McLean, 2001) in order to provide better biofidelity. Both linear and angular head acceleration can be recorded (Anderson et al, 2005). It has been validated using the results from cadaver tests, particularly in regard to femur and pelvic fracture.
- A finite element model developed by Toyota R&D Labs and Toyota Motor Corporation called THUMS (Total Human Model for Safety) (Sugimoto and Yamzaki, 2005; Snedeker et al, 2005). THUMS has been designed for use in the PAM-CRASH environment and has been validated using instrumented cadavers.
- A finite element model of the POLAR-II dummy is under development (Shin et al, 2006). Due to POLAR-II's high cost the ability to accurately simulate the crash-test dummy has obvious cost-benefits. Because it is not a human model current finite element methods should be able to replicate the dummy with a high degree of accuracy. However, once finite element models of human bodies are sufficiently accurate the need for POLAR-II and its corresponding mathematical model will be negated.
- The WSUHIM (Wayne State University Head Injury Model) model, an FE human head model, was developed using brain injury data from people injured whilst playing American football (Zhang et al, 2001 & 2003). It can model the effect of an impact on intracranial pressure distribution and stress and strain

throughout the brain, as well as linear and rotational acceleration. The researchers at Wayne State University believe that too much attention is focused on brain acceleration as the predominant parameter in brain injury and that more attention needs to be paid to intracranial pressure and brain stress and strain.

- The ULP (Louis Pasteur University) Model (Willinger et al, 1999; Willinger and Baumgartner, 2003) was created to address the perceived deficiencies of the Head Injury Criterion (HIC). The ULP Model is a finite element model of the skull and brain which models both the interaction of the skull and brain using fluid-structure interaction and skull damage from bone fracture. Injury potential is determined from intracranial pressure, Von Mises stress and cerebral-spinal fluid internal energy (CSFIF). When evaluating motorcyclist head injuries, Von Mises stress was found to be a good indicator of concussion, CSFIF was noted to predict sub-dural haematoma and the FE model accurately forecast skull fracture.

Anderson and McLean (2001) compared the head-impact speed using the JARI, MADYMO and Adelaide University full-body mathematical pedestrian models in simulated collisions with three different vehicles and two different pedestrian postures. The vehicle shapes represented were a flat-fronted vehicle, a passenger car and an SUV. Anderson obtained the most consistent results across the different pedestrian models and postures for simulations using the passenger car model. In these cases the head impact speed varied between 22% and 82% for a given impact speed. For simulations using the SUV model, the head impact speed predicted by the different pedestrian models varied by between 130% and 210% for a given impact speed whilst for the flat-fronted vehicle the head impact speed for a given impact speed varied by between 76% and 200%. Based on these results there are several possible conclusions:

- The models are inaccurate
- Head impact during a vehicle-pedestrian collision is highly variable, particularly for vehicles with a relatively high leading bonnet edge.
- A combination of the above

Anderson concludes by stating the need for further investigation.

4.7.6 Comparison of Mathematical Modelling and Real-World Pedestrian Injuries

Most studies comparing mathematically modelled, experimentally replicated and actual vehicle-pedestrian collisions focus on the kinematics of the pedestrian. Whilst this is undoubtedly useful, particularly from the viewpoint of the litigators, research on the simulation and experimental replication of pedestrian injuries provides valuable insight into the mechanisms of pedestrian injury and the development of potential methods of pedestrian injury reduction.

Coley et al (2001) scaled a 50^{th} percentile male pedestrian human model to reconstruct a real-world accident involving a small female. To validate their methodology a similarly sized scaled model was created and validated against experimental cadaver testing conducted by Ishikawa (1993). The real-world accident involved a pedestrian struck by a car that may not have had its brakes fully applied. The pedestrian was then thrown some 10.8 metres with Police calculations estimating the vehicle impact speed to be between 11.1 to 11.6 ms^{-1}. Serious injuries incurred by the pedestrian included a large subdural haemorrhage (bleeding between the dura (outer brain membrane) and the middle brain membrane) (AIS 5), an extensive subarachnoid haemorrhage (bleeding between the middle brain membrane and the brain itself) (AIS 3) and a tension pneumothorax (collapsed lung) (AIS 5) which in conjunction resulted in death. Minor injuries included AIS 2 leg injuries. The vehicle was modelled in MADYMO using 23 multibody ellipsoids. The pedestrian model was assigned a walking speed of 3 ms^{-1}. The simulation result produced AIS 2 leg and pelvic injuries and AIS 5 thoracic and head injuries. It did not appear that the authors attempted to confirm vehicle impact speed versus pedestrian throw distance.

Liu and Yang (2001) created scaled multibody models to represent children of various ages. Liu and Yang noted that pedestrian versus vehicle compatibility can influence the injury outcome to a large degree and that this was especially evident in a vehicle-pedestrian collision involving a small child (Sturtz et al, 1976; Ohashi et al, 1990) where mortality rates for children aged 6 or less were noted to be considerably higher than those involving children aged 9 years or older. Yang's validated 50^{th} percentile male multibody model (Yang et al, 2000) was scaled to represent 3, 6, 9 and 15 year

old children. Two cases were simulated. In the first case vehicle impact speed and throw distance were well documented and the simulation was found to be in agreement. Head injury was noted in the simulation but did not appear to be correlated to the real-world injury. In the second case it would appear that impact speed was uncertain and that a series of simulations were conducted to ascertain vehicle impact speed. Wrap-around distance, head strike location and pedestrian throw distance were used to corroborate the simulated and real-world outcomes in both cases. Injury correlation was noted to be good but details were omitted.

Stammen and Barsan-Anelli (2001) used MADYMO to reconstruct a vehicle-pedestrian collision in terms of both pedestrian trajectory and injury. The pedestrian was struck from behind whilst jogging and received an AIS 1 head injury but did not lose consciousness. Stammen and Barsan-Anelli's initial expectations of accurate results using approximated vehicle characteristics and pedestrian posture seem somewhat optimistic. Stammen and Barsan-Anelli discovered that both an accurate vehicle shape, with correct material properties and an accurately positioned pedestrian (including upper extremity placement) were needed for the simulated head injury to match the inflicted injury. Once the correct parameters were used in the simulation an HIC of 865 was simulated, which is consistent with an AIS of 1.

Linder et al (2005) used MADYMO 4.4.1, Easi-CRASH and Yang's pedestrian model to reconstruct six vehicle-pedestrian accidents with a specific focus on the accuracy of head injury simulation. One of the simulated vehicle-pedestrian collisions involved two pedestrians, giving a total of seven simulations. Five of the simulations predicted the pedestrian head injury with a good degree of accuracy (See Figure 4.3). Of the two cases where the simulation did not accurately determine the actual head injury it would appear that the modelling approach could not accurately replicate the specific circumstances peculiar to these two events. In case 2b the pedestrian had been forewarned by the impact of the pedestrian in case 2a and was able to prepare for the collision. This preparedness resulted in a remarkable difference between the head injuries received by the two pedestrians in case 2. The pedestrian model employed in the study was not able to respond in the same manner as the actual pedestrian in case 2a and as such the simulated head injuries were too severe. In case 4 the HIC value from the simulation is well under 1000 and is not inconsistent with MAIS 0.

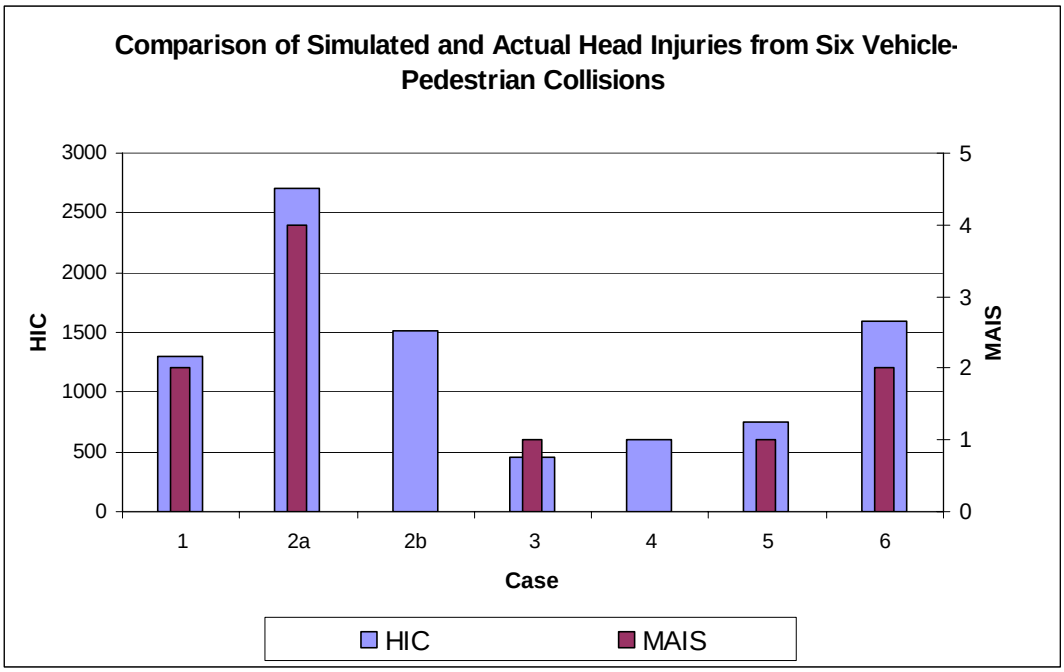

Figure 4.3 Comparison of Simulated and Actual Head Injuries from Six Vehicle-Pedestrian Collisions (Source: Linder et al, 2005)

Whilst mathematical modelling allows for pedestrian movement, orientation and the capacity for scenario-specific characteristics (size, shape, gender, age) it is obvious that these factors need to be correctly applied. Thus, whilst mathematical modelling of pedestrian injuries can be highly accurate, the results are only dependable if the necessary inputs are sufficiently accurate.

Scope for further improvement of mathematical models may include pedestrian models with artificial intelligence so that pedestrian response, particularly muscular, before and during the collision is correctly modelled. Because the mathematical models have been validated against cadaver testing it may be reasonable to assume that the mathematical models more closely resemble cadavers than living humans. With the lack of muscle stiffness, particularly in the neck as noted previously, this leads to the concern that the models may not correctly predict human kinematics and injury patterns in situations where the pedestrian has reacted in some manner to the impending collision (as per Linder's case 2a).

The more extensive use of actual vehicle-pedestrian collision data to validate mathematical human models may address some of these issues.

4.8 Pedestrian Injuries as Accident Reconstruction Parameters

Teresiński (2001a) and Mądro examined the knee joints of 357 pedestrians that received fatal injuries as a result of a vehicle-pedestrian collision. By comparing knee injury to known information regarding pedestrian orientation at time of impact and vehicle type, Teresiński was able to identify consistent ligament damage and bone damage/bruising patterns thus adding knee damage to the reconstructionist's toolbox.

Mądro (2001) and Teresiński also produced a paper on the use of pedestrian neck injuries as a reconstruction tool. It was discovered that neck injury from vehicle impact was more complicated than knee injury but with sufficiently careful inspection some deductions regarding direction of impact could be made from damage to the cervical vertebrae ligaments.

The same authors produced a third paper in 2001 (Teresiński, 2001b) on the examination of ankle injuries resulting from fatal vehicle-pedestrian collisions. It was discovered that close examination of ankle joint injury, including dislocation, bone fracture and ligament damage could be useful in determining both direction of vehicle impact and height of impact on the pedestrian, particularly when injuries are apparent in both ankles.

In 2002 Teresiński and Mądro summarised their findings with a paper that examined the combined use of all the common pedestrian injuries to reconstruct the direction of impact for a vehicle-pedestrian collision. Injury parameters examined included:

- Traditional pedestrian evidential injuries: skin detachment, crushed bone and soft tissue and fragmentation of body parts
- Soft tissue 'bumper' injuries
- Knee, ankle, spinal and pelvic injuries
- Neck muscle damage - Sternocleidomastoid muscle (front of neck along both sides) and Scalene muscle (side of neck) damage
- Lower extremity and pelvic fractures

The error risk was defined as the percentage of cases where the deduced impact direction was different to that indicated by other evidential material. Hip dislocations were found to have negligible error risk whilst deductions based on ankle injuries,

muscle injuries and bending fractures of the lower extremities were found to have minimal error risk (less than 5%). Moderate error risk (12%) was found for the traditional pedestrian evidential injuries. High error risk (between 15% and 21%) was associated with non-bending lower extremity fractures and spinal and pelvic fractures (not dislocation). Cases involving multiple vehicle-pedestrian collisions (eg impact with a vehicle followed by subsequent run-over by the same or different vehicle) and impacts involving initially prone pedestrians were not included.

4.9 Discussion and Conclusion

There is much potential to model injury incurred by the human body as a result of a vehicle impact using computer simulation. However, the accuracy depends not only on how well we can model the human body but also depends on our understanding of the underlying injury mechanisms. As there is still much to be learnt about many injury types, particularly head injury (Willinger et al, 1993 & 2003; Zhang et al, 2001 & 2003), the ability to successfully model such events in all circumstances is still in its infancy. However, advances in using FE models to correlate energy, stress and strain to head injury do appear to hold more promise than relying solely on linear acceleration (or even a combination of linear and rotational acceleration). MADYMO's multibody human model does have its limitations in comparison to FE models but that does not preclude its usefulness as a tool as long as these limitations are acknowledged.

The ability to successfully simulate pedestrian injuries following a vehicle impact has been demonstrated by a number of authors (Stammen and Barsan-Anelli, 2001; Coley et al, 2001; Liu and Yang, 2001; Linder et al, 2003), however, they did not appear to make the most of the injury prediction capability afforded by simulation to assist in reconstructing the accident, instead often basing the simulation parameters on the calculations performed by the investigators using traditional vehicle-pedestrian accident reconstruction methods. In these instances it would appear that there were missed opportunities for the validation of an accident reconstruction through the application of multiple methods of analysis (i.e. not just impact speed versus throw, but also correlation to the different injuries sustained).

The next chapter will examine the application of MADYMO's injury prediction capabilities to multiple methods of analysis of vehicle-pedestrian accident reconstruction and the influence this has on the dependability of the reconstruction.

Chapter 5

Using MADYMO's Injury Prediction Capabilities for Accident Reconstruction

5.1 Introduction

In this chapter the two case studies from Chapter 3 are analysed from an injury perspective. The material in this chapter describes the use of MADYMO's injury prediction capabilities to provide sufficient injury correlation to corroborate the vehicle speed range(s) at impact originally determined using traditional vehicle-pedestrian reconstruction methods, such as pedestrian throw distance analysis as described in Chapter 3.

The injuries incurred during three separate events are analysed:

- pedestrian struck by a large, slow-moving SUV-type vehicle
- pedestrian struck by a typical vehicle at moderate speed (20 to 35 km/h)
- pedestrian overrun by a typical vehicle

The first event relates to one case study described in Chapter 3, the second and third events are separate stages from the other case study. More information on the case studies can be found in Appendix III.

For the pedestrian impacted by the SUV, the injury analysis and correlation will focus on the minor upper body and severe head injuries, whilst for the pedestrian impacted and then overrun by a typical vehicle there will be a predominant focus on the lack of lower limb and serious head injury from the on-road collision, and a focus on abdominal and pelvic/hip injury during the subsequent over-run event.

Pedestrian kinematics and the effect of primary injuries (such as those incurred in vehicle contact) on secondary (usually ground contact) injury severity is examined.

The sensitivity of injury analysis to simulation parameters is evaluated and the differing injury patterns resulting from collisions with typical vehicles versus SUV-type vehicle is also explored.

5.2 Case Study 1: Injury Correlation for Pedestrian Impacted by an SUV-Type Vehicle

5.2.1 Injury Summary

The pedestrian died of a severe brain-stem injury resulting from a direct impact to the back of the head. Of particular note was the lack of other injuries apart from abdominal and leg bruising and some ligament damage to the right lower leg. A summary of victim pathology can be seen in Table 5.1 For more information please refer to the accident report in Appendix III: Case Study 1 - Lyttelton.

Visible Injuries	Head – Right orbital haematoma (‘black eye’). Two superficial abrasions on forehead. Abraded bruise with swelling on back of head.
	Trunk – Bruising on left and right lower abdomen
	Upper Limbs – Abrasions on knuckles of left hand and left elbow. Bruise to outer edge of left forearm.
	Lower limbs – Swelling of left lower leg, bruising on left shin, knee and ankle.
Internal Examination	Skull – Vertical linear fracture at rear, extending 145mm
	Abdomen – Bruising and muscle tears to lower abdomen
	Brain – Two hemorrhages in brain stem
	Lower limbs – Torn ligaments between tibia and fibula
Mechanism of Death	Severe impact to back of head causing lethal damage to brainstem.

Table 5.1 Victim Pathology for Pedestrian Impacted by SUV-Type Vehicle

In this case the distinguishing injuries are a severe head injury and a minor lower abdominal injury. The right orbital haematoma was readily apparent in autopsy photographs, as was the lack of injury to the left eye. It would therefore appear likely that the right orbital haematoma occurred from a direct blow, as opposed to a contrecoup injury (an injury resulting from a blow to the opposite side of the body or organ) which, as the lethal blow was to the middle of the back of the head, would be expected to affect both eyes (Knight, 1985). As noted by Adnani et al (2002) 60% of their case studies who received a blow to the face developed a black eye. It would therefore appear likely, based on the findings of Knight and Adnani et al, that the single orbital haematoma injury was caused by a direct blow to the face.

The abdominal injuries are thought to have resulted from the subsequent run-over of the pedestrian (see Appendix III). The abdominal injury analysis conducted in this Chapter is used to confirm that a more serious injury would not have resulted from primary vehicle contact and as such provide an upper bound for vehicle impact speed.

5.2.2 Simulation Methodology for Injury Analysis

The simulation methodology employed was essentially the same as described in Section 3.8 but with an emphasis on injury prediction (instead of throw distance prediction). Additionally, this section contains a brief investigation into the sensitivity of MADYMO's injury prediction to vehicle and environmental parameters.

5.2.3 Head Injury Analysis

Figures 5.1 to 5.3 show the resulting head acceleration following an impact with an SUV-type vehicle travelling at 2.8, 3.8 and 4.8 ms^{-1}.

As can be seen in Figure 5.1, with the vehicle initially travelling at 2.8 ms^{-1} the secondary impact with the ground, occurring between 1000 and 2000 milliseconds, results in higher levels of acceleration than the primary impact with the vehicle.

Figure 5.2 shows that with the vehicle initially travelling at 3.8 ms^{-1} it would appear that the head accelerations, again, are generally noticeably greater for the secondary ground contact except for when a vehicle is decelerating heavily, as can be seen in

Figure 5.2. In the latter instance the primary contact head accelerations are considerably greater than for the secondary contacts.

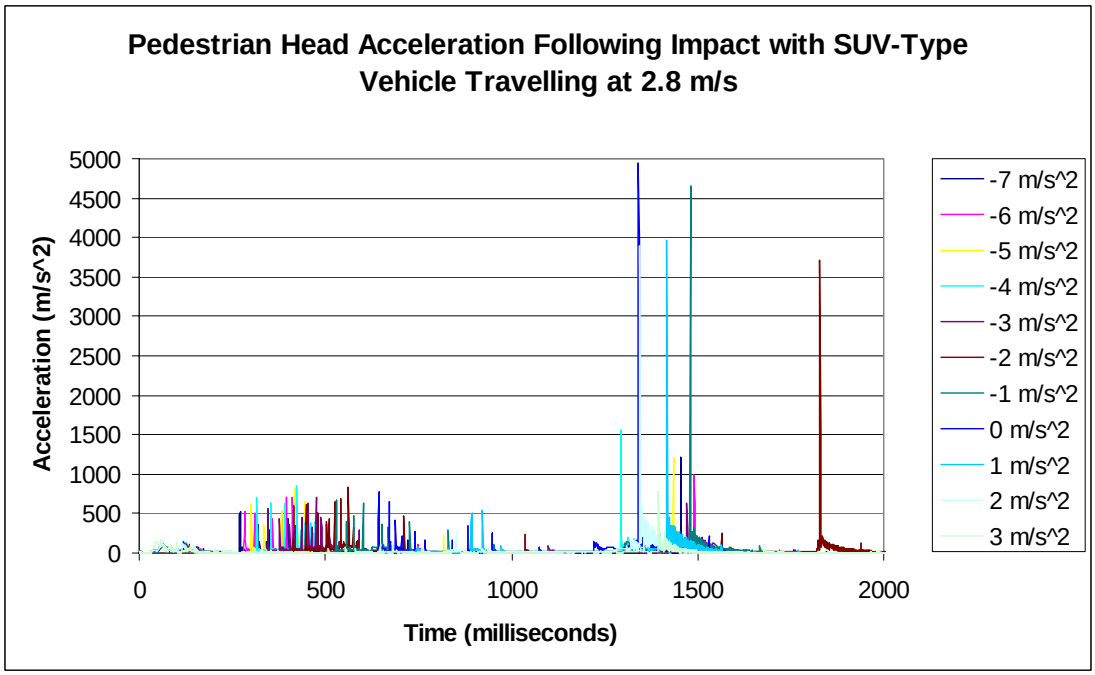

Figure 5.1 Head Acceleration for 5th Percentile Female MADYMO Human Model Struck by SUV-type Vehicle with the Vehicle Initially Travelling at 2.8 ms^{-1}

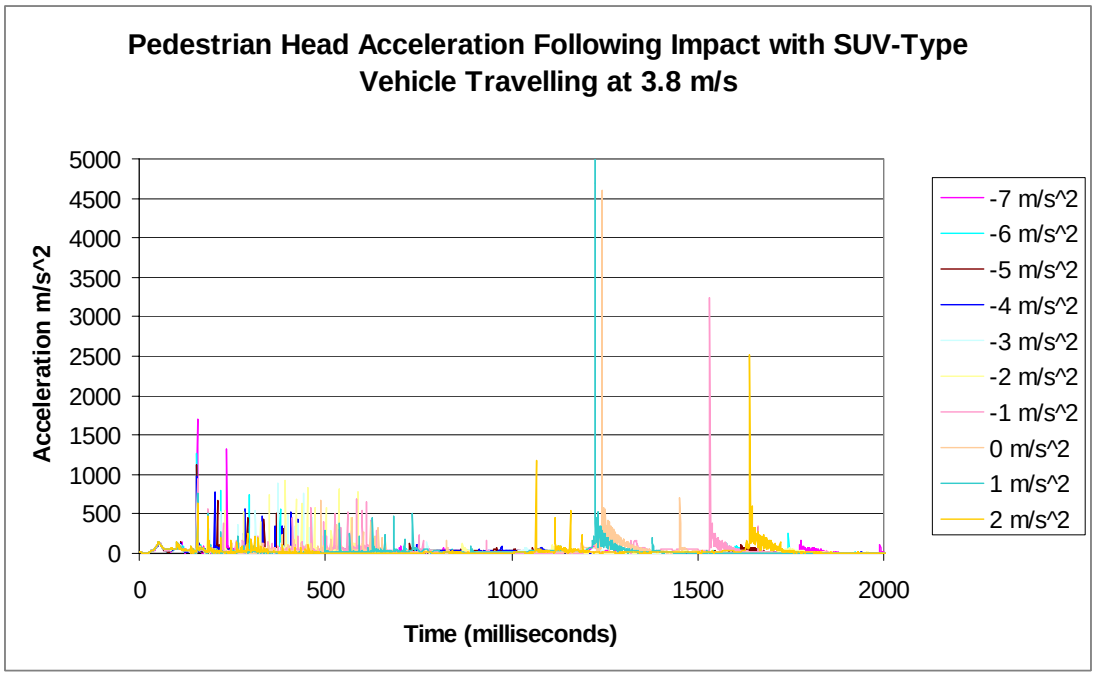

Figure 5.2 Head Acceleration for 5th Percentile Female MADYMO Human Model Struck by SUV-type Vehicle with the Vehicle Initially Travelling at 3.8 ms^{-1}

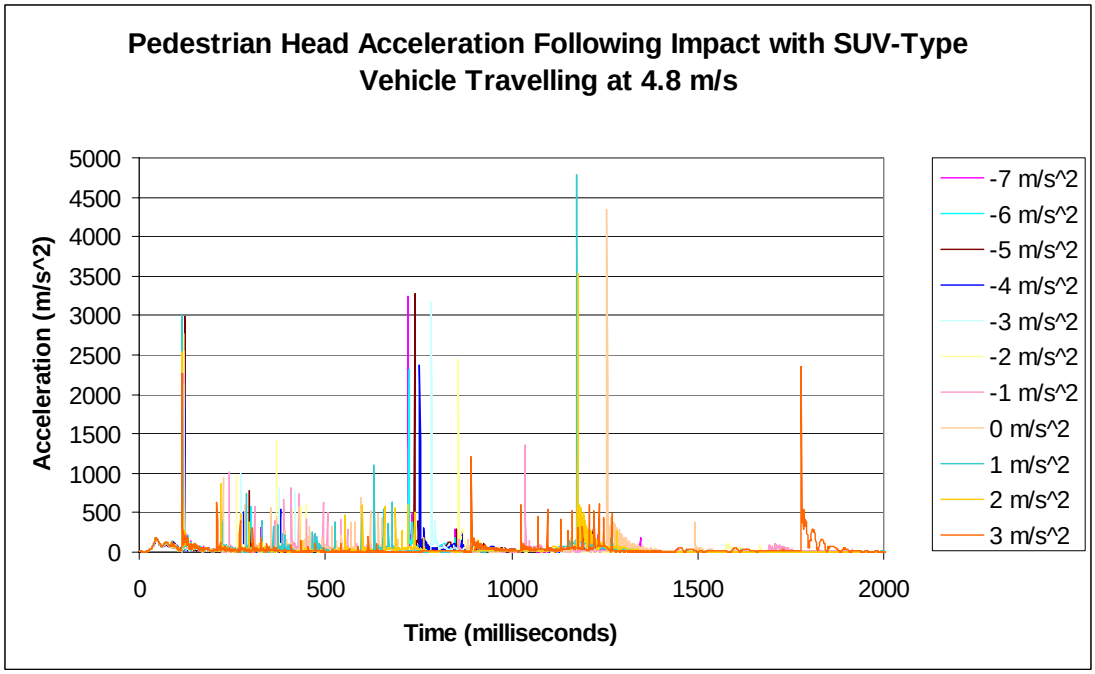

Figure 5.3 Head Acceleration for 5th Percentile Female MADYMO Human Model Struck by SUV-type Vehicle with the Vehicle Initially Travelling at 4.8 ms^{-1}

Figure 5.3 indicates secondary head-ground contact occurring between 1000 and 2000 milliseconds for a vehicle that is either accelerating or travelling at constant speed. For vehicles that are braking the secondary contact generally occurs between 500 and 1000 milliseconds. The head-ground contacts that result from an accelerating or constant speed vehicle tend to be of greater severity than the corresponding head-vehicle primary contacts. For vehicles that are braking the primary and secondary contacts result in similar levels of head acceleration.

It is also interesting to note the differences between the head acceleration resulting from vehicle contact and the head acceleration resulting from ground contact. Figures 5.4 and 5.5 show the duration of head impact for the vehicle and ground contacts, respectively.

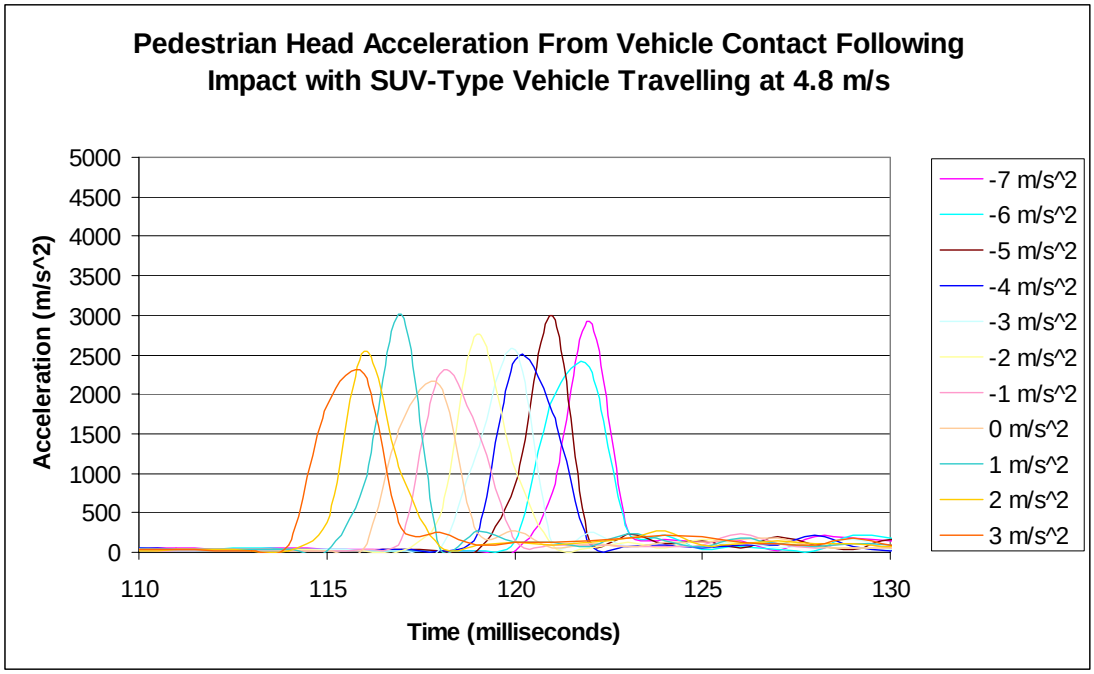

Figure 5.4 Head Acceleration Duration for Vehicle Contact for 5th Percentile Female MADYMO Human Model Struck by SUV-type Vehicle with the Vehicle Initially Travelling at 4.8 ms^{-1}

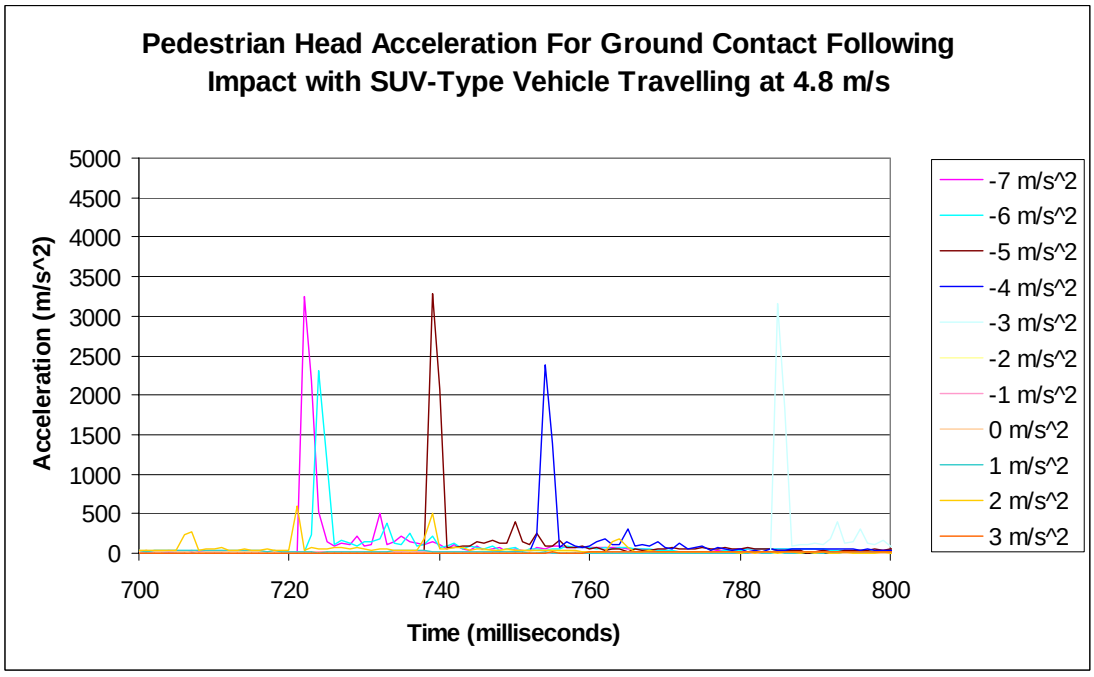

Figure 5.5 Head Acceleration Duration for Ground Contact for 5th Percentile Female MADYMO Human Model Struck by SUV-type Vehicle with the Vehicle Initially Travelling at 4.8 ms^{-1}

In Figure 5.4 the duration of contact for the vehicle contact is noted to be between approximately 2.7 (heavily braking vehicle) and 3.6 (accelerating vehicle) milliseconds. Simms and Wood (2005), in their simulations, displayed a head versus

vehicle contact duration of 20 milliseconds, although their sampling rate did not appear to be very high. Yang (2003), in both simulation and test results, showed a head versus vehicle contact duration of 10 milliseconds. It is suspected that the short duration of contact shown in Figure 5.4 has resulted from the relatively minor, in both intensity and duration, head injury potential resulting vehicle contact for a short pedestrian being struck by a tall vehicle. In such a scenario the minimal rotation required for the pedestrian's head to strike the bonnet also results in a lower head velocity at the time of head-vehicle contact in comparison to a typical, 'bonneted'-type car (Mizuno and Kajzer, 2000).

Figure 5.5 displays an impact duration for ground contact of approximately 2.7 milliseconds. Simms and Wood indicated that the contact duration for head versus ground impact was approximately 3.4 milliseconds. It would therefore appear that head contact duration for a short pedestrian struck by a tall vehicle is not significantly different to a typical-height pedestrian being struck by a 'typical'-shape vehicle. This is not surprising, as the distance to travel to the ground is not significantly different for a short person versus a tall person, whereas the head to bonnet travel distance can be significantly different for a short person versus and tall vehicle and a normal (or tall) person versus a 'typical' vehicle.

To interpret the injury potential of these accelerations the Head Injury Criterion (HIC) was used (see Chapter 4, Section 4.2.1). MADYMO's inbuilt HIC calculator was used to determine peak values and for the determination of other HIC values (such as the HIC for vehicle contact, for a simulation where the greatest HIC was for ground contact) NHTSA's HIC calculator was used (contact Nrd.OcrSoftDev@Nhtsa.Dot.Gov for more information on this tool).

With the variability evident in head acceleration (and corresponding HIC values) it is easier to see trends if averaging is applied over both vehicle acceleration and initial vehicle speed. These results can be seen in Figure 5.6.

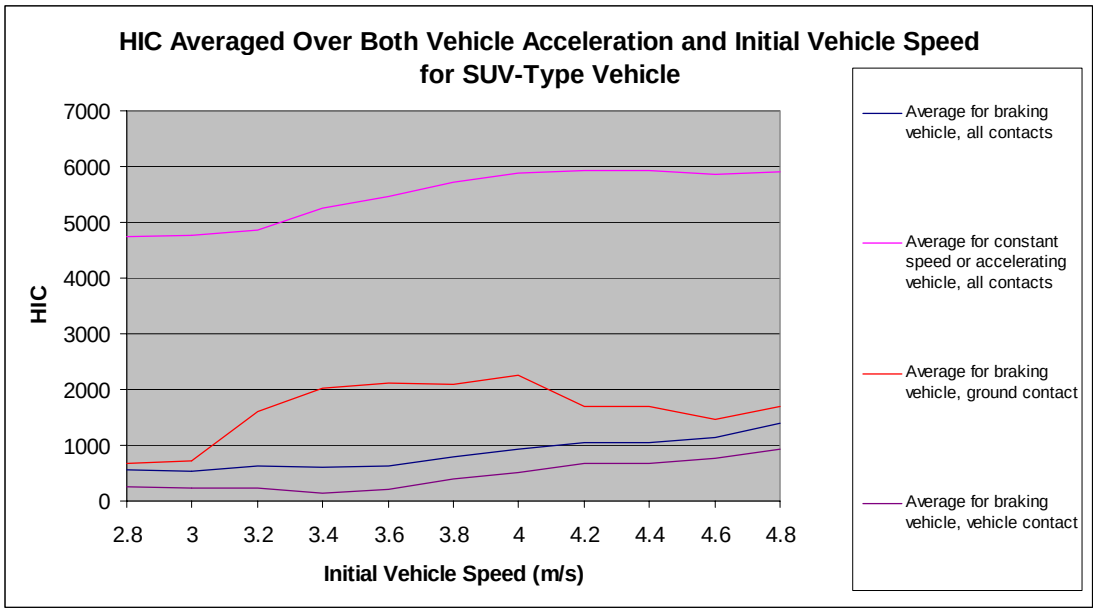

Figure 5.6 HIC Averaged Over Both Vehicle Acceleration and Initial Vehicle Speed

To obtain these results the HIC values were averaged over all the results obtained for either a braking or a constant speed/accelerating vehicle, for each initial vehicle speed. These results were then averaged over an 0.8 ms^{-1} initial speed interval to give a moving average. This method permits trends to be visible which are otherwise masked by the variability in individual HIC results. For a braking vehicle the HIC can be seen to generally increase with initial vehicle speed, from a low HIC value of approximately 500 to approximately 1500 ('Average for braking vehicle, all contacts'). A similar trend is apparent in the results for an accelerating or constant speed vehicle, where much higher HIC values are also evident with an overall HIC average approaching 5500 ('Average for constant speed or accelerating vehicle, all contacts').

The results can be divided according to whether the maximum HIC value resulted from either vehicle and these findings are also shown in Figure 5.6. It should be noted that the average HIC values resulting from ground contact for a constant speed or accelerating vehicle are unchanged from the 'All contacts' results. Additionally there were no matching results where the maximum HIC resulted from vehicle contact for a constant speed or accelerating vehicle The 'braking vehicle/Maximum HIC from ground contact' are greater than the 'all contacts' results whilst the 'braking vehicle/Maximum HIC from vehicle contact' are less. This indicates the increased

injury severity potential of ground contact in comparison to vehicle contact in these scenarios.

According to Prasad and Mertz (1985) an HIC value 2500 correlates to a 100% chance of an AIS 4 or greater head injury using the Mertz/Weber method. Linear regression indicates that there is a 100% of an AIS 4 or greater injury for an HIC value of 2350 or greater. Noting that Mertz and Prasad based their findings on cadaver tests, MacLaughlin et al (1993) established a series of risk curves based on real-world injury data. MacLaughlin et al's results indicated that the HIC threshold for a 100% risk of an AIS 4 injury may be as low as 1500. Therefore an HIC value of approximately 5500 equates to a 100% risk of serious injury with a high probability of such an injury proving fatal.

The high HIC results evident in Figure 5.6 resulted from ground contact. The average HIC resulting from ground contact (where the HIC value for ground contact was greater than for vehicle contact) following an impact with a braking vehicle was less than 2000 whereas following an impact with a vehicle travelling at constant speed it was almost 5500. In comparison, the average HIC value resulting from vehicle contact (where the HIC value for vehicle contact was greater than for ground contact) following an impact with a braking vehicle was slightly over 450 whereas there were no instances of a maximum HIC value resulting from vehicle contact for a constant speed or accelerating vehicle. These scenarios would appear to represent a situation, such as that described by Tanno et al (2000) and Simms and Wood (2005), where a pedestrian involved in a collision with a vehicle with a high-leading edge is most likely to receive the most serious injury from ground contact.

The results shown in Figure 5.6 would appear to indicate that if the vehicle was travelling at less than approximately 3.2 ms^{-1} it would be probable, for an impacted pedestrian to receive the severe head injury indicated in Table 5.1, that the vehicle was either travelling at constant speed or accelerating.

5.2.4 Thoracic Injury Analysis

Thoracic injury potential can be ascertained similarly to head injury potential. Figure 5.7 shows the sternum acceleration of the pedestrian model following an impact with

an SUV-type vehicle. Regardless of the level of vehicle acceleration the secondary impact with the ground, occurring between 1000 and 2000 milliseconds, results in higher levels of acceleration than the primary impact with the vehicle.

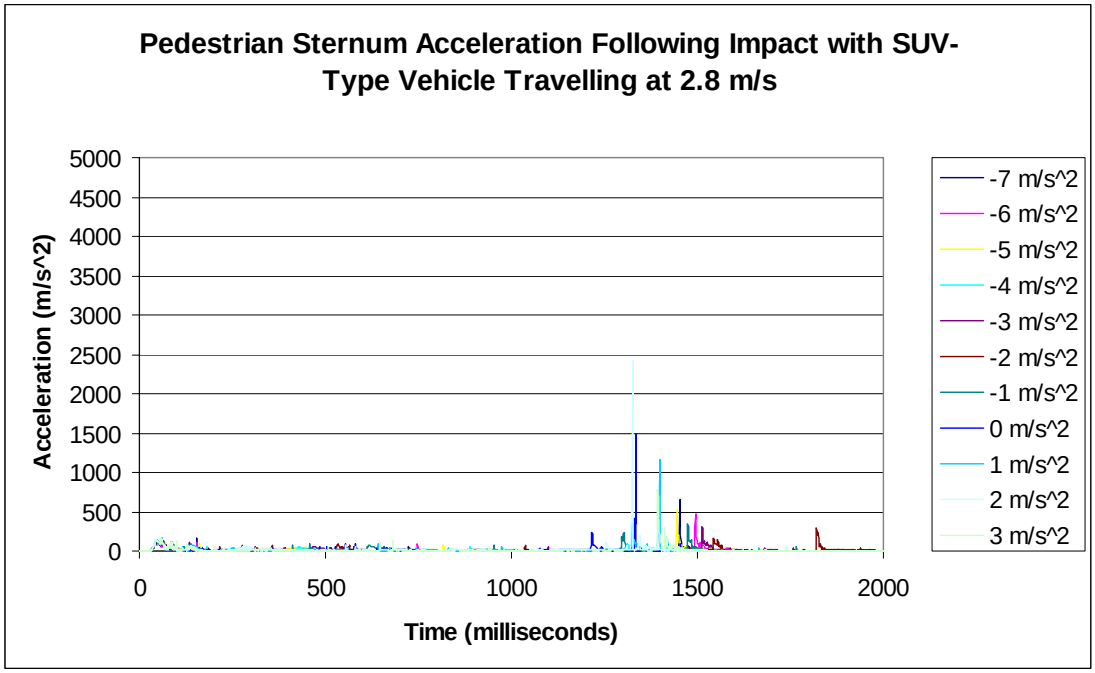

Figure 5.7 Sternum Acceleration for 5th Percentile Female MADYMO Human Model Struck by SUV-type Vehicle with the Vehicle Initially Travelling at 2.8 ms^{-1}

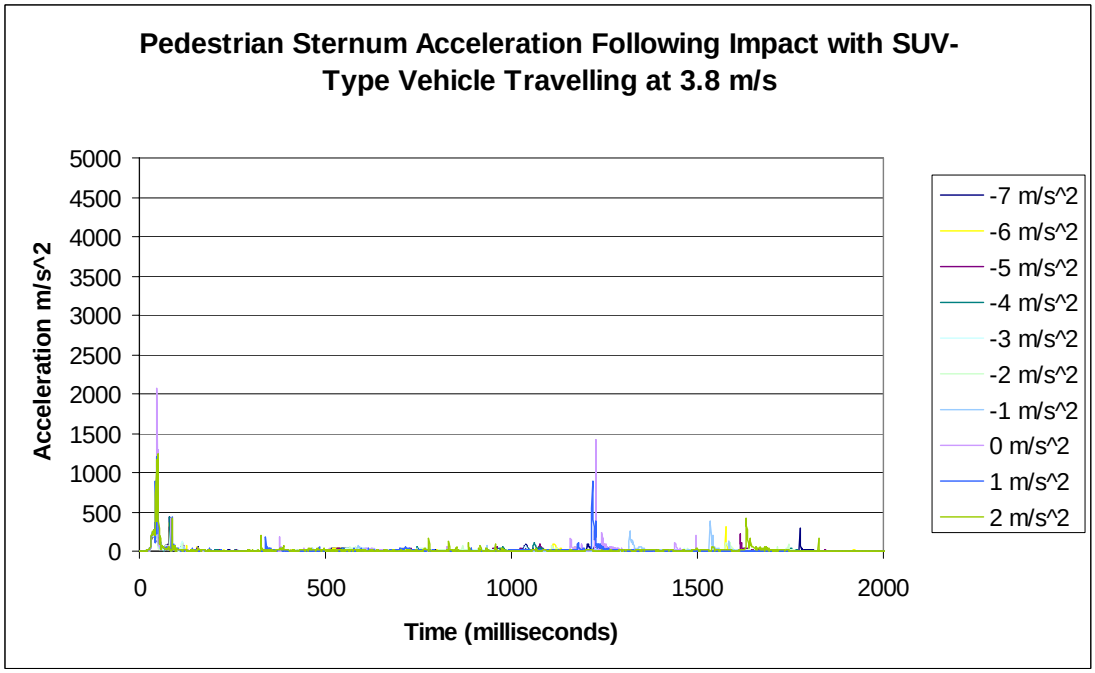

Figure 5.8 Sternum Acceleration for 5th Percentile Female MADYMO Human Model Struck by SUV-type Vehicle with the Vehicle Initially Travelling at 3.8 ms^{-1}

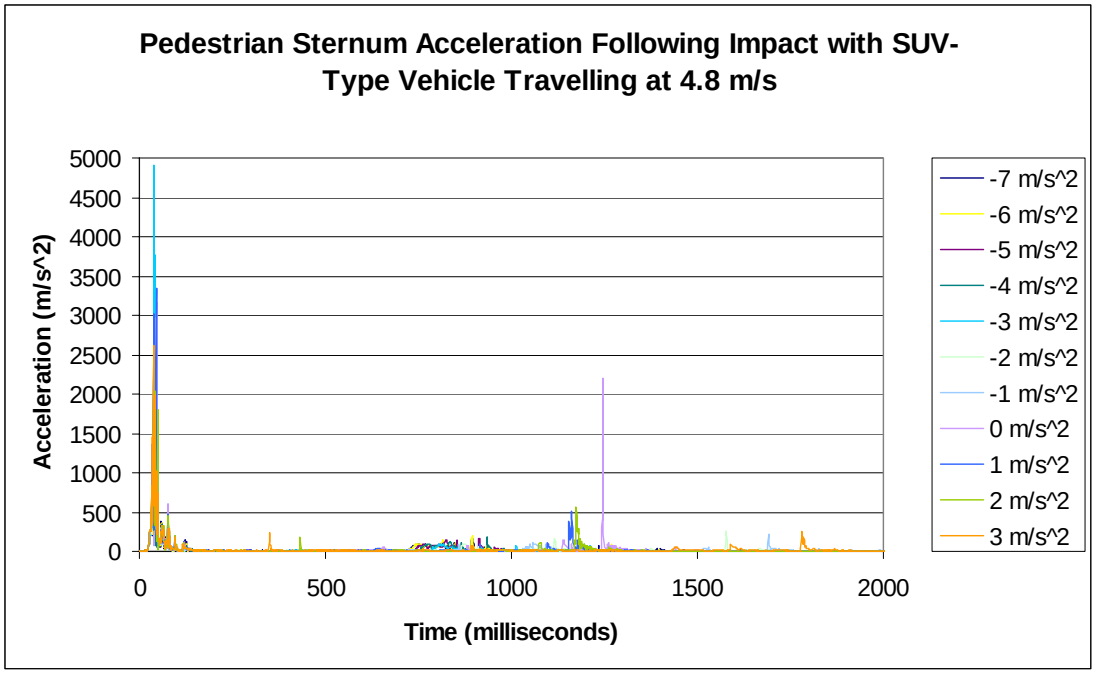

Figure 5.9 Sternum Acceleration for 5th Percentile Female MADYMO Human Model Struck by SUV-type Vehicle with the Vehicle Initially Travelling at 4.8 ms^{-1}

With the vehicle initially travelling at 3.8 ms^{-1} it can be seen in Figure 5.8 that sternum accelerations are similar for both primary and secondary contacts, with primary contact accelerations tending to be slightly higher than the secondary for an accelerating vehicle

Figure 5.9 indicates considerably greater sternum acceleration for primary contact with the vehicle relative to secondary contact with the ground. The sternum primary contact accelerations are also noticeably higher for an initial vehicle speed of 4.8 ms^{-1} in comparison to the sternum accelerations resulting from slower initial vehicle speeds as shown in Figures 5.7 and 5.8.

As is noted in Appendix I, cadaver testing has indicated that a thoracic Viscous Criteria (VC) result of 1.3 ms^{-1} indicates a 50% chance of an AIS injury of 4 or greater. A VC of 1 ms^{-1} is often used as the tolerance limit for blunt frontal thoracic impact (Cavanaugh et al, 1990). The thoracic VC results for a pedestrian impacted by an SUV-type vehicle can be seen in Figure 5.10.

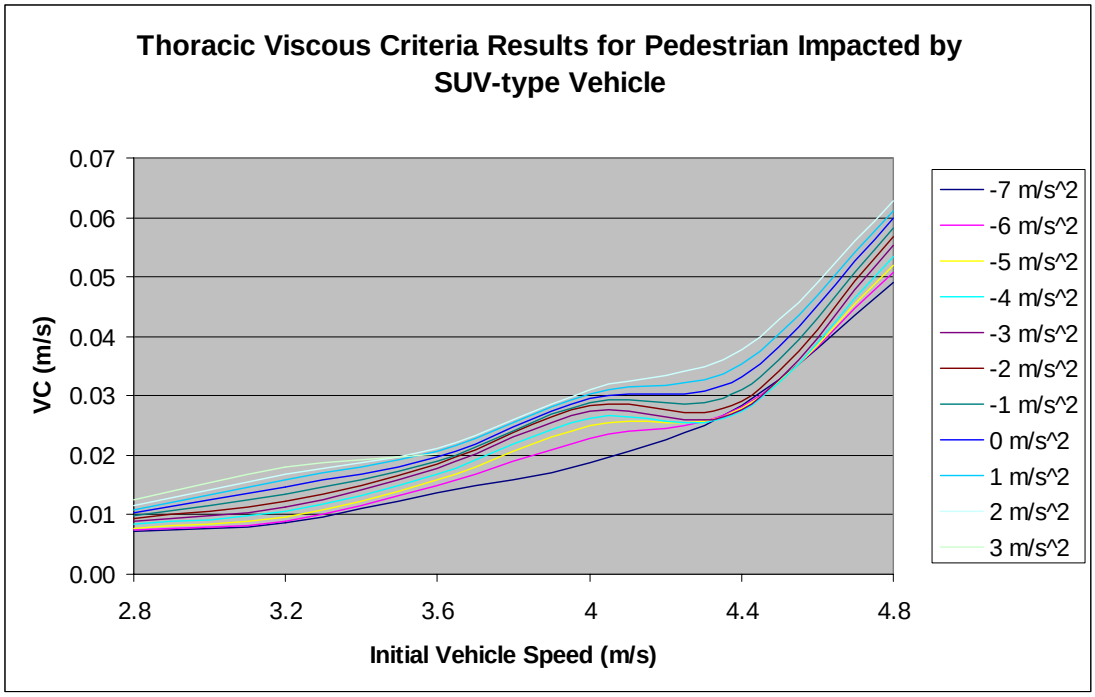

Figure 5.10 Thoracic Viscous Criteria Results for Pedestrian Impacted by SUV-Type Vehicle

For the speed range analysed there would appear to be minimal risk of thoracic injury from vehicle contact. Minor differences in VC are evident for different levels of vehicle acceleration with VC generally increasing with acceleration. VC also appears to increase exponentially with vehicle speed.

5.2.5 Abdominal Injury Analysis

The abdominal injuries described in the coroner's report and summarised in Table 5.1 are consistent with an AIS 1 injury (AAAM, 1990). Exact quantitative data on the mechanisms of abdominal trauma is limited. As noted in the US Department of Transport *Collision Avoidance and Accident Survivability Volume 3: Accident Survivability* guide produced by Calspan Corporation (1993):

> *"A large body of clinical literature has evolved over the years that documents the various forms of injuries produced by blunt abdominal trauma. In contrast, there are very little quantitative data available on the loading conditions, force levels and impact velocities that characterize typical accident situations. To date, animal testing has been the prime method for evaluating abdominal injury tolerance."*

As noted in previous sections a range of mechanisms can be related to injury risk including acceleration, compression, power and force with these mechanisms often being rate-dependant. Quantitative abdominal acceleration tolerance would not appear to be readily available, however, the thoracic acceleration tolerance is taken to be 60 G's for a period not exceeding 3 ms, which is the limit for frontal thoracic acceleration stipulated in FMVSS 208 (1997), and is the loading applied to the entire thorax, including both skeletal and soft tissues.

Alternatively, abdominal injury tolerance to frontal loading can be determined from the force applied to the abdomen. Considerable research has been conducted on the risk of abdominal injury posed by airbag deployment, steering wheel contact and seatbelt loading to vehicle drivers. Hardy et al (2001) conducted a series of tests to determine abdominal injury tolerance to frontal impact by subjecting cadavers to blows from seatbelt impactors, rigid bar impactors and airbag deployment. Johanssen and Schindler (2007) coded the resulting injuries from Hardy et al's tests and, neglecting the seatbelt injuries (which invariably were in conjunction with thoracic injuries, indicating a lessening of the load applied to the abdomen), produced a chart of risk of AIS 3 or greater injury versus frontal abdominal loading, as reproduced in Figure 5.11.

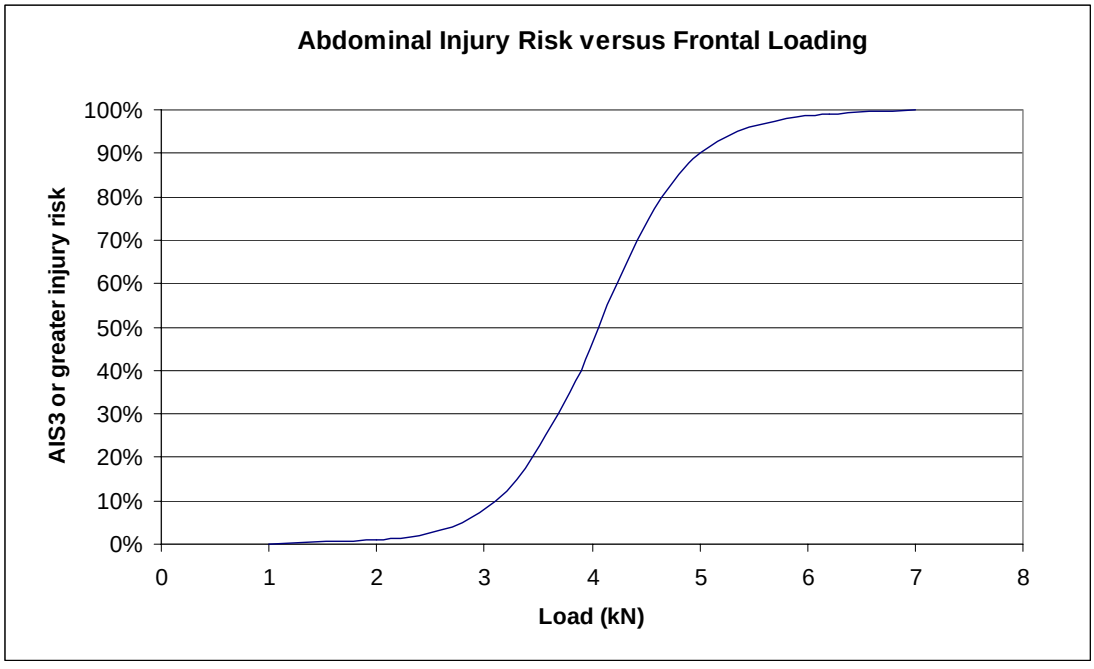

Figure 5.11 Abdominal Injury Risk versus Frontal Loading (from Johannsen and Schindler, 2007; derived from Hardy et al, 2001)

As can be seen, a loading of 4 kN indicates a 50% risk of an AIS 3 or greater injury, whilst a loading of 5 kN indicates a 90% risk of such an injury. A loading of 3 kN or less indicates a low (less than 10%) risk of serious injury.

Assuming that pedestrian injury tolerance is equivalent to that derived from testing designed to evaluate the risk of abdominal injury to vehicle occupants a simulation matrix was constructed to evaluate the influence of impact speed and vehicle acceleration for a vehicle-pedestrian collision involving a SUV-type vehicle and provide an additional correlation to the vehicle speed estimates derived from other pedestrian injuries as well as throw distance.

The simulation parameters used to evaluate abdominal injury potential were as described in Table 3.3. An abdominal force sensor was added to the pedestrian model in an attempt to correlate the injury risk to vehicle speed and acceleration. The validation results for a sensor in this location have not been located for this pedestrian model so the results should be treated as comparative only. Furthermore, the value of such a sensor in a multibody model is questionable, although it should be noted that the structure of the human abdomen, consisting mostly of soft tissues, is considerably more homogenous than the thorax (which contains a considerable skeletal component). Taking this into account, it is quite possible that modelling abdominal injuries using a multibody model is more accurate than modelling thoracic injuries using such a model. Having noted this, it should be pointed out that no abdominal injury criteria are included as standard outputs for the MADYMO pedestrian model, but 3 millisecond criteria (continuous and contiguous) and Viscous Injury Criteria (VC) for the thorax are included as standard.

A simulation matrix of five initial vehicle speeds (2, 4, 6, 8 and 10 ms^{-1}) and five levels of vehicle acceleration (-9, -6, -3, 0 and 3 ms^{-2}) were analysed and the results are shown in Figures 5.12 to 5.16..

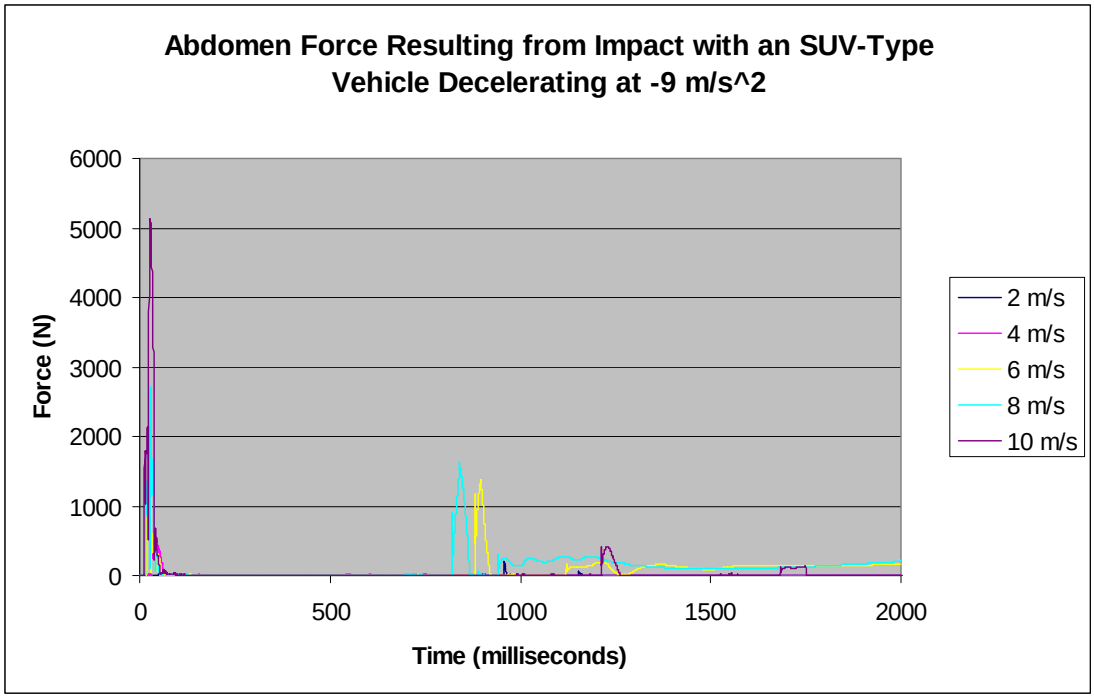

Figure 5.12 Abdominal Force Resulting from Impact with Vehicle Decelerating at -9 ms^{-2}

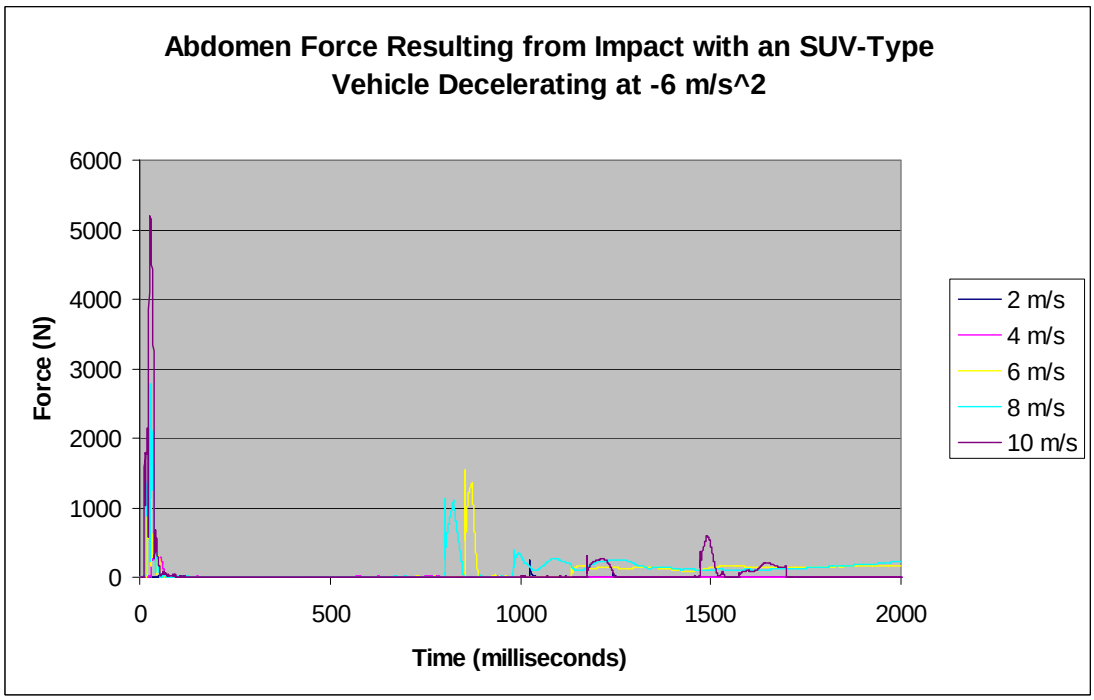

5.13 Abdominal Force Resulting from Impact with Vehicle Decelerating at -6 ms^{-2}

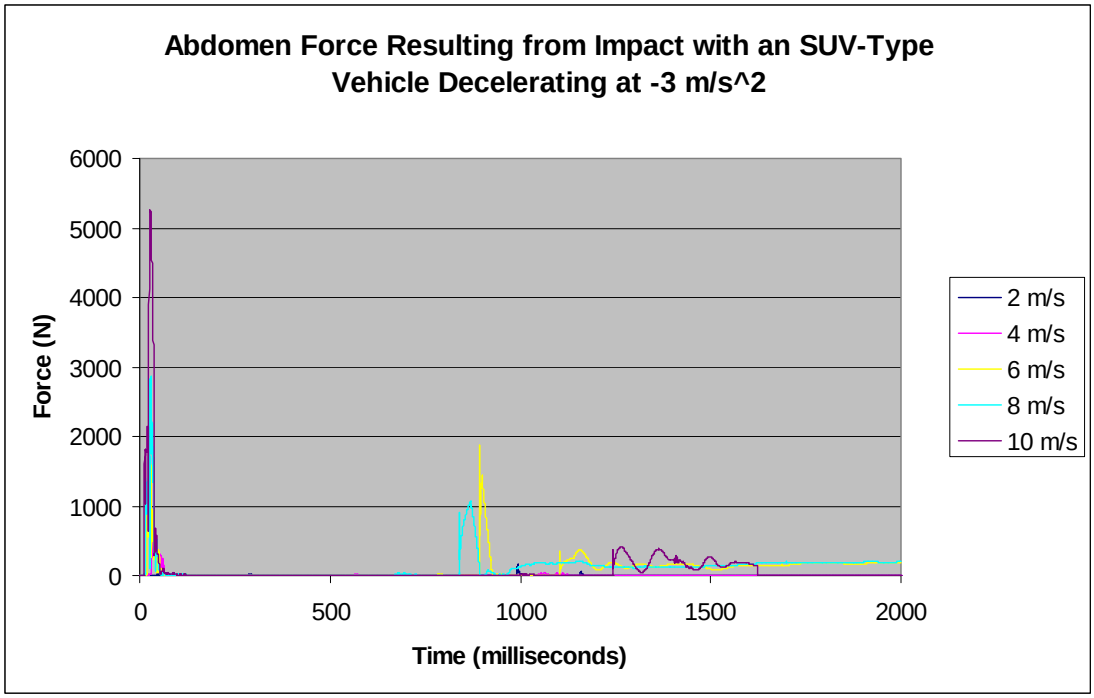

5.14 Abdominal Force Resulting from Impact with Vehicle Decelerating at -3 ms^{-2}

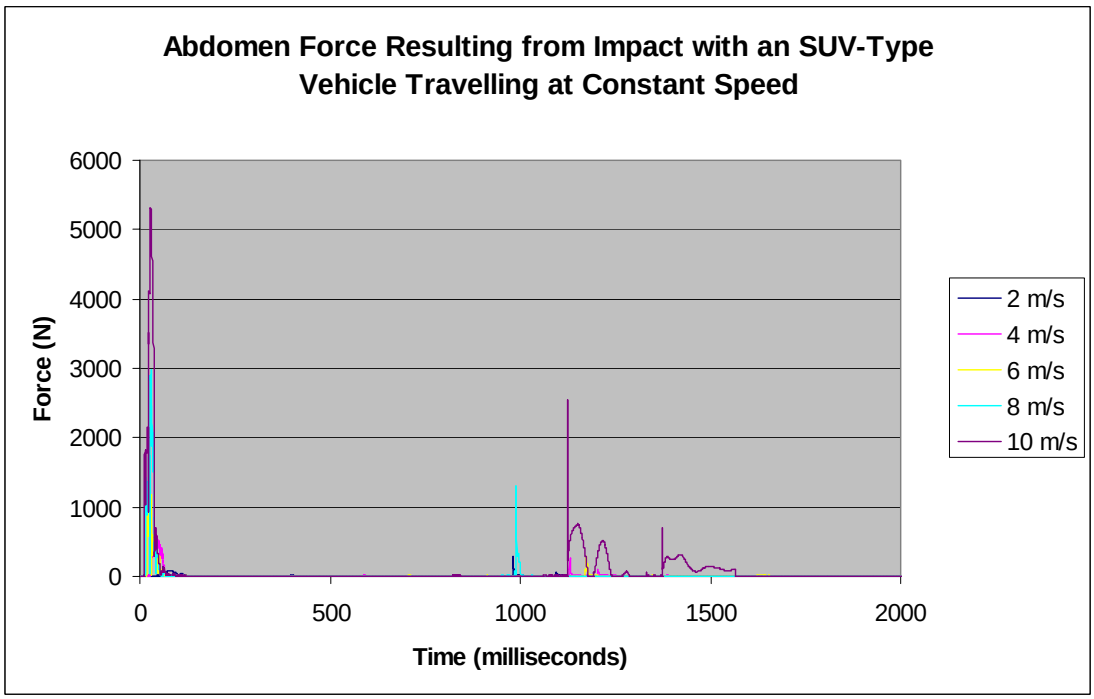

5.15 Abdominal Force Resulting from Impact with Vehicle Travelling at Constant Speed

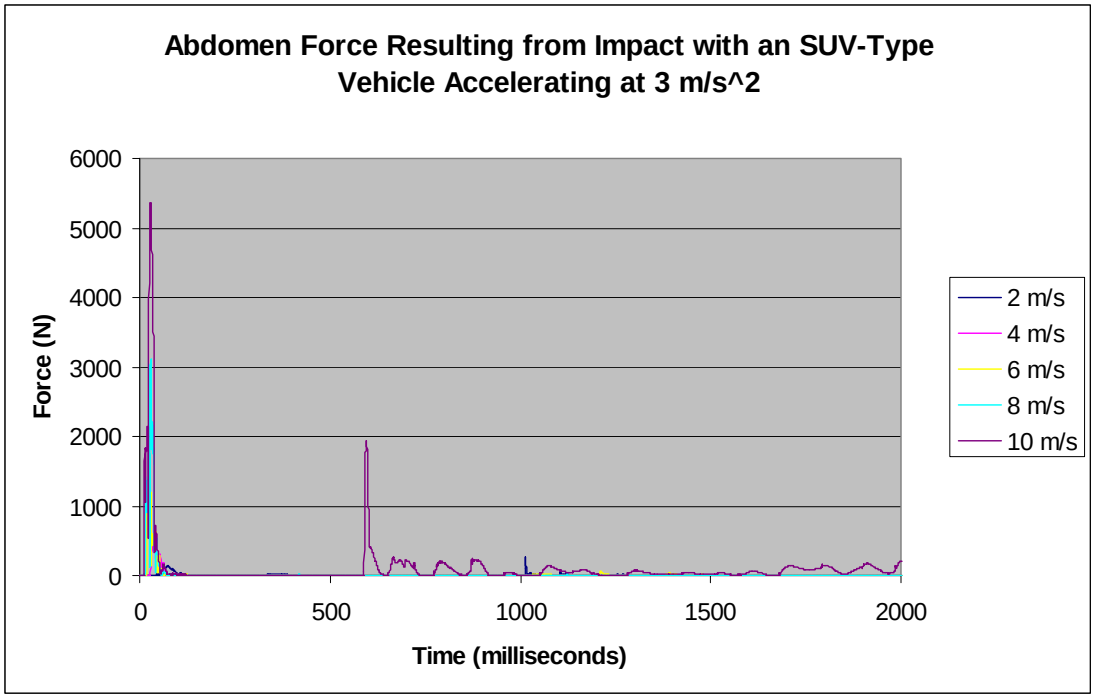

5.16 Abdominal Force Resulting from Impact with Vehicle Accelerating at 3 ms^{-2}

From the results shown in Figures 5.12 to 5.16 it can be seen that the level of vehicle acceleration/deceleration does not appear to significantly influence the results. Vehicle impact speed does appear to positively correlate with abdominal injury risk. A high risk of significant abdominal injury from vehicle contact was only apparent when the vehicle speed was at its highest, namely 10 ms^{-1}. Abdominal force as a result of a vehicle impact at 10 ms^{-1} consistently resulted in over 5 kN of abdominal force whereas impacts with the vehicle travelling at 8 ms^{-1} or lower resulted in approximately 3 kN of abdominal force or less. As noted earlier, a loading of 5 kN indicates a 90% risk of an AIS 3 or greater injury whereas a loading of 3 kN or less indicates a low (less than 10%) risk of serious injury. If the abdominal force measurements are valid then the AIS 1 abdominal injury sustained by the pedestrian in the accident case would appear to indicate that the likely vehicle impact speed was less than 8 ms^{-1} and quite possibly considerably less.

5.3 Observations Regarding Pedestrian Kinematics Post-Impact and Their Influence on Injuries

Figures 5.17 and 5.18 compare the varying pedestrian kinematics for the different speeds. In Figure 5.17 the key aspects of the pedestrian's motion following a 2.8 ms^{-1}

(10 km/h) vehicle impact are shown. With 0 milliseconds representing bumper contact, bonnet contact first occurs at 50 milliseconds. At 250 milliseconds the pedestrian is briefly lifted off the ground and the head contacts the bonnet. By 650 milliseconds the pedestrian has slid down the front of the vehicle and the heels are acting as a pivot on the ground. By 850 milliseconds there is no more contact with the bonnet and the pedestrian is being rotated backwards. At 1050 milliseconds the pedestrian's pelvis makes contact with the ground and the 1130 milliseconds the head strikes the ground also, resulting in an HIC value averaging in excess of 4200 (range 3870 to 4910) for a constant speed or accelerating vehicle. According to Prasad and Mertz (1985) an HIC of this level represents a 100% chance of an AIS 4 or greater injury and is highly likely to be fatal.

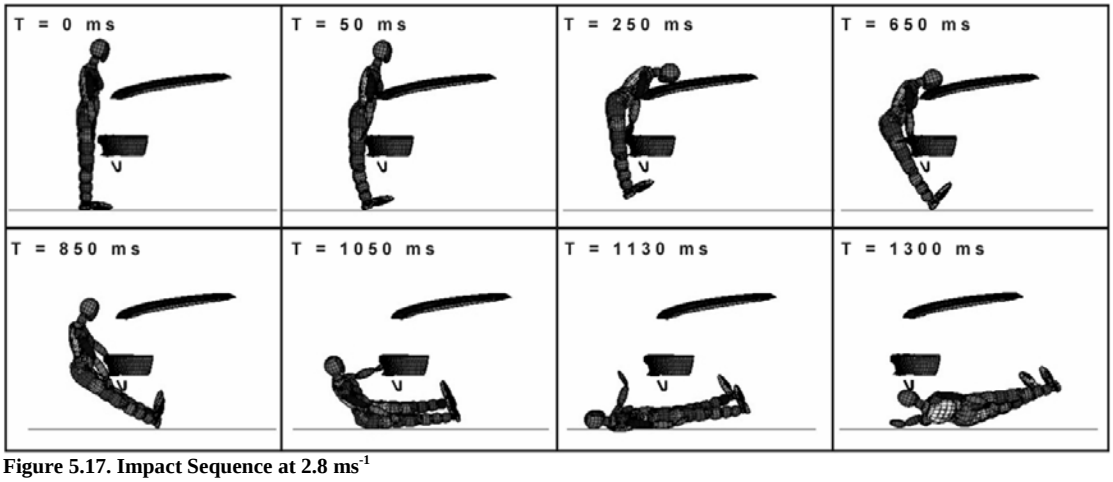

Figure 5.17. Impact Sequence at 2.8 ms^{-1}

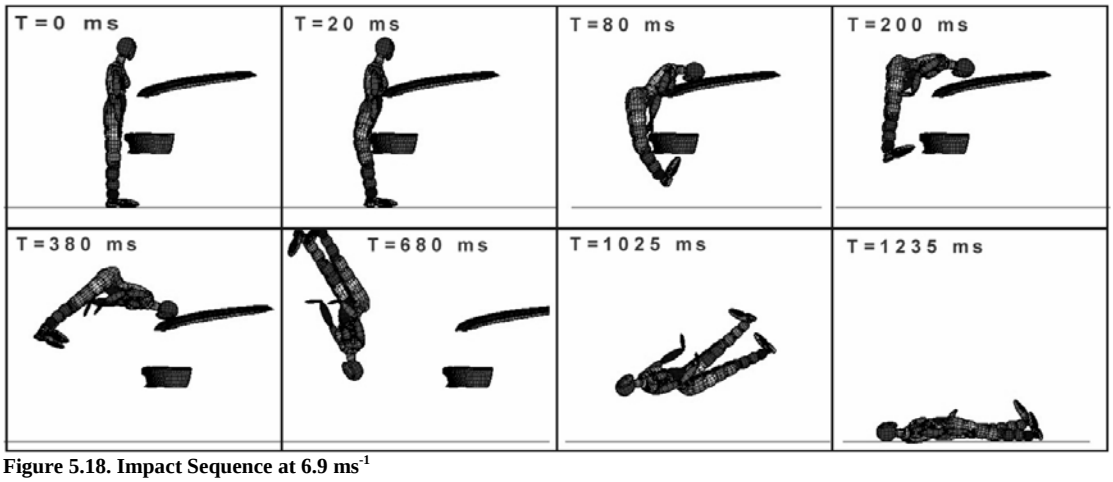

Figure 5.18. Impact Sequence at 6.9 ms^{-1}

By 1300ms the head has rebounded sufficiently for a light contact to occur between the front of the pedestrian's head and the vehicle's towing hook.

Figure 5.18 shows an impact sequence and 6.9 ms^{-1} (25 km/h). Key differences to the 2.8 ms^{-1} impact sequence include the pedestrian being knocked forward, clear of the vehicle, before falling to the ground. The resulting head injuries from ground contact are lower for the 6.9 ms^{-1} than for the 2.8 ms^{-1} impact.

Large differences in injury outcome can even result from minor variations in vehicle impact speed. Figures 5.19 and 5.20 show sequences from vehicle-pedestrian collisions at 4.4 ms^{-1} (15.8 km/h) and 4.8 ms^{-1} (17.3 km/h), respectively.

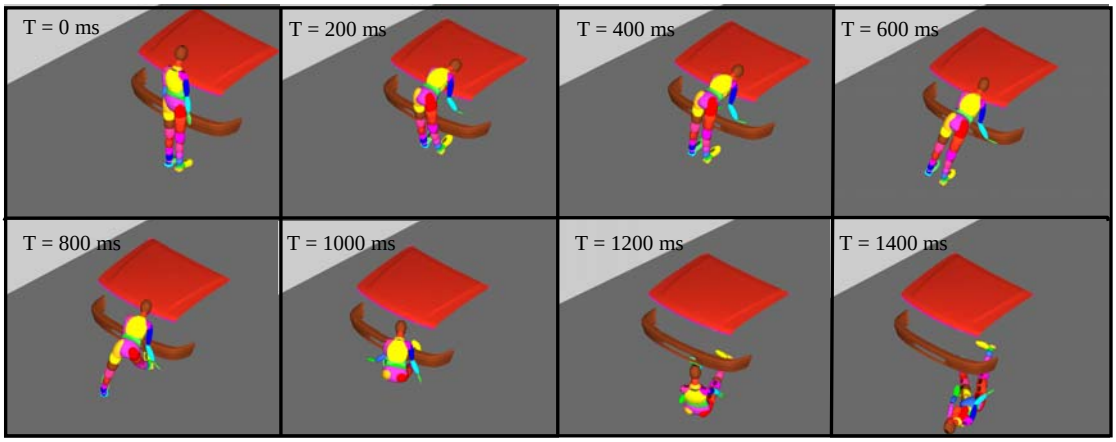

Figure 5.19 Pedestrian Motion Following Impact at 4.4 ms^{-1}

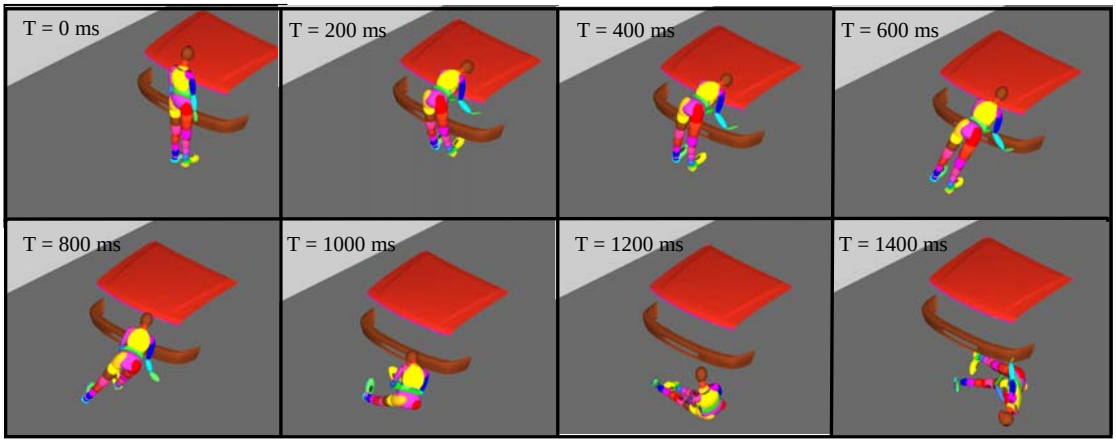

Figure 5.20 Pedestrian Motion Following Impact at 4.8 ms^{-1}

The ground contact following impact resulted in an HIC value of over 5700 for the 4.4 ms^{-1} scenario whilst for the 4.8 ms^{-1} scenario the HIC from ground contact was a

slightly under 1800. Inspection of the kinematics evident in Figures 5.19 and 5.20 indicates that more rotation is imparted to the pedestrian by the 4.8 ms^{-1} collision, resulting in the pedestrian's shoulder hitting the ground before the head causing a considerable reduction in head injury potential.

It is interesting to note a 67% reduction in HIC from a 9% impact speed increase, but such are effects of the variable kinematics during a vehicle-pedestrian collision.

5.4 Sensitivity Analysis

It is good practice to investigate the sensitivity of the results to parameter variance. In this case, neither the ground stiffness nor the vehicle panel stiffnesses were measured directly. Instead values were obtained from literature, as noted elsewhere. In this section a sensitivity analysis is conducted to evaluate the influence of various parameters.

5.4.1 Sensitivity to Other Injuries

In this section the effect and influence of other injuries (such as leg fracture from primary vehicle contact) on subsequent injuries (such as head contact with ground) is examined.

Results where the pedestrian did not fall to the ground during the simulation period were excluded.

The simulation matrix was reduced (in comparison to that used for throw distance evaluation in Chapter 3) to vehicle speeds from 2.8 to 4.8 ms^{-1}, evaluated in 0.2 ms^{-1} intervals versus vehicle acceleration of -7.0 to 3.0 ms^{-2}, evaluated in 1.0 ms^{-2} intervals. Where results in Figure 5.21 are missing it is because no results matched the criteria specified in the chart.

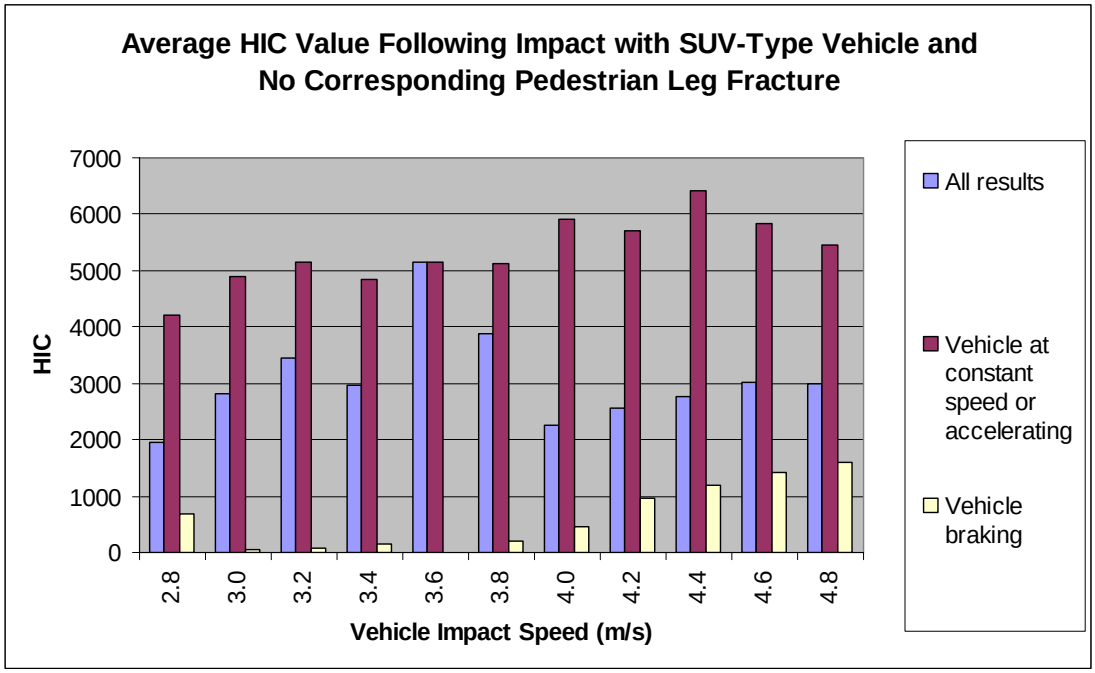

Figure 5.21. Average HIC Value Following Impact with SUV-Type Vehicle and No Corresponding Pedestrian Leg Fracture

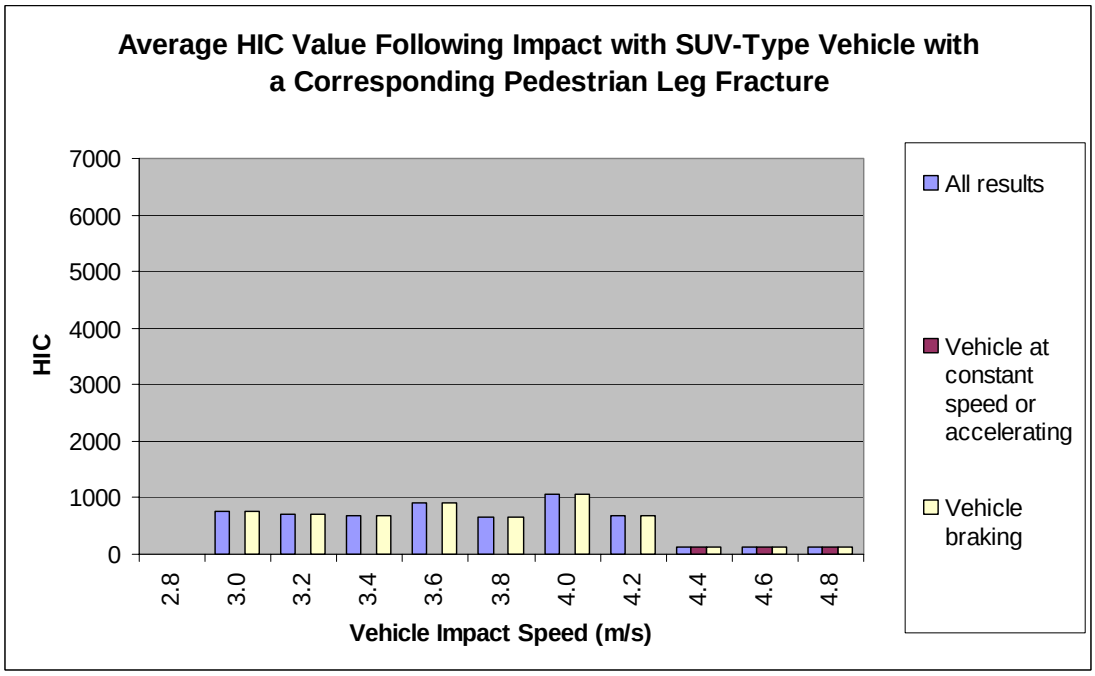

Figure 5.22. Average HIC Value Following Impact with SUV-Type Vehicle with a Corresponding Pedestrian Leg Fracture

Figures 5.21 and 5.22 show a summary of results where average HIC values for scenarios where the vehicle is either braking or accelerating are plotted against initial vehicle speed. In Figure 5.21 no leg fracture were recorded by the pedestrian model,

whereas in Figure 5.22 one or more leg fractures was determined by the pedestrian model. It is evident from these figures that leg fracture has a large influence on the risk of severe head injury.

As shown in Figure 5.21 all results for a vehicle travelling at constant speed or accelerating resulted in an HIC from ground contact of over 2500, with most results (7 out of 10) indicating an HIC in excess of 4000. As noted earlier an HIC value 2500 or greater correlates to a 100% chance of an AIS 4 or greater head injury using the Mertz/Weber method.

The results displayed in Figure 5.22 indicate much lower HIC values with only two results above 1000. It is quite obvious that the risk of serious head injury is considerably reduced for a pedestrian impacted by a slow-moving SUV-type vehicle if the pedestrian experiences leg-fracture from vehicle contact. The risk curves created by Prasad and Mertz (1985) indicate less than 20% chance of a serious head injury for an HIC value of 1000 or less.

Also of note is the correlation between vehicle acceleration and HIC, with a braking vehicle generally producing lower HIC scores in the impacted pedestrian.

5.4.2 Sensitivity to Environmental Parameters

The key environmental parameter in this instance is ground stiffness. For this sensitivity analysis the ground stiffness is varied between 2.6 $kNmm^{-1}$ (lowest value from Chadbourn et at (1997)), 40 $kNmm^{-1}$ (mid-range, 25 deg C value from Chadbourn et al), 10 $MNmm^{-1}$ (extremely stiff – approximately equivalent to a solid steel road) and infinitely stiff where the only the head characteristic is used for the calculation of the contact force and resultant acceleration, i.e. not the combined characteristic (both road and head stiffness) used previously. The vehicle impact speed was varied between 2.8 to 4.8 ms^{-1} in 0.4 ms^{-1} increments and no vehicle acceleration was applied. The results can be seen in Figure 5.23.

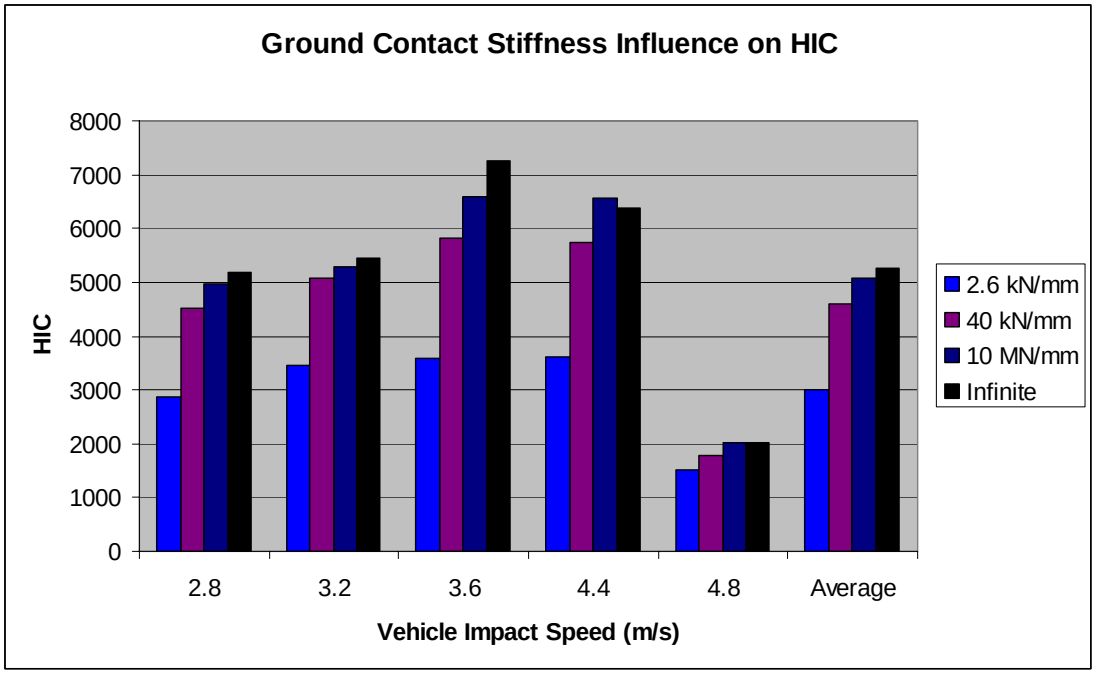

Figure 5.23 Ground Contact Stiffness Influence on HIC

The marked decrease in HIC between the 4.4 and 4.8 ms^{-1} scenarios resulted from the different pedestrian kinematics evident in Figures 5.19 and 5.20 (i.e. the shoulder impacting the ground before the head at 4.8 ms^{-1}, which was not the case at 4.4 ms^{-1}). For each of the vehicle speed scenarios the HIC values can be seen to typically increase for increasing ground contact stiffness. Of note is the relatively limited influence of different orders of magnitude of ground contact stiffness on the resulting HIC. For the averaged results, the HIC value for the scenario with 2.6 $kNmm^{-1}$ ground stiffness had an HIC value that was approximately 57% of the HIC value for the 10 $MNmm^{-1}$ scenario. A stiffness of 2.6 $kNmm^{-1}$ represents only 0.026% of the stiffness of 10 $MNmm^{-1}$. Likewise, the 40 $kNmm^{-1}$ scenario resulted in an HIC value that was 87% that of 10 $MNmm^{-1}$, but represents only 0.4% of the stiffness of 10 $MNmm^{-1}$. It would therefore appear that ground stiffness values only need to be of the correct order of magnitude to ensure reasonable results in scenarios such as these.

For softer surfaces, such as roadside verges, more care in selecting an appropriate ground stiffness would be needed.

5.4.3 Sensitivity to Vehicle Parameters

Whilst the predominant (and fatal) pedestrian injury in this instance resulted from ground contact it is nonetheless prudent to investigate the influence of vehicle parameters to ascertain the following:

i. Is the analysis of pedestrian injury likely to be valid if vehicle parameters are inexact?

ii. Do the vehicle parameters sufficiently influence the pedestrian's kinematics following vehicle contact to affect, noticeably, the severity of head injury resulting from ground contact?

To answer these questions a simulation matrix was created where three different levels of vehicle panel stiffness were used and the injury results analysed for a range of vehicle speeds from 2 to 10 ms^{-1}, evaluated in 2 ms^{-1} increments, giving a matrix of 15 simulations. Vehicle speed was constant (i.e. no acceleration or deceleration).

Minimum (or 'soft') vehicle panel stiffnesses were 75 Nmm^{-1} for bonnet top and bumper stiffness (Yang, 2000) and 850 Nmm^{-1} for the leading bonnet edge (Coley et al, 2001). Maximum (or 'hard') panel stiffnesses used were 2000 Nmm^{-1} for bumper, bonnet edge (Ishikawa et al, 1993) and bonnet top (Howard et al, 2000). Intermediate (or 'Medium') values used were the intermediate values of the above, i.e. 1037.5 Nmm^{-1} for bumper and bonnet top and 1425 Nmm^{-1} for bonnet edge.

In all other respects the simulation parameters were the same as used previously for analysing the pedestrian versus SUV-type vehicle.

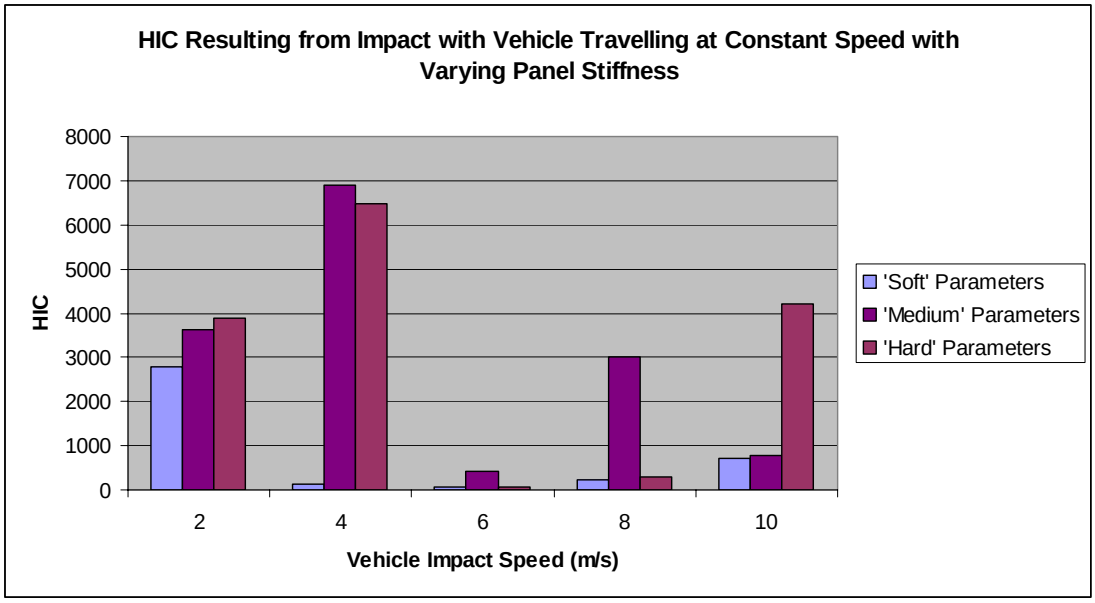

Figure 5.24. HIC Resulting from Impact with Vehicle Travelling at Constant Speed with Varying Panel Stiffness

Figure 5.24 shows the influence of panel stiffness on HIC. The most serious head injury resulted from ground contact in 10 out the 15 simulations. The HIC value at a given speed was lowest for the 'Soft' parameter scenarios. Minimal correlation between vehicle impact speed and injury severity was evident.

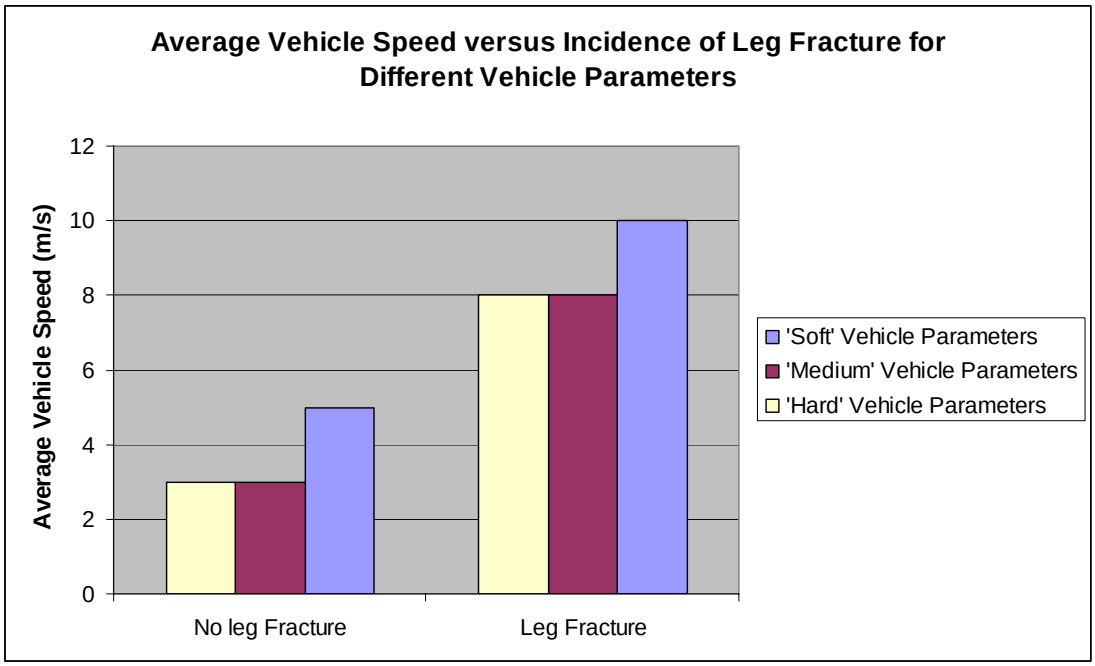

Figure 5.25. Average Vehicle Speed versus Incidence of Leg Fracture for Different Vehicle Parameters

Figure 5.25 indicates that leg fracture is more likely to occur at higher vehicle speeds, with the average speed required for leg fracture being higher for the 'Soft' vehicle

parameters. Leg fracture occurred in 7 of the 15 scenarios evaluated with only one instance of leg fracture for a ‘Soft’ vehicle parameter scenario. The incidence of fracture versus non-fracture was evenly divided for the ‘Medium’ and ‘Hard’ vehicle parameter scenarios

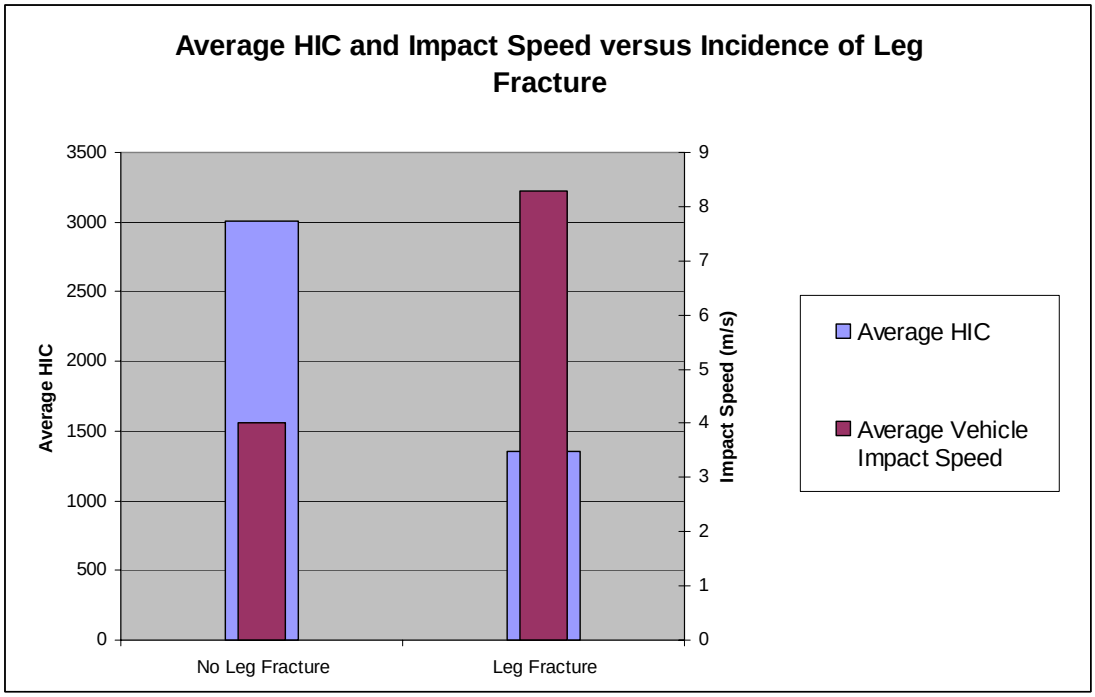

Figure 5.26. Average HIC and Impact Speed versus Incidence of Leg Fracture

Figure 5.26 shows an inverse correlation between average HIC and vehicle speed, according to the incidence of leg fracture. This result is very similar to that obtained in section 5.4.1 and indicates that severe head injury, usually resulting from ground contact, is more directly influenced by leg fracture than vehicle stiffness. The incidence of leg fracture is influenced both by impact speed and vehicle stiffness, with higher impact speeds and stiffer vehicle parameters more likely to result in leg fracture.

As the major head injury risk results from a secondary contact it is unsurprising to note poor correlation between head injury severity and vehicle panel stiffness. The abdominal force experienced by the dummy during the primary contact with the vehicle would be expected to more directly relate to the variation in vehicle panel stiffness and these results can be seen in Figures 5.27 to 5.29.

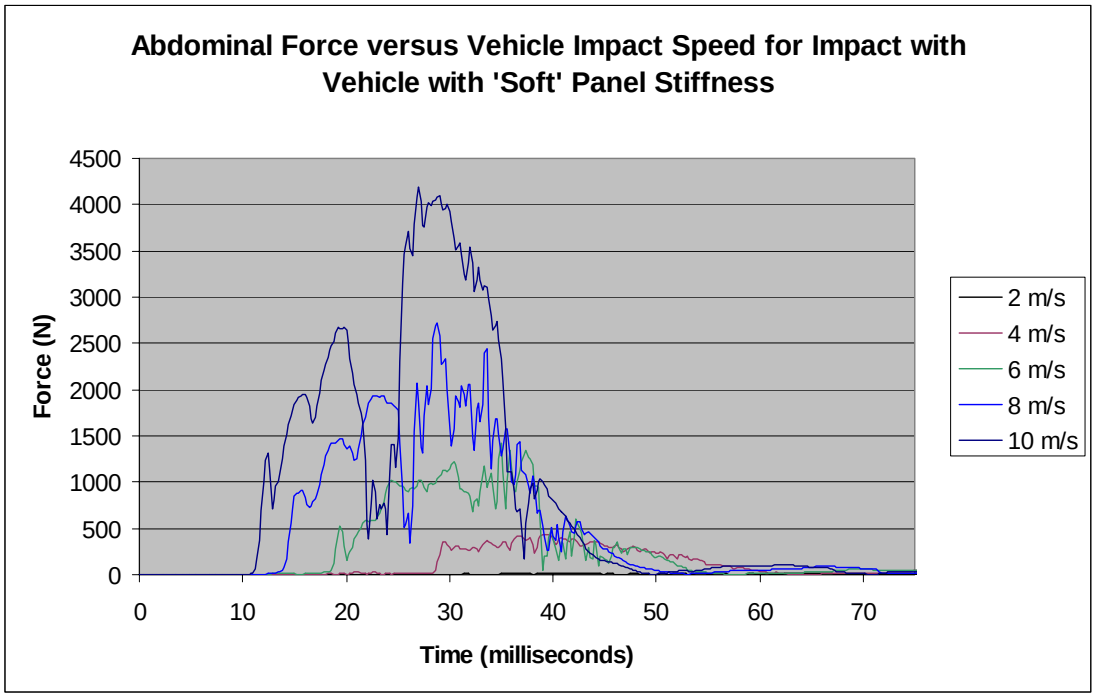

Figure 5.27 Abdominal Force versus Vehicle Impact Speed for Impact with Vehicle with 'Soft' Panel Stiffness

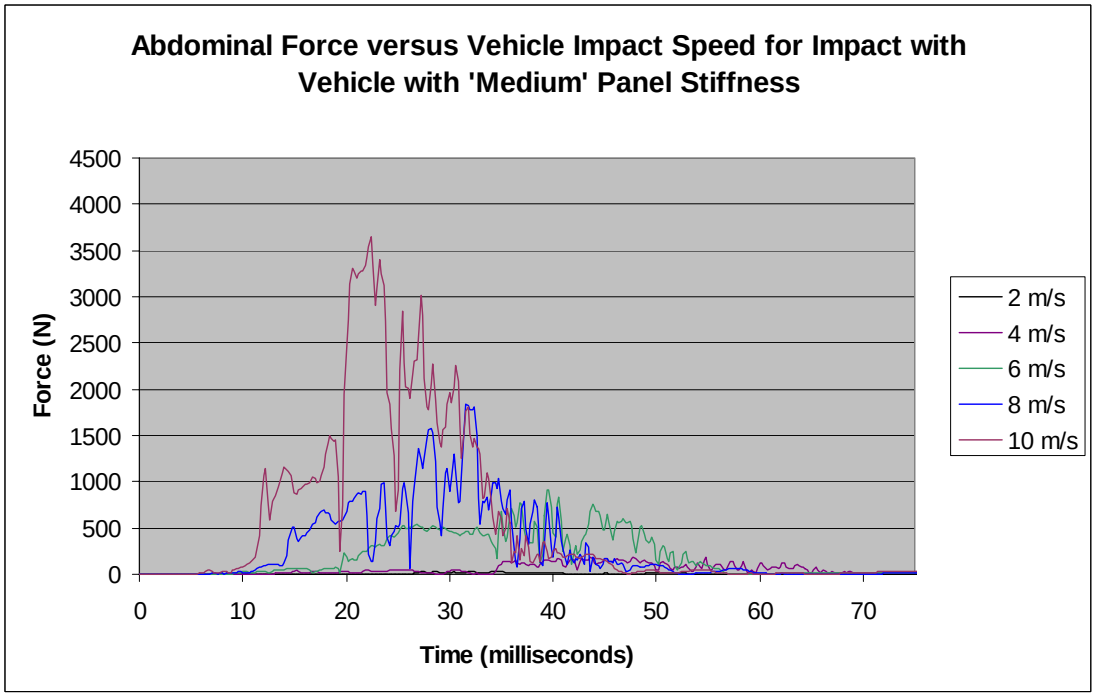

Figure 5.28 Abdominal Force versus Vehicle Impact Speed for Impact with Vehicle with 'Medium' Panel Stiffness

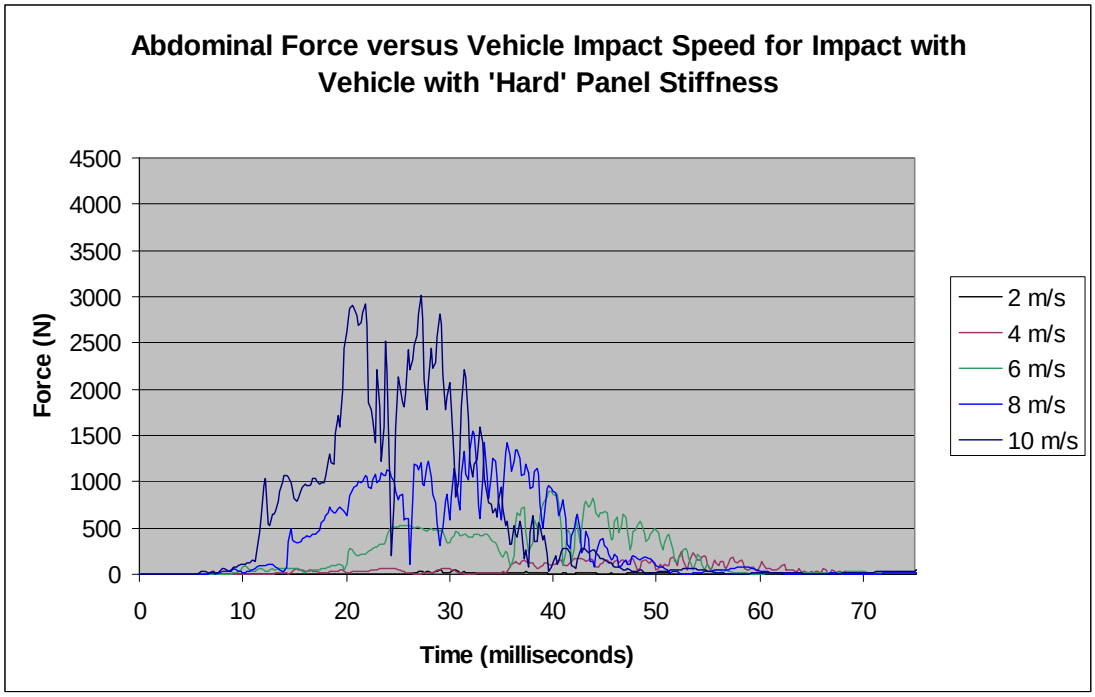

Figure 5.29 Abdominal Force versus Vehicle Impact Speed for Impact with Vehicle with 'Hard' Panel Stiffness

It is apparent that 'soft' vehicle panels accentuate abdominal injury in this instance. Liu et al (2002) noted a similar finding in their research whereby pedestrian tibia acceleration decreased considerably when increasing the vehicle bumper stiffness from 250 Nmm^{-1} to 500 Nmm^{-1}. It is thought that the more compliant vehicle panels increase the contact duration resulting in increased energy transfer to the pedestrian

To answer the questions posed at the beginning of this section it would appear that vehicle panel stiffness has limited direct influence on pedestrian head injury as, in the scenarios evaluated, the most injurious head contact is with the ground and not the vehicle.

Logically, there appears to be an increased risk of leg injury at lower speeds for stiffer vehicle panels. Therefore, the vehicle parameters can be seen to indirectly influence risk of severe injury (in this instance, head injury) via the incidence of leg fracture, as noted previously.

5.4.4 Sensitivity to Pedestrian Orientation

The original series of simulations, as described in Chapter 3, had the pedestrian oriented at 184 degrees about the z-axis and offset to the left of the vehicle centreline.

This placed the pedestrian more or less parallel with the left portion of the front bumper of the vehicle and was consistent with witness statements.

A series of simulations were then run which compared the effects of varying the orientation of the pedestrian with respect to the vehicle. Orientations modelled were between 157 and 207 degrees, in steps of 4.6 degrees (i.e. still essentially facing the vehicle, as per the witness statements, but with some allowance for error/movement). The same vehicle speed, 4.17 ms^{-1} (15 km/h) was used for each orientation.

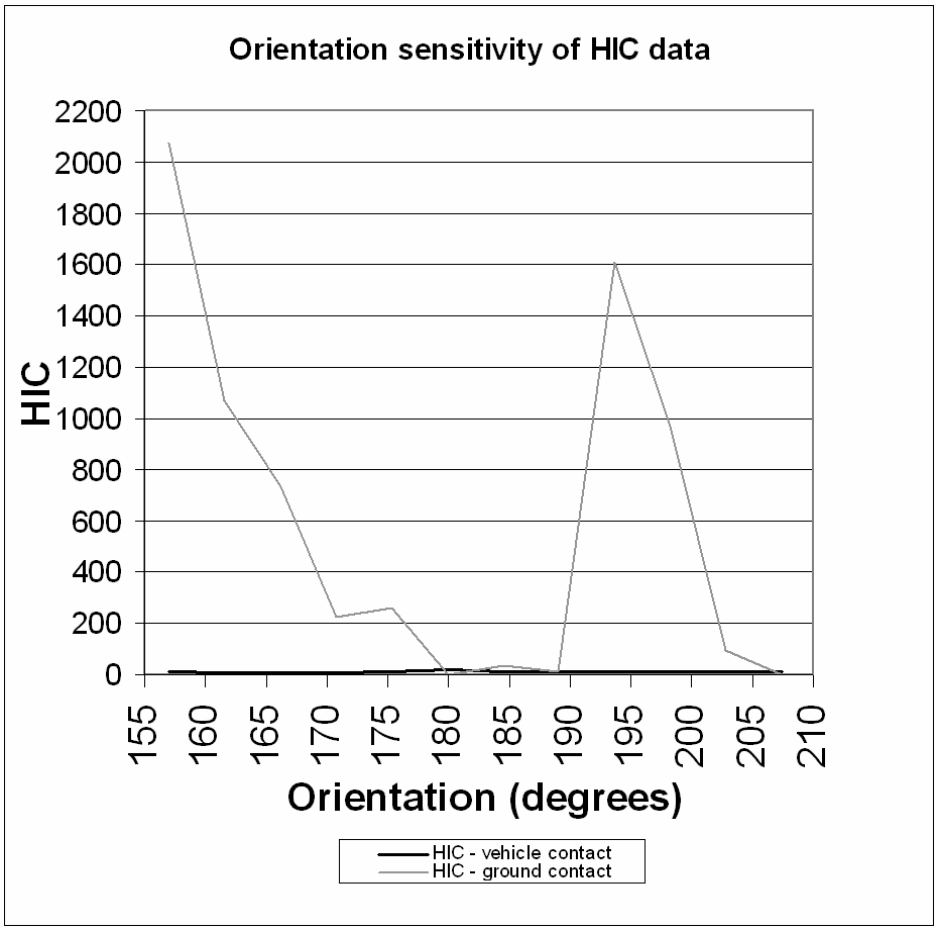

Figure 5.30. Orientation Sensitivity of HIC Data

The HIC values from vehicle contact, shown in Figure 5.30, were very low, between 7.8 and 15.7, and represent virtually no risk of head injury. The Prasad and Mertz HIC risk curves (1985) were based on data from a number of sources. Analysis of this data indicates no injury for HIC values of 400 or less. The HIC values from ground contact varied considerably, demonstrating that the pedestrian's post impact kinematics can be influenced to a large degree by the pedestrian's orientation with respect to the vehicle. In simulations where the pedestrian is more or less facing the vehicle, the

pedestrian is knocked backwards and pivots about one or both legs before falling over. This results in a low risk of head injury. In some instances head injury was negligible due to the way in which the pedestrian model 'folded-up' on the ground. Whether such movement is realistic is debatable. Side-on impacts appeared to have a higher risk of head injury as they are more likely to result in the pedestrian's head contacting the ground first, followed by the shoulders.

5.4.5 Sensitivity to Pedestrian Anthropometry

The majority of simulations in this study used a 5^{th} percentile female pedestrian model. This model best represented the actual accident analyzed. The 5^{th} percentile female model stood 1.53 m high and weighed 49.77 kg. Had a better representation been required, the MADYMO scaling software MADYSCALE could have been used, but no licence for this was available at the time the simulations were conducted.

Two simulations were also run with larger, male pedestrian models. These models represent the 50^{th} percentile male, standing 1.74 m high and weighing 75.7 kg, and the 95^{th} percentile male, which stands 1.91 m high and weighs 101.1 kg. These models were derived by TNO from the database of the RAMSIS software package. This database is itself based upon a sample of the Western European population aged 18 to 70 years in 1984 (MADYMO Human Models Manual, 2001).

The results for the three different pedestrian sizes can be seen in Figures 5.31 to 5.33.

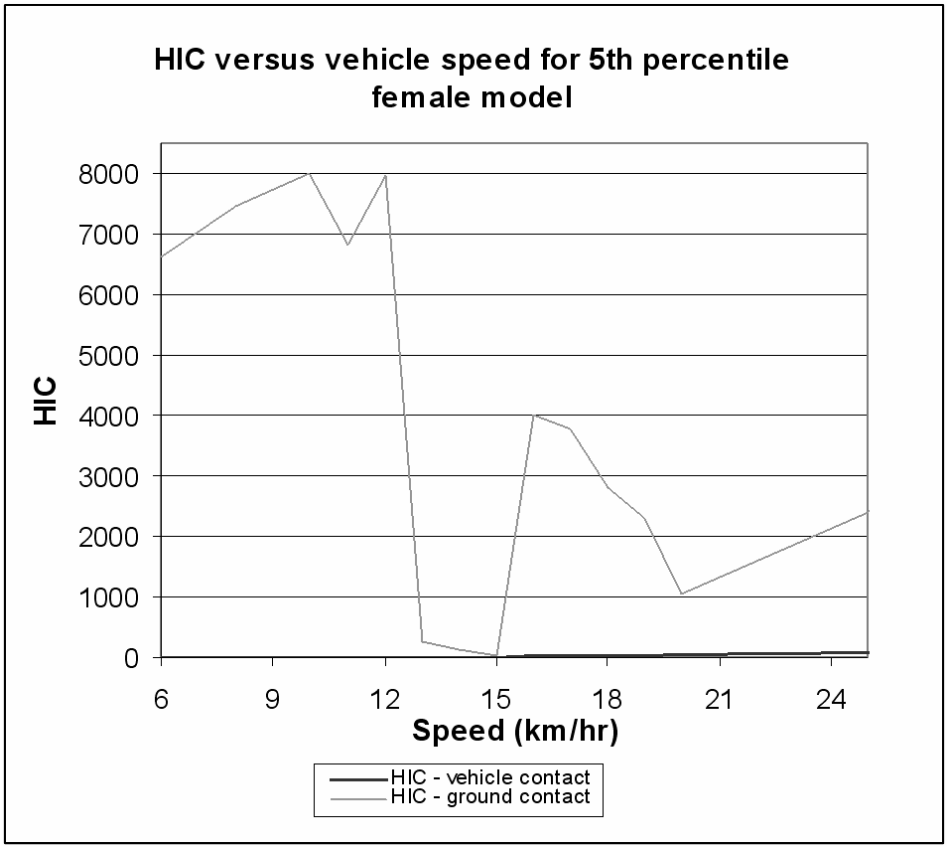

Figure 5.31: HIC Versus Vehicle Speed for 5th Percentile Female Model

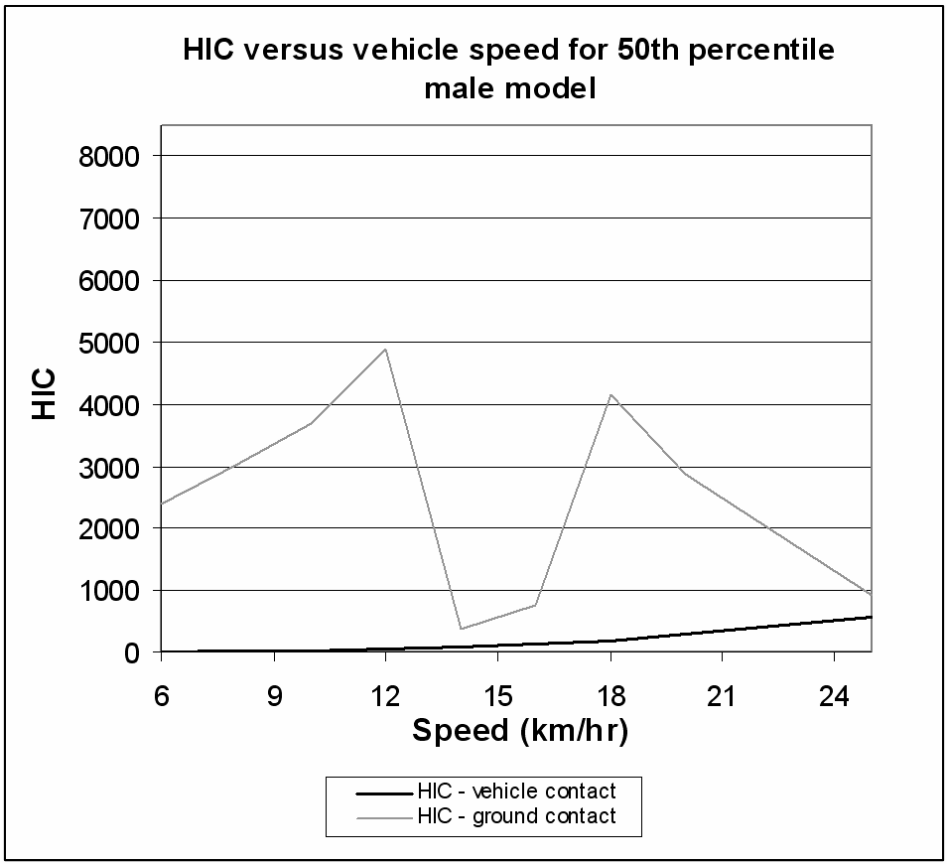

Figure 5.32. HIC Versus Vehicle Speed for 50th Percentile Male Model

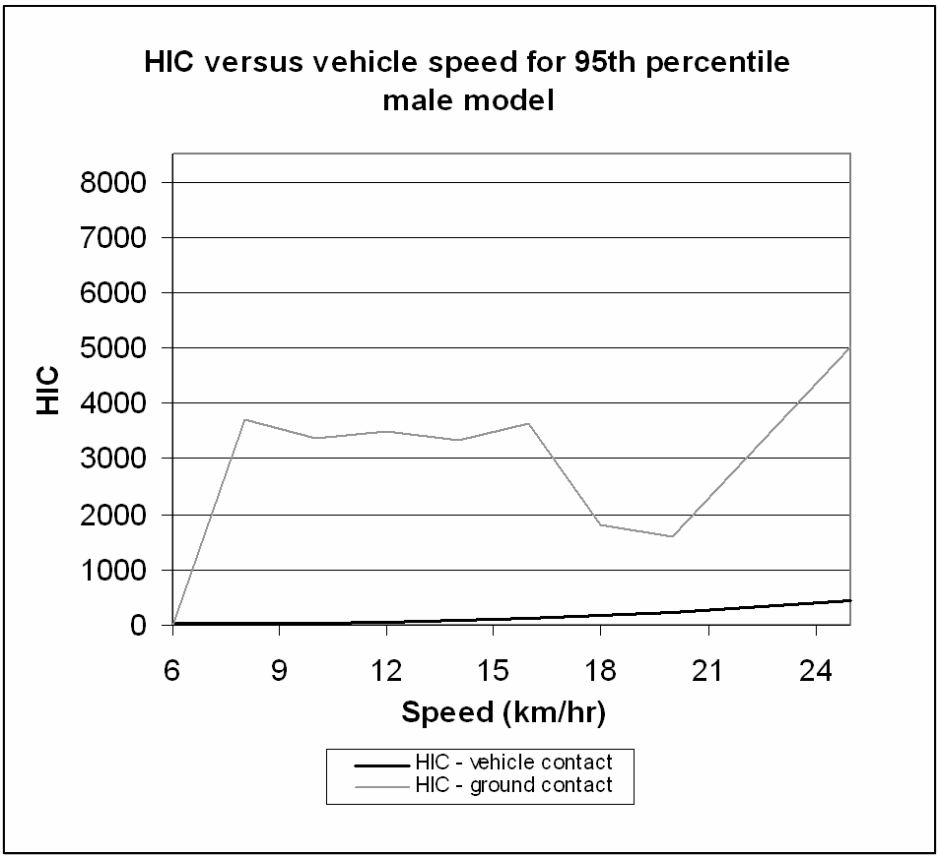

Figure 5.33. HIC Versus Vehicle Speed for 95th Percentile Male Model

The HIC values for the 5th percentile female model for vehicle contact are negligible (averaging an HIC of approximately 5) for impact speeds of 15 km/h or less. In these instances the impact speed was insufficient to cause the pedestrian model's head to contact the bonnet. This would appear to have resulted from a 'short' pedestrian being struck by a 'tall' vehicle. In such a scenario it would appear to require a reasonable amount of force to flex the short length of torso above the contact point to combine with neck flexion and permit the head to contact the bonnet. For taller pedestrians less force would appear to be required to flex the longer torso length above the contact point and again, combined with neck flexion, permit the head to contact the bonnet.

The HIC values for the 50th percentile male model display a similar trend to that of the 5th percentile female model in that there is a greater risk of head injury at low speeds (12 km/h and below for the 5th percentile female, 13 km/h for the 50th percentile male) than there is for slightly higher speeds. There is, however, a decreasing HIC trend for the 50th percentile male model for speeds of 18 km/h and above that is not evident in the data for the 5th percentile female. The HIC values for

the 95th percentile male do not show the same reduction in HIC values at moderate speeds than is evident in the simulations using the other models. This most probably occurred because the height of the centre of mass of the 95th percentile model is much closer to the height of the leading edge of the SUV bonnet and as such does not tend to lever the model backwards at low speeds

5.5 Discussion of the Injury Correlation Results for a Pedestrian Impacted by an SUV-Type Vehicle

MADYMO was able to predict injury patterns resulting from a vehicle-pedestrian collision involving a pedestrian and a large, SUV-type vehicle moving at low speed that appeared consistent with the injuries incurred and provided additional correlation with the range of vehicle speed and driver actions predicted from throw-distance analysis. In particular:

1. Abdominal injury prediction suggested an impact speed of less than 8 ms^{-1}
2. Head injury prediction suggests that if the vehicle speed was less than approximately 3.6 ms^{-1} then the vehicle was either travelling at constant speed or accelerating
3. Thoracic injury prediction, made using the Viscous Criteria, indicated minimal risk of thoracic injury from vehicle impact for impacts over the speed range analysed. This is consistent with the lack of thoracic injury in the pathology report.

In summary, the injury correlation indicates a maximum vehicle impact speed of less than 8 ms^{-1} with this reduced to approximately 3.6 ms^{-1} if the vehicle was not braking at the time of impact.

The sensitivity analysis indicated minimal influence for vehicle panel stiffness on head injury severity. This to be expected, as it would appear that ground impact was responsible for the severe head injury. Ground stiffness sensitivity was also determined to have relatively minor effect at high stiffness level of a typical road (40 kNmm^{-1}). The influence of other injuries (in this instance, leg fracture) and pedestrian kinematic variability was found to have far greater influence on pedestrian head injury severity than any variation in vehicle or environmental parameters. Any influence

from vehicle stiffness parameter variation was noted to have a relatively minor influence on leg injury and any influence on head injury severity was most noticeable via leg fracture.

Of note in this case was the low level of correlation between vehicle speed and pedestrian injury severity. A much greater correlation was observed for the incidence of pedestrian leg-fracture versus vehicle impact speed resulting in relatively low HIC values versus a lack a leg-fracture resulting in high HIC values.

Low-speed collisions between SUV-type vehicles and pedestrians appear to pose a considerable risk of fatal injury to the pedestrian through head injury following ground contact if no leg fracture is observed. This occurs through the pedestrian's body being levered backwards by the high collision contact point. In instances where the pedestrian experiences leg-fracture the pedestrian's body no longer acts as a rigid lever, thus decreasing the risk of fatal head injury.

5.6 Case Study 2 – Part 1: Multiple Contact Vehicle-Pedestrian Collision

In this section the pedestrian kinematics of a female pedestrian involved in a sequence of collisions involving a typical (car-like) vehicle will be examined, as per the scenario described in Section 3.8, and the injury predictions analysed in an attempt to use injury correlation to determine vehicle impact speed range in a similar manner to that described in Section 5.2.

5.6.1 Injury Summary

An injury summary, summarised from the pathologist's report, is given in Table 5.2.

Visible Injuries	Head – Multiple abrasions and lacerations including an extensive degloving laceration from the right forehead to the right frontoparietal scalp. Depth of laceration extending to skull.
	Trunk – Abrasions on posterior of neck, lower back, chest, front of abdomen and right shoulder. A compound fracture of the left anterior pelvis associated with a laceration in the left groin.
	Lower limbs – Abrasions on front of left leg, rear of left thigh and both knees..
Internal Examination	Ribcage – All right ribs fractured at the front.
	Bladder – Lacerated
	Brain – Diffuse axonal injury suggestive of concussion. Also implies survival of 2-3 hours following head injury.
Mechanism of Death	Hemorrhage resulting from pelvic trauma.

Table 5.2 Victim Pathology for Pedestrian Impacted by Typical Vehicle

From additional forensic information the following was surmised regarding pedestrian injuries:

- A vehicle-pedestrian collision occurred on the road where there was relatively minor injury to the pedestrian consisting of minor abrasions and possibly a relatively minor head injury from where the pedestrian's head struck the vehicle at the rear edge of the bonnet, on the cowl below the windscreen.
- At least one further vehicle-pedestrian collision occurred where substantial injury to the pedestrian occurred, including the fatal pelvic trauma. It did not

appear that this occurred on the road but was considered more likely to have occurred a short distance off-road, down an adjacent bank.

In this section only the first vehicle-pedestrian collision is considered. In section 5.8 the fatal vehicle-pedestrian collision will be analysed.

5.6.2 Simulation Methodology for Injury Analysis

The simulation methodology employed was essentially the same as described in Section 3.8 with the addition of investigating the influence of vehicle and environmental parameters on pedestrian injury.

A simulation matrix was created to determine a likely vehicle speed range and pedestrian orientation for the vehicle-pedestrian collision that occurred on the road. Vehicle speed, driver actions and pedestrian orientation with respect to the vehicle were analysed. The determination of a likely range of vehicle impact speeds and pedestrian orientations was an iterative process and is discussed in the following sections. Driver actions were analysed at the acceleration levels of 0, -4.0 and -8.5 ms^{-2} to represent constant vehicle speed, moderate braking and heavy braking.

The simulation results were appraised based on the similarity between the modelled and actual injuries in addition to the location of the head strike on the bonnet.

5.6.3 Knee Injury Severity versus Pedestrian Orientation

Knee injury (or rather, the lack thereof) was used to determine pedestrian orientation with respect to the vehicle for the first vehicle-pedestrian collision. Although the knees were not internally examined, the lack of development of any visible external trauma (eg swelling, bruising) over the period that the victim survived suggests minimal knee injury. A closer knee examination and comparison of any damage to Teresiński and Mądro's findings would have been useful, however. Furthermore, the pedestrian model used in the mathematical simulations does not have any standard sensors for measuring either shear force or bending moment at the knee, despite having three shear sensors in both the femur and tibia, as it would appear that the biofidelity of the MADYMO human pedestrian knee has not been validated (van Hoof

et al, 2003). Nonetheless, it is a relatively simple exercise to add sensors to the knees of the model, record the outputs and analyse the data produced.

As noted in the MADYMO Human Models Manual an injury tolerance of 4 kN in shear has been defined (EEVC, 1994, 1998) for pedestrian injury reduction. From McElhaney et al (1976) some findings indicated a conservative knee injury tolerance of 6.2 kN was noted for middle-aged males whilst other research indicated a knee tolerance of 5.9 kN for males and 2.3 kN for females. Kajzer et al (1999) produced the data shown in Table 5.3.

	Shearing	Bending
Impact Velocity Level (km/h)	20	20
Knee Shearing Force (kN)	2.4	1.3
Knee Bending Moment (Nm)	418	307

Table 5.3 EuroNCAP Knee Shear and Bending Tolerances (Source: Kajzer et al, 1999)

From the values shown in Table 5.3 it would appear that the EEVC tolerance levels may be too high.

The pedestrian was placed in a standing position in front of the vehicle and the orientation with respect to the vehicle varied in 45º increments. Collisions were then simulated with a range of vehicle speed and driver actions. For moderate braking a vehicle dive angle of 1° was applied and for heavy braking a dive angle of 2º was used. From the first simulation results it was immediately apparent that simulations that placed the pedestrian facing the vehicle or at 45° towards the vehicle resulted in injuries to the knees that were not indicative of the actual injuries inflicted. Simulations based on these pedestrian orientations were disregarded.

Figures 5.34 and 5.35 show the maximum bending moments for the left and right knees, respectively, as calculated by MADYMO for the various scenarios simulated. These bending moments are generally below the injury tolerance levels specified as ‘current’ by Kajzer et al, with the possible exception of the results obtained for the ‘facing away’ orientation where the vehicle speed is constant.

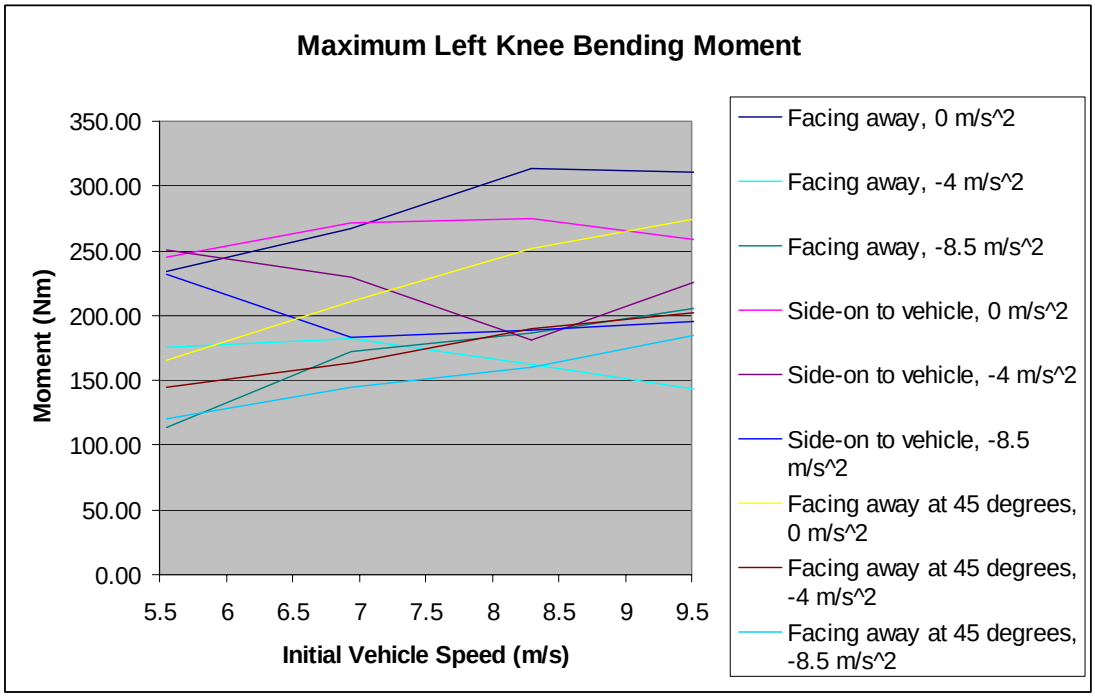

Figure 5.34 Maximum Left Knee Bending Moment

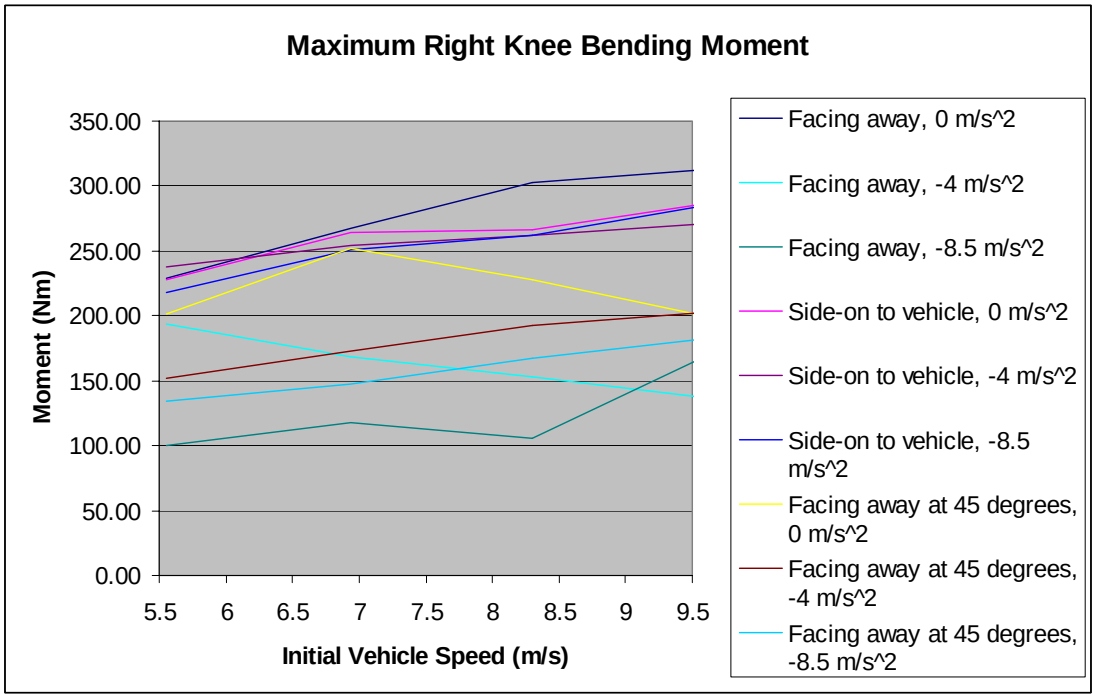

Figure 5.35 Maximum Right Knee Bending Moment

Figures 5.36 to 5.41 display the knee shear forces determined by MADYMO for the scenarios evaluated. The X, Y and Z directions specified are relative to a local co-ordinated system centred on the knee, with X representing longitudinal force, Y

representing transverse force and Z indicating vertical force. For the side-on orientation the left leg is closest to the vehicle whilst for the 'facing-away at 45°' orientation the right leg is closest. All the shear forces recorded are noted to increase with increasing vehicle speed.

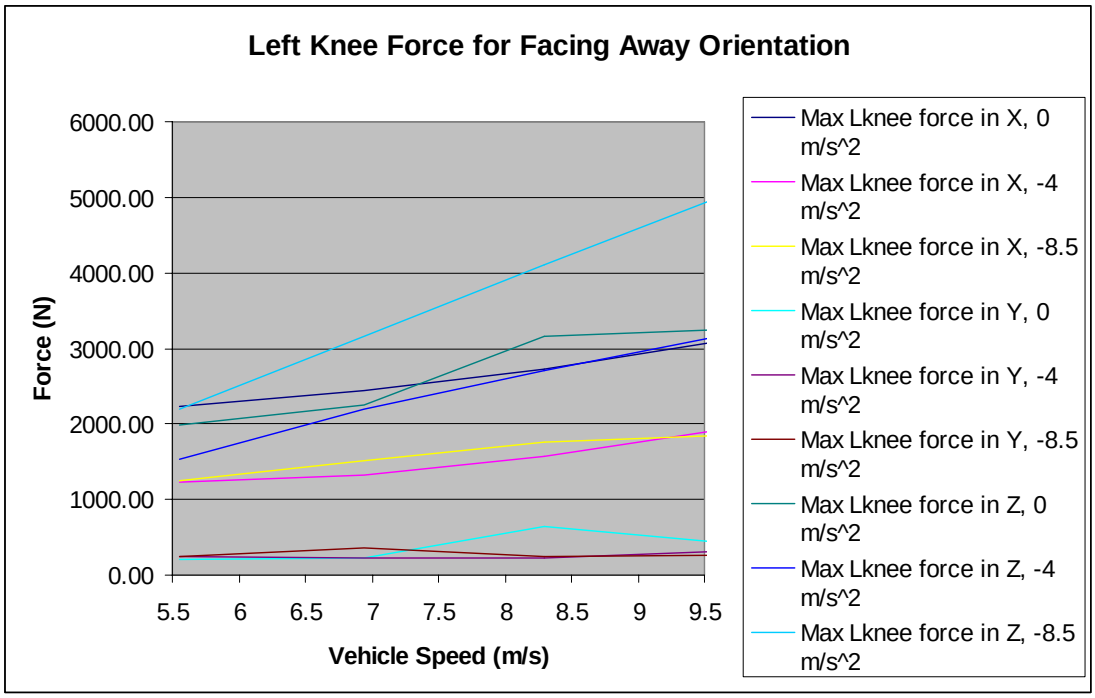

Figure 5.36 Left Knee Force for Facing Away Orientation

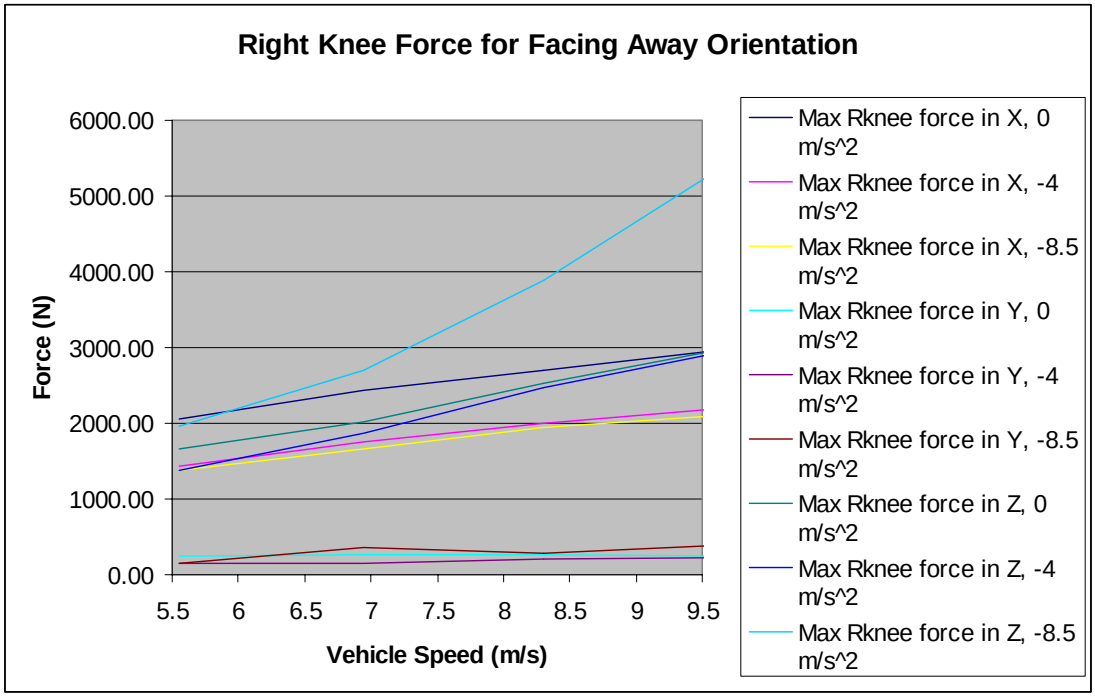

Figure 5.37 Right Knee Force for Facing Away Orientation

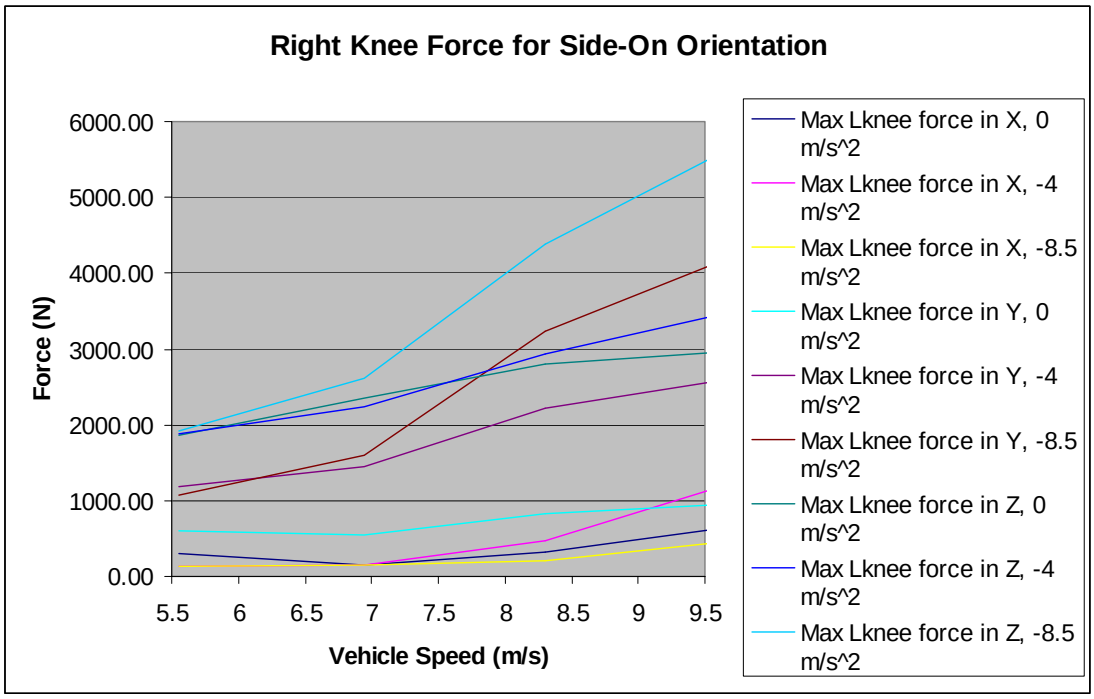

Figure 5.38 Right Knee Force for Side-On Orientation

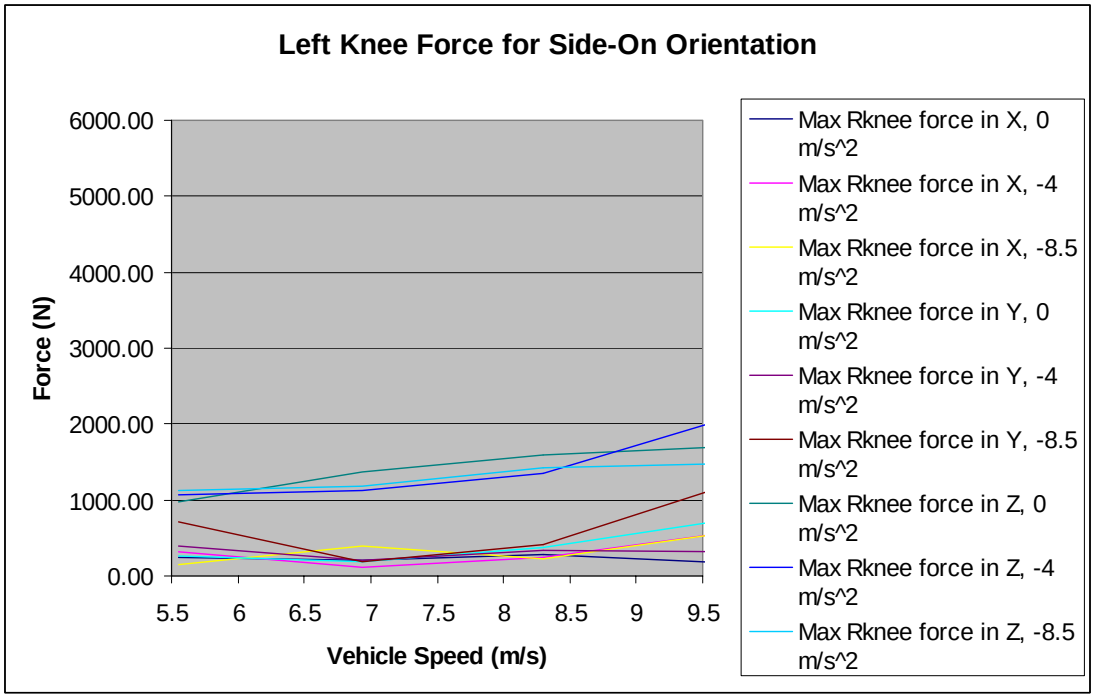

Figure 5.39 Left Knee Force for Side-On Orientation

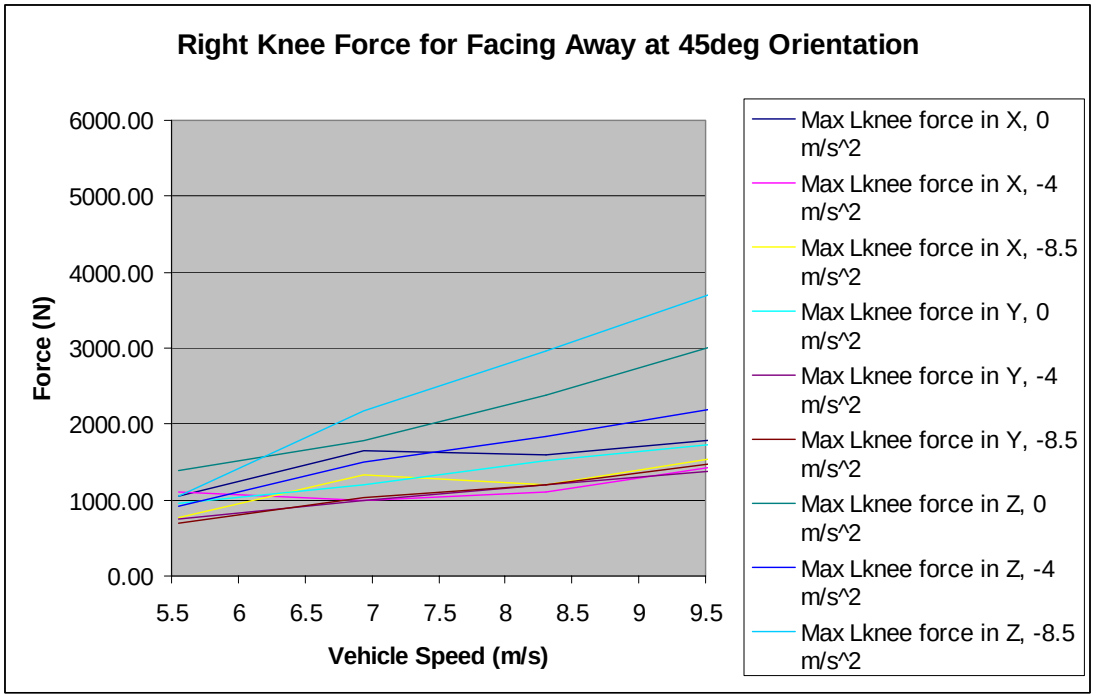

Figure 5.40 Right Knee Force for Facing Away at 45° Orientation

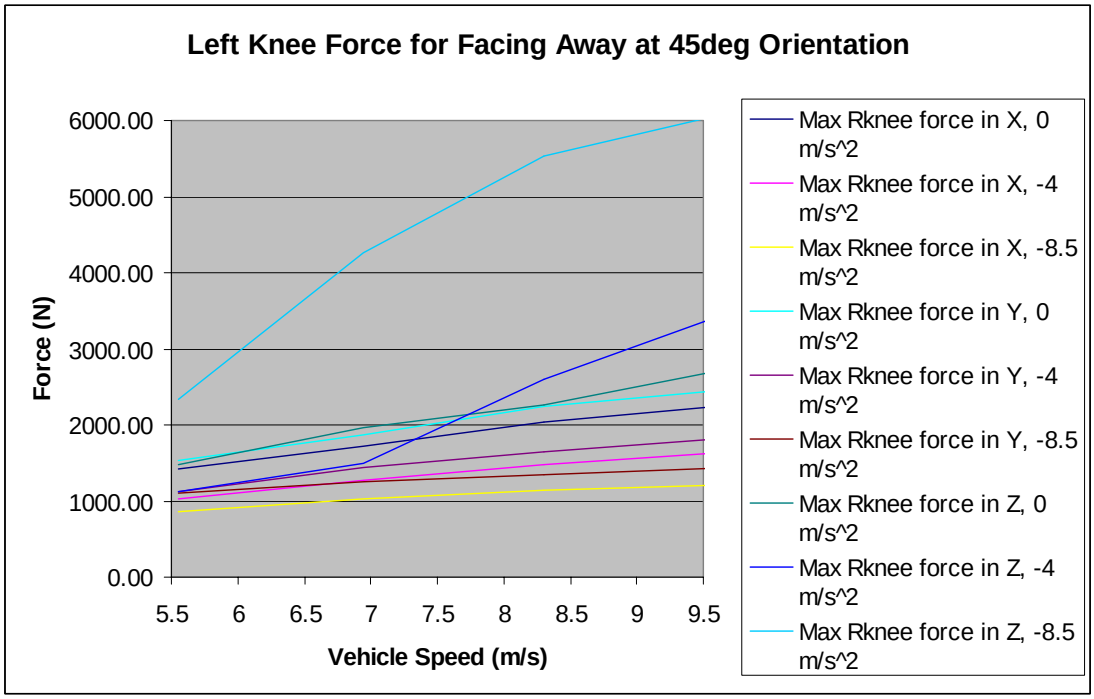

Figure 5.41 Left Knee Force for Facing Away at 45° Orientation

Depending on the tolerance level applied, most of the scenarios indicate potential for knee injury in the upper range of the vehicle speeds simulated. By considering this information with other simulation results it may be possible to reduce the number of potentially valid scenarios although it should be noted that not all scenarios have been

considered. Pedestrian movement and foot loading would be expected to have considerable influence on knee injury in these circumstances but have not been accounted for in these scenarios. With these assumptions in mind, the knee injury results would appear to point towards the lower speed range (i.e. less than 8.3 ms^{-1}) of the possible scenarios indicated by the kinematics analysis and head-strike location, namely 'side-on' orientation, vehicle decelerating heavily.

5.6.4 Pedestrian Kinematics and Head Strike Location versus Pedestrian Orientation

With a sedan-type vehicle, the pedestrian is likely to land on the bonnet of the vehicle before sliding to the ground as the vehicle brakes. This has the net effect of increasing the duration of the collision and thus reducing the severity of the deceleration impulse on the pedestrian when ground contact occurs. This can be seen in Figures 5.42 and 5.43.

The unusual kinematics evident in Figure 5.42 result from the pedestrian sliding off the bonnet and then being shunted by the vehicle travelling at constant speed. Whether or not such a sequence is realistic is debatable, but it should be remembered that this scenario is reconstructing a homicide, not an accident. Additionally, any pedestrian response in reality during the time is uncertain, particularly after the potentially stunning impact between the head and the bonnet.

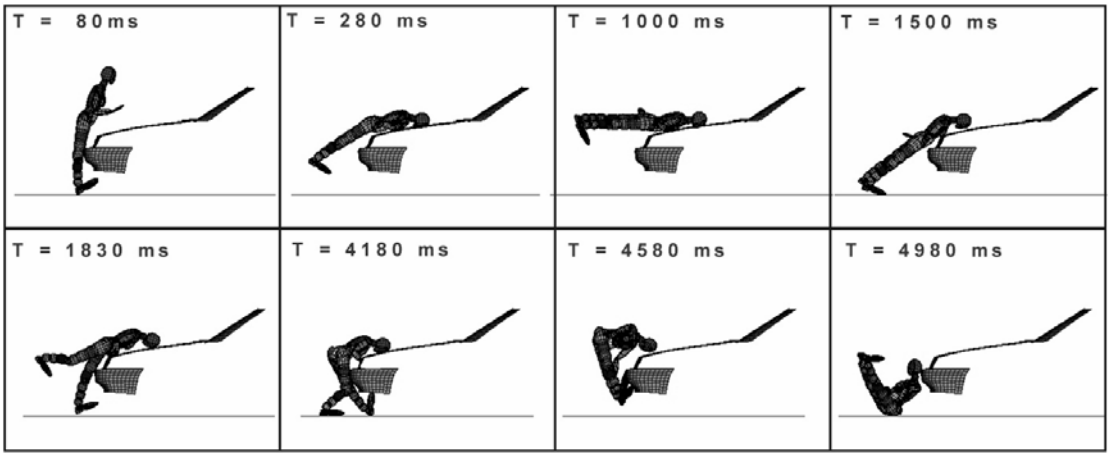

Figure 5.42. Impact Sequence at 10 km/h

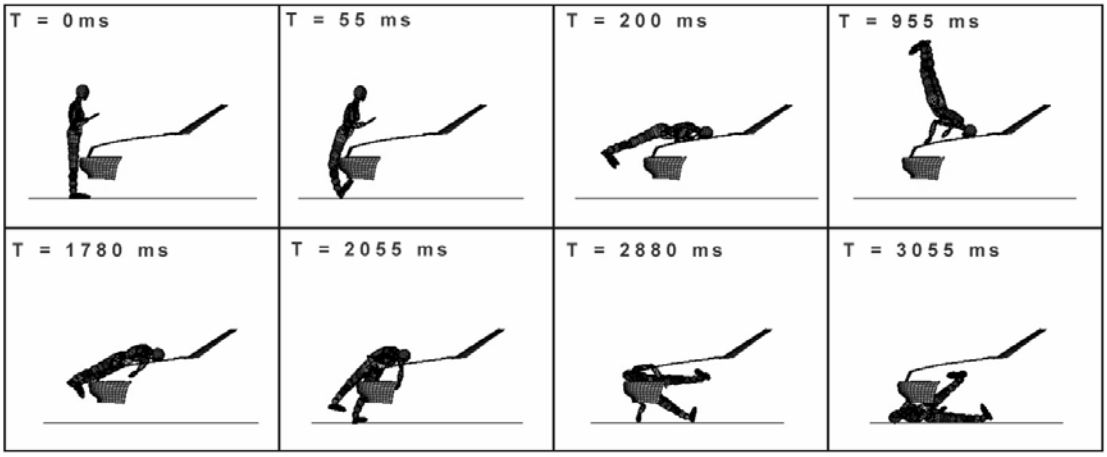

Figure 5.43. Impact Sequence at 16 km/h

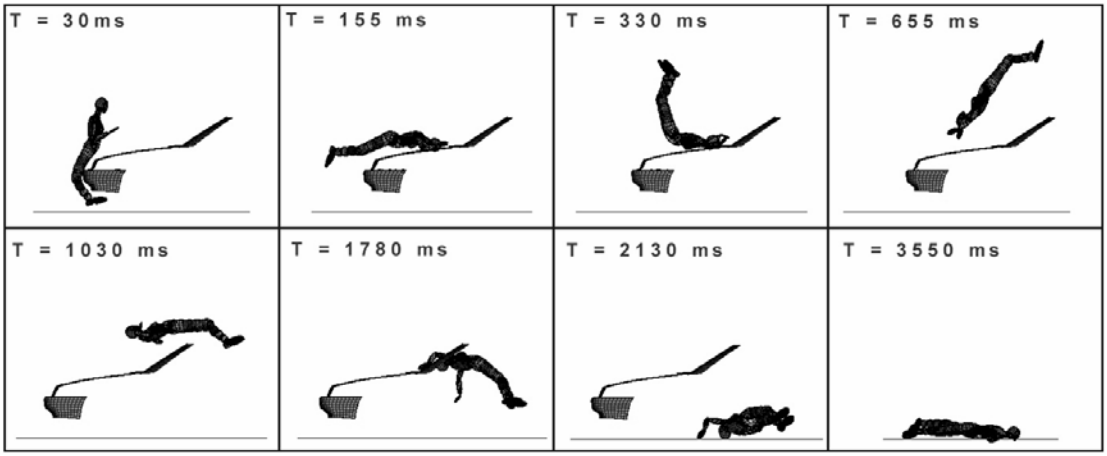

Figure 5.44. Impact Sequence at 25 km/h

For speeds of 6.9 ms^{-1} (25 km/h) or more, the pedestrian tends to vault the vehicle and, having further to fall, increases the risk of serious injuries from secondary (ground) contact, as can be seen in Figure 5.44.

Furthermore, for impact speeds of 11.1 ms^{-1} (40 km/h) or greater resulted in the pedestrian's head striking the windscreen. Neither a windscreen strike nor a vault were in agreement with either the location of the head strike on the actual vehicle or the pedestrian's injuries. Simulations with a vehicle speed of 11.1 ms^{-1} or greater were therefore disregarded.

Similarly, an impact speed of 5.6 ms^{-1} (20 km/h) or less resulted in a head-strike somewhat forward of the actual impact point. Simulations with a vehicle speed of 5.6 ms^{-1} or less were therefore also disregarded.

The location of the head strike on the vehicle and the lack of injuries to the lower extremities of the pedestrian (as per Table 5.2) indicates a pedestrian pre-impact orientation somewhere between side-on to the vehicle and facing away from the vehicle (i.e. a 180 degree range) and a vehicle impact speed range of between 6.9 to 9.7 ms^{-1} (25 to 35 km/h). The 9.7 ms^{-1} impact speed would only be likely if the vehicle was decelerating heavily at the time of impact. The kinematics from this result can be seen in Figure 5.45.

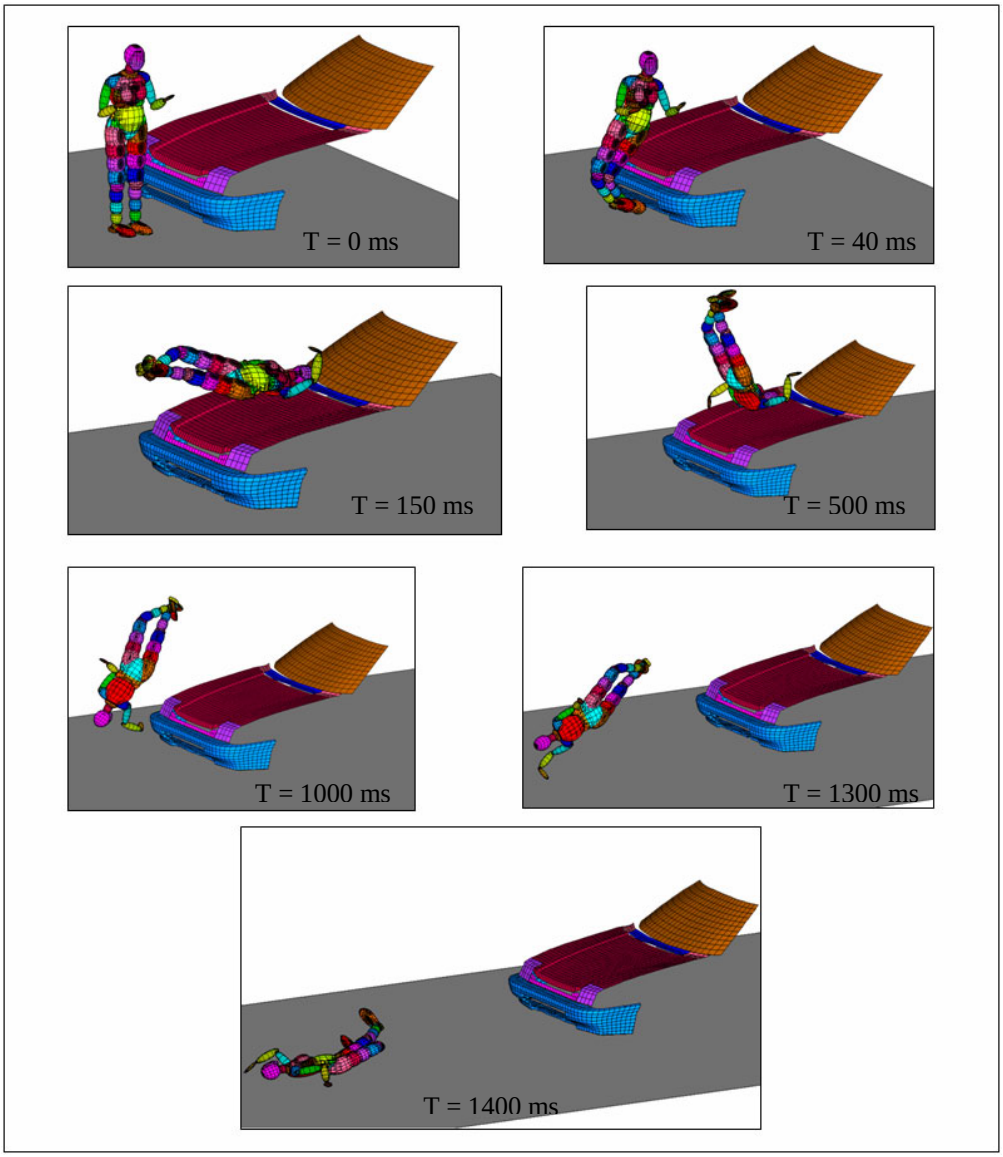

Figure 5.45: Vehicle Impact at 35 km/h, Vehicle Braking Heavily

5.6.5 Head Injury Severity versus Pedestrian Orientation

For this case study it is the lack of serious head injury, despite the apparent head strike on the vehicle bonnet, that is of interest. The resultant head acceleration and

HIC were analysed over the simulation matrix and the results are given in the following figures.

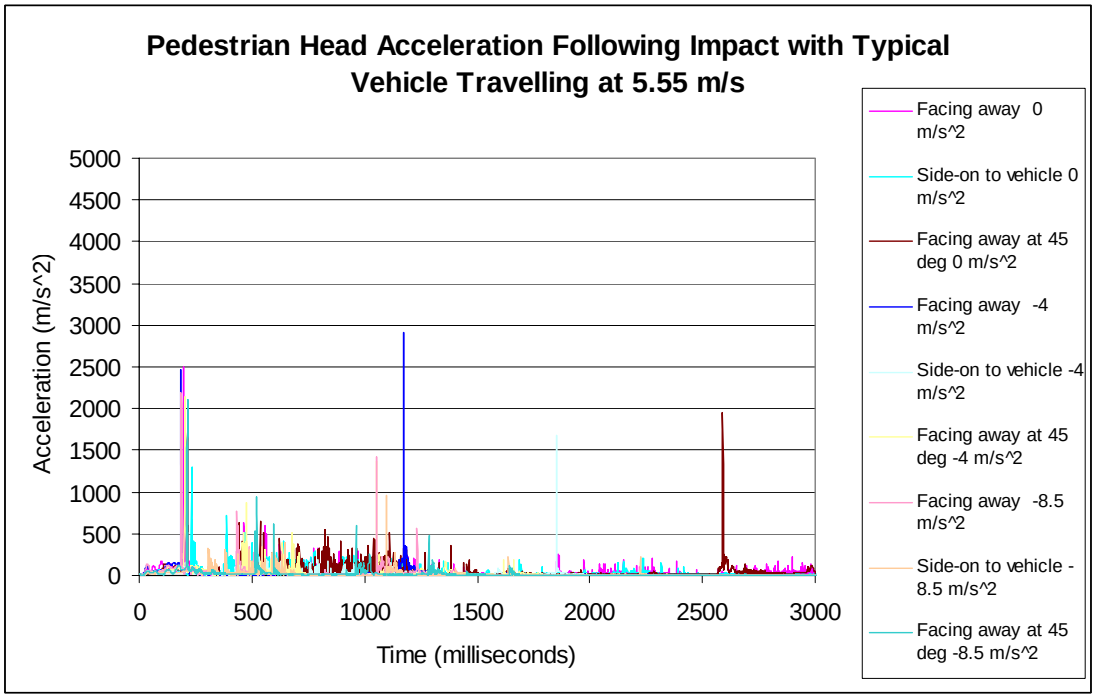

Figure 5.46 Head Acceleration for 5th Percentile Female MADYMO Human Model Struck by Typical Vehicle with the Vehicle Initially Travelling at 5.55 ms^{-1}, Three Different Driver Actions (No Action, Moderate Braking and Heavy Braking) and Three Pedestrian Orientations (Facing Away from Vehicle, Side-On to Vehicle and Facing Away at 45°).

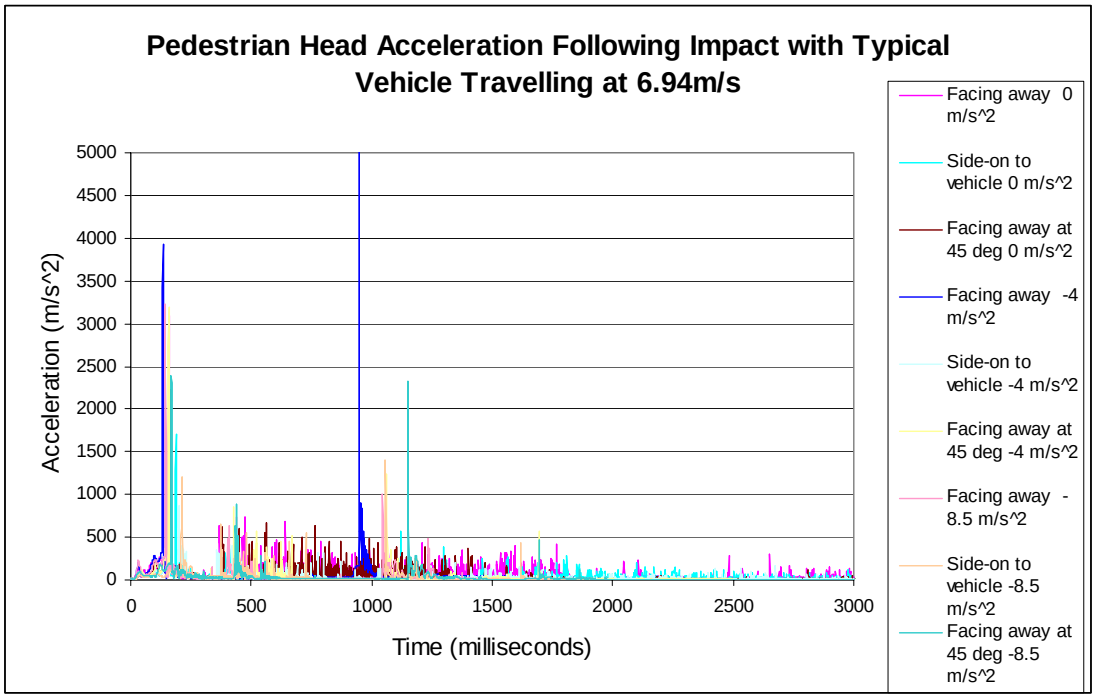

Figure 5.47 Head Acceleration for 5th Percentile Female MADYMO Human Model Struck by Typical Vehicle with the Vehicle Initially Travelling at 6.94 ms^{-1}, Three Different Driver Actions (No Action, Moderate Braking and Heavy Braking) and Three Pedestrian Orientations (Facing Away from Vehicle, Side-On to Vehicle and Facing Away at 45°).

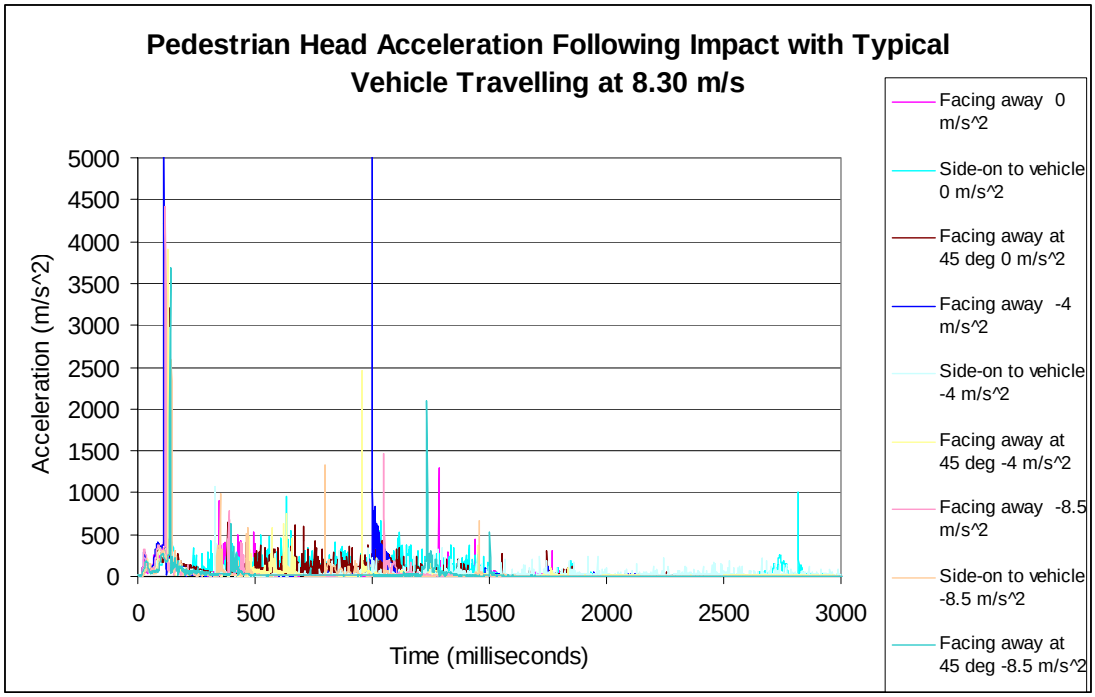

Figure 5.48 Head Acceleration for 5th Percentile Female MADYMO Human Model Struck by Typical Vehicle with the Vehicle Initially Travelling at 8.3 ms^{-1}, Three Different Driver Actions (No Action, Moderate Braking and Heavy Braking) and Three Pedestrian Orientations (Facing Away from Vehicle, Side-On to Vehicle and Facing Away at 45°).

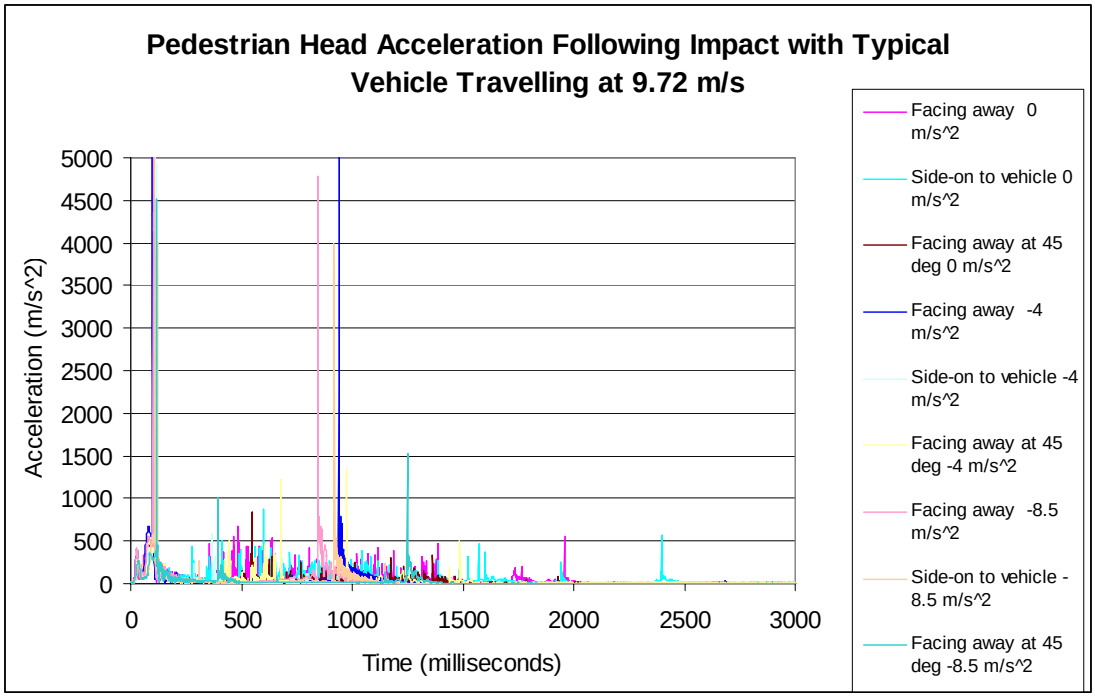

Figure 5.49 Head Acceleration for 5th Percentile Female MADYMO Human Model Struck by Typical Vehicle with the Vehicle Initially Travelling at 9.72 ms^{-1}, Three Different Driver Actions (No Action, Moderate Braking and Heavy Braking) and Three Pedestrian Orientations (Facing Away from Vehicle, Side-On to Vehicle and Facing Away at 45°).

In Figure 5.46 it is apparent that a combination of pedestrian orientation of facing away from the vehicle, with the vehicle braking moderately, resulted in the highest

level of head acceleration and this occurred from ground contact. This same scenario also produced one of the highest head accelerations from vehicle contact with the other two highest primary contact accelerations also resulting from 'facing away' orientations with different driver actions (no braking and heavy braking).

Figure 5.47 shows the same nine scenarios as Figure 5.46 except with the vehicle now having an initial speed of 6.94 ms^{-1} (25 km/h). This scenario ('facing away' pedestrian , moderately accelerating vehicle) produced the highest head acceleration for a vehicle speed of 6.94 ms^{-1}, which also resulted from ground contact, as can be seen in Figure 5.47. Aside from this scenario, the other head accelerations for a vehicle travelling at 6.94 ms^{-1} were generally higher for vehicle contact than for secondary contact, with the three 'facing away' scenarios (i.e. no braking, moderate braking and heavy braking) producing the three highest primary contact head accelerations, much as they did for a vehicle travelling at 5.55 ms^{-1}.

Figure 5.48 shows a similar pattern of head acceleration from primary and secondary contact to that displayed in Figures 5.46 and 5.47. Again, the 'facing away' pedestrian, moderately accelerating vehicle scenario produced the highest head acceleration (6915 ms^{-2}, the graph being capped at 5000 ms^{-2} to allow more accurate comparison with the lower speed scenarios) and again this resulted from ground contact. As before, the same scenario generated the greatest head acceleration from vehicle contact (5206 ms^{-2}) with the other two 'facing away' scenarios representing the next highest primary contact head accelerations.

In Figure 5.49 (again, the scale has been capped at 5000 ms^{-2} to facilitate comparison with lower speed scenarios) the head acceleration resulting from ground contact is significant in three of the scenarios, namely 6134 ms^{-2} for the 'facing away', moderate braking scenario and between 4000 and 5000 ms^{-2} for the 'facing away', heavy braking and side-on, heavy braking scenarios. All nine scenarios with a vehicle speed of 9.72 ms^{-1} resulted in head acceleration in excess of 3000 ms^{-2} as a result of vehicle contact. The three 'facing away' scenarios resulted in primary contact head accelerations of between 5000 and 6000 ms^{-2} with two of the 'facing away at 45°' scenarios (vehicle speed constant and moderate braking) scoring similarly.

The most apparent and least surprising trend noticeable in Figures 5.46 to 5.49 was the tendency for pedestrian head acceleration to increase with increasing vehicle impact velocity. Generally, the side-on pedestrian orientation produced the lowest accelerations for both primary and secondary contact with the exception of a vehicle travelling at 9.72 ms^{-2} and braking heavily. The 'facing away' orientation consistently produced the highest primary contact head acceleration, ranging between 2500 ms^{-2} for a vehicle impact speed of 5.55 ms^{-1} to almost 6000 ms^{-2} for a vehicle speed of 9.72 ms^{-1}.

The pathology report notes relatively minor head injury which was likely to have resulted in minor-moderate concussion. AAAM (1990) notes that mild (no prior unconsciousness, may have headache or dizziness known to result from head injury) and cerebral concussion (the classical definition of concussion) have AIS scores of 1 and 2, respectively. Relating this to HIC (Prasad, 1999) suggests a reasonable probability of an HIC value below 1500 and a high probability of an HIC value below 2000.

The average HIC from the preliminary results was 2350. Many scenarios resulting in high HIC values were able to be eliminated. By evaluating both head impact location and head injury severity the range of feasible scenarios were markedly narrowed. Scenarios considered highly probable, according to both impact location and severity, had HIC values of less than 1500.

The results for a simulation matrix of initial vehicle speed of 5.56, 6.94, 8.3 and 9.72 ms^{-1} and vehicle acceleration of 0, -4 and -8.5 ms^{-2} produced the HIC results indicated in Figure 5.50. As per the HIC analysis in the first case study. the results were averaged across vehicle acceleration (all levels) and vehicle speed (three speed intervals) to allow trends to be identified.

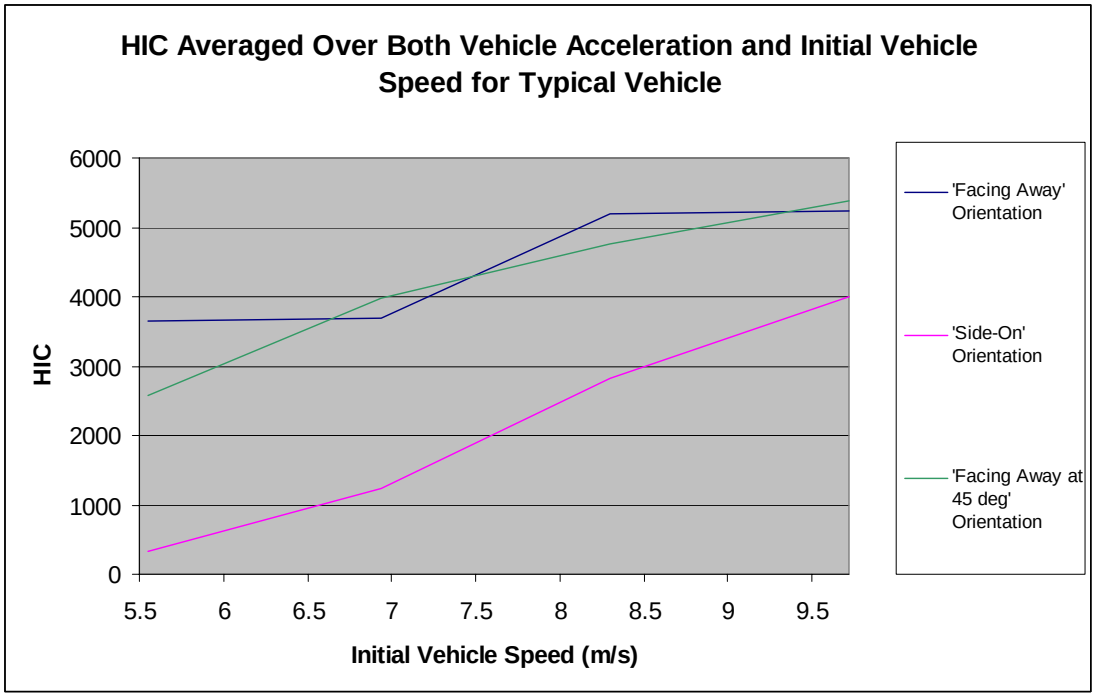

Figure 5.50. HIC Averaged Over Both Vehicle Acceleration and Initial Vehicle Speed for Typical Vehicle

For an HIC result of less than 1500 it is considered probable that the pedestrian was oriented 'side-on' to the vehicle and that the initial vehicle speed was less than approximately 7.25 ms^{-1}.

5.6.6 Thoracic Injury Severity versus Pedestrian Orientation

Similarly to head acceleration, the acceleration of the pedestrian model's sternum was also recorded, and the results are given in the following figures.

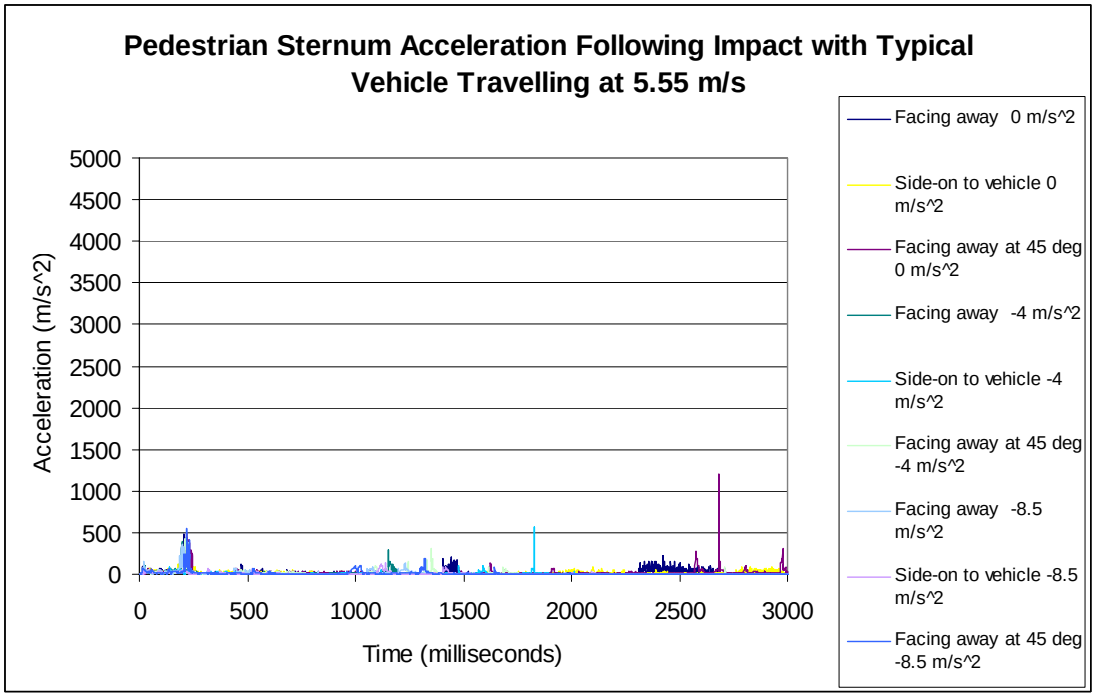

Figure 5.51 Sternum Acceleration for 5th Percentile Female MADYMO Human Model Struck by Typical Vehicle with the Vehicle Initially Travelling at 5.55 ms^{-1}, Three Different Driver Actions (No Action, Moderate Braking and Heavy Braking) and Three Pedestrian Orientations (Facing Away from Vehicle, Side-On to Vehicle and Facing Away at 45°).

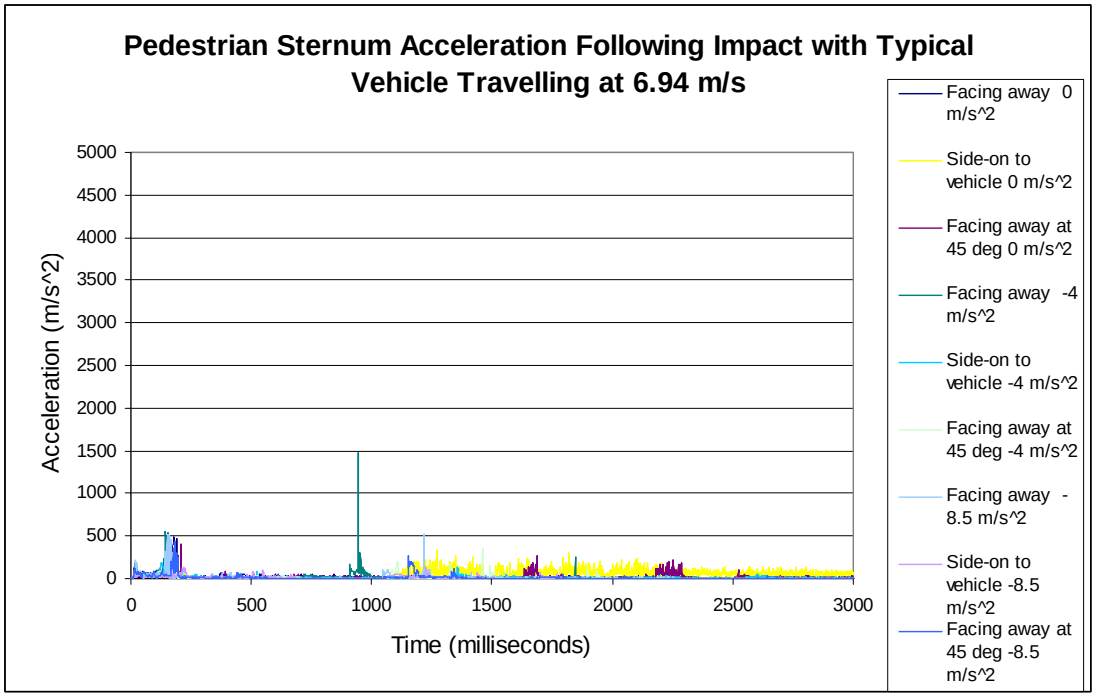

Figure 5.52 Sternum Acceleration for 5th Percentile Female MADYMO Human Model Struck by Typical Vehicle with the Vehicle Initially Travelling at 6.94 ms^{-1}, Three Different Driver Actions (No Action, Moderate Braking and Heavy Braking) and Three Pedestrian Orientations (Facing Away from Vehicle, Side-On to Vehicle and Facing Away at 45°).

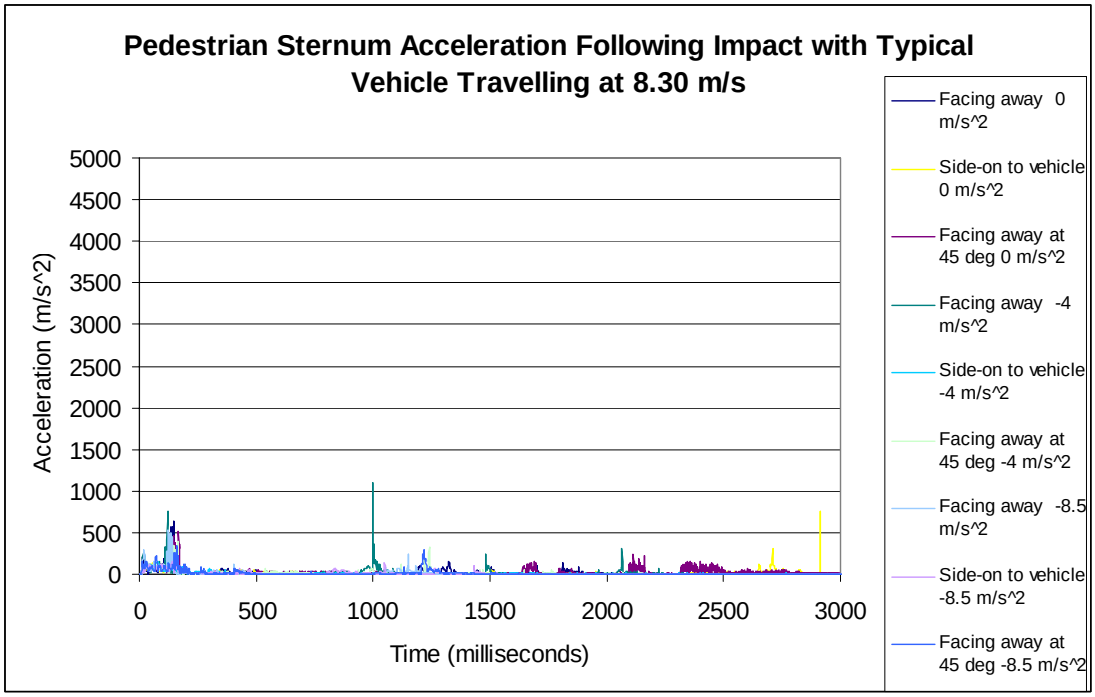

Figure 5.53 Sternum Acceleration for 5th Percentile Female MADYMO Human Model Struck by Typical Vehicle with the Vehicle Initially Travelling at 8.3 ms^{-1}, Three Different Driver Actions (No Action, Moderate Braking and Heavy Braking) and Three Pedestrian Orientations (Facing Away from Vehicle, Side-On to Vehicle and Facing Away at 45°).

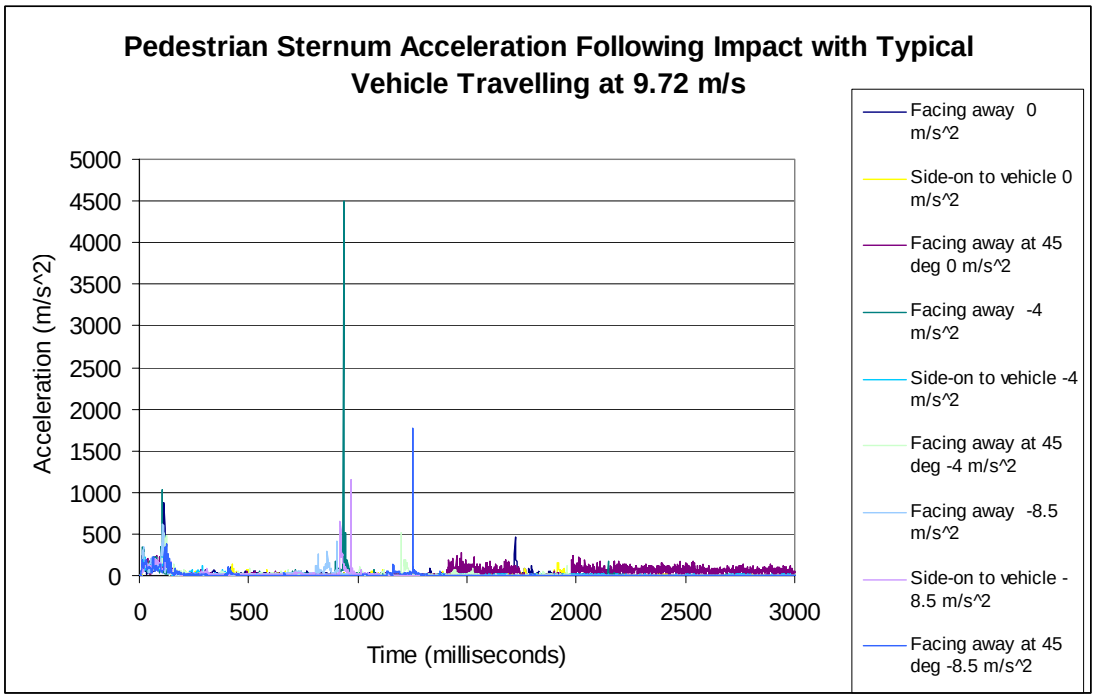

Figure 5.54 Sternum Acceleration for 5th Percentile Female MADYMO Human Model Struck by Typical Vehicle with the Vehicle Initially Travelling at 9.72 ms^{-1}, Three Different Driver Actions (No Action, Moderate Braking and Heavy Braking) and Three Pedestrian Orientations (Facing Away from Vehicle, Side-On to Vehicle and Facing Away at 45°).

Figure 5.51 shows that the sternum acceleration resulting from secondary contact (after 1000 milliseconds) is less than that resulting from primary contact except for

two out of the nine scenarios (three pedestrian orientations and three driver actions) where the initial vehicle speed was 5.55 ms^{-1} (20 km/h). In two instances (facing away from vehicle and side-on to vehicle, both with constant vehicle speed) the pedestrian failed to fall from the vehicle within the duration of the simulation (4 seconds), instead remaining on the bonnet and negating the risk of ground impact. All the sternum accelerations were of moderate to minor intensity.

Figure 5.52 shows the same nine scenarios as Figure 5.51 except with the vehicle now having an initial speed of 6.94 ms^{-1} (25 km/h). The primary contact resulted in only slightly greater sternum accelerations in comparison to the scenarios conducted at 5.55 ms^{-1} and the sternum accelerations resulting from ground contact were generally less at 6.94 ms^{-1} (as compared to 5.55 ms^{-1}) with the exception of the scenario representing a 'facing away' pedestrian and a moderately braking vehicle, which resulted in a sternum acceleration from ground contact approximately three times larger than other sternum acceleration in this set of scenarios.

Figure 5.53 displays the sternum accelerations resulting from an impact with a vehicle travelling at 8.30 ms^{-1} (30 km/h). The results for the nine scenarios are similar to those analysed for the vehicle impact speeds of 5.55 and 6.94 ms^{-1}, except that the primary contact sternum accelerations are approximately 50% higher for the scenarios resulting from a 8.30 ms^{-1} vehicle speed in comparison to those resulting from a 5.55 ms^{-1} vehicle speed, with the 6.94 ms^{-1} results falling in between.

Figure 5.54 indicates a break in the pattern, with the sternum acceleration resulting from ground contact (from 750 milliseconds onwards) of significant magnitude in two of the scenarios ('facing away', moderate braking and 'facing away at 45°', heavy braking). The sternum acceleration resulting from primary contact is greater for a vehicle impact speed of 9.72 ms^{-1} (35 km/h) in comparison to the slower vehicle speed scenarios, but the increase is not as noticeable as the escalation apparent for sternum acceleration resulting from secondary contact.

As noted for head injury potential, the most apparent and least surprising trend noticeable was the tendency for sternum acceleration to increase with increasing vehicle impact velocity. As was the case the head injury, the side-on pedestrian

orientation produced the lowest sternum accelerations for both primary and secondary contact with the exception of a vehicle travelling at 9.72 ms^{-2} and braking heavily. The 'facing away' orientation consistently produced noticeable sternum acceleration from ground contact with considerable injury potential at higher vehicle impact speeds.

Due to the extensive thoracic injuries sustained by the pedestrian in the subsequent runover event thoracic injury correlation cannot be used to assist in determining a vehicle impact speed. These results for thoracic acceleration will, however, be referred to in a comparison between the injury potential of typical vehicles and SUV-type vehicles during a vehicle-pedestrian collision.

5.7 Injury and Kinematics Correlation Summary

From the preceding sections the following observations were made:

- The knee injury prediction would appear to point towards a vehicle impact speed of less than 8.3 ms^{-1}, a pedestrian orientation that was 'side-on' to the vehicle and that the vehicle was braking heavily at the time of impact..
- Kinematic analysis indicated a pedestrian orientation somewhere between side-on to the vehicle and facing away from the vehicle (i.e. a 180 degree range) and a vehicle impact speed range of between 6.9 to 9.7 ms^{-1} (25 to 35 km/h). The 9.7 ms^{-1} impact speed was only considered likely if the vehicle was decelerating heavily at the time of impact.
- Head injury analysis suggested a probable pedestrian orientation of 'side-on' to the vehicle and that the initial vehicle speed was less than approximately 7.25 ms^{-1}.

These results indicate a likely vehicle impact speed range of between 6.9 to 7.25 ms^{-1}, a pedestrian orientation that was 'side-on' to the vehicle at the time of impact and that the vehicle was braking heavily at the time of impact.

Thoracic injury correlation could not be used for determination of vehicle speed as it was suspected that the thoracic injuries incurred by the pedestrian occurred during a subsequent runover.

5.8 Case Study 2 – Part 1: Discussion

Where pedestrian orientation was varied it was shown to have a noticeable influence on both head and sternum acceleration for both vehicle and ground contact. Simms and Wood (2005) noted that a side-on pedestrian orientation was likely to have the lowest injury potential and this is in agreement with the results shown in Figures 5.46 to 5.54. Simms and Wood noted that a front-on (or 'facing towards') orientation produced the greatest head accelerations from vehicle contact and although they did not test a 'facing away' orientation their comment that the 'facing towards' orientation had an effectively low (in comparison to the side-on orientations) radius of rotation, resulting in high impact velocities, is thought to apply also the 'facing away' orientations examined here. Simms and Wood were unable to spot any correlation between pedestrian orientation and ground contact severity.

Coley et al (2001) noted that the pedestrian orientation relative to the vehicle was the parameter with the greatest influence on pedestrian head injury from vehicle impact. Coley et al also noted that a 'facing away' orientation produced the greatest head injury values.

Bhalla et al (2002) noted that pedestrian orientation was of most influence in wrap trajectories and was less influential in collisions involving SUV-type vehicles that resulted in a forward-projection trajectory for the pedestrian.

The most apparent and least surprising trend noticeable in Figures 5.46 to 5.49 and Figures 5.51 to 5.54 was the tendency for pedestrian head and sternum acceleration to increase with increasing vehicle impact velocity. Generally, the side-on pedestrian orientation produced the lowest head and sternum accelerations for both primary and secondary contact with the exception of a vehicle travelling at 9.72 ms^{-2} and braking heavily. The 'facing away' orientation consistently produced noticeable sternum acceleration from ground contact with considerable injury potential at higher vehicle impact speeds. The same orientation also consistently resulted in the highest primary

contact head acceleration, ranging between 2500 ms^{-2} for a vehicle impact speed of 5.55 ms^{-1} to almost 6000 ms^{-2} for a vehicle speed of 9.72 ms^{-1}.

It would appear that simulation using MADYMO was able to identify a narrow range of potential vehicle speed, driver actions and pedestrian orientation with respect to vehicle at the time of impact for the case study in question. This was achieved by using injury correlation.

The consistency of the results would appear to lend credibility to the approach taken.

Improved simulation fidelity may have been possible if a finite element pedestrian model had been used which may have provided more accurate injury correlation, particularly to the lower extremities as the poor reproduction of soft-tissue injuries is a known limitation of the existing pedestrian multibody model.

The use of pedestrian injury correlation, particularly if used in conjunction with improved, validated pedestrian models, would appear to be a valid method of vehicle-pedestrian accident reconstruction for typical vehicle-pedestrian collisions not previously possible using traditional methods.

5.9 Comparison with the Results Obtained for a Collision Involving an SUV-Type Vehicle

It is interesting to compare the pedestrian head injury potential for the two different vehicle types that featured in case studies 1 and 2. Figure 5.55 shows the HIC values obtained from simulations using both a typical vehicle and an SUV-type vehicle. As per the individual case studies the HIC results are averaged across a speed range (in this instance 1.7 ms^{-1} (6 km/h)) to make general trends more apparent. The pedestrian orientation was facing the vehicle and the vehicle speed was constant.

The HIC values for ground contact following contact with the sedan-type vehicle are considerably lower than those for a pedestrian-SUV collision for speeds of 4.5 ms^{-1}

(16 km/h) or less. For speeds of 6.9 ms^{-1} (25 km/h) or more, the pedestrian tends to vault a typical vehicle and the risk of serious head injuries increases.

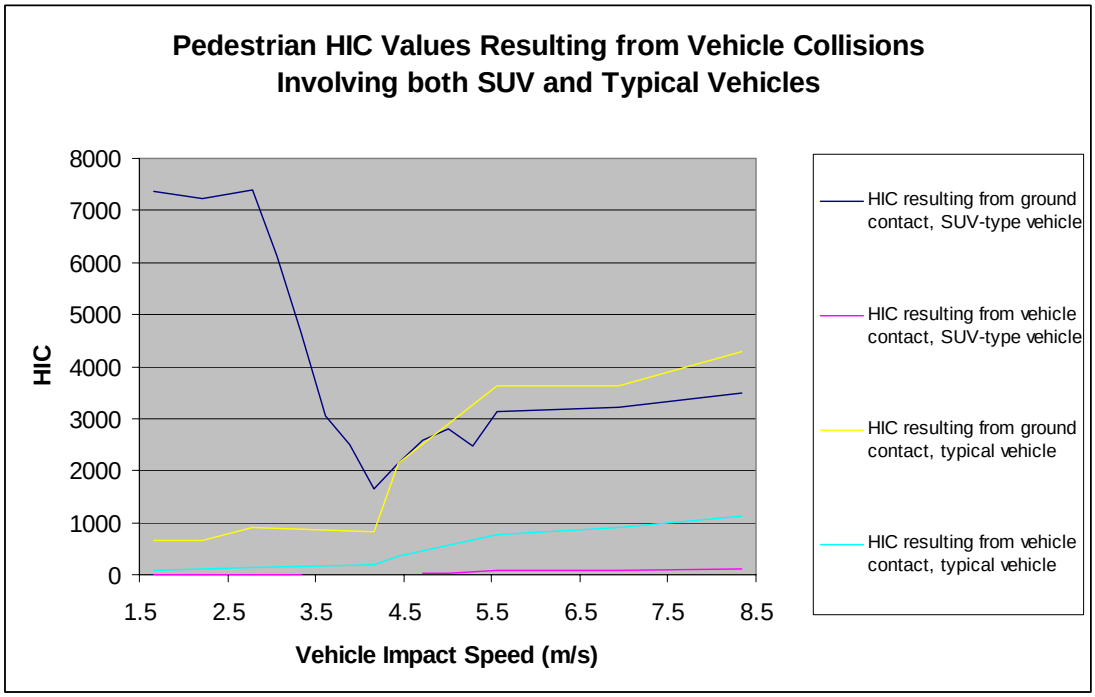

Figure 5.55 Pedestrian HIC Values Resulting from Vehicle Collisions Involving Both SUV and Typical Vehicles

Low-speed impact scenarios involving a typical vehicle did not result in a high-risk of serious head injury from ground contact as was apparent from the simulations involving a large SUV-type vehicle.

As can be seen in Figure 5.55, the HIC values from vehicle contact increase with speed more noticeably than for collisions with the higher SUV-type vehicle. This can be attributed to the higher velocity of the pedestrian's head prior to impact that is typical of impacts with lower vehicles (Mizuno and Kajzer, 2000).

The trend of increased likelihood of secondary contact injuries at lower vehicle speeds is noted by Otte and Pohlemann (2001), and this is reflected in the results for a vehicle-pedestrian collision involving an SUV-type vehicle. This trend was not apparent in the simulation series conducted involving a typical, car-like vehicle, where both the primary and secondary contact injury severity potential generally increased with vehicle speed. Otte and Pohlemann also noted that injuries from secondary contact tend to be less severe than those from primary contact, a trend which is not apparent in these simulations. It should be noted that Otte and

Pohlemann's research focussed on various vehicles travelling between 5.56 ms^{-1} and 19.4 ms^{-1} whilst the results presented in this Chapter do not exceed 10 ms^{-1}. Furthermore, the majority of collisions examined by Otte and Pohlemann usually involved a wrap trajectory (referred by Otte and Pohlemann as a 'scoop') which characteristically occurred in the simulations involving a typical vehicle whereas the simulations involving a braking SUV-type vehicle invariably resulted in a forward-projection type trajectory.

5.10 Case Study 2 – Part 2: Simulation of Vehicle Leaving Road and Subsequent Pedestrian Runover

A second simulation matrix was used to evaluate potential scenarios in a subsequent vehicle impact that resulted in severe pelvic injury. As noted in Chapter 4 the MADYMO pedestrian model has a fairly limited set of standard injury measurements. Equipping the pedestrian model with more of the occupant model's injury sensors would be very useful when correlating injury during accident reconstruction. In this instance APF (Abdominal Peak Force) would have been a useful indicator of force applied to the abdominal and pelvic regions. As it stands, it is entirely possible to equip the pedestrian model with sensors but there is no validation data available for this injury measurement.

5.10.1 Introduction

Subsequent to the initial vehicle-pedestrian collision, the vehicle went over a bank at the edge of the road and caused fatal injuries to the pedestrian. As noted previously, this case study was based on an incident that was determined to be a homicide and not an accident as maintained by the accused. Some of the unusual vehicle orientations are best examined with this information in mind.

The injury pattern and the evidence available suggested that the vehicle landed on the pedestrian a few metres down the bank, shattering the pedestrian's pelvis. It also appeared likely that the vehicle passed through a fence slightly further downhill and the lack of injuries on the pedestrian consistent with impact with the fence suggest that the vehicle passed though the fence before the pedestrian. The direction of

external injuries indicated that the pedestrian had passed underneath the vehicle feet-first.

The likely impact location and the fence location were used as constraints to investigate the vehicle speed and probable pedestrian location/orientation prior to impact as the vehicle left the road using a series of MADYMO simulations. Parameter exploration with an example vehicle can be seen in Figure 5.56. Figure 5.57 shows the fence broken by the vehicle on its downward travel.

Figure 5.56: Testing with Exemplar Vehicle at Top of Bank.

Figure 5.57: Fence Broken by Vehicle Part-way Down Bank

5.10.2 Vehicle and Environment Modelling

The same vehicle and pedestrian models from the previous modelling scenario were used as starting points for the models for this scenario. The vehicle model was modified from Case Study 2 – Part 1 to include an underside, complete with engine-sump and exhaust. The suspension modelling was enhanced to provide better accuracy over the undulating terrain. The pedestrian model's shoes were removed because (i) they were removed in reality during the on-road collision, and (ii) clearance issues between the underside of the vehicle and the ground were identified, causing high ankle forces.

Survey data was used to create surfaces that approximated the roadside bank and fence. In the absence of readily available published values for roadside verges the ground stiffness was taken to be 2 $kNmm^{-1}$ which is approximately 75% that of Chadborne et al's (1997) lowest value.

5.10.3 Simulation Matrix

The test matrix used the following variables:

- Pedestrian orientation:
    - Standing
    - Lying on vehicle bonnet
    - Lying on ground
- Pedestrian placement:
    - At edge of road
    - At top of bank
    - Partway down bank

(pedestrian placement and orientation combinations can be seen in Figure 5.58)

- A vehicle speed range of 0.56 ms^{-1} (2 km/h) (automatic transmission creep) to 3.9ms^{-1} (14 km/h) (maximum attainable speed for vehicle over available distance) in 0.56 ms^{-1} increments. No vehicle acceleration was applied because (i) there was no evidence of acceleration/deceleration on the grass verge, and (ii) once the vehicle was over the bank gravity provided the dominant accelerative force.

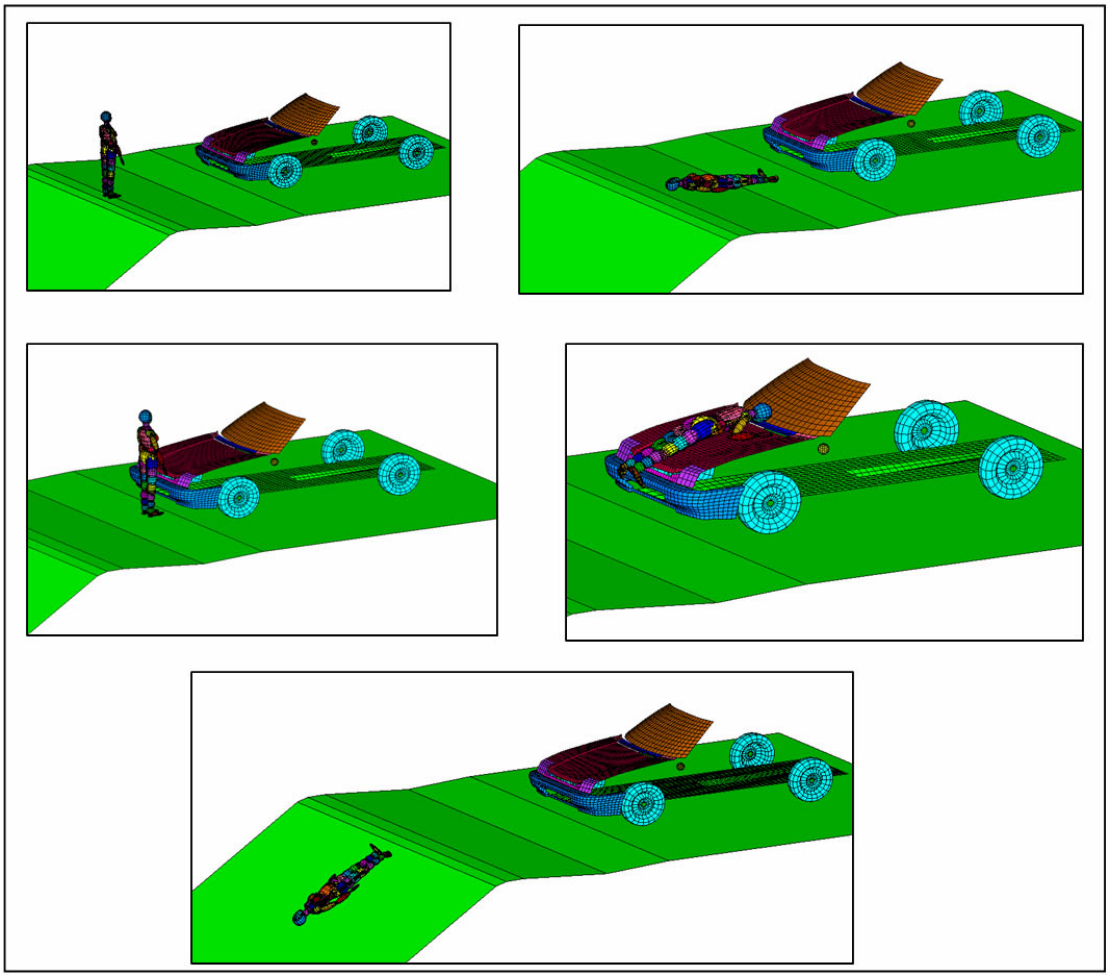

Figure 5.58: Various Pre-Impact Pedestrian Placements

5.10.4 Simulation Overview

Very few of the simulations indicated an injury pattern that matched the injuries inflicted. Some scenarios were proven unlikely for reasons other than injury correlation; when the pedestrian was placed prone on the road-side and vehicle was travelling at low speed, the vehicle became jammed on top of the pedestrian and failed to proceed down the bank.

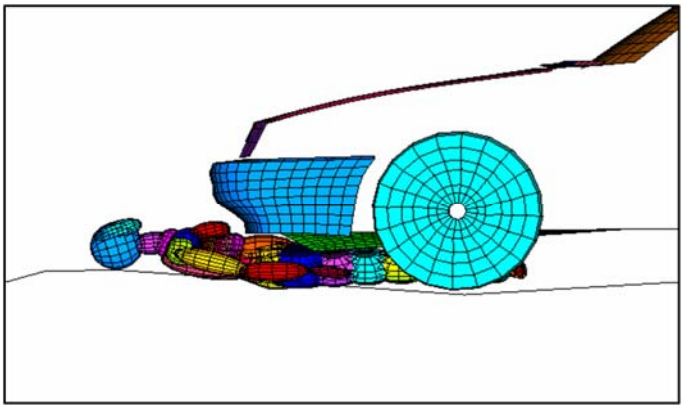

Figure 5.59: Vehicle Jammed Atop Pedestrian

It was determined from time and distance travelled that the most likely pre-impact pedestrian position/orientation placed the pedestrian on their back, feet towards the top of the bank, part way down the bank. Other pre-impact scenarios suggested events that were inconsistent with the actual injuries inflicted, including the pedestrian contacting the fence before the vehicle. From time and distance analysis it was determined that the vehicle speed as it went over the bank was approximately 3.3 ms^{-1} (12 km/h). A simulation sequence showing this result can be seen in Figure 5.60.

For a full summary of the results from the simulation matrix conducted please refer to Case Study 2: Lamar, in Appendix III.

Injury correlation was then used in an attempt to confirm the speed range.

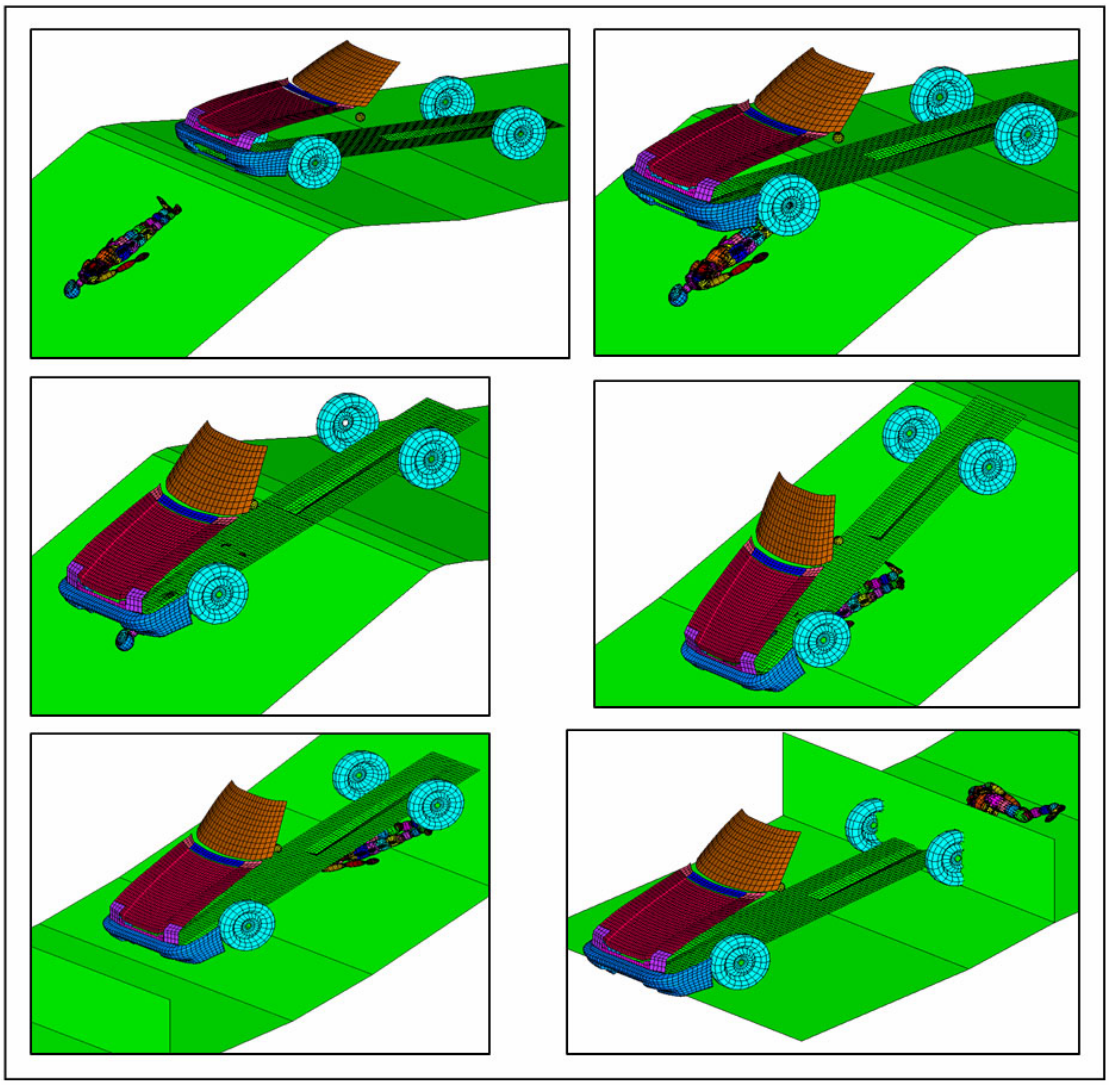

Figure 5.60: Likely Impact Sequence

5.10.5 Pedestrian Abdominal and Hip Injury Correlation

A simulation matrix was created with the vehicle given an initial speed at the top of the bank of between 1.5 to 4 ms^{-1} in 0.5 ms^{-1} increments. A vehicle speed of 1 ms^{-1} was not feasible as the vehicle failed to successfully negotiate the top of the bank at this speed or less. 4 ms^{-1} was determined to be the maximum speed achievable by the vehicle in the space available.

Figures 5.61 to 5.63 show the results for abdominal and hip force. Although the pathology report refers to a pelvic injury it would appear that in the MADYMO multibody model the hip joints are the closest measurement location for such an injury. This is not an unreasonable approach as the hip/pelvic group is often considered as a whole in injury analysis.

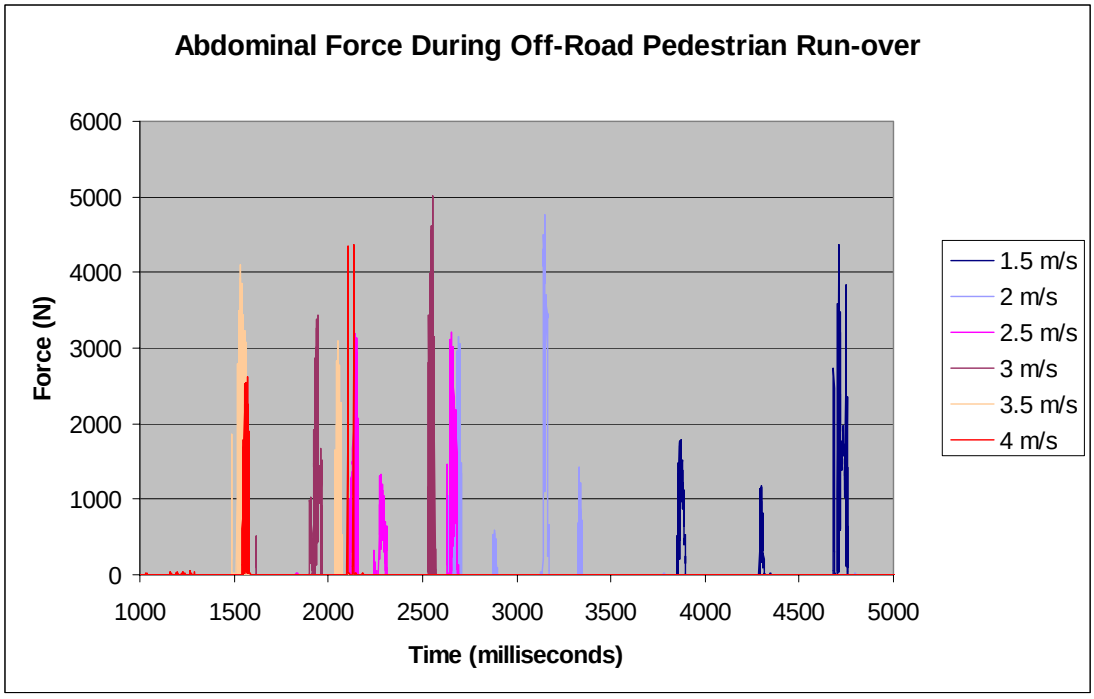

Figure 5.61: Abdominal Force during Off-Road Pedestrian Run-over

Based on the abdominal injury risk curve shown in Figure 5.11 it can be ascertained that all the scenarios indicated in Figure 5.61 pose a high risk of an AIS 3 or greater abdominal injury.

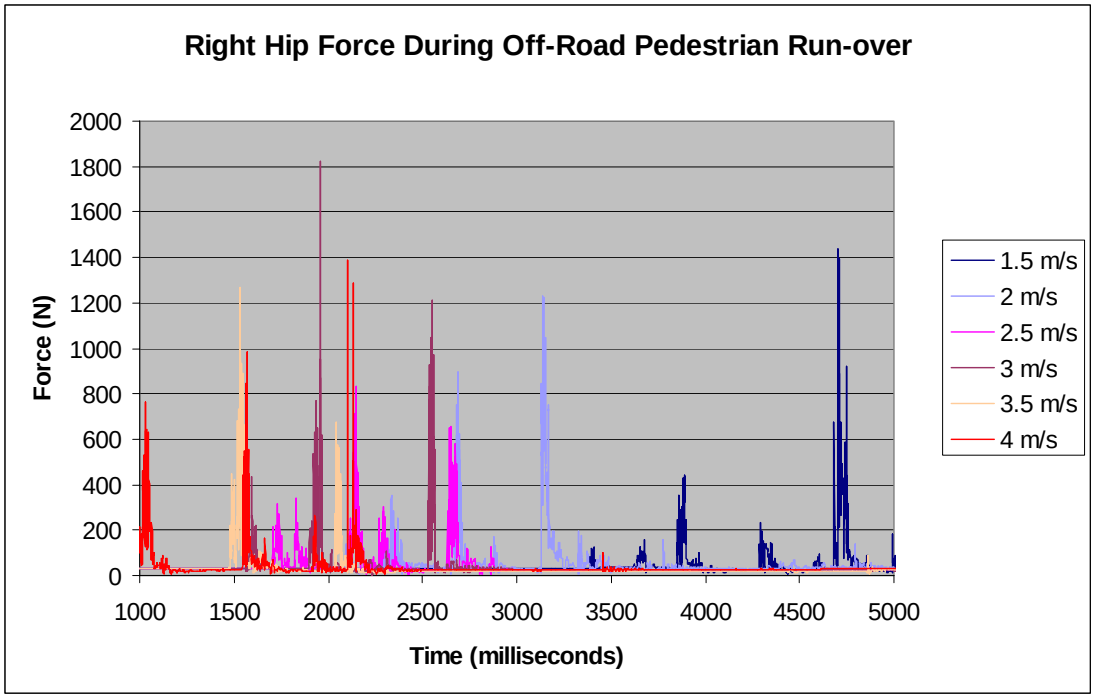

Figure 5.62: Right Hip Force during Off-Road Pedestrian Run-over

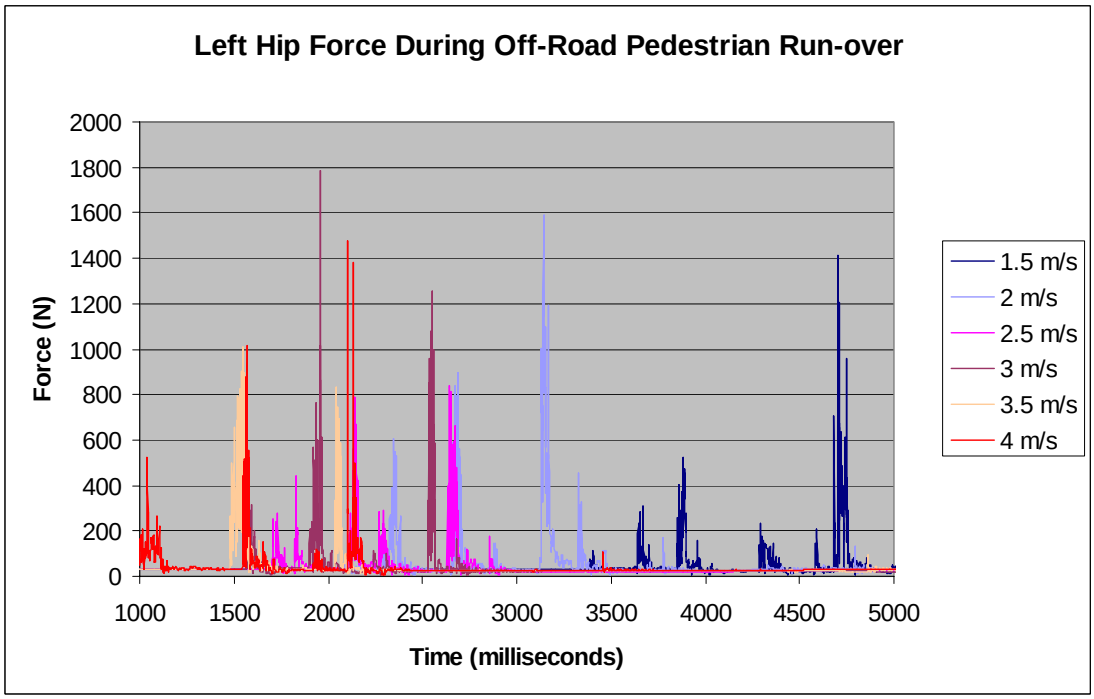

Figure 5.63: Left Hip Force during Off-Road Pedestrian Run-over

McElhaney et al (1974) refer to Messerer's (1880) findings indicating a minimum pelvis anterior-posterior loading tolerance of 170 kg or approximately 1670 N for the hip/pelvis. Most material relating to pedestrian pelvic fracture refers to lateral loading and considerably higher tolerances of between 3 to 17.1 kN (Nyquist, 1986; Snedeker

et al, 2003; King et al, 2004). If Messerer's tolerance is applicable then it would appear that the results shown in Figures 5.62 and 5.63 indicate likely hip trauma although the result is far from conclusive.

The modelling for this scenario requires scrutiny. The actual accident site was noted to include rocks and mounds not included in the simulation. Such terrain features could well cause considerably higher loadings should they coincide with the pedestrian during the vehicle impact. Although the vehicle suspension was modelled any differences between the model and reality could easily result in major differences to the load applied to the pedestrian. As Snedeker et al pointed out, a finite element pedestrian model is the preferred choice for such modelling rather than a multibody model. The vehicle underbody was only roughly approximated. Any solid objects protruding below the plane modelled (such as engine sump, transmission) could well have caused a point-loading on the pedestrian in reality.

5.10.6 Case Study 2 – Part 2: Discussion

The simulation series was able to determine a possible pedestrian placement that may have resulted in the actual injuries incurred by the pedestrian. This was determined using a time and distance method of analysis.

Injury correlation indicated the potential for severe injury, but this could also be determined by simple inspection (i.e. having a vehicle land upon a person is liable to cause injury if there is insufficient clearance between the underside of the vehicle and the ground).

Injury modelling was unable to provide additional correlation in this instance because of:

- Potential inaccuracies in terrain modelling
- Potential inaccuracies in vehicle modelling
- The use of a multibody pedestrian model instead of a finite-element model

These issues stem from the relatively unusual form of vehicle-pedestrian interaction that occurred in this instance and highlight the relative inflexibility of the modelling

method used once situations outside of the typical on-road vehicle-pedestrian interaction are considered.

5.11 Discussion and Conclusions

Simulations using MADYMO models were able to successfully predict both the kinematics and resulting injuries of a short pedestrian impacted by a tall vehicle in Case Study 1. The head injury correlation indicated massive trauma to the posterior of the head, matching the actual head injuries, for surprisingly low vehicle impact speeds. Traditional accident reconstruction methods are not capable of such predictions.

A sensitivity analysis indicated this result was not significantly affected by variation in either ground or vehicle stiffness parameters. Pedestrian kinematics were, however, shown to greatly influence head injury potential. Injuries resulting from primary vehicle contact that subsequently affected pedestrian kinematics (such as leg fracture) accordingly also influenced the head injury potential from ground contact.

Computer simulation was able to rapidly evaluate the exceedingly large number of potential scenarios encountered when evaluating the first vehicle-pedestrian impact in Case Study 2. The large number of scenarios resulted from the deliberate actions and subsequent concealment of these actions by the vehicle driver and is not something normally expected when analysing vehicle-pedestrian collisions. Injury correlation was the only method possible to substantially reduce the range of valid vehicle-pedestrian impact scenarios and it is difficult to identify any other method that would have provided such a narrow range so effectively. This injury correlation was achieved by identifying scenarios that did **not** result in either significant knee or head injury (common pedestrian injuries).

Injury correlation for the final vehicle-pedestrian impact was attempted by using the measured ground contours along the vehicle path and the vehicle measurements to create a three dimensional simulation that tracked the possible vehicle path as it left the road. The simulation's predictions regarding the vehicle's trajectory as it left the road and the resulting vehicle-pedestrian interaction were used to identify a likely

vehicle trajectory and a narrow range of vehicle speed. Traditional vehicle-pedestrian accident reconstruction methods are unable to account for the significant height differences between the vehicle and pedestrian and the three-dimensional nature of such a scenario. Accurate injury correlation in this instance was not possible, however, due to limitations of the model and modelling method.

The analysis performed on the two case studies examined in this chapter has indicated the potential for vehicle-pedestrian accident reconstruction based on pedestrian injury patterns. This method of accident reconstruction is not possible with traditional accident reconstruction techniques and demonstrates the value of computer simulation. It is also equally obvious that more research and development is needed to further improve the remarkable tool provided by mathematical modelling of human injury, particularly for the accurate modelling of off-road vehicle-pedestrian encounters.

Many of the issues surrounding the accuracy of mathematical modelling of pedestrian injury stem from the characteristics of the models themselves and the method by which these characteristics were derived. Pedestrian dummy characteristics were invariably derived using cadaver testing and pedestrian mathematical models were usually based on a combination of dummy and cadaver test results. One can therefore only reasonably expect the majority of mathematical models to duplicate the behaviour of a cadaver struck by a car.

Research based on case studies and volunteer tests is necessary to develop mathematical human models that are biofidelic and not cadaverfidelic. It is apparent to the author that the choice of virtual sensors in the mathematical models and derived injury parameters are strongly biased towards validation with experimental tests using dummies. It would appear that this has resulted from the original design goals of low-cost virtual crash testing of new car models. Unfortunately it would appear that the majority of work in this area has focussed on, and remains focussed on, the replication of crash-test methods developed and approved over a decade ago rather than improved biofidelity.

With medical researchers creating valuable, real-world injury databases it is time that this information is put to practical use. Mathematical pedestrian models need to be used more for the proactive evaluation of real-world pedestrian protection and not just as replacements for crash-test dummies. A discussion of potential methods of improving pedestrian thoracic protection will be addressed in the Appendix.

The use of MADYMO as an accident reconstruction tool has been demonstrated to be effective when applied to transport-related accidents. It is highly suited to the analysis of vehicle-pedestrian accidents and also accidents of an unusual nature, particularly those involving large vehicles with a correspondingly large number of occupants.

Computer simulation of accidents permits the analysis of a large number of scenarios quickly, cheaply and effectively. It is possible to correlate vehicle damage, pedestrian and occupant injuries and kinematics to a level of accuracy unmatched by traditional accident reconstruction techniques.

The next chapter will further introduce a standardized approach to vehicle-pedestrian accident reconstruction using computer simulation software such as MADYMO.

Chapter 6
A Generalised Approach to the Reconstruction of Real-Life Vehicle-Pedestrian Accidents Using Computer Simulation

6.1 Foreword

After the initial version of the thesis had been completed, Dr Robert Anderson (Centre for Automotive Safety Research, University of Adelaide) suggested that a new chapter should be added formalising the methodological approach used for the reconstruction of real-life pedestrian crashed such that it could be applied by others. This chapter is intended to meet that request but it should be noted that the analysis in the earlier chapters was conducted using an earlier version of MADYMO. Subsequently, there is some repetition of the simulation work described in this chapter with the discussion in the present chapter relating to a recent MADYMO version.

6.2 Introduction

This Chapter examines the issues surrounding the use of computer-simulation in a context where the most likely application is in the field of litigation. Very often the most important factor in the legal debate is the vehicle speed at the time of impact.

The value of computer-produced simulations and animation in a forensic context is widely debated (Mustard, 1987; Bohan, 1991; Leeman et al, 1991; Grimes, 1992; Stickney, 1993; McLay et al, 1994; Hull et al, 1996; Fay, 1997; Grimes et al, 1998; Bohan and Yergin, 1999; Day and Garvey, 2000; Schofield et al, 2002) and is generally only deemed acceptable if based on demonstrably sound principles.

Unfortunately, this is not easily tested. In a historic case, long before computer simulation was even imagined, the validity of scientific evidence was questioned (Frye, 1923) and the following ruling was made:

> *“Expert opinion based on a scientific technique is inadmissible unless the technique is "generally accepted" as reliable in the relevant scientific community”*

This ruling had the unfortunate effect that it could be manipulated to admit or exclude particular evidence. Indeed, it is unlikely that Darwin's theory of evolution or Galileo's planetary theories would have passed the Frye test when first proposed (Eckstein and Thumma, 1998). Because of this, it was recognised that it was more useful to apply a series of tests, such as:

> *(1) whether the proffered scientific theory or technique can be (and has been) empirically tested (i.e., whether the scientific method is falsifiable and refutable);*
> *(2) whether the theory or technique has been subject to peer review and publication (although publication "is not a sine qua non of admissibility");*
> *(3) whether the known or potential error rate of the theory or technique is acceptable, and whether the existence and maintenance of standards controls the technique's operation; and, echoing Frye,*
> *(4) whether the theory or technique has attained general acceptance*.
> (Daubert, 1993)

It is necessary to clearly distinguish between computer animations and simulation. In this thesis 'simulation' is taken to mean the application of the laws of physics in a consistent and repeatable manner to replicate real world events by analysing forces, energy, acceleration and motion at discrete time intervals. An 'animation' is the process of visual creation of a scenario that may or may not be representative of physics. At times it is not easy to determine whether an exhibit is an animation, a simulation or both. Definitions described by other authors (in particular Bohan, 1991 and 1999) provide the following classifications:

1. An animation equivalent to a series of chart drawings or diagrams. The depicted motion was derived from calculations separate to the method of creating the animation.
2. An animation produced using traditional vehicle accident reconstruction methods and calculations (usually empirical) where the calculations are performed automatically.
3. A simulation produced using computer software that relies on the laws of physics integrated over discrete time-steps. The accuracy is determined by

the input parameters, integration method and assumptions relating to the application of the laws of physics.

Animations are usually produced for illustrative purposes. In the first classification above the animation is completely separate from any calculations. In the second method any animations produced are usually bound by the restrictions imposed by the fairly simple calculation methods. Indeed, the majority of traditional vehicle-pedestrian accident reconstruction only 2-dimensional calculations are performed, although often these are used to produce animations that appear to move through 3-dimensions.

In this chapter the third classification described above is examined and a process is suggested for reliable simulation of vehicle-pedestrian accidents. As a matter of definition in this thesis, the animations produced by computer simulation are considered to be an integral output of the simulation process and in the remainder of this chapter any animation referred to has been produced by simulation.

6.3 Looking Forwards, Looking Backwards

An important point to note is that traditional accident reconstruction methods tend to operate on a ‘looking backwards’ principle (Grimes et al, 1998). The ‘looking backwards’ approach typically starts with final positions (vehicles, people, debris) and traces the approach paths backwards to determine initial positions and velocities. The scenarios deemed to be likely are those that appear to match witness statements and other evidence.

Simulations, on the other hand, are ‘looking forwards’ and start with an initial set of conditions that are applied to the objects of interest. The motion of these objects, their interaction with the environment and each other and the final rest positions are determined by physics and the assumptions applied. Commonly, an iterative approach is needed in order to match the end condition to the scenario being replicated.

Often, a ‘looking backwards’ method (or methods) is used to determine the input parameters for a ‘looking forwards’ simulation and to provide cross-checking.

6.4 Type of Simulation

As has been discussed in previous chapters, a number of software packages exist to assist in the calculation of forces, accelerations and vectors associated with a collision between two objects. Unsurprisingly, the majority of software packages are targeted at vehicle-to-vehicle automotive accidents. For the simulation of accidents such as these, the objects (vehicles), are usually treated as monolithic objects of stipulated mass and inertia properties and that may or may not have stiffness and deformation characteristics. The vast majority of vehicle-accident simulation software also only function on a two-dimensional plane, referred to here as the *x-y* plane, which is coplanar with the vehicles direction(s) of travel.

It is therefore apparent that it is necessary to determine the most appropriate simulation method relative to the scenario under examination. In the vast majority of vehicle-pedestrian collisions the pedestrian is displaced not only across the *x-y* plane but also undergoes a height displacement. Depending on the height of the pedestrian, the vehicle shape and the relative directions of travel of both the vehicle and the pedestrian, the pedestrian may have a positive or negative launch angle. In scenarios with a positive launch angle the maximum height attained by the pedestrian post-collision may be considerable. In these scenarios three-dimensional analysis is a necessity.

6.5 Determination of Simulation Parameters

Parameters that require consideration in vehicle-pedestrian accident reconstruction include the following:

Environmental Parameters

- Surfaces
- Gravity
- Primary Objects
- Secondary Objects

Pedestrian Factors

- Size
- Shape
- Mass
- Pre-impact motion
- Injuries

Pedestrian Factors (continued):

- Distance travelled between primary and secondary vehicle impacts
- Launch angle
- Centre of mass height at launch
- Relative speed between vehicle and pedestrian at launch
- Distance from launch to ground impact (airborne travel)
- Distance from ground impact to rest position (tumbling/sliding distance)
- Pedestrian versus ground coefficient of friction

Vehicle Factors

- Size
- Shape
- Mass
- Driver actions
- Post-impact vehicle travel distance and deceleration

Collision Factors

- Air drag
- Projection Efficiency
- Pedestrian Trajectory Type
- Pedestrian versus vehicle coefficient of friction
- Vehicle Damage
- Secondary/other vehicle-pedestrian interaction
- Contact Characteristics
- Other Debris

These factors will now be examined in more detail.

6.5.1 Environment

Surfaces

The degree to which the environment is represented can vary widely. Some authors would appear to focus their attention almost entirely on the model and have limited regard for the environment. Such instances included head versus ground impact where the ground is modelled as a rigid plate with no discussion or justification as to the appropriateness of such an approach (Horgan, 2005). For instances where the ground is extremely hard (eg concrete) such an approach may be reasonable, but the issue should be addressed in the discussion. In many instances the ground is not infinitely

hard (grassed roadside verges, for example) and the corresponding stiffness characteristics need to be defined.

Gravity

Obviously, for all earth-bound simulations gravitational acceleration needs to be included. Noting that the gravitational constant is one of the most inexactly determined physical constants, but taking it to have a value of approximately 6.655×10^{-11} $m^3kg^{-1}s^{-2}$, the acceleration due to gravity can be determined using:

$$g = \frac{GM_E}{{R_E}^2}$$

where g is acceleration due to gravity

G is the gravitational constant

M_E is the mass of the Earth

R_E is the radius of the Earth

It should be noted that as the Earth is an ellipsoid the radius varies between 6356.75 km at the poles to 6378.135 km at the equator, at sea level. The standard value for g is 9.80665 ms^{-2} which is taken at an arbitrary geodetic latitude of about 45.5°. In the Southern Hemisphere this would correspond to the city of Dunedin in New Zealand. For other locations the Earth's radius can be determined using the formula:

$$R = \sqrt{\frac{\left(a^2\cos(\phi)\right)^2 + \left(b^2\sin(\phi)\right)^2}{\left(a\cos(\phi)\right)^2 + \left(b\sin(\phi)\right)^2}}$$

where a and b are the major and minor semi-axis of the Earth, respectively

$ø$ is the latitude, in degrees

Thus g will typically lie in the range of 9.78 to 9.83 ms^{-2} at sea level. Re-examining equation 2.14 for the launch velocity of a tumbling and sliding point object, namely:

$$v = \sqrt{g\left(\frac{d_a}{h + d_a} + 2\mu d_g\right)}$$

It can be seen that for airborne distance of 10 m, a sliding distance of 10 m, a centre of mass height of 1 m and a coefficient of friction of 0.6 that the calculated launch velocity varies according to latitude (and corresponding variation of *g*) in the following manner:

Latitude	Calculated Launch Velocity
0	11.24 ms^{-1}
45	11.25 ms^{-1}
90	11.27 ms^{-1}

For the example given the variation is seen to be less than 0.3%. It is therefore apparent that if acceleration due to gravity is taken to be 9.81 ms^{-2} any error introduced would be negligible.

Primary Objects

Any entities whose interaction influences the outcome of a simulation is a primary object. It includes surfaces (mentioned above) and also includes other objects that are struck during the simulation. Examples include roadside furniture and banks.

Primary objects require accurate modelling, as their parameters influence the outcome of the simulation.

Secondary Objects

Any object that does not interact with the objects of interest during the course of a simulation is a secondary object. They are generally incorporated as reference points and often include trees, painted road markings and signs. Secondary objects do not require to be as accurately modelled (unless there is evidence that they were narrowly avoided).

For further reference on both primary and secondary objects and their importance in litigation it is recommended to refer to either Bohan (1991)(where they are referred to as ‘Illustrative Evidence’), Grimes (1992) and Grimes et al (1998).

6.5.2 Pedestrian Factors

Size, Shape and Mass

A number of authors have noted the influence of pedestrian size on the resulting kinematics following a vehicle-pedestrian collision (Eubanks and Hill, 1994; Han and Brach, 2001; Toor et al, 2002). In fact, it is the relative size and contact heights of both the vehicle and pedestrian that is of importance. Mizuno and Kajzer (2000), as noted in Chapter 5, reiterated the importance of wrap-around distance (WAD) in head-injury severity. If the pedestrian size is modelled incorrectly, the WAD will be incorrect and the injury potential incorrectly determined.

The mass and height of the centre of mass of the pedestrian require accurate modelling. Whilst the 55% rule (as per Chapter 2) may prove accurate for finding the height centre of mass for the majority of the population it does not necessarily hold true for children, the elderly or the physically disabled. If the mass properties of the pedestrian are modelled incorrectly then the pedestrian's motion following impact, particularly rotation, is unlikely to be accurate.

Pre-Impact Motion

The pedestrian orientation with respect to the vehicle, gait and velocity need to be taken into consideration. They can also be very difficult to model correctly, for the following reasons:

- pedestrian orientation immediately prior to impact may be difficult to determine, as the pedestrian often reacts during the last moments before impact. Wakim et al (2004) discuss this at length
- pedestrian velocity can vary considerably, even before any reaction effects are considered (Zhao and Wu, 2003; Ishaque, 2006)
- ground reaction force varies constantly during perambulatory motion (Giddings et al, 1999).

Injuries

Damage models have been developed that allow for pedestrian injury correlation from the simulation of vehicle-pedestrian accidents. Peak Virtual Power allows for thoracic

and head injury evaluation and correlation (Neal-Sturgess, 2002; Neal-Sturgess et al, 2002). Lower limb injury models have been extensively developed by Yang (1997) and Yang et al (2000, 2002, 2005).

It is important to ensure that the correct injury model is used. Soft-tissue injury models should only be used for evaluating appropriate injuries and likewise for hard-tissue (skeletal) injuries. For more information on pedestrian injury correlation please refer to Chapter 5.

6.5.3 Vehicle Factors

Size and Shape

As noted under pedestrian factors, it is the interaction between vehicle geometry and the pedestrian geometry that determines the resulting kinematics. Authors that have drawn attention to the influence of vehicle geometry on vehicle-pedestrian interaction include Eubanks and Hill (1994), Mizuno and Kajzer (2000), Roudsari et al (2004 & 2005), and Simms (2006) amongst others.

In order to save considerable computation time it is entirely feasible to only model the parts of the vehicle that interact with the pedestrian. Other vehicle parts may either be omitted or included in a simplified manner (ie lacking in physical attributes and interaction definitions) as secondary objects for visualisation and reference purposes.

Mass

Vehicle mass usually requires accurate modelling only if the vehicle is moderately small and the pedestrian moderately large. Manufacturer data and likely loading will provide a sufficiently accurate mass for most simulations. Exceptions to this include scenarios where the vehicle either drives over or lands on the pedestrian (as per Chapter 4, Section 4.5).

Driver actions

Driver actions pre-collision should be considered. Evidence of heavy braking prior to impact should be taken into account and appropriately simulated. Heavy braking will tend to lower the front of the vehicle (from load shift), altering the contact

characteristics between the vehicle and the pedestrian. Heavy braking will also tend to extend the contact period between the vehicle and pedestrian and increase the likelihood of both vehicle and pedestrian attaining a common velocity. A turning or swerving vehicle will have implications relating the positions of primary and secondary vehicle contact. An accelerating vehicle is likely to have the shortest duration of contact with a pedestrian.

Indications of Vehicle Speed

Any evidence relating to a possible speed range for the impacting vehicle requires examination. As noted earlier, 'Looking Backwards' using traditional vehicle accident reconstruction techniques can be applied. Often, a probabilistic speed range can be determined and used in subsequent simulations although care should be taken to ensure that the methodology employed and the range of results obtained is reasonable. Coefficient of friction testing should be conduced in a manner that replicates as closely as possible the circumstances of the collision. If the vehicle involved is substantially damaged or unavailable rolling resistance values should be obtained from the literature with a suitably wide range considered, especially if vehicle transmission type, gear selection and tyre pressures are uncertain (Cliff and Bowler, 1998).

6.5.4 Collision Factors

Pedestrian Trajectory Type

As per Chapter 2, Section 2.4, five unique pedestrian trajectories are commonly described:

6. Wrap trajectory
7. Fender vault
8. Roof vault
9. Somersault
10. Forward projection

The type of pedestrian trajectory should be correlated with vehicle type, vehicle damage, driver actions, throw distance and pedestrian injuries.

Projection Efficiency

Chapter 2, Section 2.14 notes that the pedestrian seldom attains the vehicle's linear velocity during a collision. Often rotational motion is imparted to the pedestrian, giving rise to reduced linear throw distance. In other cases it would appear that considerable kinetic energy is absorbed by damage to the vehicle and/or the pedestrian. A useful term to employ is *projection efficiency*. This relates the proportion of vehicle velocity attained by the pedestrian at the point of separation and should be applied to traditional vehicle-pedestrian equations, either when used as a standalone solution or as a simulation cross-check.

Furthermore, in the case of large pedestrians impacted by small vehicles momentum exchange dictates that the collision may noticeably slow the vehicle, further reducing the effective projection efficiency. For example, a collision between a stationary large male weighing 120 kg impacted by small (but boxy) Suzuki Wagon R weighing 950 kg (including driver and cargo) and travelling at 50 km/h would result in a reduction of vehicle velocity of almost 6 km/h (based on conservation of linear momentum). At the other extreme, a small child impacted by a large truck would have negligible influence on vehicle velocity.

Happer et al (2000) provide some suggested projection efficiencies for forward projection and wrap trajectories, with a range of between 81% and 99.9% for forward projection and with 23% to 89% as minimum values, based on height of pedestrian centre of mass above the vehicle bonnet for wrap trajectory.

It should be noted that if a simulation is created correctly there is no need to apply projection efficiency to the results, other than when using traditional methods to validate the simulation results.

Air drag

Many simulations treat the model as if it were in a vacuum. For low model velocities this suffices as a reasonable approximation, but at higher velocities air-drag becomes an important factor. As noted by Collins and Morris (1979) air drag may be safely ignored for pedestrian launch speeds of less than 40 km/h. Aronberg (1990) provides some guidelines for speed loss from air drag for launch velocities over 40 km/h. It

should be noted, however, that these guidelines were developed from skydiving data, with the skydiver in a 'spread' stance. It can be safely assumed that the drag on a tumbling pedestrian may be somewhat different. Aronberg notes that speed loss from air drag is proportional to the total airborne distance travelled by the pedestrian and not the total throw distance. Therefore, pedestrian trajectories with a high apogee will be more affected by air drag than those with a lower apogee. It should also be noted that moderate to high winds will have an influence on airborne pedestrian air drag, particularly where higher vehicle speeds are suspected.

Empirically-derived vehicle-pedestrian equations will account for air-drag only in typical, relatively low pedestrian apogee, scenarios where high vehicle and wind speeds are not a factor. As noted in Chapter 2, the basic projectile motion equation derived therein neglects air drag.

A paper of note is that by Bhat et al (2002) describing the computation of the physical parameters of an airborne object based on video footage. The method described involves the simultaneous analysis of all video frames for a best fit solution for velocity (both linear and rotational) and air drag, assuming known mass and inertial properties. Such an approach could be applied to digitised video footage of pedestrian accidents, such as that from Helsinki analysed by Randles et al (2001), but where higher impact speeds are typical. Probable air drag factors for airborne pedestrians could then be determined.

It should be noted that the vehicle-pedestrian scenario simulations described in this thesis all involved vehicle-pedestrian impacts below 40 km/h. Accordingly, air drag was not taken into account.

Projection Distance

In some instances projection distance is well defined. In other instances there are uncertainties relating to the impact point and/or the rest position of the pedestrian. Furthermore, there are uncertainties relating to the proportion of airborne travel versus tumbling/sliding along the ground, as well as potential unknowns relating to launch angle and apogee height. Empirically-derived and other traditional vehicle-pedestrian equations do not always distinguish between the different factors noted above and

some do not distinguish between any of them. For some factors this is not of great concern, as it is often impossible to determine launch angle and apogee. For litigation purposes a launch angle of 45° is often used, as this indicates a minimum launch velocity for a given throw distance. As noted in Chapter 2, a launch angle range of between 20º and 50º changes the calculated launch velocity by less than 4% and that for a range of 10º to 60º the computed launch velocity is changed by less than 10%.

In comparison, the airborne versus tumbling/sliding portions of travel are often well defined (usually from fluid-splatter or other debris at the landing point) and provide useful correlation data. For such situations partial simulation validation may be obtained from matching the airborne and tumbling/sliding travel portions.

Coefficient of Friction (for both vehicle and pedestrian)
The coefficient of friction between the vehicle's tyres and the ground is usually fairly easily obtained using methods widely described elsewhere (Brach et al (1998) is a useful reference). The coefficient of friction between the pedestrian and the ground is not so easily obtained. As described in Chapter 2, Section 2.11, a fairly wide range of pedestrian friction factors is described within the literature. It is also difficult to test without causing injury. Furthermore, many authors appear to use an effective coefficient of friction over the entire throw distance, which is an average over the airborne and tumbling/sliding portions of travel.

The friction between the pedestrian's shoe and ground surface also requires consideration, especially in respect to leg forces generated during bumper contact. Stammen and Barsan-Anelli (2001) used a coefficient of friction of 0.67 between the foot of the pedestrian model and the ground. The author of this thesis considers that the friction between a rubber-soled shoe and a road-surface and the friction between a vehicle's tyre and the road may indeed be similar. In this context, a value of 0.67 does not seem unreasonable.

The coefficient of friction between the pedestrian and vehicle also needs to be determined to effectively simulate vehicle-pedestrian interaction. A brief literature appraisal reveals a range of values. Simms (2006) recommends a value of 0.2, scarcely different from Yoshida et al (1998) and Stammen and Barsan-Anelli (2001)

who used a value of 0.25. Alternatively Carter et al (2005) use a value of 0.5 from Yang et al (2000). Ashton et al (1983) experimented with a range from 0 – 0.5 for vehicle-pedestrian friction for their modelling. Eubanks (1994) quotes Wood as using a value of 0.4 and Galli a range of 0.25 – 0.35. Variability in pedestrian clothing would appear to influence the disparity of values and case by case testing may have merit.

Vehicle Damage

Damage to the vehicle as a result of the pedestrian impact should be closely examined, photographed and measured. Marks left by clothing, fluid splatter, hair and other debris from the pedestrian can be correlated to injuries and marks on the pedestrian. Happer et al (2000) and Toor et al (2002) provide useful look-up tables relating vehicle damage to impact speed for forward-projection and wrap-trajectories. Resources such as these can provide helpful starting points but should not be relied-on too heavily.

Secondary/Other Vehicle-Pedestrian Interaction

Any additional vehicle-pedestrian interaction that occurs after the initial impact needs to be considered. Impacts by the pedestrian's head or other body parts on bonnets, windscreens, vehicle roof or elsewhere provide valuable insight into the pedestrian dynamics. Subsequent run-overs of impacted pedestrians need to be noted, as they indicate a vehicle that is either not braking or braking only lightly (Eubanks, 1994).

Contact Characteristics

Appropriate pedestrian contact characteristics should be used. Should head injury be under consideration, then the contact stiffness of the head needs to be correctly modelled. A stiffness of 6500 Nmm^{-1} is quoted by the MADYMO Human Models Manual (via Neal-Sturgess et al, 2002) whereas a range of 3500 Nmm^{-1} to 1400 Nmm^{-1} for anterior-posterior head loading and 2800 Nmm^{-1} to 700 Nmm^{-1} for lateral head loading is quoted by McElhaney et al (1976). Ishikawa et al (1993) used a head stiffness of 900 Nmm^{-1} based on JARI cadaver testing. Yang et al (2000) quoted a range of 1730 to 3570 Nmm^{-1}, attributable to Voigt et al (1973) and Allsop et al (1991). Yang then used a value of 2500 Nmm^{-1} in a later paper (2003). It would appear that the value used by default in earlier MADYMO models was based on the

stiffness of a dummy, and not an actual head. The expected range is therefore between 700 – 3570 Nmm^{-1}. If the loading direction is known, then the ranges of 700 Nmm^{-1} to 2800 Nmm^{-1} for lateral loading and 1400 Nmm^{-1} to 3570 Nmm^{-1} for anterior-posterior loading appear reasonable.

It should be noted that none of these values take either rate-dependence or non-linearity into account. The issues that arise due to rate-independent, linear contact models in respect to the validity of results over a range of crash conditions is noted by Anderson et al (2005).

The contact interaction models available in the MADYMO release (6.0.1) used for the simulations described in this thesis have a considerable number of constraints which would be expected to reduce the accuracy of results under certain circumstances. MADYMO's elastic contact model calculates the elastic contact force based on either force-penetration, stress-penetration or a penalty factor (MADYMO Theory Manual). However, when modelling a finite-element vehicle impacting a pedestrian, it is not possible to select that both vehicle and pedestrian characteristics are utilised in an elastic contact model, unless one defines a custom contact model for each interaction of interest (as defined within the MADYMO User Manual). If a kinematic contact model is selected this constraint does not apply. One must therefore be careful which contact model is selected to evaluate interactions between objects of different stiffnesses.

The damping force present in an elastic collision is calculated in MADYMO according to:

$$F_d = F_{ampl}(F_e)\left[C_d\left|v_{norm}\right| + F_{damp}\right]$$

where F_d is the damping force

C_d is the damping coefficient

F_{damp} is the damping velocity function

F_{ampl} is the amplification function dependent of the elastic force

F_e is the elastic force

Of particular interest is the damping applied to head contacts due to the influence on calculated head injury.

Anderson et al (2005) discuss at length the importance of accurate contact definitions for the correct simulation of vehicle-pedestrian contact interaction and note the limitations of using multibody objects for modelling such scenarios.

The relationship between vehicle panel stiffness and pedestrian injuries has been examined by other authors (Neal-Sturgess et al, 2002). Ishikawa et al (1993) used a linear stiffness of 2000 Nmm^{-1} for both bumper and bonnet edge. Yang et al (2000) used a bumper stiffness of 300 Nmm^{-1} and a bonnet edge stiffness of 2000 Nmm^{-1}. Howard et al (2000) indicated a bumper and bonnet stiffness of 2000 Nmm^{-1}. Yang (2003) analysed the influence of bonnet top stiffness over a range of 75 to 300 Nmm^{-1}. Coley et al (2001) used values of 200 Nmm^{-1} for bumper stiffness, 850 Nmm^{-1} for the leading edge of the bonnet, 300 Nmm^{-1} for the bonnet top and 1250 Nmm^{-1} for the windscreen. As noted by the authors, these values do not represent the variation that occurs across a panel surface due to design creases, sub-structure or other vehicle components underneath or the distance from rigid boundaries (such as the influence of the A-pillars on windscreen stiffness). Stammen and Barsan-Anelli (2001) conducted a series of tests to determine the windscreen stiffness of a Honda Civic subjected to impact from a head impactor. Their results indicated a windscreen stiffness of 860 Nmm^{-1} prior to failure.

Chadbourn et al (1997) measured a stiffness range of 26.5 to 60 $kNmm^{-1}$ for asphalt roads at 25ºC. Timm et al (1999) noted the temperature influence on the stiffness of asphalt, indicating a modulus of 345 MPa at 40 ºC to 14,000 MPa at -20ºC, with a design modulus of 3500 MPA at 25ºC.

Other Debris

Any evidence of other debris, either from the vehicle or pedestrian, should be examined. Projectile motion can be applied to objects originating from the pedestrian, especially those loosely retained (e.g. eye-glasses, shopping bags etc) can assist in identifying the point of impact. Whether debris are used in ‘Backwards Looking’

checks, as a part of the simulation or disregarded would need to be determined in a case by case basis. Glass fragments are good candidates for ‘Backwards Looking ‘ analysis, as the spread of glass debris can be compared to a theoretical launch angle range if the glass is known to have originated from the same region to give an indication of launch speed. Larger debris components, such as a dislodged vehicle bumper may be best modelled using simulation in order to determine object motion following separation from the vehicle. The motion of some debris objects, such as hand-held water bottles is very difficult to model due to the low ground resistance when rolling and the correspondingly large influence of ground contours and wind. In such instances debris analysis is often impossible.

6.6 Determination of Simulation Bounds

6.6.1 Time Step

As noted in Chapter 3, Section 3.3.3, simulations that utilise finite element analysis can use either implicit or explicit solvers. To recap, implicit solvers use a forward difference algorithm and assume constant acceleration over the integration time step. The smaller the time-step, the greater the accuracy.

On the other hand, explicit solvers typically use the central difference method where displacements are assumed to occur linearly and the resulting accelerations and velocities are determined. Unless the time step is smaller than a value based on the media stress wave velocity and the smallest element dimension the solver will tend to be unstable.

A large time step results in fast computation but at the risk of inaccuracy where implicit solvers are used and instability in the case of explicit solvers.

6.6.2 Duration

The duration of a vehicle-pedestrian collision may extend for several seconds before the pedestrian comes to rest. The majority of this period consists of the pedestrian’s vault and tumbling/sliding trajectory. The actual interaction with the vehicle usually has a duration of less 1 second, although an exact range of values is hard to locate in

the literature. Wood et al (2005) refer to the duration of impact (t_{impact}) during which the momentum exchange between the vehicle and the pedestrian is completed. Wood et al refer to a range between 56 to 140 milliseconds for t_{impact}, based on research from Aldman et al (1980). Reference to Aldman et al reveals that the 56 to 140 millisecond range is for leg to bumper contact only. Further vehicle-pedestrian interaction, such as bonnet or windscreen contact, extends the total duration of contact considerably.

Schreurs et al (2001), when simulating a 50th percentile male impacted by a bonneted vehicle, noted that the head did not impact the windscreen until 120 milliseconds after initial leg-bumper contact. Svoboda and Čížek (2003) determined an impact duration of approximately 27 milliseconds for a typical pedestrian head-vehicle contact during testing involving a 40 km/h vehicle impact speed. Summing these results indicates a total t_{impact} of about 150 milliseconds. Chawla et al (2003), when simulating the interaction between three-wheeled scooter taxis and pedestrians, determined a duration of contact of 175 milliseconds.

Vehicle shape, type of pedestrian impact (eg wrap, forward projection etc) and relative vehicle mass (in the case of smaller vehicles, all have some influence on duration of impact. Vehicle impact speed has the greatest influence, with shorter impact durations resulting from higher-speed collisions.

In the interests of efficient computation an initial simulation series of short duration can be conducted to evaluate pedestrian contact points on the vehicle. Such a simulation would need to replicate the scenario for between 150 to 500 milliseconds depending on the impact speed. Once a reasonable match between contact points is established, longer simulation durations can be used to evaluate pedestrian motion post vehicle separation, subsequent ground contact and throw distance.

6.6.3 Model Detail

Primary objects require sufficient detail to behave in a realistic manner. This includes size, shape, mass and other physical properties such as stiffness and coefficients of friction. Vehicles are considerably easier to model than pedestrians, especially if the vehicle is a recent model and the manufacturer has released public domain FEA models based on those used in the design process. As discussed in Chapter 3, a truly

biofidelic human model does not yet exist. Indeed, because of such complex issues as muscular response it is possible that such a model may never exist. There are however, as discussed previously, a number of human models that have been validated under various vehicle-pedestrian impact scenarios. It is therefore necessary to compare the circumstances under which the model was validated to the scenario under consideration and judge whether the model is appropriate for the task. A pedestrian model such as that used by Yang et al (2000) has well validated lower extremities and would be suited to modelling a scenario where knee injury (for example) is of interest. Where head injury is of interest a model such as that described by Willinger et al (1999) would be advisable.

6.6.4 Test Runs for Overview, Detailed Runs for More Exact Results

It can be useful to conduct test simulations to gain an overview of the scenario, with more detailed and focused simulations targeting specific events or sequences of interest. This approach results in computational efficiency but requires user judgement.

6.6.5 Deterministic versus Probabilistic Analysis

Whilst deterministic simulation has been determined suitable for virtual vehicle testing its appropriateness for accident analysis is debateable. Probabilistic analysis with the results expressed in terms of likelihood is gaining favour in the accident reconstruction community

6.7 Uncertainty and Error

Many of the simulation parameters, as described in this chapter, are not exact, known quantities. The coefficient of friction between a pedestrian and the ground is a good example of an uncertain parameter. The following sections provide examples of how the uncertainties arise and how to account for them.

6.7.1 Technique/Application Error

Errors resulting from incorrect technique or misapplication are hard to correct for. They are best removed from the problem by re-examining and identifying the correct method of measurement. An example would be using a tyre drag-sled, normally used

to determine the vehicle-to-ground coefficient of friction, to determine the coefficient of friction for a tumbling pedestrian. In this instance the parameter should be preferably re-measured, preferably with a suitably attired dummy (and possibly thrown from a moving vehicle) or, failing that, corresponding values from literature (although such a course of action has inherent potential for error also).

6.7.2 Measurement Error

Measurement errors can arise in a number of ways. Equipment can be poorly calibrated, displays can be misread (the swinging needle on a spring-balance whilst dragging an object over a surface is a case in point) and measurements can be mis-recorded. Units can also be mistakenly applied. Usually common sense can be applied to identify these errors. Re-measurement is usually the best method of correction.

6.7.3 Interpretation Error

Uncertainties and error can result from misinterpretation of a phenomenon. As noted in Chapter 2, Wood (1988) suggests that the coefficient of friction for a pedestrian sliding on the ground decreases as a function of the pedestrian's velocity. Therefore, one would tend to use, when applying traditional reconstruction methods, the equation Wood suggests, integrated over the expected speed range traversed by the pedestrian. However, Wood's equation is based on a 'low-speed' coefficient of friction of 0.772 and should the surface in question have a different 'low-speed' coefficient of friction then this method is unlikely to prove accurate.

Wood (with Simms) offers a different approach in a paper written in 2000, where it is suggested that the coefficient of friction between a tumbling/sliding pedestrian is independent of speed. One therefore must be careful when applying other author's (mis)interpretations.

6.7.4 Statistical Uncertainty

It is often impossible to exactly duplicate a scenario and obtain exact parameter measurements. In such a situation a range of scenarios may be created or explored and sample measurements made. Statistical methods can then be used to analyse the spread of results. But how many samples are enough? Time, cost and feasibility

constraints often limit the amount of testing that can be performed, resulting in inadequate sampling. In worst case scenarios only a single sample may be taken.

6.8 Accounting for Error and Uncertainty

Measurement errors often cannot be corrected during the calculation stage but the ability to recognise them gives rise to the ability to rectify the situation by replacing the data with correct measurements or by referring to literature values.

Uncertainty, the other hand, needs to be adequately addressed so that resulting effect on the final outcome can be quantified. There are a number of ways of accomplishing this and the following methods, by no means a complete list, are commonly used. For more information on uncertainty in accident reconstruction it is recommended to refer to Brach (1994), Kost and Werner (1994) and Bartlett and Fonda (2003).

6.8.1 Upper/Lower Bounds

This is probably the simplest method to account for uncertainty. The calculations are performed using both the highest and lowest values known and the resulting answer is expressed as a range. Unfortunately, this method give no indicating which value(s) within that range are the most likely or any other form of discrimination.

6.8.2 Monte Carlo Method

The Monte Carlo method is a brute force stochastic technique that typically involves the repeated calculation of a set of parameters with the value of these parameters randomly varied according to a determined statistical distribution (see also Chapter 3, Section 3.2.2). As many as 25,000 repetitions are performed to establish the distribution of the result (Bartlett and Fonda, 2003). A means to utilise common spreadsheet software for Monte Carlo analysis is described by Bartlett (2003).

Results obtained using Monte Carlo analysis are more useful than those obtained from Upper/Lower bounds as the probability distribution is also indicated.

6.8.3 Finite Difference Method

The Finite Difference method involves numerical partial differentiation to relate the quantity being determined to the input variables without the need for algebraic partial differentiation. It requires that the same probability level is chosen for the variables in question (eg one standard deviation) and is based on the premise that the variance of the sums equates to the sum of the variances. It is less computation intensive than the Monte Carlo method and has the added benefit of an in-built sensitivity analysis.

6.8.4 Applying These Methods to a Forwards-Looking Simulation

Both the Upper/Lower Bounds and the Monte Carlo method can be easily applied to a vehicle-pedestrian accident simulation. Previous studies (Reuter and Watermann (1999), Reuter and Hülsmann (2000) and Shah and Danne (2003)) have shown promising results when applying the Monte Carlo method to MADYMO simulations for vehicle design when assessing occupant injury risk. Moser et al (2003) used the Monte Carlo method for stability analysis of solutions obtained using the CRASH software (See Chapter 3, Section 3.3.1). It was noted by Moser et al that the probabilistic outcomes were well received by the local judiciary.

As noted by Reuter and Watermann, model resolution is not necessarily the key to obtaining robust results. Instead, testing the model across a range of input parameters and observing the influence on the results can indicate model weaknesses and inconsistencies with improved confidence. Shah and Danne state that between 50 to 100 model runs using the Monte Carlo method is sufficient to test the robustness of a model. Reuter and Hülsmann used 100 model runs each for two different systems to compare airbag effectiveness.

Dalbey et al (2006) however note that the number of trials needed to obtain a given level of accuracy of the Monte Carlo method is given by the inverse square of the desired level of accuracy. Thus, for three significant figures of accuracy the error needs to be 0.001 or less, therefore the number of trials is $\frac{1}{0.001^2} = 10^6$ trials. Dalbey et al propose a method based on spectral expansion theory that they refer to as the Polynomial Chaos Quadrature Method. Gaussian Quadrature is used to determine values of input variables across the expected distribution. For a small number of input

variables the number of sample calculations can be several orders of magnitude less than that required by the Monte Carlo method for similar levels of accuracy. Dalbey et al noted, however, that Polynomial Chaos Quadrature Method was not suited to the evaluation of models where a large number of parameters need to be varied as the number of simulations required increased according to a power factor equal to the number of variables.

However, recent advances in multi-core and multi-cpu computing reduce the time and cost penalties traditionally associated with brute-force stochastic techniques needed with a large number of variables exist.

6.9 Stochastic Analysis of Body-Armour Simulation and Thoracic Injury

Dalenoort et al (2005) utilised stochastic sampling to evaluate the effect of scatter on thoracic injury response of a Hybrid III MADYMO occupant model. Three hundred simulations were run using variables altered according to the Monte Carlo method. Correlations were then made relating the variation of input variables and injury outcomes.

A similar approach can be applied to optimise the design of protective equipment and could be applied to the pedestrian thoracic protective device detailed in Appendix I.

6.10 Stochastic Analysis of Pedestrian Throw Distance and HIC

In a manner similar to Section 6.9 above, the effect of pedestrian orientation on pedestrian throw distance can be examined. The MADYMO simulations described in Chapter 3, Sections 3.7 and 3.8 could be evaluated by varying the pedestrian walking speed (Zhao and Wu, 2003; Ishaque, 2006), orientation (Wakim et al, 2004), gait (Curio et al, 2000) and corresponding ground reaction force as per Giddings et al (1999) according to the parameter distribution specified in the literature. Further information on the application of vehicle mass, pedestrian mass, pedestrian height, radius of gyration and centre of mass height for Monte Carlo analysis is provided by Wood et al (2005).

6.11 Simulation Validation

There are some key difficulties in validating vehicle-pedestrian collision reconstruction. Moral and ethical considerations render both live subject and cadaver testing difficult. Cost considerations can limit dummy testing, as both dummies and vehicles are often damaged during testing. The difficulties associated with validating the simulation of vehicle-pedestrian interaction have been noted by a number of researchers, including but not limited to Iwamoto et al, (2003), Ruan et al (2003), Toor et al (2003), Leglatin et al (2006). One of the greatest issues relating to the validation of vehicle-pedestrian interaction pertains to the variability of the human form and the inherent difficulty of kinematic replication of such a variable object using a deterministic modelling method.

Alternatively, the use of stochastic methods can provide a cost effective method of testing the robustness of a simulation in lieu of traditional validation techniques. Whilst one-off, deterministic simulation results can be difficult to compare to the work of other researchers, a range of stochastically determined results that corroborate comparable research are much more likely to be accepted by the accident reconstruction community.

6.12 Flow-Diagrams for the Simulation of Vehicle-Pedestrian Interaction

It can be useful to use a flow diagram to correlate the desired analysis outcome with the information available and a suggested process can be seen in Figure 6.1:

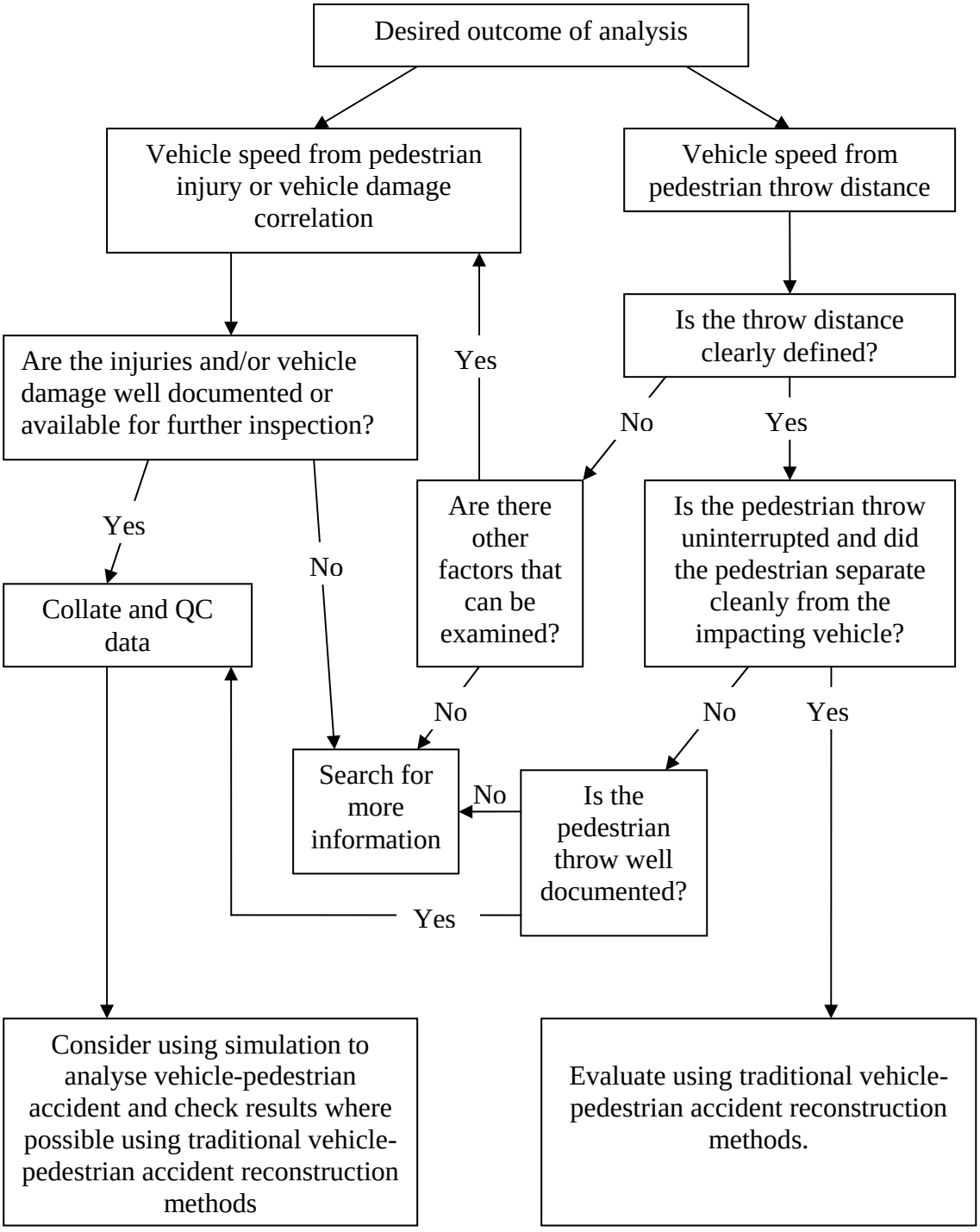

Figure 6.1 Flow-Diagram of Analysis Method versus Information Available

If simulation is chosen as the analysis method the procedure to follow can also be quantified in a flow chart, as suggested by the method described in Figure 6.2:

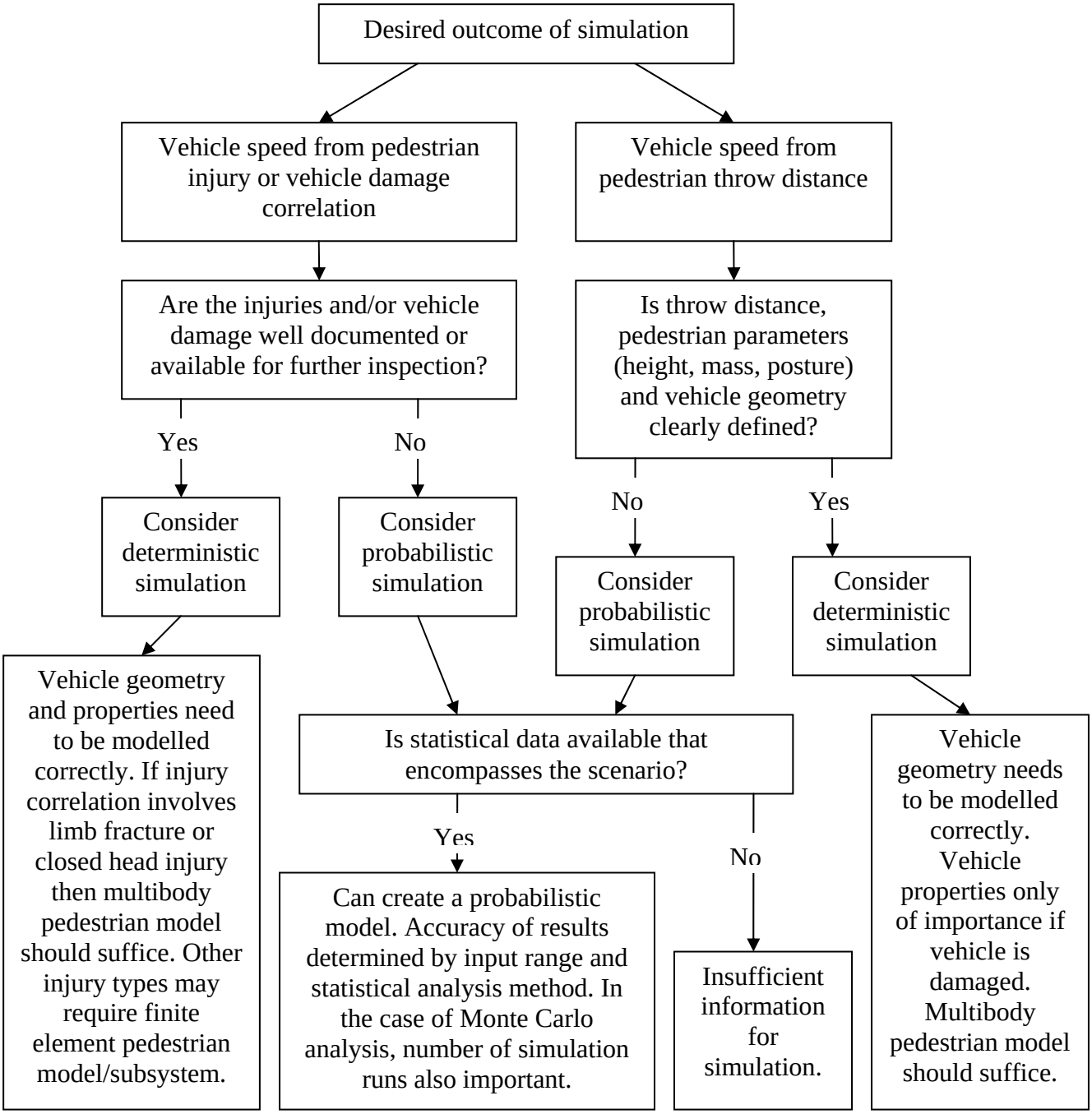

Figure 6.2 Flow-Diagram of Simulation Method

6.13 Classifying the Inputs

When investigating a vehicle-pedestrian collision it is necessary to gather as much data as possible. This data may be obtained by direct measurement by the reconstructionist or their agent (e.g. a surveyor), may be obtained second-hand from a law-enforcement agency or other reconstructionist or may be interpreted from other material (e.g. location of debris from photographs, driver actions from witness

statements). For the most basic of analysis only the throw distance is required. A range of pedestrian-ground coefficient of friction is applied to an equation such as Searle's (see Chapter 2, Section 2.8.2) and a range of impact speeds are obtained. There is a good chance that the speed range derived may indeed encompass the vehicle's speed at time of impact, especially if the range is broad and the vehicle-pedestrian interaction is consistent with the assumptions inherent to the calculation used (again, refer Chapter 2).

However, should a more exact speed range be required, or if the throw distance is not known, or if the vehicle-pedestrian interaction is atypical (e.g. a vehicle with bullbars) then the above approach may not suffice. At this point the reconstructionist needs to evaluate what data is available to them. Parameters of interest, to recap, may include any of the following:

- throw distance of pedestrian
- distance from launch to ground impact (airborne travel)
- distance from ground impact to rest position (tumbling/sliding distance)
- distance travelled by pedestrian between primary and secondary vehicle impacts
- pedestrian versus ground coefficient of friction
- centre of pedestrian mass height at launch
- pedestrian size, shape and mass
- pedestrian pre-impact motion including relative speed between vehicle and pedestrian at launch
- pedestrian injuries
- vehicle size, shape and mass
- driver actions before, during and post-impact
- post-impact vehicle travel distance and deceleration
- vehicle damage
- type and location of other debris

The parameters that are available need to be divided into specific groups, namely:

- known
- assumed
- uncertain
- unknown

Known parameters may include such values as pedestrian mass and vehicle geometry. Known parameters are typically easily measured with the measurements displaying excellent repeatability with limited or no influence from the environment and will lie within ranges stipulated in literature.

Assumed parameters would typically include acceleration due to gravity and may include height of pedestrian centre of mass. They will also agree with the ranges stipulated in the literature. It should be noted that many traditional vehicle-pedestrian accident reconstruction methods have hidden assumptions, such as launch angle (Bonnett, 2005). Computer simulation using multibody and finite element models in a time domain has the advantage that launch angle is not an input, as it is determined during the course of the simulation.

Uncertain parameters often include pedestrian-to-ground coefficient of friction, vehicle-to-ground co-efficient of friction, impact point, vehicle deceleration and throw distance. Uncertain parameters should usually be expressed as range and possibly as a probability distribution.

Unknown parameters are those for which no range can be attributed with any certainty. They may also include parameters which may not be relevant to the case at hand.

6.14 Achieving the Desired Outputs

The desired outputs also need to be ascertained. The most common output is typically vehicle speed at time of impact and may, in some circumstances, include driver action at the time of impact e.g. braking. The available input parameters need to be correlated to the available outputs. In best practice circumstances several different approaches will be used, using different groupings of input parameters to achieve a range of output values.

Correlation of pedestrian injuries can be conducted using either MADYMO's injury evaluation models or from forces and accelerations calculated during the simulation and a comparison made to the values for human tolerance stated in the literature (eg.

McElhaney et al, 1976). Alternatively energy-based injury analysis such as Peak Virtual Power (Neal-Sturgess, 2002) could be applied.

If the outputs do not agree then a sensitivity analysis should be conducted to create a feedback system, whereby the input variables with the greatest range of values and influence on the outputs are inspected and corrected in order to achieve consistent outputs.

6.15 A Sample Approach to the Reconstruction of Real-Life Vehicle-Pedestrian Accidents Using Computer Simulation

This example is loosely based on the pedestrian versus SUV-type vehicle discussed in Chapter 5.

6.15.1 Identify Desired Outcome

The desired output in this instance is a likely range of impact speed.

6.15.2 Quantifying the Inputs and Parameters Regarding the Pedestrian

The inputs and parameters relating to the pedestrian were, in this instance, generally obtained from the pathologist's report and witness statements. Data from the pathologist's report is generally regarded as more reliable than witness statements, so inferences relating to pedestrian orientation relating to the vehicle should usually be preferred to witness statements although in this case they appeared to be in agreement.

Other parameters, such as pedestrian head stiffness, were used on an 'as validated' basis, i.e. as supplied by TNO Automotive.

Parameter	Status	Example Range (if applicable)	Comments
Throw Distance	Uncertain	3 to 5 metres	From witness statements
Proportion of airborne pedestrian travel versus travel on ground	Unknown		
Pedestrian height and mass	Known	1660 mm tall, 80 kg	From pathologist's report
Pedestrian shape	Assumed, based on height and mass	Overweight, slightly taller than average female	Shape apparent in photographs and a brief description given in the pathology report. Body Mass Index (BMI) of 29
Pedestrian pre-impact motion and orientation	Known	Stationary, facing vehicle	From witness statements
Secondary/other vehicle-pedestrian interaction	Known		Pedestrian run over by both left side wheels. Tyre marks visible on her thigh(s) – from witness statements.
Secondary/other vehicle-pedestrian interaction	Unknown		Pedestrian has a substantial black-eye
Pedestrian injuries	Known	Lethal injury was determined to be a significant impact to the back of the head, resulting in a skull fracture, inevitably lethal damage to the brainstem and a contre-coup injury to the front of the head.	Other injuries included: right orbital haematoma ("black eye"); a 70 mm wide x 40 mm high stippled abraded bruise to back of head, with underlying boggy swelling; superficial cuts, abrasions and bruising to the upper limbs; significant bruising to the left leg along with focally torn ligaments; abdominal wall bruising on both left and right sides, centred 940 mm above the sole of the foot.
Pedestrian head stiffness	Assumed	1400 Nmm^{-1} to 3570 Nmm^{-1}	As per literature for anterior-posterior loading.
Other pedestrian stiffnesses	Assumed	As per standard MADYMO female pedestrian model	

Table 6.1 Pedestrian Parameters and Inputs

6.15.3 Quantifying the Inputs and Parameters Regarding the Vehicle and Driver Actions

With the vehicle available for inspection the vehicle parameters were relatively easy to determine, however, given the undamaged state of the vehicle panel stiffness testing was undesirable. The large number of witness statements available provided some insight into driver actions but as witness statements are often unreliable parameters relating to driver actions are noted as 'uncertain'. The range of inputs and parameters relating to the vehicle and driver actions can be seen in Table 6.2.

Parameter	Status	Example Range (if applicable)	Comments
Vehicle geometry, size, shape and mass	Known		Vehicle available for inspection.
Vehicle speed range at time of impact.	Uncertain	2.8 to 5.4 ms^{-1}	Vehicle accelerated from standstill, travelling between 4 to 5 metres prior to pedestrian impact. Speed range derived from acceleration range of 1.0 to 2.9 ms^{-2} based on witness statements and vehicle manufacturer performance data over a distance of between 4 and 5 metres.
Driver actions before, during and post-impact	Uncertain	Acceleration during impact, not braking noticeably thereafter.	Witness statements indicate vehicle accelerating (moderately to hard) at time of impact. Subsequent runover indicative of lack of braking post-impact.
Post-impact vehicle travel distance	Unknown	Not relevant as vehicle not braking noticeably during incident	
Vehicle damage from pedestrian impact.	None apparent.		
Stiffness of vehicle bumper	Assumed	200 to 300 Nmm^{-1}	As per literature.
Stiffness of vehicle bonnet edge	Assumed	850 to 2000 Nmm^{-1}	As per literature.
Stiffness of vehicle bonnet top	Assumed	300 Nmm^{-1}	As per literature.

Table 6.2 Vehicle/Driver Action Parameters and Inputs

6.15.4 Quantifying the Inputs and Parameters Regarding the Environment and the Interaction between the Objects of Interest

Table 6.3 shows the inputs and parameters for the environment and also the relevant interaction parameters for the interaction between the different objects contained with the system (vehicle and pedestrian) and also between these objects and the environment (road, gravitational and frictional forces, etc). The collision scene was available for inspection but only some time after the collision had occurred.

Debris location and tyre marks are often useful for the determination of a possible vehicle speed range using traditional vehicle-pedestrian accident reconstruction methods. Unfortunately they are not always present or recorded.

Ambient temperature and weather conditions at the time of the collision should, if possible, be noted. These factors can be useful for identifying if other parameters such

as road stiffness (temperature dependant, as noted in Section 6.5.4) and coefficient of friction between vehicle and road (often weather dependant) are within the appropriate range.

Parameter	Status	Example Range (if applicable)	Comments
Type and location of other debris.	None apparent.		
Length and type of tyre marks	None apparent.		
Coefficient of friction between vehicle and road	Unknown	Not applicable as vehicle not braking (and insufficiently powerful for friction to be a limiting factor under acceleration)	
Coefficient of friction between vehicle and pedestrian	Assumed	Range of 0.2 – 0.5, as per literature.	
Pedestrian head stiffness	Assumed	1400 Nmm^{-1} to 3570 Nmm^{-1}	As per literature for anterior-posterior loading.
Stiffness of road	Assumed	26.5 to 60 $kNmm^{-1}$	Range determined by Chadbourn et al (1997)
Acceleration due to Gravity	Assumed	9.81 ms^{-2}	As per discussion in Section 6.5.1
Road/ground slope	Known	Negligible	
Ambient temperature at time of collision	Unknown		
Weather conditions at time of collision	Dry		

Table 6.3 Environment and Interaction Parameters and Inputs

6.15.5 Choosing the Modelling Method

Once the parameters and inputs have been identified the most appropriate and practical modelling method should be identified. As per the flow-diagram shown in Figure 6.2, for a well documented vehicle-pedestrian collision where throw distance is unknown but vehicle damage (none apparent) and pedestrian injuries are clearly defined a deterministic modelling method would appear most suitable.

A simple multibody pedestrian model and a geometrically accurate model of the vehicle front end (bumper and bonnet) on a flat plane were considered adequate in this situation.

Simulation parameters should always be correctly defined, even if it does not appear that they are going to be used. As an example: defining the contact characteristics of a rigid FE surface even though impacting multibody characteristics are used in the determination of the contact forces. This way, if it becomes apparent that a different modelling approach is needed later (e.g. the substitution of the multibody model for a FE model) the chance of incorrectly defined attributes is reduced.

6.15.6 Creating the System

Once the parameters and inputs have been identified and the most appropriate modelling method identified, the simulation system can be assembled.

In the case study an existing finite-element vehicle model was modified to closely replicate the actual vehicle characteristics. The standard MADYMO 5^{th} percentile female model was used in the orientation described by the witness statements (and consistent with the pathologist's report. The road surface was modelled using a flat plane with an appropriate stiffness (see input ranges for values applied).

6.15.7 Creating a Simulation Matrix

Whilst it would be ideal to evaluate every potential scenario this is seldom practicable or even possible. In this instance an appraisal of probable vehicle speed at impact had been requested, however, it would appear possible that the vehicle was accelerating at the time of the collision.

A simulation matrix was constructed with the variables of initial vehicle speed and vehicle acceleration. Initial vehicle speed was examined from 2.8 to 4.8 ms^{-1}, based on witness statements and evaluated in 0.2 ms^{-1} increments. Vehicle acceleration was taken to be between 0 and 3 ms^{-2} and this was evaluated in 0.2 ms^{-2} increments, creating a matrix of 176 simulations.

Once a likely range of scenarios has been identified a sensitivity analysis should be conducted to examine the influence of other parameters (such as vehicle panel stiffness) on the results.

6.15.8 Determining Other Simulation Parameters

Other simulation parameters also need to be determined. These include:

- Integration method choice of Euler, fourth order Runge-Kutta, fifth order Runge-Kutta Merson or user defined via MATLAB. The MADYMO Human Models Manual recommends EULER integration when using pedestrian models.
- Solver time step. A time step of 1.0E-5 seconds was used so that the potential for pedestrian leg fracture could be ascertained (such a fracture did not occur in reality – both injury presence and absence can be used for scenario validation).
- Simulation duration should be sufficiently long to permit a comparison of pedestrian throw distance to the (wide) range given in witness statements. In this instance a three second simulation duration was determined to be sufficient. For higher speed scenarios or if extended vehicle-pedestrian interaction is suspected, a longer simulation duration may be required.
- Depending on availability of computational capacity a sensitivity appraisal of the model may be advisable. In this instance a finite-element vehicle model was used and the HIC resulting from ground contact for a range of vehicle acceleration was examined. A comparison was then made with a facet vehicle model to determine the influence of vehicle parameters on pedestrian HIC.

6.15.9 Noting Assumptions

The assumptions inherent in the simulation, in addition to those specified in Tables 6.1 to 6.3, include:

- Vehicle acceleration is uniform, within the period specified. For acceleration from standstill, this assumption would appear to be justifiable, as the manufacturer data upon which this information is based, would have been derived under similar circumstances (ie launch from a standstill) and any non-uniformity of acceleration (especially within the first 0.5 second or so) is automatically accounted for.
- That the manufacturer performance data is relevant to this vehicle. There is nothing to indicate that age or defects would have resulted in the vehicle in question performing substantially differently to the manufacturer data. As the

acceleration data is considered over a range, any performance loss particular to this vehicle would mean that it is still included in the range considered. There was no indication of any performance enhancement to the vehicle.

- The stiffness values used in some of the contact definitions are assumed to be rate-independent and linear in effect. This may not be unreasonable in circumstances where the values are applied are similar to the situation from which they were derived. In other situations rate-dependence effects will cause unrealistic results.

The general assumptions inherent in mathematical modelling, as noted in previous Chapters, are also applicable.

6.15.10 Documenting the Simulation Process

It is important to document all stages and aspects of the research. Before conducting any simulation it is important to document the following:

- the hypothesis to be tested or examined
- the rationale behind the approach taken
- the methodology employed
- all parameters of relevance
- the origin of any models sourced externally
- the validation of all models used
- the range of variables to be examined and the variable sample frequency

By following these steps it is often possible to spot methodological errors prior to expending any computational time. Simulation results should be documented carefully and a quick result examination, analysis and comparison should be performed as soon as practicable after each simulation so that any issues (e.g. FE model instability, missing or incorrect contact definitions) can be attended to in a time effective manner (which may include starting over). Early determination and solid documentation of errors assists in the identification of the source of the problem and the best method of rectification.

Simulation result documentation should include:

- a brief description of the graphical output of the simulation. This output is often the first examined after performing the simulation, at least for a new input deck. Simulation errors such as missing contact definitions are often most easily spotted using graphical output.
- a graphical analysis of the outputs of interest, e.g. acceleration, displacement, injury parameters etc
- a comparison of the outputs of interest from different simulations and the determination of whether the input variables are influencing the outputs.

If the inputs are not influencing the outputs, then either:

- the original hypothesis is incorrect
- the methodology is invalid
- the effect is too small to determine, or
- a simulation error exists

All notes, discussion and conclusions regarding inputs versus outputs should also be documented.

By strictly documenting all stages of the simulation process, even if some details are initially recorded only quick, handwritten notes it is much easier for both one's own reference and for others to examine and evaluate the methods employed.

6.15.11 Establishing Valid Output Boundaries

The outputs of interest in this scenario are throw distance and head injury. An expected range of throw distance can be determined using appropriate traditional vehicle-pedestrian accident reconstruction equations (in this instance Collins would be the logical choice) although, as the vehicle is possibly accelerating any prediction is likely to be conservative.

Head injury can be appraised on either the basis of an injury criterion (such as HIC, 3ms Criterion) with an expected result equivalent to an AIS 5 or 6 injury.

The animation produced by the simulation can be a useful tool for checking the validity of the results. A visual animation of the collision makes it easy to identify that all contact interactions have been included and that the contact behaviour appears realistic. Pedestrian and vehicle motion can be visually inspected and compared to witness statements.

6.15.12 Analysing and Documenting the Results

The results should be analysed as the simulation matrix is progressively solved and compared to the boundaries determined in the previous section. This will permit the early identification of simulation, method or model errors.

Results can be analysed in a number of ways, including:

- DOE (Design-of-experiment) Software. Many examples of DOE Software simplify much of the simulation process by automatically generating input decks based on the simulation matrix, 'data-mining' the results and correlating the inputs and the outputs. They also permit stochastic and other forms of analysis if there are sufficient input variables to render a simulation matrix (or series of matrices) unfeasible.
- Spreadsheet software is readily available and often familiar, making it an attractive proposition for the evaluation of small simulation matrices. However, when there are a large number of variables to evaluate DOE can offer considerable time savings.
- Tabulation of peak values is the simplest way to present results but do not lend themselves to in-depth analysis.

Regardless of the analysis method it is important to ensure that the results of the analysis are adequately qualified. Therefore, in addition to the presentation of the preferred results, it is desirable that the complete range of valid results is expressed, the probability distribution across that range (if applicable) as well as the assumptions made to obtain those results.

A clear and concise result summary should be provided to permit rapid comprehension and appraisal of the findings. Additionally, located in the bulk of the

report, the result documentation should be suitably comprehensive to permit a reader to conduct sufficient analysis to either confirm or disprove the findings. Finally, a comparison to the findings of other authors is invariably useful.

6.16 Conclusion

This chapter described the general inputs and parameters required for the computer simulation of a vehicle-pedestrian accident and suggested a basis for the methodology required to:

- Identify the desired goals(s) of the analysis
- Identify the available inputs and parameters
- Identify the best approach to use the available inputs and parameters to determine the desired goal(s)
- Adequately document not only the results but also the process used to achieve them
- Recognise and state the assumptions inherent to the analysis
- Recognise and state the error and uncertainty associated with the results

It is hoped that the approach described in this Chapter is of use to other researchers and that it be extended, refined and generally improved-upon.

The next, and final, Chapter will offer a summary of the thesis and will discuss the conclusions that can be drawn from the findings.

Chapter 7

Summary, Discussion and Conclusions

7.1 Traditional Vehicle-Pedestrian Accident Reconstruction Methods

The derivation for a number of traditional vehicle-pedestrian accident reconstruction equations was analysed and in some cases were found to simply consist of a combination of projectile motion and slide-to-rest equations. Other methods employed the findings from actual vehicle-pedestrian collisions or analysed the results of dummy and cadaver tests. Some methods were also identified that used relatively sophisticated two-dimensional physics.

The vast majority of vehicle-pedestrian accident reconstruction equations relate vehicle impact speed to pedestrian throw distance. These predictions are of obvious interest to litigators and law enforcers. What should be of equal interest to these parties is the accuracy, assumptions and limitations of these equations and, in particular, when they should and shouldn't be used.

For a situation consisting of a decelerating vehicle with a typical, car-like shape impacting a pedestrian with a centre of mass above the contact point on the vehicle it would appear that Searle's 1993 equation offers reasonable and consistent results in many instances.

Where the contact point of the impacting vehicle is above the pedestrian's centre of mass the use of Collins' equation is preferable.

All of the mathematical equations studied were unable to provide an accurate pedestrian throw-distance versus vehicle impact speed relationship with 100% accuracy for all cases.

In the instance of a constant speed or accelerating vehicle the impact speed prediction offered by traditional vehicle-pedestrian accident reconstruction methods is usually highly inaccurate, tending to over-predict vehicle impact speed by a considerable margin. In the context of litigation such a tendency for over-prediction is alarming.

Furthermore, it is not possible to correlate vehicle damage or pedestrian injury versus vehicle impact speed using traditional vehicle-pedestrian accident reconstruction methods. Where no impact point is defined throw-distance based methods of impact speed prediction cannot be used. In such circumstances it would appear that there is a need for alternative means of establishing vehicle impact speed if there is no roadside evidence other than the pedestrian.

In summary, traditional methods of vehicle-pedestrian accident reconstruction methods can, in the correct circumstances, provide a useful indication of vehicle impact speed based on pedestrian throw distance. However, in many circumstances the prediction offered is incorrect, often by a significant margin. Traditional methods of vehicle-pedestrian accident reconstruction therefore need to be used with care and with the knowledge of the limits of their applicability.

7.2 Comparing Traditional Vehicle-Pedestrian Accident Reconstruction Methods and Computer Simulation

The progress of computers from clumsy calculators capable of out-of-order instructions to powerful, convenient and inexpensive desktop PC's was chronicled. Alongside the development of these number-crunchers mathematical modelling progressed in leaps and bounds.

The automotive manufacturing industry was one of the early adopters of mathematical modelling and the tools created for the design and optimisation of motor vehicles were easily adapted to the reconstruction of motor vehicle accidents.

The large number of variables and iterative requirements associated with accident reconstruction, in comparison to automotive design, made large demands on the computational power available. The traditional methods of accident reconstruction, particularly in regard to the reconstruction of the complex kinematics of pedestrian accidents, remained popular due to their simplicity and accessibility.

As computational cost decreased the popularity of software-based accident reconstruction programs such as CRASH and SMAC increased during the 1970's and 80's. In the 1980's vehicle-pedestrian collision reconstruction using multibody analysis was studied by a number of researchers and excellent correlation with experimental tests was reported. More advanced simulation methods such as finite-element analysis, however, were still in their infancy and the modelling of vehicle-pedestrian accidents using such methods was considered too difficult.

By the end of the 1990's however, the situation changed with the addition of finite-element modelling capability to the previously multibody only simulation program MADYMO. By combining multibody models with finite-element models an excellent balance of computational speed and accuracy was obtained.

7.3 Using Computer Simulation to Reconstruct Vehicle-Pedestrian Accidents

The MADYMO simulation program was used to reconstruct two vehicle-pedestrian accidents. One of the 'accidents', determined to be a homicide, involved repeated vehicle-pedestrian collisions. This had proved to be very difficult to reconstruct using traditional accident reconstruction methods and so computer simulation was employed. A methodical sequence of computer simulations was used to evaluate the validity of proposed scenarios and to establish likely parameters for vehicle speed and pedestrian orientation at time of impact.

One of the correlations provided by computer simulation was the location of the pedestrian's head-strike on the vehicle versus vehicle impact speed and pedestrian orientation. Although the literature does note that pedestrian head-strike location is related to vehicle impact speed (which may also be determined intuitively) such literature only provides wide speed ranges for broad strike locations on the vehicle. Furthermore the literature does not clearly specify the influence of vehicle shape, pedestrian height or pedestrian orientation on the head-strike location.

The other case study involved a vehicle-pedestrian collision where investigator's estimates, witness statements and the victim's injuries displayed considerable disagreement in regard to vehicle impact speed. Computer simulation was used to

reconstruct the accident to relate the pedestrian's injuries to vehicle impact speed, a correlation that traditional accident reconstruction techniques were unable to provide. It was discovered that the pedestrian's orientation to the vehicle and the height difference between the pedestrian's centre of mass and the leading edge of the impacting vehicle resulted in unexpected pedestrian kinematics and severe head injury for a vehicle speed that was considerably lower than would normally be expected for such an injury.

7.4 The Injury Prediction Capabilities of MADYMO

The injury patterns in vehicle-pedestrian accidents have traditionally been underutilised by accident reconstructionists. Research conducted by the author has shown that injury prediction using computer simulation can provide additional methods for vehicle speed prediction in vehicle-pedestrian accident reconstruction. The replication of pedestrian injury patterns (including the lack of injury, in some circumstances) using the injury prediction capabilities of MADYMO's multibody pedestrian model for several accident reconstruction scenarios provided additional correlation of vehicle impact speed for two out of three scenarios.

Although some shortcomings were recognised in the injury prediction process the current injury prediction capability for on-road vehicle pedestrian collisions is nonetheless impressive when correlated against case studies. In the instance of an off-road collision involving complex terrain coupled with an interaction between the underside of the vehicle and the pedestrian that may be considered highly unusual, the injury correlation capability was not as evident as for the on-road scenarios. Many of the deficiencies noted in the off-road example are being actively rectified by researchers around the world with improved modelling techniques including finite-element pedestrian models with considerably improved biofidelity in comparison to multibody models.

In the author's opinion the primary deficiency of many of the current human mathematical models is their basis on cadaver and dummy data. One cannot reasonably expect the mathematical models to replicate with complete accuracy the characteristics of living humans until such models are indeed actually based on the

characteristics of living humans. This deficiency does detract somewhat from MADYMO's capacity as a forensic tool when using the standard multibody pedestrian model and must be kept in mind when used for accident reconstruction.

7.5 Limitations of the Mathematical Modelling of Vehicle-Pedestrian Accidents

As has been noted there are a number of limitations inherent within mathematical modelling. These limitations include the assumptions that must be made when replicating the world with numbers, our limited understanding of ourselves and our environment and the intrinsic need of current simulation methods to render both time and space into discrete units to create mathematically solvable sub-systems. Even when and where a reasonable understanding exists and the system is modelled with a high degree of accuracy the resulting problem is often difficult and time-consuming to solve.

Being able to use mathematical modelling effectively requires an understanding of which compromises are acceptable, the degree to which the compromise can be extended and the likely consequences of the compromises made. Examples of such compromises include the discretisation of time into defined intervals and the reduction of physical objects into a system of interconnected elements. Adaptability on the part of the modeller is also necessary in order to effectively implement new concepts as software systems change, understanding progresses and technology advances.

The mathematical modelling of vehicle-pedestrian collisions was not widely considered 50 years ago. The mathematical modelling of vehicle-pedestrian collisions using computer simulation was unusual 30 years ago. Whilst great advances have been made over the last two decades it is still a science in its infancy with much scope for advancement.

7.6 Potential Improvements for the Simulation of Vehicle-Pedestrian Collisions

The simulation of vehicle-pedestrian collisions has much capacity for improvement. The accumulative and application of knowledge gained from actual vehicle-pedestrian

collisions using databases resulting from initiatives such as SARAC II (as described in Section 4.5) will hopefully improve the biofidelity of and kinematic responses of pedestrian models. Accounting for geographic, demographic, gender, age and obesity factors in the creation of pedestrian models and using scaling software such as MADYSCALE improves the accuracy of vehicle-pedestrian reconstructions where the pedestrian is not an exact 5^{th}, 50^{th} or 95^{th} percentile representation of the European population.

More consistency and compatibility between the simulation software suites from different vendors may decrease learning times and increase information transfer. Optimised software than ran faster on relatively modest computer systems would have enabled the author of this thesis to have conducted a greater range of simulations in the time available.

The use of several reconstruction methods for each analysis and comparing the results to other research enabled the identification of spurious results, lending more credibility to the results of this research.

The increased use of computer simulation in analysing vehicle-pedestrian accidents needs to be focused more on identifying methods of reducing pedestrian injury and less on litigious finger-pointing after the fact.

7.7 Evaluating and Reducing Pedestrian Injury

A survey of the research that has been conducted and is ongoing on the safety and injury reduction of road users indicates a strong bias towards the safety of vehicle occupants. It is suspected that this bias results from the consideration of the automotive manufacturers that the greatest financial gain and the highest rate of return result from the development, implementation and marketing of vehicle safety features that benefit vehicle occupants. The research and standards that exist in relation to pedestrian safety tend to focus on the reduction of head and lower extremity injuries. Whilst lower extremity pedestrian injuries are extremely prevalent some research indicates that pedestrian thoracic injuries are more costly to society.

Mindful of the relatively limited research on pedestrian thoracic injuries, in spite of their significance, the author evaluated MADYMO's effectiveness in evaluating pedestrian thoracic injury and attempted to identify a method of pedestrian thoracic injury reduction.

The complicated nature of the thorax creates difficulties when attempting to simulate thoracic injury. A large proportion of the thorax is occupied with vital organs that contain time-variant quantities of fluids and gases, conditions that are not replicated during experimental tests using cadavers to determine physical thoracic characteristics and injury tolerances. The presence, importance and fragility of these vital organs, however, preclude all but the most limited volunteer testing.

The current MADYMO multibody pedestrian model is based upon previous occupant models which were, in turn, based upon occupant dummies. The biofidelity of the MADYMO multibody pedestrian model is therefore questionable in many areas where pedestrian characteristics have not been well validated, including frontal thoracic loading. The results obtained for the simulation of the effectiveness of body-armour in pedestrian thoracic injury reduction as noted in Appendix I should therefore be treated as broadly indicative rather than definitive.

The initial findings, as described in Appendix I, indicate that certain armour configurations and parameters have the potential to reduce pedestrian thoracic injury in the event of a vehicle impact. Other armour configurations and parameters appeared to exacerbate the injury potential.

Further research needs to be conducted to identify whether or not the injury exacerbation simulated is realistic, as there is both research and anecdotal evidence that point both ways.

7.8 Conclusions

After conducting this research the author can conclude the following:

I. The strengths of vehicle-pedestrian accident reconstruction using computer simulation, and the software package MADYMO in particular, lie in:

i. The ability to more accurately model the pedestrian throw-distance versus vehicle impact speed relationship than traditional methods. This increased accuracy results from the ability to account for different vehicle shapes and sizes, driver actions (i.e. braking versus accelerating) as well as varying pedestrian shapes, sizes, postures and orientation with respect to the impacting vehicle.

ii. The ability to predict injury patterns with sufficient accuracy for forensic applications in certain circumstances. There are no other methods available that can be used to predict such a wide range of injury with such comparative ease.

iii. The ability to model three dimensional events that traditional methods struggle with.

II. The weaknesses of vehicle-pedestrian accident reconstruction using computer simulation, and the software package MADYMO in particular, lie in:

i. The ease with which erroneous results can be created and the difficulties associated with finding the error(s).

ii. The power and versatility of the software comes at the cost of a long familiarity timeframe.

iii. The inability of current software to account for pedestrian responses and in particular muscle tension.

iv. The majority of characteristic of the human models are not based on living humans, but rather cadaver and dummy tests.

v. The fairly limited number of pedestrian models available and the characteristics of the model scaling software offered means that only certain representatives of the human race can presently be modelled.

vi. That the majority of pedestrian models that do exist are of a multibody form, thus not realising the potential for greater accuracy and biofidelity afforded by finite element human models.

vii. The fairly radical and developing nature of the software has resulted in a large number of changes between versions. Whilst this is necessary for improvement it does requires considerable adjustment.

In accordance with these conclusions the findings related to the original research aims are as follows:

I. The pedestrian throw distance versus vehicle impact speed relationship determined by MADYMO is more likely to be accurate than existing methods of vehicle-pedestrian accident reconstruction, particularly if the vehicle is either accelerating or travelling at constant speed. Existing methods of traditional vehicle-pedestrian accident reconstruction appear to assume that the vehicle is decelerating, and usually decelerating heavily.
II. The pedestrian injury patterns predicted by the MADYMO multibody pedestrian model appear to be reasonably accurate for lower limb and head injuries but not necessarily thoracic or abdominal injuries.
III. The modelling of thoracic injury was found to be more difficult than first thought. Accordingly the modelling of thoracic injury reduction methods did not achieve any definite conclusions.

The author is excited by the progress that is being made in the field of mathematical modelling, especially as it is a field still in its infancy. Each generation of human mathematical models are more accurate and biofidelic than the last. The author has identified some of the strengths of mathematical modelling in the context of vehicle-pedestrian collision analysis and in view of current research expects the weaknesses to diminish considerably over the next few years. It is hoped that improved mathematical models will result not only in improved research but also in valuable practical applications.

The author would also like to note the following: Mathematical modelling is a tool that must be carefully wielded. Although numbers do not lie they can be manipulated both well and poorly. The author hopes that his research is considered to fall in the former category.

The author would like to finish by expressing his hope that this research is of positive benefit to humanity and that it contributes to pedestrian injury and mortality reduction.

References

AAAM (Association for the Advancement of Automotive Medicine): The Abbreviated Injury Scale. AAAM, Des Plaines, IL, USA. 1990.

Adnani, K., Shastri, M., Thakkar, V., Gajjar, A. and Billore, M. Ocular Manifestations of Head Injury - A Study of 150 Cases. Proceedings of the All India Ophthalmological Society. Edited by N. Raju, Kerala, India. 2002.

Aldman, B., Thorngren, L., Bunketorp, O. and Romanus, B. An Experimental Model for the Study of Lower Leg and Knee Injuries in Car Pedestrian Impacts. IRCOBI, pp. 180–193. 1980.

Allsop, D., Perl, T., Warner, C. et al. Force/deflection and fracture characteristics of the temporo-parietal region of the human head. Proceedings of the 35th Stapp Car Crash Conference, pp. 269–278. 1991.

Anderson R. W. G. and McLean A. J. Vehicle Design and Speed and Pedestrian Injury: Australia's Involvement in the International Harmonised Research Activities Pedestrian Safety Expert Group. Road Safety, Education and Policing Conference, Melbourne, Australia. 2001.

Anderson R. W. G., McLean A. J., Dokko Y. Determining Accurate Contact Definitions in Multibody Simulations for DOE-Type Reconstruction of Head Impacts in Pedestrian Accidents, 19th Enhanced Safety of Vehicles Conference, Washington DC, USA. 6-9 June 2005.

Aronberg, R. Airborne Trajectory Analysis Derivation for Use in Accident Reconstruction, SAE 900367, 1990.

Ashton, S. The Cause and Nature of Head Injuries Sustained by Pedestrians. Proc. of the 2nd Int. Conf. on Biomechanics of Serious Trauma, Birmingham, September 9-11. IRCOBI Bron France. pp. 101-113. 1975

Ashton, S., Cesari, D. and Wijk, J. Experimental Reconstruction and Mathematical Modelling of Real World Pedestrian Accidents. SAE Paper 830189, presented at the Society of Automotive Engineers International Congress and Exposition, Detroit, Michigan, USA. February - March, 1983.

Ashton, S. and Mackay, G. Benefits from Changes in Vehicle Exterior Design – Field Accident and Experimental Work in Europe. Society of Automotive Engineers - Paper 830626. Pedestrian Safety (PT-112), 119-27. Warrendale, PA, USA. 1983

AUSTROADS: Pavement Design - A Guide to the Structural Design of Road Pavements. AUSTROADS, Sydney, Australia. 1992

Babbage, C., Morrison, P. and Morrison, E. Charles Babbage and His Calculating Engines: Selected Writings by Charles Babbage. Dover Science Books, New York, USA. 1961

Bartlett, W. Conducting Monte Carlo Analysis with Spreadsheet Programs, SAE Paper 2003-01-0487, presented at the Society of Automotive Engineers World Congress and Exposition, Detroit, Michigan, USA, Session: Accident Reconstruction (Part 1&2 of 4). March 2003.

Bartlett, W. and Fonda, A. Evaluating Uncertainty in Accident Reconstruction with Finite Differences. SAE Paper 2003-01-0489, presented at the Society of Automotive Engineers World Congress and Exposition, Detroit, Michigan, USA, Session: Accident Reconstruction (Part 1&2 of 4). March 2003.

Bathe, J. K., Wilson, E. L. and Iding, R. H. NONSAP: A Structural Analysis Program for Static and Dynamic Response of Nonlinear Systems. Department of Civil Engineering, University of California, USA. 164 pages. 1974

Bathe, J. K. Nonlinear Finite Element Analysis and ADINA, Proceedings of the 11th ADINA Conference. Computers & Structures. Vol. 64, no. 5-6, pp. 881-1297. Sept. 1997

Baughman, L. D. Development of an Interactive Computer Program to Produce Body Description Data. AFAMRL-TR-83-058, Air Force Aerospace Medical Research Laboratory, Wright-Patterson Air Force Base, Ohio, USA, 1983

Bhalla, K., Montazemi, P., Crandall, J., Yang, J., Liu, X., Dokko, Y., Takahashi, Y., Kikuchi, Y., and Longhitano, D. Vehicle impact velocity prediction from pedestrian throw distance: Trade-offs between throw formulae, crash simulators, and detailed multibody modelling. IRCOBI Conference on the Biomechanics of Impacts. 2002.

Bhat, K., Seitz, S., Popvic, J. and Khosla, P. Computing the Physical Parameters of Rigid-Body Motion from Video. Computer Vision - ECCV 2002: 7th European Conference on Computer Vision, Proceedings, Part I, Copenhagen, Denmark, May 28-31, 2002.

Bohan, T. L. Computer-Aided Accident Reconstruction: Its Role in Court. SAE Paper 910370, presented at the Society of Automotive Engineers International Congress and Exposition, Detroit, Michigan, USA. February - March, 1991.

Bohan, T. L. and Yergin, A. A. Computer-Generated Trial Exhibits: A Post-Daubert Update. SAE Paper 1999-01-0101, presented at Society of Automotive Engineers International Congress and Exposition, Detroit, Michigan, USA. March, 1999.

Bonnett, G. Pedestrian Vaults – Humans Going Ballistic. Institute of Police Technology and Management, University of North Florida, Jacksonville, Florida, USA. 2005.

Bovington Results. Impact – Journal of ITAI, p83-85, Autumn 1999.

Brach, R. Uncertainty in Accident Reconstruction Calculations. SAE Paper 940722, presented at the Society of Automotive Engineers International Congress and Exposition, Detroit, Michigan, USA. February - March, 1994.

Brach, R., Rudny, D. and Sallmann, D. Comparison of Tire Friction Test Methodologies Used in Accident Reconstruction. SAE Paper 980367, presented at the

Society of Automotive Engineers International Congress and Exposition, Detroit, Michigan, USA. February, 1998.

Brands, D., Happee, R. and Oakley, C. Minutes of the PSN Workshop on Human Body Modelling. Eindhoven University of Technology, Eindhoven, The Netherlands. March, 2001.

Brands, D. W. A. Predicting Brain Mechanics During Closed Head Impact : Numerical and Constitutive Aspects. Technische Universiteit Eindhoven, The Netherlands. ISBN 90-386-2713-0. 2002

Calspan History and Timeline, http://www.calspan.com/history, accessed May 2006.

Cameron, M., Peden, M., Scurfield, R., Sleet, D., Mohan, D., Hyder, A., Jarawan, E. and Mathers, C. World Report on Road Traffic Injury Prevention. World Health Organization, Geneva. 2004.

Campbell, K. Energy Basis for Collision Severity. SAE Paper 740565 presented at the 3rd International Conference on Occupant Protection, Troy, Michigan, USA. July, 1974.

Carter, E., Ebdon, S. and Neal-Sturgess, C. Optimization of Passenger Car design for the Mitigation of Pedestrian Head Injury Using a Genetic Algorithm. Proceedings of the 2005 Conference on Genetic and Evolutionary Computation GECCO. ACM Press. June, 2005

Chadbourn, B., Newcomb, D. and Timm, D. Measured and Theoretical Comparisons of Traffic Loads and Pavement Response Distributions. Proceedings, 8th International Conference on Asphalt Pavements, Seattle, WA, USA. pp 229 – 238. 1997.

Chawla, A., Mukherjee, S., Mohan, D., Singh, J., Rizvi, N. Crash Simulations of a Three Wheeled Scooter Taxi (TST). Proceedings of ESV 2003, Nagoya, Japan. May 2003.

Chen, S. The Unofficial History of Ansys. http://www.fea-optimization.com/ans_macro/ANS-history.txt (last accessed May 2006)

Cheng, P. H., Sens, M. J., Wiechel, J. F. and Guenther, D. A. An Overview of the Evolution of Computer Assisted Motor Vehicle Accident Reconstruction. SAE 871991. SAE Passenger Car Meeting and Exposition, Dearborn, USA. 1987.

Cheng, H., Rizzer, A. and Obergefell, L. Articulated Total Body Model Version V User's Manual. United States Air Force Research Laboratory, Wright-Patterson Air Force Base, Ohio, USA February 1998.

Cliff, W. and Bowler, J. The Measured Rolling Resistance of Vehicles for Accident Reconstruction. SAE Paper 980368. 1998.

Coley, G., de Lange, R., de Oliveira, P., Neal-Sturgess, C. and Happee, R. Pedestrian Human Body Validation Using Detailed Real-World Accidents. International IRCOBI Conference on the Biomechanics of Impact, pp 89 – 102. October 2001.

Collins J. C. and Morris, J. L., Accident Reconstruction, Highway Collision Analysis, Thomas Publishing. 1979.

Cooperrider, N. K., Hammoud, S. A., Colwell, J. Characteristics of Soil-tripped Rollovers. SAE980022, 1998.

Crandall J., Wiley K., Longhitano D., Akiyama A. Development of Performance Specifications for a Pedestrian Research Dummy, Proceedings of the 19th International Technical Conference on the Enhanced Safety of Vehicles (ESV) Washington DC, USA. Paper no. 05-0389-0. 6-9 June 2005.

Curio, C., Edelbrunner, J., Kalinke, T., Tzomakas, C. and von Seelen, W. Walking Pedestrian Recognition. Intelligent Transportation Systems, IEEE Transactions on Volume 01, Issue 3, Page(s):155 – 163. Sept. 2000.

Dalbey, K., Patra, A., Pateel, V. Arumugasundaram, S., Hatziprokopiou, I. and Galganski, R. Incorporating Input Data Uncertainties in Computer Models of Vehicle Systems using the Polynomial Chaos Quadrature Method. SAE Paper 2006-01-1139, presented at SAE 2006 World Congress & Exhibition, Detroit, MI, USA, Session: Occupant Restraints (Part 1 of 2). April, 2006.

Dalenoort, A., Griotto, G., Mooi, H., Baldauf, H. and Weissenbach, G. A Stochastic Virtual Testing Approach in Vehicle Passive Safety Design: Effect of Scatter on Injury Response. SAE Paper 2005-01-1763, presented at SAE 2005 World Congress & Exhibition, Detroit, MI, USA, Session: Reliability and Robust Design in Automotive Engineering - Applications (Part 3 of 3). April, 2005.

Daubert vs Merrell Dow Pharmaceuticals, 509 U.S. 579. 1993

Day, T. D. and Garvey, J. T. Applications and Limitations of 3-Dimensional Vehicle Rollover Simulation. SAE Paper 2000-01-0852. Progress in Technology, Vol 101, pp 742-755, USA, 2004.

Du Bois, P., Chou, C., Filet, B., Khalil, T., King, A., Mahmood, H., Mertz, H. and Wismans, J. Vehicle Crashworthiness and Occupant Protection. American Iron and Steel Institute, Southfield, USA. 2004.

Eckstein, P. F. and Thumma, S. A. Novel Scientific Expert Evidence in Arizona State Courts. Arizona Attorney, USA. June 1998.

EEVC Working Group 10 Report (1994): Proposals for methods to evaluate pedestrian protection for passenger cars. November 1994.

EEVC Working Group 17 Report (1998): Improved test methods to evaluate pedestrian protection afforded by passenger cars. December 1998.

Emori, R. I. Analytical Approach to Automobile Collisions. Automotive Congress and Exposition, Detroit, USA. SAE 680016. 1968.

Eubanks, J. and Hill, P. F. Pedestrian Accident Reconstruction and Litigation. Lawyers & Judges Publishing Company, Tucson, Arizona, USA. 1994.

EuroNCAP Pedestrian Testing Protocol Version 4.1. www.euroncap.com. March, 2004.

European Road Safety Observatory (2006) Vehicles. (www.erso.eu) 2007

FAA Advisory Circular: Methodology for Dynamic Seat Certification by Analysis for Use in Parts 23. 25. 27 and 29 Airplanes and Rotorcraft. U.S Department of Transportation, Federal Aviation Authority. AC No. 20-146, 2003

Fasanella E. L., Jackson, K. E., Jones, Y. T., Fings, G. and Vu, T. Crash Simulatin of a Boeing 737 Fuselage Section Vertical Drop Test. Aircraft Design, Testing and Performance, NASA Langley Research Centre, 2001

Fay, R. J. Computer Images and Animations in Court. SAE Paper 970965, presented at the Society of Automotive Engineers International Congress and Exposition, Detroit, Michigan, USA. February, 1997.

Fitzgerald, M. P. and Armstrong, T. R. A New Determination of the Newtonian Gravitational Constant at MSL. Conference on Precision Electromagnetic Measurements, 16-21 June, 2002

Fleisher, H. J. and Benaroya, H. Investigation of Monte Carlo Simulation in FAA Program KRASH. Journal of Aircraft, Vol 31 No 2, 1994.

FMVSS (Federal Motor Vehicle Safety Standards): 208 – Occupant Crash Protection. National Highway Traffic Safety Administration, Office of Vehicle Safety Compliance, Washington, DC. USA. 1997.

Foret-Bruno J. Y., Faverjon G., Le Coz J. Y. Injury Pattern of Pedestrians Hit by Cars of Recent Design, Proceedings of the 16th International Technical Conference on Enhanced Safety of Vehicles (ESV), Windsor, Canada. pp 2122-2130. 1998.

Fredriksson R., Håland Y., Yang J. Evaluation of a New Pedestrian Head Injury Protection System with a Sensor in the Bumper and Lifting of the Bonnet's Rear Edge, Proceedings of the 17th International Technical Conference on the Enhanced Safety of Vehicles, Amsterdam, The Netherlands. 4-7 June 2001.

Fricke, L. B. Traffic Accident Reconstruction, Vol 2 of the Traffic Accident Investigation Manual, 1990

Frye v. United States, 54 App. D. C. 46, 47, 293 F. 1013, 1014. 1923.

Fugger, T., Randles, B., Wobrock, J. and Eubanks, J. Pedestrian Throw Kinematics in Forward Projection Collisions. SAE Paper 2002-01-0019, presented at the Society of Automotive Engineers 2002 World Congress & Exhibition, Session: Biomechanics (Part A&B). Detroit, MI, USA. March 2002

Gadd C. M. Use of a Weighted Impulse Criterion for Estimating Injury Hazard, Proceedings of the 10th Stapp Car Crash Conference, Society of Automotive Engineers, New York. pp 164-174. 1966.

Garthe E., Mango N., States J. D. AIS Unification: The Case for a Unified Injury System for Global Use, Proceedings of the 16th International Technical Conference on the Enhanced Safety of Vehicles (ESV) Windsor, Ontario, Canada. Paper No. 98-S6-O-50. pp 1276-1290. 1998.

Gibson, T., Fildes, B., Deery, H., Sparke, L., Benetatos, E., Fitzharris, M.m McLean, J. and Vulcan, P. Improved Side Impact Protection: A Review of Injury Patterns, Injury Tolerance and Dummy Measurement Capabilities. A Monash University Accident Research Centre Report. Report No. 147, Melbourne, Australia. August, 2001.

Giddings, V., Beaupre, G., Whalen, R. and Carter, D. Calcaneal Loading during Walking and Running. Medicine & Science in Sports and Exercise, American College of Sports Medicine, Indianapolis, USA. July 1999.

Graillet, D. and Ponthot, J. Numerical Simulation of Crashworthiness with an Implicit Finite Element Code. Aircraft Engineering and Aerospace Technology: An International Journal. MCB University Press, Bradford, United Kingdom. Vol. 71 No. 1, pp 12 -20, 1999

Grimes, W. D. Computer Animation Techniques for Use in Collision Reconstruction. SAE Paper 920755, presented at the Society of Automotive Engineers International Congress and Exposition, Detroit, Michigan, USA. February, 1992.

Grimes, W. D. Using ATB Under the HVE Environment. SAE International Congress and Exposition, Detroit, USA. SAE 970967. February 1997.

Grimes, W. D., Dickerson, C. P. and Smith, C. D. Documenting Scientific Visualizations and Computer Animations Used in Collision Reconstruction Presentations. SAE Paper 980018, presented at the Society of Automotive Engineers International Congress and Exposition, Detroit, Michigan, USA. February, 1998.

Grosse, R. 25 Years of the Personal Computer. Department of Computer Science. University of Saskatchewan, Saskatoon, Canada. 2004

Gurdjian E. S., Roberts V. L., Thomas L. M. Tolerance Curves of Acceleration and Intracranial Pressure and Protective Index in Experimental Head Injury, Journal of Trauma, 6(5): 600-604. 1966.

Han, I. and Brach, R. Throw Model for Frontal Pedestrian Collisions. SAE Paper 2001-01-0898, presented at the Society of Automotive Engineers World Congress and Exposition, Detroit, Michigan, USA. March 2001.

Happee, R., Hoofman, M., Kroonenberg, A., Morsink, P. and Wismans, J. A Mathematical Humand Body Model for Frontal and Rearward Seated Automotive Impact Loading. Proceedings of the 42nd Stapp Car Crash Conference, SAE Paper 983150, Warrendale, Pennsylvania, USA. 1998.

Happee, R. and Wismans, J. Pedestrian Protection Full-Body Simulations, Dummy Validation. Proceedings VDA Technical Congress, Frankfurt, Germany. 1999.

Happer, A., Araszewski, M., Toor, A., Overgaard, R. and Johal, R. Comprehensive Analysis Method for Vehicle/Pedestrian Collisions. SAE Paper 2000-01-0846, presented at the Society of Automotive Engineers International Congress and Exposition, Detroit, Michigan, USA, Session: Accident Reconstruction: Simulation & Animation (Part C&D). March 2000.

Hardy, W., Schneider, W. and Rouhana, S. Abdominal Impact Response to Rigid-Bar Seatbelt and Airbag Loading. 45th Stapp Conference, 2001

Highway Accident Report, NTSB. 15-Passenger Child Care Van Run-Off-Road Accident Memphis, Tennessee, April 2002, NTSB/HAR-04/02

Hill, D. K. Dissecting Trajectories: Galileo's Early Experiments on Projectile Motion and the Law of Fall**.** *Isis*, pp. 646-668 Vol. 79, No. 4, Dec 1988

Hill, G. S. Calculations of Vehicle Speed from Pedestrian Throw – Journal of ITAI, p18-20, Spring 1994.

Hira and Gupta, *Operations Research*, Dhanpatrai & Sons, 1998, 1999

Hoof J. van, Lange R. de, Wismans J. Improving Pedestrian Safety Using Numerical Human Models. SAE Report No. 2003-22-0018Stapp Car Crash journal. Vol. 47, pp. 401-436. 2003

Horgan, T. J. A Finite Element Model of the Human Head for Use in the Study of Pedestrian Accidents. A thesis submitted for the degree of Doctor of Philosophy of the National University of Ireland. Department of Mechanical Engineering, Faculty of Engineering and Architecture, University College of Dublin, Dublin, Ireland. February, 2005.

Howard, M., Thomas, A., Koch, W., Watson, J. and Hardy, R. Validation and Application of a Finite Element Pedestrian Humanoid Model for Use in Pedestrian Accident Simulations. IRCOBI Conference, Montpellier, France. September 2000,

Huang, Y., King, A. and Cavanaugh, J. A MADYMO Model of Near-Side Human Occupants in Side Impacts. Journal of Biomechanical Engineering, Vol 116, pages 228-235. 1994a

Huang, Y., King, A. and Cavanaugh, J. Finite Element Modelling of Gross Motion of Human Cadavers in Side Impact. Proceedings of the 38th Stapp Car Crash Conference, SAE Paper 942207, Warrendale, Pennsylvania, USA. 1994b

Hull, W. C., Newton, B. E., Macaw, C. R. and Miller, R. R. Functional Classifications and Critique Methods for Litigation Support Forensic/Accident Reconstruction Animations. SAE Paper 960651, presented at the Society of Automotive Engineers International Congress and Exposition, Detroit, Michigan, USA. February, 1996.

Hulme, K.F., Patra, A., Galganski, R, and Vusirikala, N. Development of a Visualization Module for Madymo-based Child Restraint System (CRS) Safety Simulation. TNO MADYMO 5th Users' Meeting of The Americas, Troy, Michigan, October, 2003.

Idnani, S. An ACSL Interface for DYMOLA. Masters Thesis, Department of Electrical and Computer Engineering, University of Arizona, USA. 1991

IHRA (International Harmonized Research Activities) Pedestrian Safety Working Group 2001 Report. IHRA-PS-200. December 2001.

Ishaque, M. Policies for Pedestrian Access: Multi-modal Trade-off Analysis using Micro-simulation Techniques. A thesis submitted as fulfilment of the requirements for the degree of Doctor of Philosophy of the University of London and for the Diploma of Membership of Imperial College. Centre for Transport Studies, Imperial College, London, United Kingdom. October 2006.

Ishikawa, H., Kajzer, J. and Schroeder, G. Computer Simulation of Impact Response of the Human Body in Car-Pedestrian Accidents. 37th Stapp Car Crash Conference, San Antonio, Texas, USA. November, 1993.

Iwamoto, M., Kisanuki, Y., Watanabe, I., Furusu, K., Miki, K. and Hasegawa, J. Development of a Finite Element Model of the Total Human Model for Safety (THUMS) and Application to Injury Reconstruction. IRCOBI Conference, pages 31-42. 2002.

Iwamoto, M., Omori, K., Kimpara, H., Nakahira, Y., Tamura, A., Watanabe, I., Miki, K., Hasegaw, J., Oshita, F. Recent Advances in THUMS: Development of Individual Internal Organs, Brain, Small Female and Pedestrian Model. Proceedings of the 4th European LS-DYNA Users Conference, Ulm, Germany, 2003

Jackson, K. E., Boitnott, R. L., Fasanella, E. L., Jones, L. E. and Lyle, K. H. A History of Full-Scale Aircraft and Rotorcraft Crash Testing and Simulation at NASA Langley Research Center. 4th Triennial International Fire and Cabin Safety Research Conference Proceedings, Lisbon, Portugal, November 2004

Jain, R. and Ramachandra, K. Bird Impact Analysis of Pre-Stressed Fan Blades Using Explicit Finite Element Code. Proceedings of the International Gas Turbine Conference, Tokyo, Japan, November 2003

Johannsen, H. and Schindler, V. Development and Assessment of a Surface Force Abdominal Sensor. Proceedings of the 20th International Technical Conference on the Enhanced Safety of Vehicles (ESV), Lyon, France. June 18 – 21, 2007.

Karger B., Teige K., Fuchs M., Brinkmann B. Was the Pedestrian Hit in an Erect Position Before Being Run Over? Forensic Science International Vol. 119 pp 217-220. 2001.

Kajzer, J., Matsui, Y., Ishikawa, H., Schroeder, G. and Bosch, U. Shearing and Bending Effect at the Knee Joint at Low Speed Lateral Loading. SAE Paper 1999-01-

0712 presented at the SAE International Congress and Exposition, Detroit, Michigan, USA. March, 1999.

Kerrigan, J. R., Drinkwater D. C., Murphy D. B., Kam C. Y., Crandall J. R. Comparison of Full Scale Pedestrian Impact Tests with PMHS and a Pedestrian Dummy, unpublished report, Center for Applied Biomechanics, University of Virginia. 2005.

Kimpara, H., Lee, J, Yang, K., King, A., Iwamoto, M., Watanabe, I. and Miki, K. Development of a Three-Dimensional Finite Element Chest Model for the 5th Percentile Female. Stapp Car Crash Journal, Vol. 49, pages 251-269. November 2005.

King A. I., Yang K. H., Zhang L., Hardy W., Viano D. C. Is Head Injury Caused by Linear or Angular Acceleration? IRCOBI Conference, Lisbon (Portugal), September 2003.

King, A. I., Du Bois, P., Chou, C. C., Fileta, B. B., Khalil, T. B., Mahmood, H. F., Mertz, H. J., Wismans, J. Vehicle Crashworthiness and Occupant Protection, published by Automotive Applications Committee, American Iron and Steel Institute, Southfield, Michigan, USA. 2004.

Knight, B. Forensic Medicine. Mosby International. December, 1985.

Konosu A., Ishikawa H., Kant R. Development of Computer Simulation Models for Pedestrian Subsystem Impact Tests, JSAE Review Vol. 21 pp 109-115. 2000.

Konosu A. Reconstruction Analysis for Car-Pedestrian Accidents Using a Computer Simulation Model, Society of Automotive Engineers of Japan, Inc. and Elsevier Science B.V. JSAE Review Vol. 23 pp 357-363. 2002.

Kost, G. and Werner, S. Use of Monte Carlo Simulation Techniques in Accident Reconstruction. SAE Paper 940719, presented at the Society of Automotive Engineers International Congress and Exposition, Detroit, Michigan, USA. February - March, 1994.

Kreja, I. Stability Analysis of Cylindrical Composite Shells in MSC/NASTRAN. Archives of Civil and Mechanical Engineering, Gdansk University of Technology, Gdansk, Poland, Vol 5 No. 3, pp 31 – 41, 2005

Kuehn M., Froeming R., Schindler V. Assessment of Vehicle Related Pedestrian Safety, Proceedings of the 19th International Technical Conference on the Enhanced Safety of Vehicles (ESV) Washington DC, USA. Paper no. 05-0044-0. 6-9 June 2005.

Kühnel, A. Vehicle-Pedestrian Collision Experiments with the use of a Moving Dummy. *Proceedings of the 18th conference of the American Association for Automotive Medicine*. Lake Bluff, Ill: American Association for Automotive Medicine. pp 223-245, 1974

Lange, R., Rooij, L., Mooi, H. and Wismans, J. Objective Biofidelity Rating of a Numerical Human Occupant Model in Frontal To Lateral Impact. Stapp Car Crash Journal No. 49. 2005

Langwieder, K., Fildes, B., Ernvall, T. and Cameron. M. SARAC – Safety Rating Based on Real-World Crashes for Supplementation of New Car Assessment Programs. Proceedings of the 18th International Technical Conference on the Enhanced Safety of Vehicles (ESV). Paper Number 175. 12 pp. http://www-nrd.nhtsa.dot.gov/pdf/nrd-01/esv/esv18/CD/Files/18ESV-000175.pdf. Nagoya, Japan, May 19-22, 2003.

Lawrence, G., Hardy, B., Carroll, J., Donaldson, W., Visvikis, C., Peel, D. and Knight, I. A Study on the Feasibilty of Measures Relating to the Protection of Pedestrians and Other Vulnerable Road Users. UPR/VE/045/06 TRL Project Report, U.K. 2006.

Lee C. and Abdel-Aty M. Comprehensive Analysis of Vehicle-Pedestrian Crashes at Intersections in Florida. Accident Analysis & Prevention 37 pp 775-786. 2005.

Lewerenz, M. Monte Carlo Methods: Overview and Basics. Quantum Simulations of Complex Many-Body Systems: From Theory to Algorithms. Grotendorst, J., Marx, D. and Muramatsu, A. John von Neumann Institute for Computing, Julich, NIC Series Vol 10, ISBN 3-00-009057, pp 1- 24, 2002

Leeman, R. W., Brown, D. R., Stansifer, R. L., Uldricks, D. B. and Guenther, D. A. Computer Accident Simulation – Pretty Pictures and the Real World. SAE Paper 910368, presented at the Society of Automotive Engineers International Congress and Exposition, Detroit, Michigan, USA. February - March, 1991.

Leglatin, N., Blundell, M. and Blount, G. The Simulation of Pedestrian Impact with a Combined Multibody Finite Elements System Model. Journal of Engineering Design, Vol. 17, No. 5, pages 463-477. October 2006.

Lin, J., Zywicz, E. and Raboin, P. DYNA3D Code Practices and Developments. Lawrence Livermore National Laboratory, U.S. Department of Energy, UCRL-ID-138654. April 2000.

Linder A., Douglas C., Clark A., Fildes B., Yang J., Otte D. Mathematical Simulations of Real World Pedestrian-Vehicle Collisions, Proceedings of the 19th International Technical Conference on the Enhanced Safety of Vehicles (ESV) Washington DC, USA. Paper no. 05-0285-0. 6-9 June 2005.

Liu, X. and Yang, K. Development of Child Pedestrian Mathematical Models and Evaluation with Accident Reconstructions. IRCOBI Conference, Isle of Man, UK. October, 2001.

Liu, X., Yang, J. and Lövsund, P. A Study of Influences of Vehicle Speed and Front Structure on Pedestrian Impact Responses Using Mathematical Models. Journal of Traffic Injury Prevention, 3:31-42. 2002.

Lizee, E., Robin, S., Song, E., Bertholon, N., Le Coz, J., Besnault, B. and Lavaste, F. Development of a 3D Finite-Element Model of the Human Body. Proceedings of the

42nd Stapp Car Crash Conference. SAE Paper 983152, Warrendale, Pennsylvania, USA. 1998.

Long A. and Anderson R. The Development and Validation of the IHRA Pedestrian Model Using MADYMO and AutoDOE, Proceedings of the 2005 Madymo Users Meeting. November 2005.

Longhitano D., Ivarsson J., Henary B., Crandall J. Torso Injury Trends for Pedestrians Struck by Cars and LTVs, Proceedings of the 19th International Technical Conference on the Enhanced Safety of Vehicles (ESV) Washington DC, USA. Paper no. 05-0411-0. 6-9 June 2005.

Louden, R. K., Lukey, I. Computer Simulation of Automotive Fuel Economy and Acceleration. Society of Automotive Engineers, Warrendale, Pennsylvania, USA. SAE 600132. 1960

Lucchini, E. and Weissner, R. Differences Between the Kinematics and Loadings of Impacted Adults and Children; Results from Dummy Tests. Proc. of the Fifth International IRCOBI Conference on the Biomechanics of Impacts, Lyon, pp. 165-179. 1980

MacLaughlin, T., Wiechel, J. and Guenther, D. Head Impact Reconstruction – HIC Validation and Pedestrian Injury Risk. SAE Paper 930895, presented at the SAE International Congress and Exposition, Detroit, Michigan, USA. March, 1993.

Mądro R. and Teresiński G. Neck Injuries as a Reconstructive Parameter in Car-to-Pedestrian Accidents. Forensic Science International 118 pp 57-63. 2001.

Madymo Theory Manual, TNO Automotive, Delft, 2001

Madymo Human Models Manual, TNO Automotive, Delft, 2001

MARC Datasheet: Nonlinear Analysis for Engineering Applications and Manufacturing Processes. MSC Software website

http://www.mscsoftware.com/assets/MA2005JULZZZLTDAT.pdf (accessed May 2006)

Marzougui, D., Kan, C. and Eskandarian, A. Safety Performance Evaluation of Roadside Hardware Using Finite Element Simulation. 14th Engineering Mechanics Conference, American Society of Civil Engineers, Austin, USA. May 2000

McElhaney, J. H., Roberts, V. L., and Hilyard, J. F. Handbook of Human Tolerance, Japan Automobile Research Institute, Inc, Tokyo, Japan, 1976

McHenry, R. R. and Naab, K. N. Computer Simulation of the Crash Victim – A Validation Study. Proceedings of the 10th Stapp Car Crash Conference, New Mexico, USA. SAE 660792. 1966.

McHenry, R. R. Research in Automobile Dynamics – A Computer Simulation of General Three-Dimensional Motions. International Mid-Year Meeting, Montreal Quebec, Canada. SAE 710361. 1971

McHenry, R. R. Computer Program for Reconstruction of Highway Accidents. Proceedings of the 17th Stapp Car Crash Conference, Oklahoma City, USA. SAE 730980. 1973

McHenry B. G. and McHenry, R. R. SMAC-87. SAE International Congress and Exposition, Detroit, USA. SAE 880227. 1987.

McHenry B. G. and McHenry, R. R. SMAC-97: Refinement of the Collision Algorithm. SAE International Congress and Exposition, Detroit, USA. SAE 970947. 1997.

McLay, R. W., Kiely, S. J. and Sheehan, M. L. Case Studies in Animation Foundation. SAE Paper 940920, presented at the Society of Automotive Engineers International Congress and Exposition, Detroit, Michigan, USA. February - March, 1994.

McLean, A. J., Anderson, R. W. G., Farmer, M. J. B., Lee, B. H. and Brooks, C. G. Vehicle Travel Speeds and the Incidence of Fatal Pedestrian Collisions, Road Accident Research Unit, Adelaide University, Australia, 1994.

Mertz HJ, Prasad P, Irwin AL. Injury Risk Curves for Children and Adults in Front and Rear Collisions, Society for Automotive Engineers, SAE#973318, 1997

Messerer, O. Elasticity and Strength of Human Bones. Verlag der J. G. Cotta'schen Buchhandlung, Stuttgart. 1880.

Miles-Doan R. Alcohol Use Among Pedestrians and the Odds of Surviving an Injury: Evidence from Florida Law Enforcement Data, published by Elsevier Science Ltd, Accident Analysis and Prevention Vol 28(1): 23-31. 1995.

Mizuno K. and Kajzer J. Head Injuries in Vehicle Pedestrian Impact, Proceedings of SAE 2000 World Congress, Detroit, USA. SAE 2000-01-0157, 2000.

Monash University Accident Research Centre. Feasibility of Occupant Protection Measures, Report CR 100, Federal Office of Road Safety, Canberra, Australia. 1992.

Moser, A., Steffan, H., Spek, A. and Makkinga, W. Application of the Monte Carlo Methods for Stability Analysis within the Accident Reconstruction Software PC-CRASH. SAE Paper 2003-01-0488, presented at the Society of Automotive Engineers World Congress and Exposition, Detroit, Michigan, USA, Session: Accident Reconstruction (Part 1&2 of 4). March 2003.

Mustard, J. D. Computers in Motor Vehicle Accident Reconstruction: A Review. SAE Paper 871995, presented at the Society of Automotive Engineers Passenger Car Meeting and Exposition, Dearborn, Michigan, USA. October, 1987.

Nagatomi, K., Hanayama K., Ishizaki T., Sasaki S., Matsuda K. Development and Full-Scale Dummy Tests of a Pop-Up Hood System for Pedestrian Protection, Proceedings of the 19th International Technical Conference on the Enhanced Safety of Vehicles (ESV) Washington DC, USA. Paper no. 05-0113-0. 6-9 June 2005.

NASA Technical Standard 7001: Payload Vibroacoustic Test Criteria, NASA-STD-7001, 1996

Nash, C. E. CRASH 3:Current Status. SAE International Congress and Exposition, Detroit, USA. SAE 870040. 1987.

National Highway Traffic Safety Administration (NHTSA) Regulation 571, 49 CFR 500-599. Superintendent of Documents, U.S. Government Printing Office, P.O. Box 371954 Pittsburgh, PA 15250-7954, USA. May, 2005.

Neale, M. S., Hardy, B. J. and Lawrence, G. J. L. Development and Review of the IHRA (JARI) and TNO Pedestrian Models. Proceedings of the 18th International Technical Conference on the Enhanced Safety of Vehicles (ESV), Nagoya, Japan. Paper no. 499. May 2003.

Neal-Sturgess, C., Coley, G. and Oliveira, P. Pedestrian Injury – Effects in Impact Speed and Contact Stiffness. Vehicle Safety, IMechE. Publication: 3982. London, U.K. 2002.

Neal-Sturgess, C. A Thermomechanical Theory of Impact Trauma. Proceedings of the Institution of Mechanical Engineers, 216, pg 883-895. 2002.

Newman, J. A Generalized Acceleration Model for Brain Injury Threshold (GAMBIT). International Conference on the Biomechanics of Impact (IRCOBI). 1986.

Newman, J., Barr, C., Beusenberg, M., Fourner, E., Shewchenko, N., Withnall, C., Biokenetics and Associates Ltd, King, Y., Yang, K., Zhang, L., EcElhaney, J., Thibault, L. and McGinnis, G. A New Biomechanical Assessment of Mild Traumatic Brain Injury – Part I – Methodology. Presented at the International Conference on the Biomechanics of Impact (IRCOBI), Sitges, Spain. 1999.

Newman, J., Barr, C., Beusenberg, M., Fourner, E., Shewchenko, N., Welbourne, E., Withnall, C. and Biokenetics and Associates Ltd. A New Biomechanical Assessment of Mild Traumatic Brain Injury - Part II - Results. Presented at the International Conference on the Biomechanics of Impact (IRCOBI), Monpellier, France. 2000.

Noon, W. D. Computer Simulated Vehicle Performance. Society of Automotive Engineers, Warrendale, Pennsylvania, USA. SAE 620573. 1962

Nyquist, G. Injury Tolerance Characteristics of the Adult Human Lower Extremities under Static and Dynamic Loading. Symposium on Biomechanics and Medical Aspects of Lower Limb Injuries, Sand Diego, California, USA. October, 1986.

Ohashi, H., Ono, K., Sasaki, A., Ohashi, N., Misawa, S. The Present Situation of Pedestrian Accidents in Japan. Proceedings of the International IRCOBI Conference on the Biomechanics of Impacts, pp. 283-292. 1990

Okamoto, Y., Sugimoto, T., Enomoto, K. and Kikuchi, J. Pedestrian Head Impact Conditions Depending on Vehicle Front Shape and its Construction – Full Model Simulation. Proceedings of the International IRCOBI Conference on the Biomechanics of Impacts, Montpellier, France. pp 281 – 291. 2000

Open Channel Foundation, Research and Academic Software Publishers, http://www.openchannelfoundation.org/projects/NASTRAN/ (last accessed May, 2006)

Ören, T. I. SCS and Computer Simulation: Fifty Years of Progress. 50th Anniversary Issue, Modelling and Simulation, 1:3 pp 32-33. San Diego, USA. 2002

Orsborn R., Haley K., Hammond S., Falcone R.E. Pediatric Pedestrian Versus Motor Vehicle Patterns of Injury: Debunking the Myth, Air Medical Journal, 18:3 July-September 1999.

Oshita, F., Omori, K., Nakahira, Y., Miki, K. Development of a Finite Element Model of the Human Body. Proceedings 7th International LS-DYNA Users Conference, Detroit, USA, pp 3-37 to 3-48, 2002

Otte, D. Design and Structure of the Windscreen as Part of Injury Reduction for Car Occupants, Pedestrians and Bicyclists. Proc. of the 38th Stapp Car Crash Conference, Fort Lauderdale, USA. November 1994.

Otte, D. and Pohlemann, T. Analysis and Load Assessment of Secondary Impact to Adult Pedestrians After Car Collisions on Roads. IRCOBI (International Research Council On the Biomechanics of Impact). Isle of Man, UK. October, 2001.

Parent, D., Tyrell, D., Perlman, A. B. Crashworthiness Analysis of the Placenia, CA Rail Collision. International Crashworthiness Conference, San Francisco, 2004

Park, K., Shin, S., Cho, H. and Jinn, J. Application of the Finite Element Method for Improvement of Vehicle Crashworthiness. Proceedings of the 6th International Pacific Conference on Automotive Engineering, Seoul, South Korea. Oct 28 – Nov 1, 1991.

Piguet, C. Electronic Computer History: 1940-2000. CSEM Centre Suisse d'Electronique et de Microtechnique SA. Maladière 71, Neuchâtel, Switzerland, 2000

Poland, K. M., McCray, L., Barsan-Anelli, A. Occupant Safety in Large School Buses: Crash Investigations, Testing and Modelling. NTSB Journal of Accident Investigation, Vol 2, Issue 1, 2006

Prasad, P. An Overview of Major Occupant Simulation Models. SAE Government Industry Meeting and Exposition, Washington, USA. SAE 840855. May 1984.

Prasad, P. and Mertz, H. The Position of the United States Delegation to the ISO Working Group 6 on the Use of HIC in the Automotive Environment. SAE, PT-43, Biomechanics of Impact Injury and Injury Tolerance of the Head-Neck Complex, Published by Society of Automotive Engineers, Inc., 1985.

Prasad, P. Biomechanical Basis for Injury Criteria Used in Crashworthiness Regulations. Proceedings of 1999 International IRCOBI Conference on the Biomechanics of Impact, Sitges, Spain. pp 1 - 16 September 1999

Randles, B., Fugger, T., Eubanks, J. and Pasanen, E. Investigation and Analysis of Real-Life Pedestrian Collisions. SAE Paper 2001-01-0171, presented at the Society of Automotive Engineers World Congress and Exposition, Detroit, Michigan, USA. March 2001.

Ravini, B., Brougham, D., Mason, R. T. Pedestrian Post-Impact Kinematics and Injury Patterns, Proceedings of the 25th Stapp Car Crash Conference, San Francisco, USA. SAE 811024. 1981.

Ray, M. H. The Use of Finite Element Analysis in Roadside Hardware Design. Roadside Safety Issues Revisited, Irvine, USA. Transportation Research Circular Issue No 453. 1996

Reitman, J. A Concise History of the Ups and Downs of Simulation. Proceedings of the Winter Simulation Conference, San Diego, USA, 1988.

Reuter, R. and Watermann, A. Application of Uncertainty Management to MADYMO Occupant Simulations. 2nd European MADYMO User's Conference, Stuttgart, Germany. 1999.

Reuter, R. and Hülsmann, J. Achieving Design Targets throught Stochastic Simulations. 3rd European MADYMO User's Conference, Paris, France. 2000.

Rich, A. S. Estimating Vault Distance and Speed after Motorcycle or Bicycle Ejection, NJAAR, The Newsletter for Accident Reconstructionists, Vol. 3 No. 2, 1997

Robin, S. HUMOS: Human Model for Safety – a Joint Effort Towards the Development of Refined Human-Like Car Occupant Models. 17th International Technical Conference on the Enhanced Safety of Vehicles, paper 297, 2001.

Roudsari B. S., Mock C. N., Kaufman R., Grossman D., Henary B. Y., Crandall, J. Pedestrian Crashes: Higher Injury Severity and Mortality Rate for Light Truck Vehicles Compared with Passenger Vehicles, Injury Prevention 2004 Vol. 10, pp 154-158. 2004.

Roudsari, B., Mock, C. and Kaufman, R. An Evaluation of the Association Between Vehicle Type and the Source and Severity of Pedestrian Injuries. Traffic Injury Prevention, p185-192. 2005.

Ruan, J., El-Jawahri, R., Chai, L., Barbat, S. and Prasad, P. Prediction and Analysis of Human Thoracic Impact Responses and Injuries in Cadaver Impacts Using a Full Human Body Finite Element Model. Proceedings of the 47th Stapp Car Crash Conference, pages 299-321. October 2003.

Russell, A. Physics and Acoustics of Baseball & Softball Bats: Why Aluminium Bats Can Perform Better than Wood Bats. http://www.kettering.edu/~drussell/bats-new/alumwood.html October, 2006.

Sarath K. B. MADYMO Modelling of the IHRA Pedestrian Head-Form Impactor, Masters Thesis, Department of Mechanical Engineering, Ohio State University, USA. 2004.

Schofield, D., Noond, J., Goodwin, L. and March, J. Interactive Evidence: New Ways To Present Accident Investigation Information, Proceedings of the Workshop on the Investigation and Reporting of Incidents and Accidents, University of Glasgow, United Kingdom. pp. 194-203. July, 2002.

Schreurs, A., Schönekäs, A. and Chapman, S. Pedestrian Dummy Models Used in the Development of Active Safety Systems. 3rd European MADYMO User's Meeting, Stuttgart, Germany. September 2001.

Searle, J. A. and Searle, A., The Trajectories of Pedestrians, Motorcycles, Motorcyclists etc following a Road Accident, SAE Technical Paper #831622, 1983

Searle, J. The Physics of Throw Distance in Accident Reconstruction, SAE 930659. 1993

Severy, D. and Brink, H. Auto-pedestrian Collision Experiments Using Full-Scale Accident Simulation, SAE Paper 660080 presented at the Automotive Engineering Congress and Exposition, Detroit, Michigan, USA. January, 1966.

Shah, P. and Danne, A. Stochastic Analysis of Frontal Crash Model. NAFEMS Seminar: Use of Stochastics in FEM Analyses, Wiesbaden, Germany. May 7-9, 2003.

Shin J., Lee S. H., Kerrigan J., Darvish K., Crandall J., Akiyama A., Takahashi Y., Okamoto M., Kikuchi Y. Development and Validation of a Finite Element Model for the POLAR-II Upper Body, accepted for the 2006 SAE International Congress, Detroit, MI, USA. 2006

Simms C. K. and Wood D. P. Pedestrian Impact: The Effect of Pedestrian Motion on Head Contact Forces with Vehicle and Ground, 2005 International IRCOBI Conference on the Biomechanics of Impact, Prague (Czech Republic). 21-23 September, 2005.

Simms, C. The Relationship Between Vehicle Front-End Shape and Pedestrian Injuries. Bioengineering in Ireland Conference, Galway, Ireland. January 27-28, 2006.

Smith, R. A. and Noga, J. T. Accuracy and Sensitivity of CRASH. Proceeding of the 26th Stapp Car Crash Conference, Ann Arbor, USA. SAE 821169. 1982

Snedeker, J., Muser, M. and Walz, F. Assessment of Pelvis and Upper Leg Injury Risk in Car-Pedestrian Collisions: Comparison of Accident Statistics, Impactor Test and a Human Body Finite Element Model. Stapp Car Crash Journal, Vol. 47, pg 437 – 457. October, 2003.

Snedeker J. G., Walz F. H., Muser M. H., Lanz C., Schroeder G. Assessing Femur and Pelvis Injury Risk in Car-Pedestrian Collisions: Comparison of Full Body PMTO Impacts, and a Human Body Finite Element Model, Proceedings of the 19th

International Technical Conference on the Enhanced Safety of Vehicles (ESV) Washington DC, USA. Paper no. 05-0103-0. 6-9 June 2005.

Stammen J. and Barsan-Anelli A. Adaptation of a Human Body Mathematical Model to Simulation of Pedestrian/Vehicle Interactions, 4th MADYMO User's Meeting of The America's, Detroit, USA. 24 October 2001.

Stevenson, T. J. and Raine, J. K. Low-speed Pedestrian versus SUV Collisions, Proceedings of the International Traffic Accident Investigators 2003 Conference, Stratford-Upon-Avon, United Kingdom. pp 143-152. 2003.

Stickney, M. E. Computer Simulation: The Beginning of a New Era. SAE Paper 930885, presented at the Society of Automotive Engineers International Congress and Exposition, Detroit, Michigan, USA. March, 1993.

Sturtz, G. and Suren, E. Kinematic of Real Pedestrian and Two Wheel Rider Accidents and Special Aspects of the Pedestrian Accident. Proc. of IRCOBI Meeting on Biomechanics of Injury to Pedestrians, Cyclists and Motorcyclists, Amsterdam, 7-8 Sept. 1976

Sugimoto T. and Yamazaki K. First Results from the JAMA Human Body Model Project, Proceedings of the 19th International Technical Conference on the Enhanced Safety of Vehicles (ESV) Washington DC, USA. Paper no. 05-0291-0. 6-9 June 2005.

Svoboda J., Čížek V. Pedestrian-Vehicle collision: Vehicle Design Analysis. SAE Paper 2003-01-0896, presented at the Society of Automotive Engineers World Congress and Exposition, March 3-6, Cobo Center, Detroit, Michigan, USA. 2003

Takubo N. and Mizuno K. Accident Analysis of Sports Utility Vehicles: Human Factors from Statistical Analysis and Case Studies, Society of Automotive Engineers of Japan, Inc. JSAE Review Vol. 21 pp 103-108. 2000.

Tanno K., Kohno, M., Ohashi N., Ono K., Aita K., Oikawa H., Oo M. T., Honda K., Misawa S. Patterns and Mechanisms of Pedestrian Injuries Induced by Vehicles with Flat-Front Shape, Legal Medicine Vol 2(2): 68-74. 2000.

Teresiński G. and Mądro R. Knee Joint Injuries as a Reconstructive Factors in Car-to-Pedestrian Accidents. Forensic Science International 124 pp 74-82. 2001a.

Teresiński G. and Mądro R. Ankle Joint Injuries as a Reconstruction Parameter in Car-to-Pedestrian Accidents. Forensic Science International Vol. 118 pp 65-73. 2001b.

Teresiński G. and Mądro R. Evidential Value of Injuries Useful for Reconstruction of the Pedestrian-Vehicle Location at the Moment of Collision, published by Elsevier Science Ireland Ltd, Forensic Science International 128 pp 127-135. 2002.

Tharp KJ, Tsongos NG. Injury severity factors – traffic pedestrian collisions. Proceedings of the Meeting on Biomechanics of Injury to Pedestrians, Cyclists and Motorcyclists; Sep 7-8; Amsterdam. Bron, France; International Research Committee on the Biokenetics of Impacts, 55-64, 1976

Tilp, J., Walther R., Carstens-Behrens S., Zehder C., Zott C., Fischer T., Ruhs M., Sohnke T., Wieland O., Busse A., Suhling F. Pedestrian Protection Based on Combined Sensor Systems, Proceedings of the 19th International Technical Conference on the Enhanced Safety of Vehicles (ESV) Washington DC, USA. Paper no. 05-0156-0. 6-9 June 2005

Timm, D., Birgisson, B. and Newcomb, D. Mechanistic-Empirical Flexible Pavement Thickness Design: The Minnesota Method. Department of Civil Engineering, University of Minnesota, Minneapolis, MN, USA. 1999.

Toor, A., Araszewski, M., Johal, R., Overgaard, R. and Happer, A. Revision and Validaton of Vehicle/Pedestrian Collision Analysis Method. SAE Paper 2002-01-0550, presented at the Society of Automotive Engineers World Congress and

Exposition, Detroit, Michigan, USA, Session: Accident Reconstruction (Part B&C). March 2002.

Troutbeck, R., Barker, T. and Thambiratnam, D. Roadside Barrier Design and Vehicle Occupant Safety. Australian Transport Safety Bureau Road Safety Research Grant Final Report, T2000/0736. School of Civil Engineering, Queensland University of Technology, Brisbane, Australia. November 2001.

Untaroiu, C., Darvish, K., Crandall, J., Deng, B. and Wang, J. Characterization of the Lower Limb Soft Tissue in Pedestrian Finite Element Models. Proceedings of the 19th International Technical Conference on the Enhanced Safety of Vehicles (ESV) Washington DC, USA. Paper no. 05-0156-0. 6-9 June 2005.

US Department of Transport. Collision Avoidance and Accident Survivability Volume 3: Accident Survivability. Calspan Corporation, Syracuse, NY, USA. DOT/FRA/ORD-93/02.III 1993

van Hoof, J., Lange, R. and Wismans, J. Improving Pedestrian Safety Using Numerical Human Models. Stapp Car Crash Journal No. 47, pgs 401 – on. October 2003.

van Rooij, L., Bhalla, K., Meissner, M., Ivarsson, J., Crandall, J., Longhitano, D., Takahashi, Y., Dokko, Y., and Kikuchi, Y. Pedestrian crash reconstruction using multibody modelling with geometrically detailed, validated vehicle models and advanced pedestrian injury criteria. In Proceedings of the 17th International ESV Conference, Nagoya, Japan. Paper 468. 2003.

Verma, M. and Repa, B. Pedestrian Impact Simulation – A Preliminary Study. Proceedings of the 27th Stapp Car Crash Conference with IRCOBI and Child Injury and Restraint Conference , San Diego, California, USA. 1983.

Versace J. A Review of the Severity Index, Proceedings of the 15th Stapp Car Crash Conference, Society of Automotive Engineers, New York. pp 771-796. 1971.

Vezin, P. and Verriest, J. Development of a Set of Numerical Human Models for Safety. Paper 05-0163 presented at the 19th International Technical Conference on the Enhanced Safety of Vehicles (ESV), Washington D.C., USA. June 2005.

Vilenius A. T. S., Ryan G. A., Kloeden C., McLean A. J., Dolinis J. A Method of Estimating Linear and Angular Accelerations in Head Impacts to Pedestrians, Accident Analysis and Prevention Vol 26(5): 563-570. 1993.

Voigt, G. E., Hodgson, V.R., Thomas, L.M. (1973). Breaking Strength of the Human Skull vs. ImpactSurface Curvature. Report Contract No. DOT HS 146.2.230.

Wakim, C., Capperon, S. and Oksman, J. A Markovian Model of Pedestrian Behavior. IEEE International Conference on Systems, Man and Cybernetics, Volume 4, Page(s):4028 – 4033. 10-13 Oct. 2004

Walfisch, G., Fayon, A., Tarriere, C., Rosey, J., Guillon, F., Got, F., Patel, C. and Stalnaker, R. Designing of a Dummy's Abdomen for Detecting Injuries in Side Impact Collisions. IRCOBI, 1980.

Waller, J. A. Injury Control. D.C Heath, Lexington, Massachusetts, USA. 1985

Waller P. F., Stewart R., Hansen A. R., Stutts J. C., Popkin C. L., Rodgman E. A. The Potentiating Effects of Alcohol on Driver Injury. JAMA 256(11): 1461-1466. 1986.

Warner, C. Y. and Perl, T. R. The Accuracy and Usefulness of SMAC. Proceedings of the 22nd Stapp Car Crash Conference, Ann Arbor, USA. SAE 780902. 1978

Warner, C. Y., Smith, G. C., James, M. B. and Germane, G. J. Friction Applications in Accident Reconstruction. SAE 830612. 1983

Wijk, J., Wismans, J., Maltha, J. and Wittebrood, L. MADYMO Pedestrian Simulations. SAE International Congress and Exposition, Detroit, USA, SAE 830060. March 1983.

Willinger, R., Kang, H. and Diaw, B. Three-Dimensional Human Head Finite-Element Model Validation Against Two Experimental Impacts. Journal of Biomedical Engineering, Vol. 27, pp 403-410. 1999.

Willinger, R. and Baumgartner, D. Numerical and Physical Modelling of the Human Head Under Impact – Towards New Injury Criteria. International Journal of Vehicle Design, Vol. 32, No. 1/2, pp 94 – 115. 2003.

Wood, D. P., Impact and Movement of Pedestrians in Frontal Collisions with Vehicles, Proceedings of the Institution of Mechanical Engineers Col 202 No D2, Pages 101-110 ImechE 1988

Wood, D. and Simms, C. Coefficient of Friction in Pedestrian Throw. Impact, Journal of ITAI, Vol 9, No 1, p12-14. January 2000.

Wood, D., Simms, C. and Walsh, D. Vehicle-pedestrian Collisions – Validated Models for Pedestrian Impact and Projection. Proceedings of the Institute of Mechanical Engineers Part D, 219, p183 – 195. 2005.

Yang, J. and Kajzer, J. Computer Simulation of Impact Response of the Human Knee Join in Car-Pedestrian Accidents. SAE 922525, Proceedings of the 36th Stapp Car Crash Conference, Seattle, USA, pp 203-217, 1992

Yang, J. K., Kajzer, J., Cavallero, C. and Bonnoit, J. (1995) Computer Simulation of Shearing and Bending Response of the Knee Joint to a Lateral Impact. Proceedings of the 39th Stapp Car Crash Conference, Coronado, California, USA, pp 251-264, 1995

Yang, J. K. Mathematical Simulation of Knee Responses Associated with Leg Fracture in Car-Pedestrian Accidents. International Journal of Crashworthiness, Vol. 2, No 3, 1997

Yang, J. K., Wittek, A. and Kajzer, J. Finite Element Model of the Human Lower Extremity Skeleton in a Lateral Impact. Journal of Biomechanical Engineering. 1997

Yang, J. K. and Lővsund, P. Development and Validation of a Human Body Mathematical Model for Simulation of Car-Pedestrian Impacts. Proceedings of the International IRCOBI Conference on the Biomechanics of Impacts. Hanover, Germany, 1997.

Yang, J. Injury Biomechanics in Car-Pedestrian Collisions: Development, Validation and Application of Human-Body Models. Doctoral Thesis. Department of Injury Prevention, Chalmers University of Technology, Gőteburg, Sweden, September 1997

Yang, J. K., Lovsund, P. J., Cavallero, C., Bonnoit, J. A. Human-Body 3D Mathematical Model for Simulation of Car-Pedestrian Impacts. International Journal of Crash Prevention and Injury Control, Vol 2(2), page 131 – 149, 2000.

Yang, K. Review of Mathematical Human Models for Incorporation into Vehicle Safety Design. International Journal of Vehicle Design, Vol. 26, No. 4. 2001

Yang, J. Pedestrian Head Protection from Car Impacts. International Journal of Vehicle Design, Vol. 32, Nos. 1/2. 2003

Yang J., Yao J., Otte D. Correlation of Different Impact Conditions to the Injury Severity of Pedestrians in Real World Accidents, Proceedings of the 19th International Technical Conference on the Enhanced Safety of Vehicles (ESV) Washington DC, USA. Paper no. 05-0352-0. 6-9 June 2005.

Yang, K., Hu, J., White, N., King, A., Chou, C. and Prasad, P. Development of Numerical Models for Injury Biomechanics Research: A Review of 50 Years of Publications in the Stapp Car Crash Conference. Stapp Car Crash Journal, Vol. 50, pages 429-490, November 2006.

Yoganandan, N., Pintar, F. A., Zhang, J., Gennarelli, T. A. and Beuse, N. Biomechanical Aspects of Blunt and Penetrating Head Injuries. Symposium on Biomechanics of Impact: from Fundamental Insights to Applications, University College, Dublin, Ireland. July, 2005

Yoshida, S., Matsuhashi, T. and Matsuoka, Y. Simulation of Car Pedestrian Accident for Evaluate Car Structure. Proc. of the 16th International ESV Conference, Windsor, Canada, Paper no 98-S10-W-18, pp 2344-2348. 1998.

Zajac S. S. and Ivan J. N. Factors Influencing Injury Severity of Motor Vehicle-Crossing Pedestrian Crashes in Rural Connecticut. Accident Analysis & Prevention Vol. 35 pp 369-379. 2003.

Zhang, L., Yang, K., Dwarampudi, R., Omori, K., Li, T. Chang, K., Hardy, W., Khalil, T. and King, A. Recent Advance in Brain Injury Research: A New Human Head Model Development and Validation. Stapp Car Crash Journal, Vol. 45, pp 369-394. November, 2001.

Zhang, L., Yang, K., King, A. and Viano, D. A New Biomechanical Predictor for Mild Traumatic Brain Injury – A Preliminary Finding. Bioengineering Conference, Key Biscayne, Florida, USA. June, 2003.

Zhao, J. and Wu, J. Analysis of Pedestrian Behavior with Mixed Traffic Flow at Intersection. Intelligent Transportation Systems, Proceedings IEEE. Page(s): 323 - 327 vol.1. 12-15 Oct. 2003.

Appendix I: Evaluation of the Effectiveness of Computer Simulation as a Tool to Assess Apparatus used to Reduce Pedestrian Thoracic Injury

A(I).1 Introduction

In this Chapter pedestrian injuries and current methods of protection for road-users in general is discussed. A closer look is taken at methods of pedestrian injury reduction and the current state of the IHRA (International Harmonised Research Activities) Pedestrian Safety Working Group and EEVC (European Enhanced Vehicle-Safety Committee) pedestrian injury reduction programmes.

The occurrence of pedestrian injuries and, in particular, the occurrence of chest and thoracic injuries is examined. The influence of population and vehicle population demographics is considered. The mechanisms, measurement of and tolerance to thoracic injury is studied. Possible future methods of thoracic measurement are discussed.

The computer simulation of the thorax is analysed with reference to both military and automotive applications. Some preliminary simulation results are offered regarding the influence of the stiffness of a thoracic protection device when employed during a vehicle-pedestrian interaction. The effect of a polycarbonate disc as a part of this device is also briefly examined.

The Chapter is concluded with thoughts on the development of pedestrian thoracic protection apparatus.

A(I).2 Pedestrian Injury Reduction and Prevention

A(I).2.1 Road-User Injury Distribution and Existing Methods of Protection from Motor Vehicle Injury

A moderate volume of research has been conducted into the distribution of pedestrian injuries following a motor vehicle collision. A survey of the available research produced the ranking shown in Figure A(I).1.

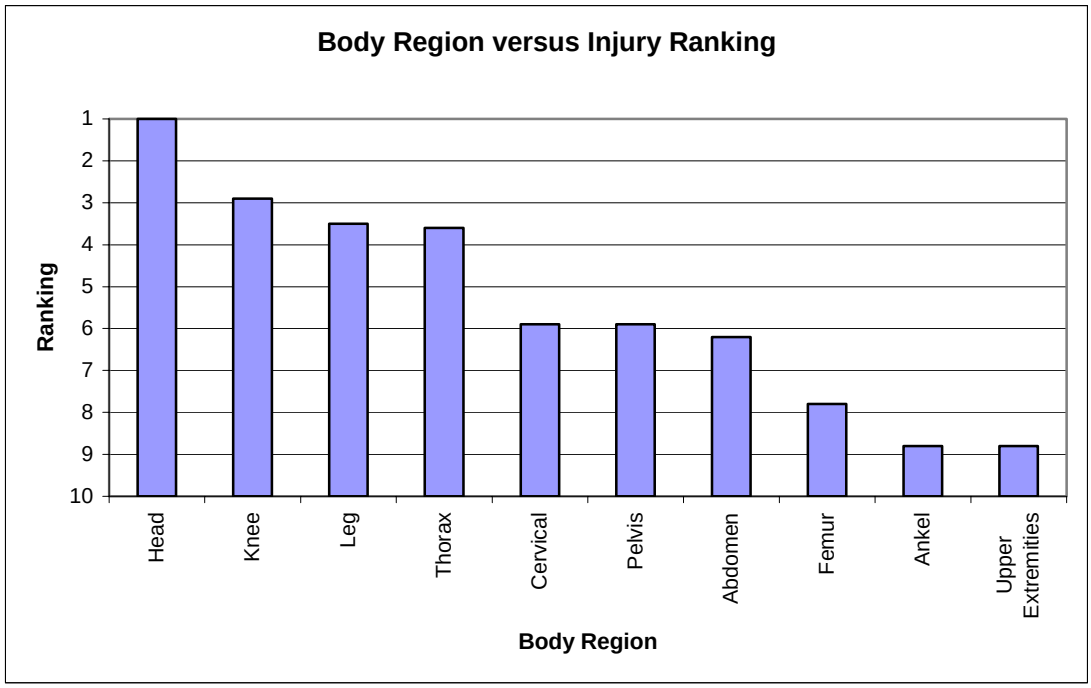

Figure A(I).1 Body Region Versus Injury Ranking (Source: Crandall et al, 2005)

Although thoracic injuries are ranked 4th, they are the second-most likely cause of pedestrian fatality following a vehicle-pedestrian collision (Harruff, 1997). Indeed, as has already been noted, the incidence of serious chest injury is higher for vehicle-pedestrian collision involving an LTV/SUV than those involving passenger cars. With the increasing popularity of LTV/SUVs one can reasonably expect an increase in the number of vehicle-pedestrian collisions that result in serious chest injury and fatality.

Langley et al (1992) compared the number of patients admitted to hospital as a result of a road accident, on a percentage basis (based on length of stay) versus the patient cost across five categories of road user; occupants (of passenger cars), motorcyclists, pedestrians, cyclists and 'other'. See Figure A(I).2 for the comparison. Despite pedestrians accounting for only 10% of road user patients the high average injury severity results in pedestrians absorbing 18% of the cost required for road user medical care.

In a subsequent paper Langley and Marshall (1993) examined this disproportionate severity distribution further, as can be seen in Figure A(I).3. It would appear that pedestrians have a better chance of an AIS 4 or 5 injury than any other type of road user.

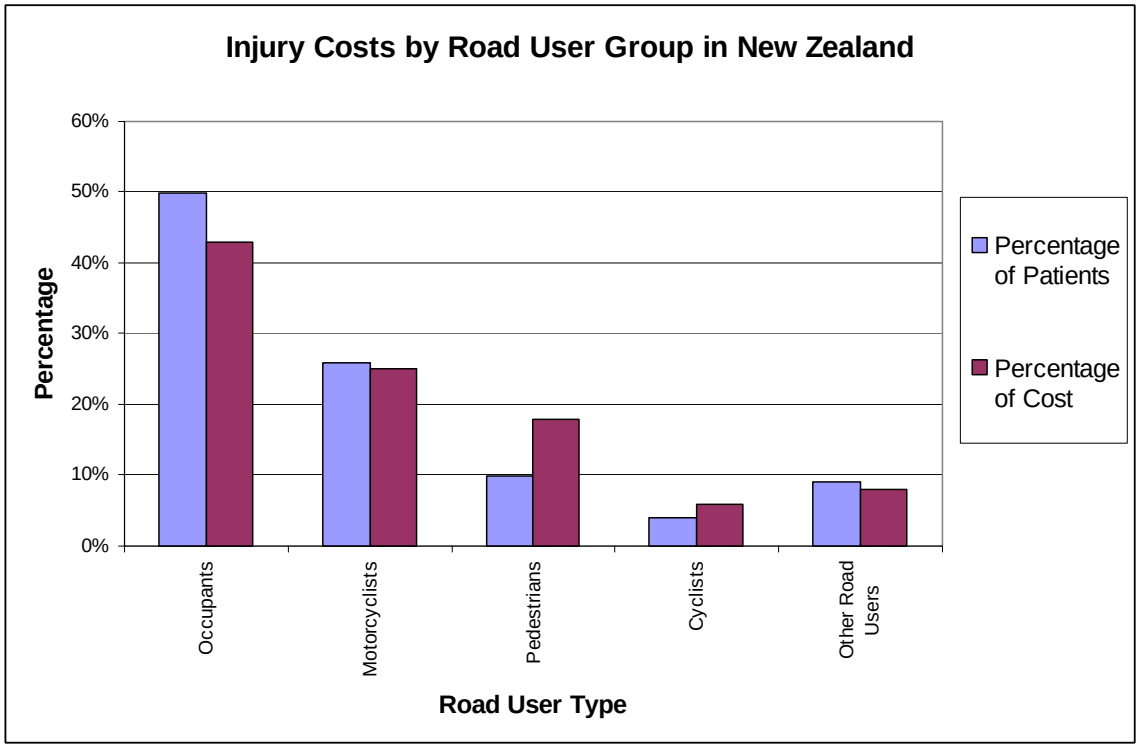

Figure A(I).2 Injury Costs by Road User Group in New Zealand (Source: Langley et al, 1992)

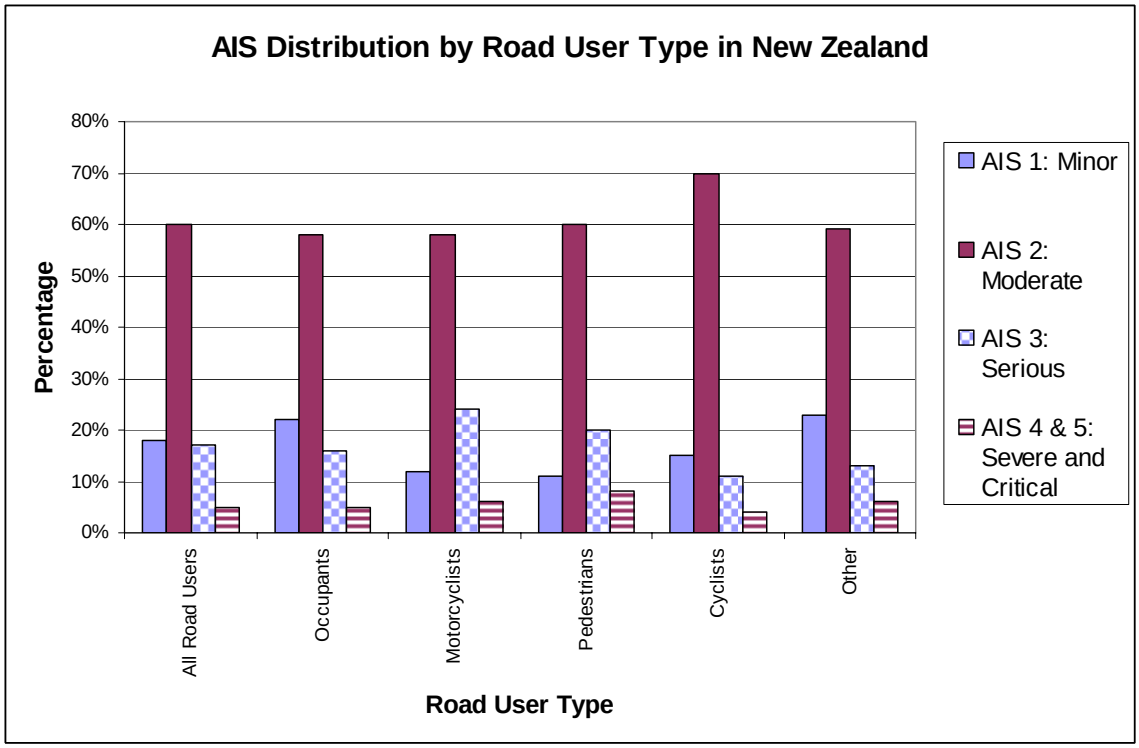

Figure A(I).3 AIS Distribution by Road User Type in New Zealand (Source: Langley and Marshall, 1993)

Langley had the following to say on road user injury distribution:

> *"The higher severity levels among pedestrians and motorcyclists are probably attributable to that they were, with the exception of helmets,*

largely unprotected from the high mechanical forces involved in the crashes… In contrast to this situation, the relatively low severity levels among occupants is probably attributable in part to the protection offered by the car body and restraint use."

Törő et al (2005), however, noted a different injury distribution in Europe with head injuries predominating in the pedestrian/cyclist group. This may well have resulted from a lower incidence of cyclist helmet use in Europe in comparison to New Zealand, coupled with a higher incidence of cyclist-vehicle collisions in Europe in contrast to the large number of single-'vehicle' cyclist collisions in New Zealand resulting in generally lower cyclist injury severity (Langley, 1993). Therefore the road environment, interaction with other road users and the use of protective equipment can be seen to influence road user injury patterns.

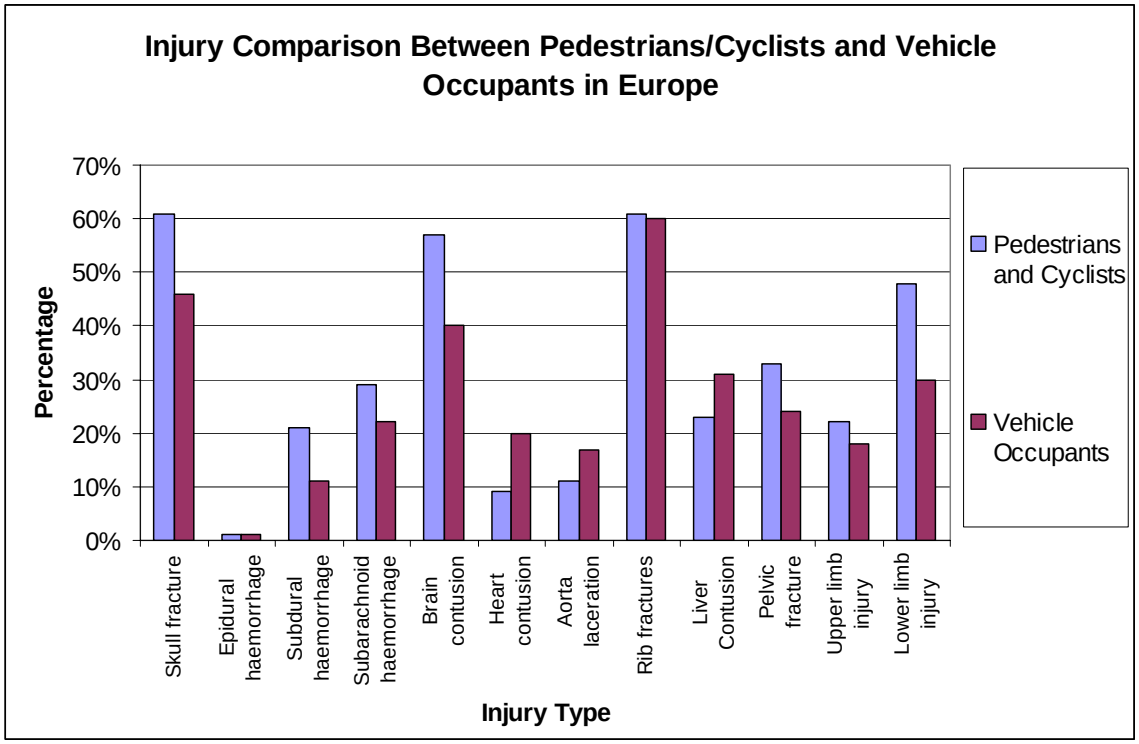

Figure A(I).4 Injury Comparison between Pedestrians/Cyclists and Vehicle Occupants (Source: Toro et al, 2005)

Other, similarly geographic, differences can be seen in the IHRA (International Harmonized Research Activities) Pedestrian Safety Working Group Reports of 2003 and 2005 (Mizuno, 2003, 2005) whose reported pedestrian injury distribution can be seen in Figure A(I).5. Pedestrian injuries in Japan are more prevalent in the lower limbs and less prevalent in the chest, abdomen and pelvis than for other countries. One possible explanation for this difference are the average adult height differences

that exist between the different countries. As can be seen in Figure A(I).6, Japanese males tend to be between 9-13 cm shorter than their American, German and Australian counterparts, whilst Japanese females tend to be about 9 cm shorter than their overseas counterparts. The large number of researchers and research institutions that have conducted or are conducting work on pedestrian safety research in Japan includes:

- Yamazaki K., 2005; Konosu A., 2002, 2000; Ishikawa H., 2000; McElhaney et al, 1976; JARI, Japan.
- Okamoto Y., Sugimoto T., Enomoto K., 2003; Nagatomi, K., Hanayama K., Ishizaki T., Sasaki S., Matsuda K., 2005; Honda R&D Co. Ltd, Japan.
- Omori K., Nakahira Y., Miki K., 2002; Iwamoto M., Omori K., Kimpara H., Nakahira Y., Tamura A., Watanabe I., Miki K., 2003; Toyota Central R&D Labs., Inc., Japan.
- Oshita F., 2002, 2003, Japan Research Institute Ltd, Japan.
- Kikuchi J., 2003, PSG Co. Ltd, Japan.
- Hasegawa J., 2003, Toyota Motor Corporation, Japan.
- Kajzer, J., 2000, Nagoya University, Japan.
- Sugimoto T., 2005, Japan Automobile Manufacturers Association Inc., Japan.
- Takubo N., 2000, National Research Institute of Police Science, Japan.
- Mizuno K., 2000, Traffic Safety and Nuisance Research Institute, Japan.
- Tanno K., Ohashi N., Misawa S., 2000, Tsukuba Medical Examiner's Office, Japan.
- Kohno M., 2000, Tsukuba Medical Center Hospital, Japan.
- Ono K., 2000, Institute for Traffic Accident Research and Data Analysis, Japan.
- Aita K., Oikawa H., Oo M. T., 2000, Department of Legal Medicine, Institute of Community Medicine, University of Tsukuba, Japan.
- Honda K., 2000, Medical University Graduate School Japan.
- Mizuno 2003, 2005, Japan Automobile Standards Internationalization Center, Japan.
- Mimasaka, Yajima, Hashiyada, Nata, Oba, Funayama M., 2003; Tohoku School of Medicine and Furakawa Hospital, Japan.

This is by no means a complete list. With the large amount of research conducted in Japan it is unsurprisingly that so much research has been devoted to lower limb injuries. Indeed, in Mizuno's 2003 IHRA report he states that there is a need for the "*clarification of injury mechanisms to areas other than the head and legs, also R & D on impactors to confirm such injury mechanisms"* and whilst the same statement is repeated in his 2005 IHRA report there is no evidence that any progress has been made outside the areas of research in head and lower limb injuries.

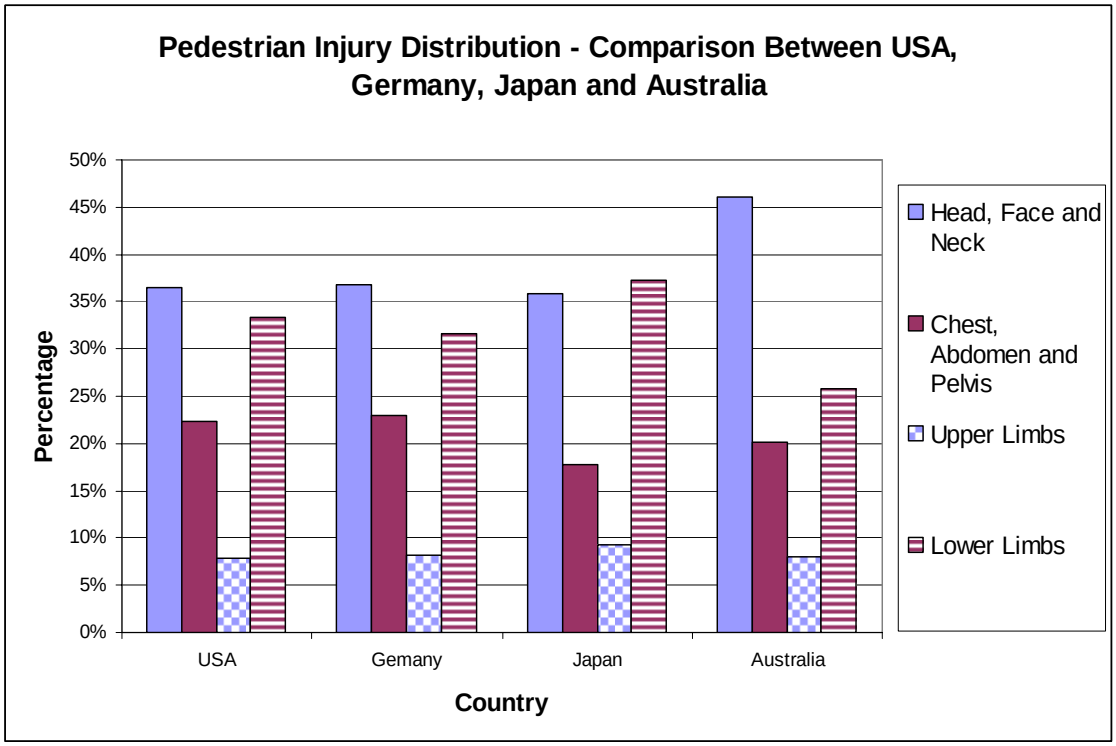

Figure A(I).5 Pedestrian Injury Distribution - Comparison Between USA, Germany, Japan and Australia (Source: Mizuno, 2003)

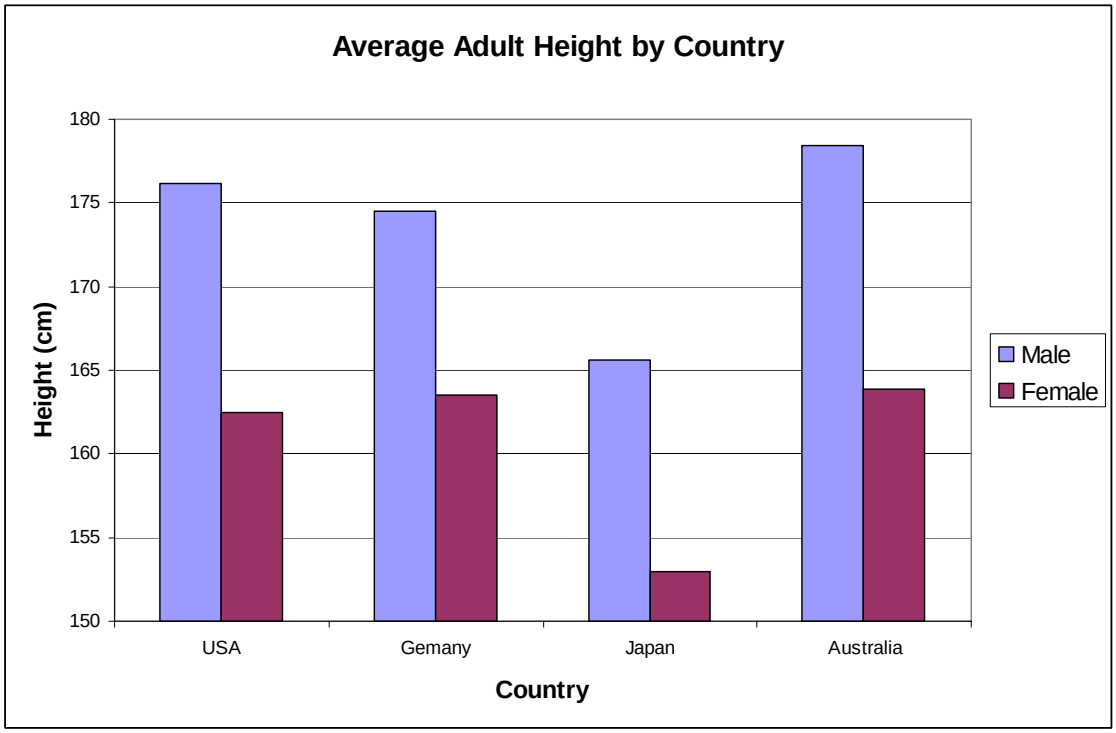

Figure A(I).6 Average Adult Height by Country (Source: http://en.wikipedia.org/wiki/Human_height - unverified)

The difference between the injury distribution in vehicle occupants and pedestrians is less surprising than the geographic differences that exist in pedestrian injury distribution. Occupant safety has been a high priority for automotive manufacturers

since the 1960's, presumably as it is vehicle occupants that buy vehicles. Indeed, vehicle occupants are very well protected by a veritable plethora of safety devices including restraints (seatbelts), strong safety cells (with padded interiors) and airbags (in an ever increasing number of locations). Cyclists and motorcyclists wear helmets to protect their heads and if the Centre for Automotive Safety Research (CASR) in Adelaide recommendations are followed then vehicle occupants will get helmets too (Anderson, 2000). Pedestrians are almost totally unprotected and this has an obvious effect on the type of injuries they receive in a vehicle-pedestrian collision. The next section will explore what steps are being taken to reduce the incidence of pedestrian injury.

A(I).2.2 Pedestrian Protection from Motor Vehicle Injury

The EEVC (European Enhance Vehicle-Safety Committee) Working Group 17 Report: Improved Test Methods to Evaluate Pedestrian Protection Afforded by Passenger Cars (1998, update 2002) noted a high incidence of thoracic injury in children and adult thoracic injuries from the bonnet. 20% of adult injuries from the bonnet were thoracic. The Working Group 17 report noted that Working Group 10 concluded that bonnet leading edge causes thoracic injuries but that Working Group 10 considered existing upper leg-form impactors sufficient for the measurement of thoracic injury potential. Later in the Working Group 17 report, when discussing the injury patterns caused by tall, off-road vehicles (SUVs), the merits of a chest impactor are discussed, particularly in regard to child impacts. However, as per the Working Group 10 Report, Working Group 17 consider the existing leg-form impactor adequate for the task:

> *"However, WG17 believes that design changes to meet the upper legform test would also result in an improvement from current practice and would reduce injuries, as the upper legform requirements are considered to be roughly similar to those for the protection of the abdomen and chest."*

The similarities between the upper leg, abdomen and chest do not strike the author as being particularly noticeable, other than all being parts of the human body. Following

this rationale, surely an upper legform impactor would suffice for all parts of the human body, including the head.

At least the IHRA, as mentioned in the previous section, acknowledges the need for the appropriate evaluation of injury mechanisms of body areas other than the head and legs even if no progress has been made in this area.

Various vehicle safety improvements such as pop-up bonnets and windscreen airbags (as noted in Chapter 4) were designed for pedestrian head injury reduction but also, incidentally, provide thoracic injury benefits. The EEVC Working Group 19 Report (2006) includes the deployable bonnet as one of four vehicle safety features worthy of further analysis and implantation. However, a lack of cohesion in vehicle design in regard to pedestrian injury minimisation may well result in shortcomings and unnecessary compromises. Lawrence (2005) notes that a lack of integration with pedestrian sub-system tests (i.e. legform, upper legform and head impactors) can create problems: *"… a more violent bumper impact might reduce the severity of the bonnet leading edge impact"* and thus presumably not acting in the best interests of minimisation of the most severe sources of injury potential.

A(I).3 Pedestrian Thoracic Injury

A(I).3.1 Occurrence and Cost of Pedestrian Thoracic Injury

Using the Harm Analysis method developed by Monash University Accident Research Centre (1992), a road trauma measurement combining frequency and cost, Longhitano (2005) identified and ranked the various pedestrian torso injuries as per Figure A.7. The lungs, the largest internal organ, rank at the top of the Harm Analysis followed by the aorta, the largest artery in the body. Any injury to either organ can be life-threatening and coupled with the large organ size (and correspondingly high incidence of injury given the improved chances of an impact affecting one or both of them relating to their considerable physical distribution or, in other words, the bigger something is the easier it is to hit) their high ranking in the Harm Analysis is unsurprising.

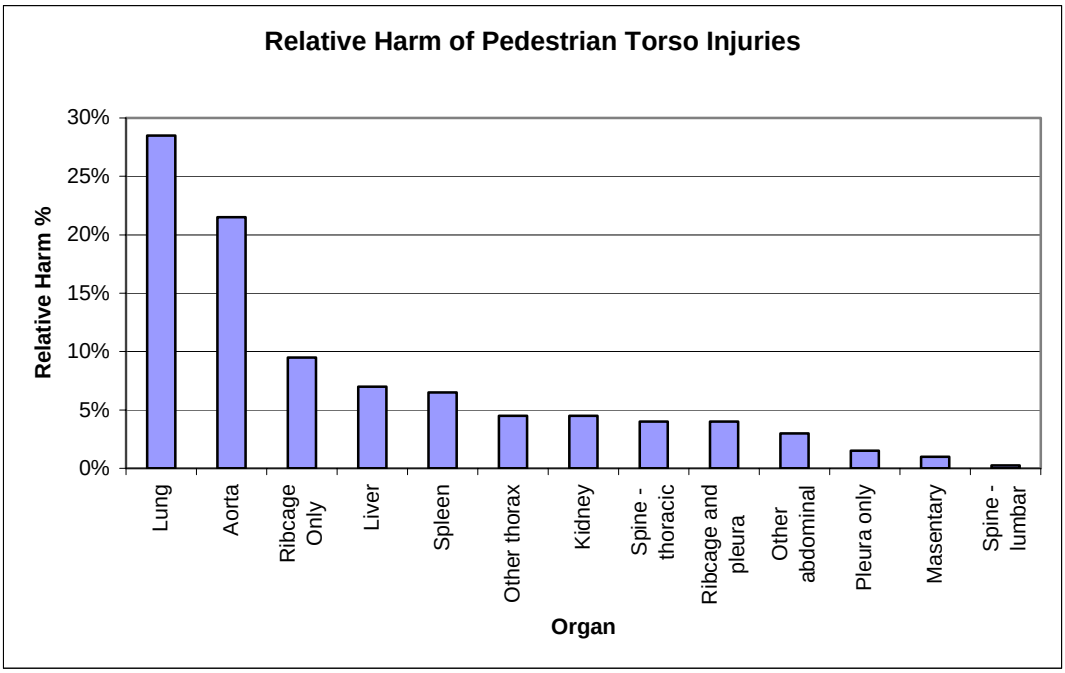

Figure A(I).7 Relative Harm of Pedestrian Torso Injuries (Source: Longhitano, 2005)

So how do these injuries arise? As noted by Yang (2002) pedestrian thoracic trauma usually results from a blunt impact with either the bonnet top or leading bonnet edge of the impacting vehicle. Adults and older children are more likely to receive thorax injuries from the bonnet top whereas children are more likely to receive thorax injuries from the leading edge. The resulting injuries are often quite similar to those received by vehicle occupants in a side-impact collision. Indeed, Törő et al (2005) noted that it is vehicle occupants that are more likely to receive thoracic injuries than pedestrians. Generally speaking, however, the severity of occupant thoracic injuries is less than that of pedestrians (Langley, 1992, 1993).

Furthermore, this disparity between the thoracic injury severity of occupants and pedestrians will become more pronounced as SUVs/LTVs gain in popularity, as SUV/LTV occupants are less likely to receive severe thoracic trauma in a side-impact in contrast to the increased thoracic trauma of a pedestrian hit by an SUV/LTV. SUV/LTV sales increased from 20% of car sales in the US in 1980 to being almost 50% in 1999 (Lefler, 2002) with similar trends observable in much of the developed world. As noted by Ballesteros et al (2004) pedestrians hit by an SUV/LTV had a higher percentage of traumatic brain, thoracic, abdominal, and spinal injuries than pedestrians hit by a passenger car. For vehicle impact speeds below 48 km/h a pedestrian hit by an SUV was twice as likely to receive traumatic thoracic injury as a

pedestrian hit by a passenger car, based on American Police, trauma registry and autopsy data. Simms (2006) produced the same results using MADYMO simulation and the 3 millisecond criterion.

Garrett (1981) provided three case examples he classified as indicative of the typical injury pattern and sequence for vehicle-pedestrian collisions involving a small car, large car and a van:

- Small Car, Wrap: Pedestrian struck in centre front of car, First contact with bumper results in tibia and fibula fractures (AIS 4), second contact involves contact of left chest on bonnet resulting in multiple rib fractures (AIS 4), third contact occurs as passenger rotates, resulting in multiple rib fractures on right of chest (AIS 3). Continued pedestrian rotation results in fourth contact: fibula fracture on leading edge of roof (AIS 2). Car braked to a halt and pedestrian slides to ground and sustains a concussion (AIS 2) and contusions (AIS 1).
- Large Car, Fender Vault: Initial bumper contact resulted in femur fracture (AIS 4). Second contact with top edge of front guard produced head, shoulder and chest contusions (AIS 1). Pedestrian rolls over guard onto ground, receiving skull fracture (AIS 3) and multiple abrasions and lacerations (AIS 1, AIS 2).
- Van, Forward Projection: Initial contact between hood edge and chest, lacerated heart and aorta (AIS 5), bilateral hemothorax (bleeding between lung and chest wall, both sides) (AIS 4), lacerations of the lung, kidney, liver and spleen (AIS 4) and multiple rib fractures (AIS 3). Subsequent ground contact resulted in abrasions and lacerations (AIS 1).

For a generic description of the wrap, fender vault and forward projection trajectories please refer to Chapter 2, Section 2.4. Note that in two of the cases the most serious injuries were thoracic with the most serious occurring from the van impact. The high leading edges of vans and SUVs (usually above the pedestrian's centre of mass) often result in a single vehicle-pedestrian contact of short duration but very high energy. Such impacts tend to be exceedingly injurious to the pedestrian. Garrett also noted the AIS distribution of fatally injured pedestrians. As can be seen in Figure A(I).8 chest and abdominal injuries are the most common form of AIS 2, 3, 4 and 5 injuries in fatally injured pedestrians.

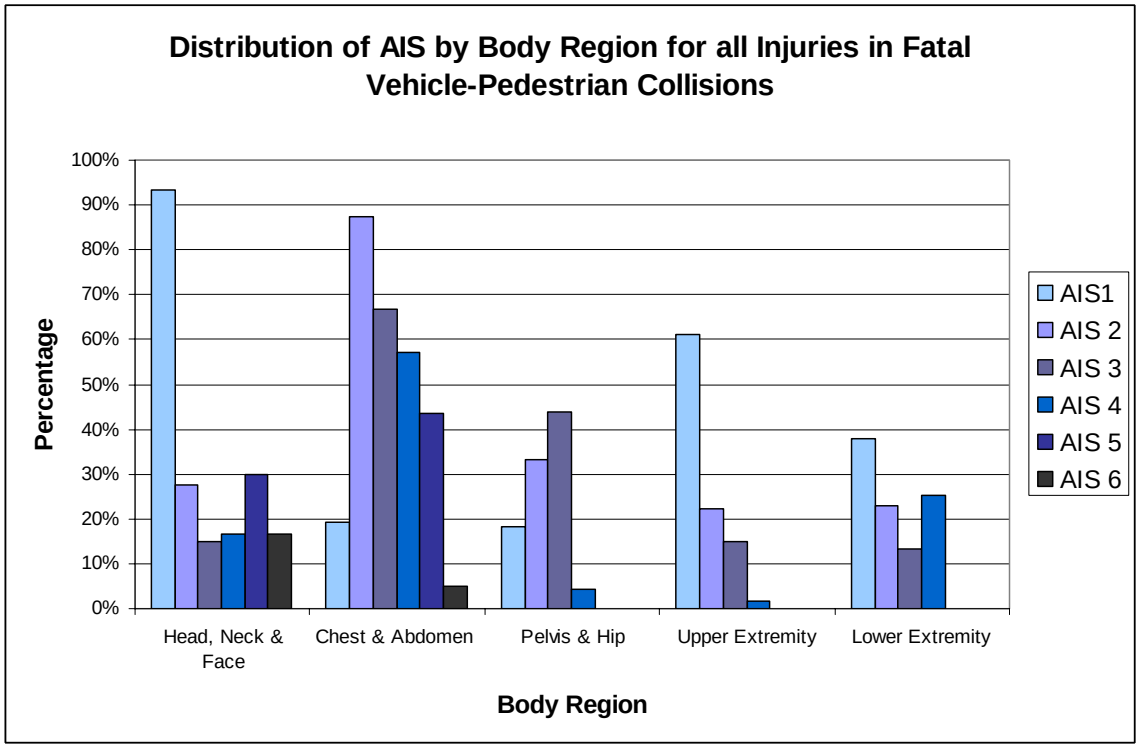

Figure A(I).8 Distribution of AIS by Body Region for all Injuries in Fatal Vehicle-Pedestrian Collisions (Source: Garrett, 1981)

Balci et al (2004) noted the incidence of thoracic trauma in children often occurred as a result of a vehicle-pedestrian collision. 29.9% of children admitted to hospital for blunt chest trauma had been hit as a pedestrian, compared to 15.3% who had been a vehicle occupant and 5.8% who were cycling at the time of injury.

This section highlighted the high incidence of thoracic trauma to pedestrians as a result of a vehicle-pedestrian collision and the relation to treatment cost via a Harm Analysis was shown. The influence of vehicle shape and pedestrian size relative to thoracic injuries was examined. Three typical vehicle-pedestrian collisions were discussed involving three different vehicle shapes and the relationship between vehicle shape, pedestrian trajectory and incidence of thoracic injury was indicated. In the next section the physical mechanisms of thoracic injury are considered.

A(I).3.2 Thoracic Structure and Mechanisms of Thoracic Injury

Classification of the thoracic skeletal structure typically includes the following (Lobuono, 2001):

- The twelve dorsal vertebrae (there are 33 vertebrae in the spine) which form the thoracic curve in the spine.

- The 24 ribs that construct the ribcage, with the first rib pair attached to the first dorsal vertebrae and the twelfth rib pair attached to the twelfth dorsal vertebrae. The first seven rib pairs attach to the sternum at the front of the thorax, rib pairs eight, nine and ten attach to the cartilage of the first seven rib pairs whilst the eleventh and twelfth rib pairs are free at the anterior of the thorax.
- The sternum in the centre of the chest.

Organs located in the thorax include the following:

- The two lungs, located in the pleura cavities.
- The heart located in the mediastinum cavity.

Other thoracic structures include:

- The trachea and bronchi respiratory airways.
- The aorta, the largest artery in the body, which distributes oxygenated blood to the body from the heart's left ventricle.
- The superior and inferior vena cavae, the two veins which return oxygen depleted blood to the right atrium of the heart.
- The pulmonary arteries and veins, which transport blood to and from the lungs, respectively, from and to the right ventricle and left atrium of the heart, respectively. There are two pulmonary arteries and four pulmonary veins.

Blunt trauma as a result of lateral impact to the pedestrian's thorax commonly results from the pedestrian contacting the vehicle's bonnet leading edge or bonnet top during a vehicle-pedestrian collision (Yang, 2002). In a frontal collision with a typical vehicle the first interaction with the pedestrian occurs between the bumper and pedestrian's lower extremities. As this is below the pedestrian's centre of mass rotation is imparted to the pedestrian causing the pedestrian's upper body to attain a velocity vector towards the vehicle. This velocity vector commonly causes a combination of the pedestrian's head, thorax and/or upper extremities to impact the vehicle's bonnet leading edge, bonnet top and or windscreen and occasionally the vehicle's roof in a high speed impact. Thoracic deceleration as a result of this impact results in three possible injury mechanisms: compression of the thorax, viscous loading within the thoracic cavity and inertial movement of the thoracic organs (Yang, 2002).

Thoracic compression can result in the following injuries:

- Fracture of the thoracic skeletal structure. If several ribs are fractured a 'fail chest' can result where fractured rib segments are sucked inwards, preventing the lung from expanding (Frey, 1970). Rib fractures can also result in lacerations to thoracic organs
- Hemothorax and pneumothorax (the collection of blood and air, respectively, in the pleural cavities) which can cause lung collapse
- Lung collapse from chest deflection
- Cardiac, pericardial (the pericardium envelops the heart) and/or aortic compression, contusion, lacerations and/or transaction (Mimasaka et al, 2003)

Viscous loading and inertial loading within the thoracic cavity can result in:

- Lung contusion and/or collapse
- Vessel disruption, including aortic shearing (one of the most common causes of death in motor-vehicle accident victims (Frey, 1970))

The term 'Viscous Loading' is used to describe the loading applied to viscous organs (which are most commonly hollow, fluid filled organs in the thoracic and abdominal cavities and include the bladder, bowel, colon and lungs).

The correlation between examples of skeletal and soft-tissue thoracic injury and AIS score can be seen in Tables A(I).1 and A(I).2.

Examples of Skeletal Thoracic Injury and Corresponding AIS Score					
AIS 1	AIS 2	AIS 3	AIS 4	AIS 5	AIS 6
Minor fracture	2-3 Rib Fractures; sternal fracture	3 rib fractures; fracture in conjunction with hemo/pneumothorax	Flail (unstable chest wall); more than 3 rib fractures on one side	Flail (unstable chest wall) for patients < 15 yrs old	None, unless in conjunction in soft-tissue injuries

Table A(I).1 Examples of Skeletal Thoracic Injury and Corresponding AIS Score (Source: AAAM, 1990)

Examples of Soft-tissue Thoracic Injury and Corresponding AIS Score					
AIS 1	AIS 2	AIS 3	AIS 4	AIS 5	AIS 6
Contusion; minor skin laceration	Breast avulsion (female); major skin laceration	Hemo/pneumothorax; contusion to one lung; ruptured diaphragm	Contusions to both lungs; ruptured diaphragm with herniation	Perforated atrium or ventricle; major tracheo-bronchial injury	Multiple lacerations of the heart

Table A(I).2 Examples of Soft-tissue Thoracic Injury and Corresponding AIS Score (Source: AAAM, 1990)

The incidence of thoracic injury in pedestrians is often associated with abdominal injuries (Cooper, 2004). Diaphragm injuries can result in abdominal contents entering the chest cavity (Frey, 1970). The most commonly injured abdominal organs from blunt trauma include the spleen, liver, kidneys, pancreas and intestines.

This section covered a brief overview of the human thorax and associated injury mechanisms related to blunt thoracic trauma. The next section will discuss measurement of thoracic injury and the tolerance levels relating to the different forms of trauma.

A(I).3.3 Measurement and Human Tolerance of Thoracic Injury

The measurement of thoracic deformation and trauma has typically been achieved using cadaver and volunteer thoracic impact tests (Lobdell et al, 1973; Kroell et al 1971, 1974; Patrick, 1967).

Lobdell et al (1973) compared cadaver and volunteer thoracic impact test results with dummy tests and mathematical models. The dummy chests, based on automotive occupant crash test dummies, were found to be unbiofidelic. Lobdell, disappointed with the results obtained using the crash-test dummies, created a mathematical model for both dummy and cadaver thoracic impact response. The mathematical model consisted of a mechanical analog using masses, springs and dampers and was solved using a digital computer. Masses representing impactor, chest mass and remaining body mass. Springs and dampers model elasticity and viscous response of rib cage

and thoracic viscera, air removal from lungs and blood removal from vessels during impact.

The parameters used in the mathematical model were based on averaged cadaver results. The effective mass of the thorax was found to be 27 kg with an initial deflection rate of 2.7 $kgmm^{-1}$ for the first 38 mm of deflection, stiffening to 8 $kgmm^{-1}$ thereafter. Impactor speeds ranged between 5 - 7 ms^{-1} and impact duration was between 50 - 60 milliseconds. Lobdell did not draw any quantitative conclusions regarding rate dependence.

Tests by the author using a volunteer have indicated 0.69 $kgmm^{-1}$ for initial 15 mm deflection and 1.76 $kgmm^{-1}$ thereafter during quasi-static loading therefore indicating that impact rate has a considerable influence. Also of considerable importance are the physical differences between the physical properties of living volunteers and cadavers. As noted by Kroell:

> *"Age, anatomical characteristics, pre-mortem physiological and post-mortem physical conditions frequently are not representative of the populations of greatest interest. Respiration, the cardiac cycle, and muscular action are absent."*

Other thoracic stiffness values in anterior-posterior quasi-static loading obtained by researchers have ranged from 0.89 - 1.78 $kgmm^{-1}$ (Fayon et al, 1975), which is very similar to the results obtained by the author, to 4.1 - 9.7 $kgmm^{-1}$ (L'Abbe et al, 1982) which is higher than the dynamic results from Lobdell. Fayon and L'Abbe's results were obtained using volunteers. Verriest et al (1981), when measuring the stiffness of living and dead pig thoraxes, discovered the thoracic stiffness of the living pigs was only half that of the dead animals. Presumably this casts additional doubt on the findings obtained using human cadavers.

Kroell et al's 1974 paper included the results of further cadaver tests at a greater range of impact speeds to identify rate dependence parameters and a good fit was obtained with the results predicted by Lobdell's mathematical model. The results from Kroell's, Patrick's and Lobdell's tests formed the basis for the Thoracic Trauma Index

(TTI) injury parameter. They, and other researchers, also determined the importance of load distribution in relation to resultant thoracic injury (Horsch et al, 1991), furthering the development of airbags for occupant protection.

The following injury parameters are commonly used for measuring thoracic trauma:

- TTI is based on the results on 84 cadavers tests indicating the occurrence of injuries to the thoracic skeletal structure were related to the peak lateral acceleration of the impacted rib cage. TTI was originally developed as a measurement for occupant injury in side-impact vehicle testing. TTI can be calculated using:

$$TTI = 1.4 \times Age + \frac{0.5 \times \left(Rib_g + T12_g\right) \times m}{m_{ref}}$$

  Where Age = age of test subject in years

  Rib_g = maximum absolute acceleration of 4th and 8th rib on struck side, in lateral direction

  $T12_g$ = maximum absolute acceleration of the 12th vertebrae, in lateral direction

  m = mass of test subject, in kg

  m_{ref} = mass of 50th percentile adult male, which is 75 kg

  For a 50th percentile crash test dummy (which is ageless) the following formula is used:

$$TTI_d = 0.5 \times \left(Rib_g + T12_g\right)$$

  Occupant crash-test requirements indicate a maximum TTI of 85 G for four-door cars and 90 G for two-door cars.

- The 3 millisecond criterion states that the limit for severe chest injury is a peak acceleration of 60 G or greater, sustained for 3 milliseconds or longer over either a cumulative or contiguous time period. The 3 millisecond criterion was based on work by Stapp (1970) and Gadd (1968).
- Viscous Criterion (VC) accounts for injury to the thoracic organs, unlike 3 millisecond and TTI which were based on skeletal tolerances. VC accounts for the pressure response of the thoracic cavity during rate-sensitive deformation of the chest. Examples of injury type best evaluated by VC include bullet-

strikes on body-armour and baseball impacts on the chest. VC is calculated using:

$$VC = SF \times \max\left(\frac{dD(t)}{dt} \times \frac{D(t)}{SZ}\right)$$

Where *SF* and *SZ* are prescribed dummy size and scale factors (see SAE standard J1727) and *D(t)* is deflection in metres. Cadaver testing has indicated that a VC of 1.3 ms^{-1} results in a 50% chance of an AIS injury of 4 or greater. A VC of 1 ms^{-1} is often used as the tolerance limit for blunt frontal thoracic impact (Cavanaugh et al, 1990). As Grimal et al (2004) notes in reference to high-energy, short duration impacts to the human thorax:

> *"In automobile accidents, the paramount mechanisms of injury are compression of the thorax and viscous dissipation of energy by soft tissues."*

Janda et al (1992) conducted a series of experiments on the effects of baseball impacts using live animals, a child crash test dummy and a 5^{th} percentile Hybrid III female dummy. With an impact speed of 42.8 ms^{-1} and an impactor mass of 150 grams an average VC of 2.0 ms^{-1} was obtained with a good chance of fatality. Experimentation with padding decreased peak force measured but impact duration was considerably extended, resulting in higher energy transfer, higher VC scores and increased mortality rates.

- Newman proposed a Generalised Acceleration Model for Brain Injury Threshold (GAMBIT) in 1985. This model incorporated both linear and rotational acceleration to predict head injury potential. A subsequent pair of papers by Newman et al (2000 & 2001) extended this by examining the six degrees of freedom and the rate of change of kinetic energy (i.e. power) in each of these degrees of freedom. This lead to the formation of the Head Injury Power (HIP) method of head injury assessment, which does not at first appear applicable to thoracic injury. However, Neal-Sturgess (2002), recognised the general applicability of the concept of power-based injury measurement and developed Peak Virtual Power (PVP). PVP is based on the premise that injury may be predicted based on the rate of energy transfer to body tissues (originally attributed to Waller, 1985). Soft-biological tissues are commonly modelled as virtually incompressible visco-elastic elements that exhibit elastic behaviour at high strain rates. It would appear that injuries

result during the energy dissipative processes following an impact. The peak specific power during this process is proportional to the maximum rate of entropy production. It can therefore be stated that injuries are contributing chaos. This theory can be applied to any part of the body, including the thorax. PVP for unrestrained vehicle occupants may be expressed as:

$$\frac{1}{m}\left(\frac{\partial \tilde{\mathrm{U}}}{\partial \mathrm{t}}\right) = a^2 \Delta t = V^3 \cong \Delta V^3$$

where U is strain energy, m is mass, t is time, V is velocity and the Δ's representing the duration and velocity change over the crash pulse. PVP is stated to be linearly proportional to AIS, simplifying injury correlation. PVP would appear to be applicable to both soft tissue and skeletal injury prediction. Using NASA data Neal-Sturgess found good correlation between HIC and PVP. MADYMO simulations also revealed similar predictions for HIC and PVP. Research data from other authors regarding bone fracture and thoracic VC injury parameters also showed good agreement with the injury predictions afforded by PVP. Scalars need to be applied for different scenarios (occupant, pedestrian, cyclist etc), gender, age, direction of force and location of impact (on body). Neal-Sturgess concludes by suggesting the potential for PVP as a universal injury criterion.

Other researchers have reported the following thoracic injury tolerances:

- Chest compression resulting in a reduction in chest depth of 35% is the limit for rib cage collapse (Lau and Viano, 1988)
- Chest compression of 35% deflection results in a 50% chance of rib fracture for a 30 year old whereas chest compression of 13% deflection results in a 50% chance of rib fracture for a 70 year old (Kent and Patrie, 2005)
- Chest compression of 50 mm has a 40% chance of injury whilst a compression of 75 mm has a 95% chance of injury (Mertz, 1991)
- A lateral force of 7.4 kN results in no injury (AIS 0) (Tarrierre et al, 1979)
- A lateral force of 10.2 kN is likely to result in a AIS 3 injury (Tarrierre et al, 1979)
- Grimal et al also compare different rate-dependant thoracic injury mechanisms, particularly to the lung, in their 2005 paper, including

comparison between blast-induced injuries, impacts from 'non-lethal' munitions and ballistics impacts on body-armour. A common injury mechanism appeared to be the propagation of a significant local pressure differential in the lung resulting from an impinging shockwave. An injury tolerance of a localised lung-wall acceleration of 10,000 ms^{-2}, resulting in a critical pressure differential of 1500 Pa, is referred to.

- Bir et al (2004) noted the influence of rate dependence in their comparison of automotive impacts to the thorax and ballistic impacts to the thorax. Thoracic injury tolerance for automotive impacts was reported to be 6.5 kN for an impact duration of 40 - 60 milliseconds whilst for ballistic impacts it was 12 kN for impact durations of less than 1 millisecond. Automotive impact speeds were considered to be 20 ms^{-1} or less whilst ballistic speeds were considered to be 20 ms^{-1} or greater.
- King (2004) compared the work of several researchers to create Table A.3, showing the relationship between chest compression and AIS:

Chest Compression and AIS		
Chest Compression (%)	50^{th} Percentile Chest Compression (mm)	AIS
30%	69 mm	2
33%	76 mm	3
40%	92 mm	4

Table A.3 Chest Compression Versus AIS (Source: King, 2004)

The majority of thoracic injury tolerance levels noted above do not appear to offer much compensation for variation between subjects, such as age, size, gender or muscle/bone/fat mass ratios. Sirmali et al (2003) note the flexible nature of children's ribs, the brittle and comparatively weak nature of the ribs of the elderly and comments on the influence these factors have on thoracic injury tolerance for these population groups. TTI's age compensation, if accurate, only accounts for the effects of age in the elderly and not the young.

Kleinberger et al (1998) have recognised some of the deficiencies of existing thoracic trauma measurement and have noted possible improvements in the context of vehicle

occupant impact testing. To allow for different combinations of thoracic compression and acceleration a Combined Thoracic Index was proposed, allowing 85 G's of acceleration for zero compression and 102 mm of compression with zero acceleration. To compensate for the lower tolerance of children reduced tolerance levels were proposed, based on age. To compensate for differences resulting from increasing age various injury risk curves can be applied.

The suggestions by Kleinberger et al would appear to be improvements over the traditional thoracic injury criteria. Their methodology, however, is based upon vehicle occupant injury analysis which is not always entirely applicable to pedestrian injury analysis. The existing thoracic injury criteria and tolerance levels are based on either force, deflection or acceleration and are generally only applicable to a given loading direction – either frontal or lateral. Thoracic injury from oblique impacts and rate-dependant injury mechanism are not well researched or understood. The possibility of an energy-based thoracic injury criteria based on the work by Bir et al (2004) and Grimal et al (2004, 2005) may well be useful as it would account for impact rate, mass and duration. This warrants further investigation.

This section has covered the basics of thoracic injury measurement and tolerance. The next section will examine the application of thoracic injury measurement in computer simulation.

A(I).4 Computer Simulation of Thoracic Injury

The literature appears to offer a relative paucity of research on the mathematical modelling of pedestrian thoracic injury. Kovandova, Svoboda, Solc and Kovanda (2001) used a MANIKIN dummy (an occupant restraint analysis dummy manufactured by USMD/Dekra under licence to TNO, The Netherlands) as a pedestrian surrogate in a frontal vehicle-pedestrian collision with a small car travelling at 27 ms^{-1} and decelerating at 6.5 ms^{-2}. Accelerometers were fitted to the centre of mass of the dummy's head and thorax. The collision was modelled using MADYMO where the mathematical simulation estimated the peak 3 millisecond value to be some 18% less than that obtained experimentally, possibly due to the dummy's thorax being stiffer than that of the mathematical human model.

Svoboda and Cizek (2003) reviewed Kovandova et al's data during a study on mathematical optimisation of the vehicle bonnet structure to minimise pedestrian injury. Although they report on the thoracic injury measurements from the previous study and state that thoracic injury evaluation is one of the focus points of the study, they fail to state any conclusions regarding the reduction of thoracic injury potential achieved.

Based on a literature survey the majority of thoracic injury modelling has been performed in vehicle occupant analysis and for military and law-enforcement applications, most noticeably body-armour.

Lobuono (2001) created a finite element model of the human torso to evaluate the biodynamic response of the thorax due to the forces transferred to the thorax via body-armour following bullet impact. The model was validated using the results from cadaver tests. The simulations were conducted to evaluate the 2 millisecond period following impact. Good correlation between the model and experimental result was achieved for sternum acceleration, velocity and displacement for the first 1ms; however for the 1 – 2 millisecond period good correlation was only achieved for sternum displacement. Similar results were achieved for spinal acceleration, velocity and displacement. Pulmonary artery acceleration was accurately modelled but trachea acceleration was not. Lobuono suspected that model limitations (i.e. the lack of a neck and head) influenced the trachea acceleration results. Another simulation was conducted using a larger calibre bullet (9mm) travelling at about half the speed of the bullet in the first simulation series. Much better agreement was noted between the model and the experimental results. However, according to the author's calculations, the bullet in the first simulation had about 4.5 times the energy of the bullet in the second simulation series (9.7 G @ 966 ms^{-1} vs 8.0 G @ 500 ms^{-1}). Sternum displacement was noted to achieve a maximum of 30 mm, indicated an average force exerting in stopping the smaller calibre, faster bullet of over 150 kN. According to Bir et al's research this force, although extremely transient, is highly likely to cause injury. It is therefore suspected that the smaller calibre bullet caused damage to the subject in the cadaver tests, such as multiple rib fracture, which could not be replicated in Lobuono's model. Rib fracture at 1 millisecond would account for the differences between the simulation and experimental results. Lobuono's explanation

for the differences was based on inadequate instrumentation in the cadaver tests and whilst this may have influenced the results it would also appear that Lobuono's model may have had shortcomings in predicating thoracic dynamics following injury. Additionally, injury potential from shockwave, as per Grimal et al's research, is not modelled.

More advanced thoracic mathematical models can be found in the work by Richens et al (2004), Grimal et al (2004, 2005) and Roberts et al (2005). The research by Richens et al focussed on modelling aortic rupture from blunt trauma using an LS-DYNA finite element model for vehicle occupant research. Positive attributes of the model included being able to modify tissue properties to account for disease, age and existing defects, as well as the ability to scale the model for different thoracic sizes. The researchers encountered difficulties in approximating tissue properties using finite element methods and the need to incorporate fluid dynamics to account for respiration and cardiac cycle as both lung air-volume and cardiac fluid volume were found to have considerable influence on thoracic injury tolerance. Richens et al were confident, however, of being able to improve the model for better biofidelity.

Roberts et al (2005) also used LS-DYNA to create a finite element model of the human thorax but in this instance were interested in modelling ballistic impact. Roberts et al's choice of modelling a 5^{th} percentile male seems unusual, as most of the ballistic validation studies have used subjects closer to 50^{th} percentile. The researcher's also note the lack of dummies designed for thoracic injury measurement subject to a frontal loading. Most side-impact occupant dummies have been designed for lateral impact and are too stiff in the anterior-posterior direction. The researchers therefore designed and built their own Human Surrogate Torso Model (HSTM). Experimental testing of the HSTM was conducted using a 9 mm bullet at speeds of 150 - 360 ms^{-1}. The researchers could not obtain good correlation between the experimental results using the HSTM and the result predicted by mathematical modelling. Robert's et al appeared to focus their blame for the discrepancies on the construction of the HSTM. It does not appear that the researchers have compared the predictions offered by their finite element model to the predictions obtained by other mathematical models or to cadaver tests.

Grimal et al (2004, 2005) used an LS-DYNA finite element model to simulate the shockwave resulting from ballistic impacts on thoracic body armour. Grimal et al only modelled the first 300 microseconds of impact and therefore did not account for any displacement or acceleration response of the thorax. Nonetheless, their model brings useful insight into thoracic shockwave injury mechanisms.

This section has examined some of the limited literature available on the computer simulation of thoracic injury. It would appear that a lack of cohesion and occasionally dubious methodology exists in comparison to the mathematical models developed for human head and leg injury analysis. This presumably stems from the legislative requirements enforced upon vehicle manufactures in regard to occupant and pedestrian injury reduction. As previously noted, only vehicle occupant testing includes thoracic injury measurement. Pedestrian injury measurement does not include thoracic injury.

The next section will discuss the author's thoughts and findings regarding pedestrian thoracic injury resulting from the use of thoracic protection apparatus.

A(I).5 Development of Pedestrian Thoracic Protection Apparatus

The benefits of increasing load distribution and decreasing peak acceleration in injury reduction are well known. For vehicle occupants airbags have been the most important safety development since the seatbelt and the cost benefits are indisputable (Fildes, 2001). Whilst external airbags on vehicles for pedestrian protection have been developed it is uncertain how widespread their adoption will become. Furthermore, even if such airbags do become commonplace there will be the potential for a pedestrian to be hit by an older vehicle sans-pedestrian airbags.

Of interest to the author are the number of examples of law-enforcement members protected by ballistic body armour when involved in vehicle-related accident, both as vehicle occupants and pedestrians. For anecdotal reports on this phenomenon please refer to Appendix IV.

A(I).5.1 Simulation Methodology and Parameters

Body armour originally designed for use by motorcyclists (See Figure A(I).9) was modelled using finite element methods and was placed on a MADYMO multibody pedestrian model. The armour model can be seen in Figure A.10. The pedestrian model used was the 50^{th} percentile male. A face-on pedestrian orientation was chosen to remove any protection to the pedestrian's thorax afforded by the shoulders. The vehicle model was the same as that used for the case studies examining pedestrian impacts involving a typical vehicle. Vehicle speed was set to 6.94 ms^{-1} and vehicle deceleration was 4 ms^{-2}. 1º of brake dive was applied to the vehicle model. Figure A.11 illustrates the pre-impact orientation of the pedestrian and the vehicle.

Figure A(I).9 Body Armour

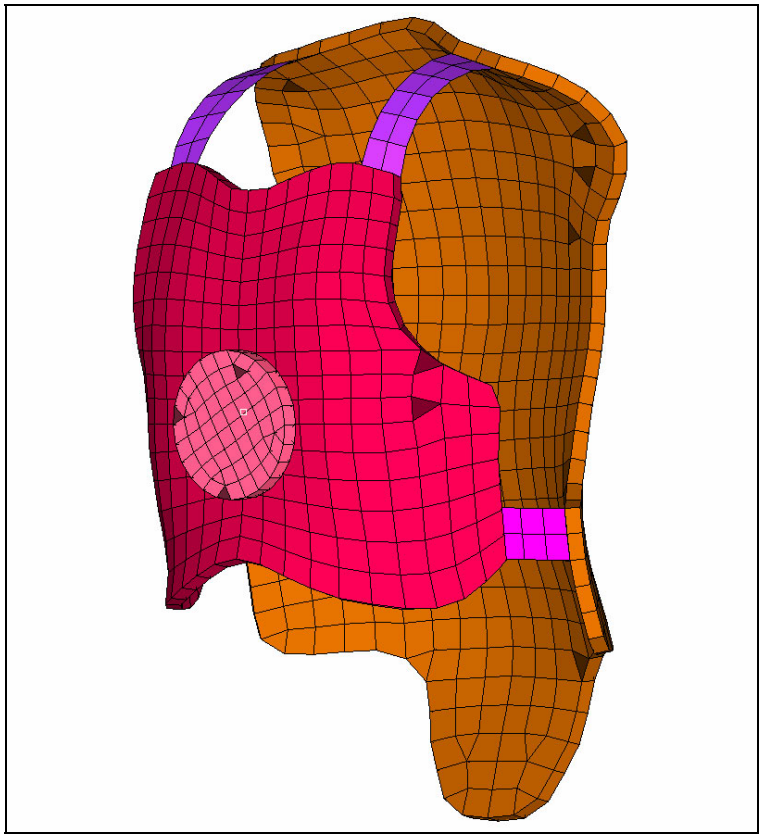

Figure A(I).10 Finite-Element Body Armour Model

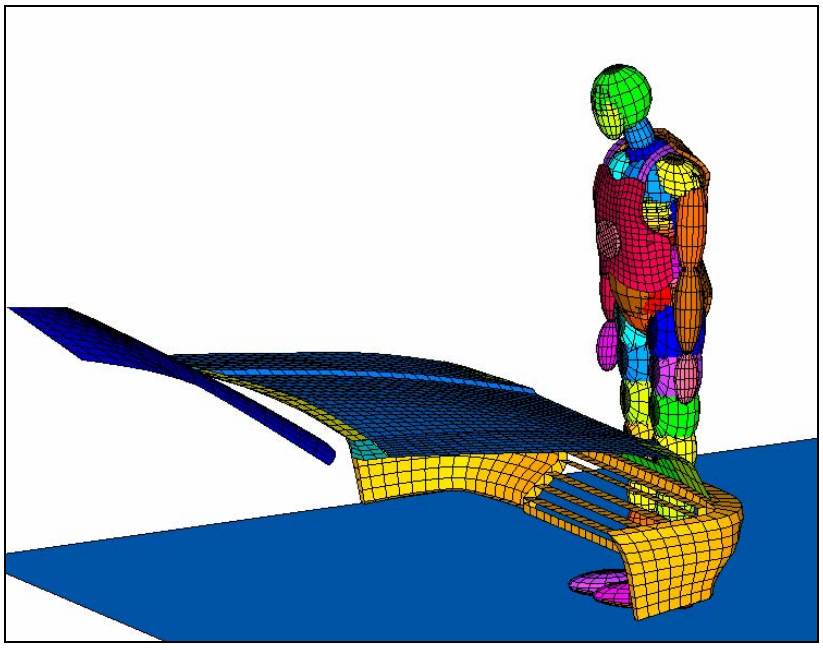

Figure A(I).11 Dummy Wearing Thoracic Protection, Pre-Impact

General simulation parameters can be seen in Table A(I).4.

Parameter	Values	Comment
Coefficient of friction between vehicle and pedestrian	0.45	Within range of values reported in literature
Coefficient of friction between pedestrian and ground	0.55 for pedestrian on ground, 0.7 for shoe contact on ground	Value indicated to be within literature values and those determined by author
Vehicle speed at impact	6.94 ms^{-1}	Range appropriate for chest to bonnet impact
Vehicle acceleration	-4.0 ms^{-2}	Middle of vehicle achievable range
Stiffness of vehicle bumper	200 Nmm^{-1}	As per literature.
Stiffness of vehicle bonnet top	300 Nmm^{-1}	As per literature.

Table A(I).4 Simulation Parameters

Table A(I).5 shows the three levels of armour stiffness modelled. The polycarbonate disc was modelled as having a stiffness of 1250 Nmm^{-1}.

Load (kN) versus Deflection			
Deflection (mm)	Soft	Medium	Firm
5	10	20	40
10	80	200	400
20	200	400	1000

Table A(I).5 Armour Stiffness Values

A(I).5.2 Simulation Results

Figure A(I).12 shows the impact sequence at 170, 190 and 240 milliseconds. Head injury was not evaluated.

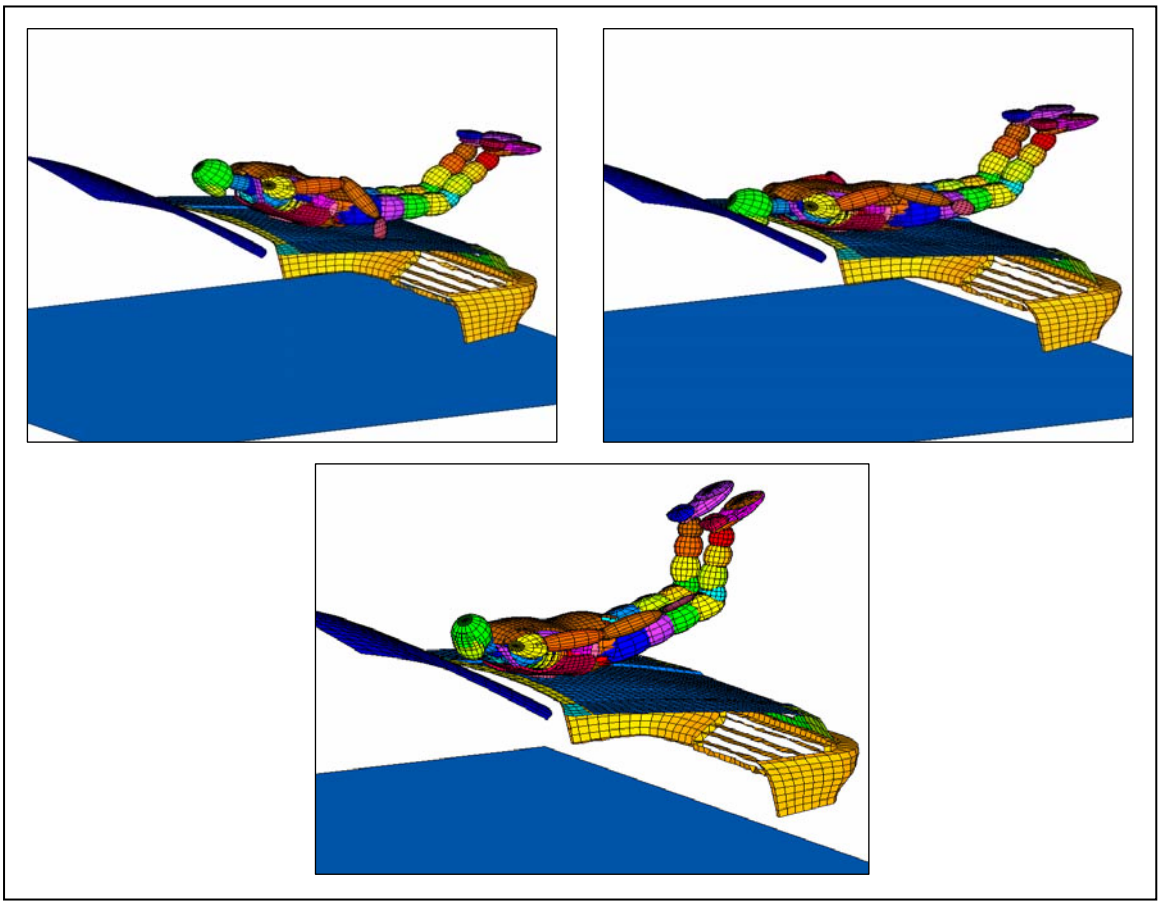

Figure A(I).12 Impact Sequence With Dummy Wearing Thoracic Protection

The upper torso and sternum acceleration for the model wearing armour of varying stiffnesses, both with and without the polycarbonate disc, as well as the upper torso and sternum acceleration for an unprotected pedestrian, can be seen in Figures A(I).13 and A(I).14.

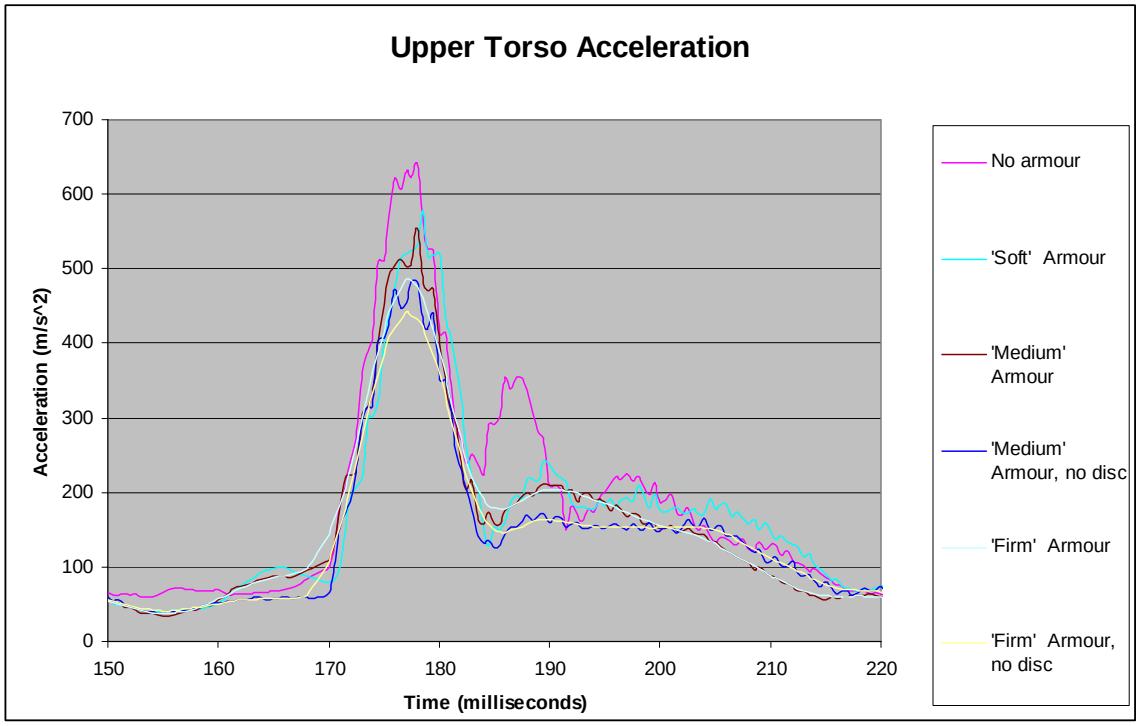

Figure A(I).13 Torso Acceleration

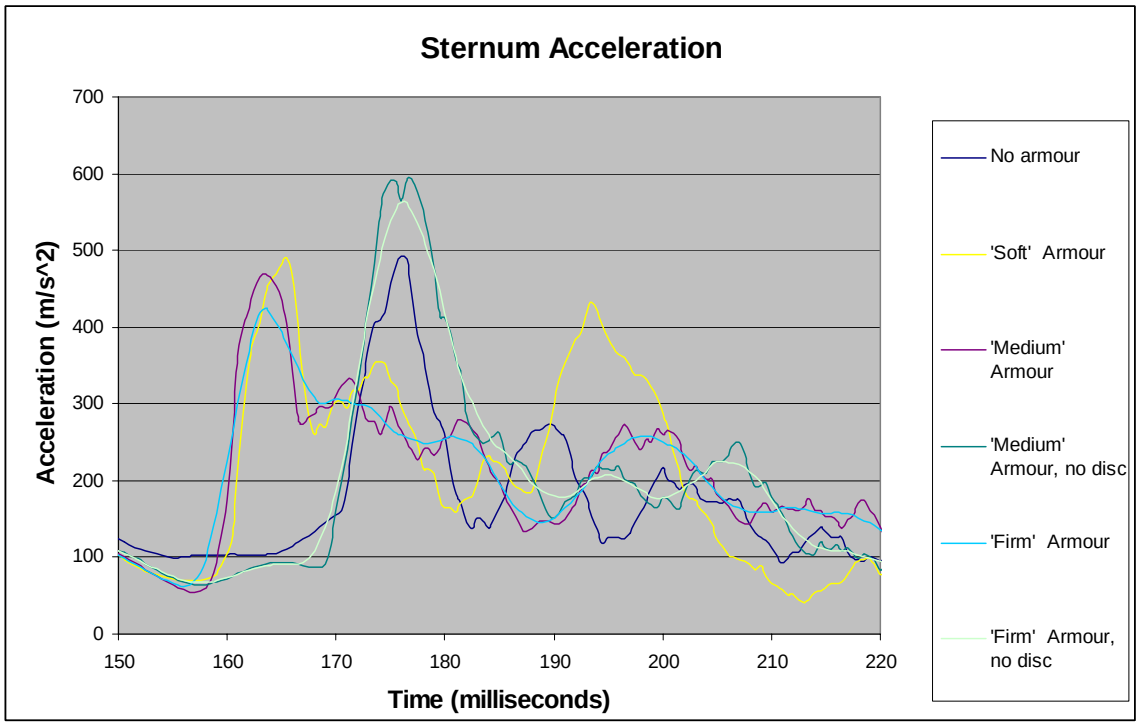

Figure A(I).14 Sternum Acceleration

A(I).5.3 Discussion and Conclusions

All armour stiffnesses and configurations (i.e. with disc; without disc) reduced upper torso acceleration in comparison to the unprotected pedestrian. The best result was

achieved with the ‘firm’ armour properties, minus the polycarbonate disc. In this instance a reduction of over 30% in upper torso acceleration was achieved, in comparison to the unprotected pedestrian. Of note is the reduction in the secondary acceleration pulse for the protected pedestrians, evident at approximately 187 milliseconds for the unprotected pedestrian.

It is also apparent that body armour without the disc is increasing the sternum acceleration during impact, in the worst case scenario (‘Medium’ armour stiffness, no disc) by over 20% in comparison to the unprotected pedestrian. These results are not dissimilar to the findings by Janda et al, whose research indicated the use of some chest protectors may well increase the risk of mortality from baseball impact. In this instance the best result was achieved with the ‘Firm’ armour, this time with the polycarbonate disc, resulting in an approximately 15% reduction in sternum acceleration in comparison to the unprotected pedestrian.

From these results it would appear that the ‘Firm’ armour, with the polycarbonate disc, offered the most consistent protection in regard to both sternum and upper torso acceleration during a vehicle pedestrian collision using the parameters specified previously and for the scenario examined.

Further research is necessary, particularly as the findings from these simulations appear in some instances to be inconsistent with the anecdotal evidence of ballistic body armour protecting law enforcement officers during vehicle and vehicle-pedestrian collisions. The author suspects that a fairly complex relationship exists between the different levels of hysteresis present in the various body armour examples, the impact rate, impact force and the rate dependant injury tolerance levels of the individual which may well depend on the cardiac and pulmonary cycles (which were obviously absent from the simulations). Further research needs to be conducted to establish the parameters involved and the relative importance of each, preferably using a mathematical model that breathes and has a pulse.

The use of a finite element pedestrian model to further examine the effect of body armour on pedestrian protection would be valuable. At the time these simulations were conducted finite element pedestrian models were not widely available. The

multibody model used has been validated for anterior-posterior thoracic impact, as shown in Figure A(I).15, although it should be noted that the impactor location used during the validation is offset.

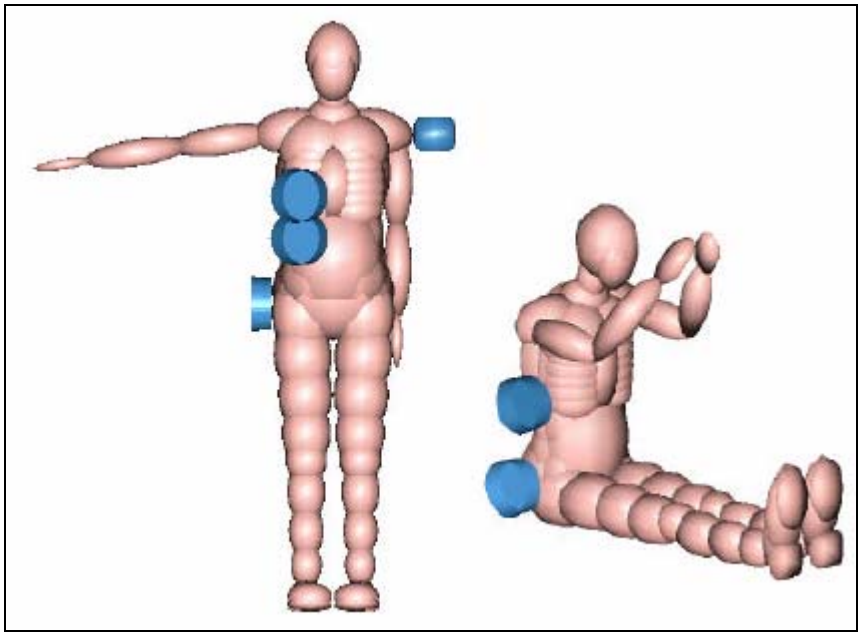

Figure A(I).15 MADYMO Multibody Pedestrian Model Validation Test Locations (Source: MADYMO Human Models Manual)

Acceleration was chosen to evaluate the effectiveness of the body armour, as a general measurement suitable for comparative purposes was preferred over a specific injury measurement which may or may not be indicative of the level of protection offered, given that many injury parameters have been developed with specific test configurations in mind. The energy-based injury criteria discussed earlier show much better versatility than existing injury criteria and once these energy-based methods are better validated they would make excellent criteria, when used in conjunction with a finite element pedestrian model, to better evaluate the effectiveness of body armour for the thoracic protection of pedestrians.

Therefore, in terms of the effectiveness of computer simulation as a tool to assess apparatus for thoracic injury reduction, it would appear that there is considerable potential for computer simulation in such a context but that more development, particularly in regard to human body and injury modelling, is required for the full potential to be realised.

Appendix II: Data from CASR (formerly RARU) Study

Case Number		Throw distance (m)	Angle for pedestrian between impact and rest point, relative to vehicle travel direction at impact (-ve for left hand angle, +ve for right, degrees)	Actual throw distance (dped x cos(theta)) (m)	Braking (before or after impact, no braking)	Vehicle stopping distance (m)	Angle between vehicle travel at time of impact and rest point, relative to vehicle travel direction at impact (-ve for left hand angle, +ve for right, degrees)	Actual stopping distance (dveh x cos(theta)) (m)	Deceleration rate (G's)	Calculation type	Vehicle type (Sedan/wagon/small utility, Motorcycle, SUV/4wd/large utility/van, Truck/Bus, Sports coupe)	Vehicle size (small, med, large)	Impact speed (km/hr)	Impact speed (m/s)	Impact speed source (Driver, Skid mark, Projection Distance)	Impact point (11, 12, 1 etc o'clock)	Pedestrian age
Year	Case															
83	H002	16	9	15.80	Before	16	0	16.00	0.72	2.1	Sedan/wagon/small utility	med	54	15.00	Skid marks	12	81
83	H005	39.5	0	39.50	After	22	-3.5	21.96	0.71	2.1	Sedan/wagon/small utility	large	63	17.50	Skid marks	12	27
83	H009	9	-18	8.56	swerve	6	10	5.91	0.96	3.1	SUV/4wd/large utility/van	med	38	10.56	projection distance	12	59
83	H012	43	0	43.00	After	142.6	0.75	142.59	0.19	3.1	Sedan/wagon/small utility	med	83	23.06	projection distance	11	15
84	H012	54.5	0	54.50	Before	38	3	37.95	0.47	2.1	Truck/Bus	large	67	18.61	Skid marks	1	22
84	H014	16.2	-13	15.78	Before	16.6	0	16.60	0.50	2.1	Sedan/wagon/small utility	large	46	12.78	Skid marks	11	18
84	H015	22.4	2	22.39	no action	40.6	-8.5	40.15	0.35	1	Sedan/wagon/small utility	large	60	16.67	driver	1	42
84	H023	13	0	13.00	no action	no info	no info	no info	no info	1	Sedan/wagon/small utility	med	60	16.67	driver	12	79
84	H029	3	-54	1.76	Before	5	0	5.00	0.71	2.1	Sedan/wagon/small utility	large	30	8.33	Skid marks	11	76
84	H045	10.5	-2	10.49	Before	3.9	-2	3.90	0.74	2.1	Sedan/wagon/small utility	large	27	7.50	Skid marks	12	69
84	H051	17.3	-4	17.26	After	62.6	-5	62.36	0.16	1	Sedan/wagon/small utility	large	50	13.89	driver	1	60
84	H054	33.6	-2.5	33.57	no action	no info	no info	no info	no info	3.1	Sedan/wagon/small utility	med	74	20.56	projection distance	11	18
85	H001	18.5	-6	18.40	Before	31.8	-5	31.68	0.38	3.1	Sedan/wagon/small utility	med	55	15.28	projection distance	12	8
85	H002	4.5	-37	3.59	slowed	no info	no info	no info	no info	3.1	Sedan/wagon/small utility	med	25	6.94	projection distance	12	65
85	H003	12.9	-2	12.89	Before	7.3	0	7.30	0.74	2.1	SUV/4wd/large utility/van	large	37	10.28	Skid marks	12	74
85	H005	43.1	7	42.78	Before	no info	no info	no info	no info	2.3	Motorcycle	small	87	24.17	momentum calculation	12	9
85	H012	6.9	-4	6.88	swerve	6	-4	5.99	1.00	2.3	Motorcycle	small	39	10.83	momentum calculation	1	75
85	H017	47	3	46.94	Before	34	0	34.00	0.29	1	Sedan/wagon/small utility	med	50	13.89	driver	12	33
85	H020	23	-2	22.99	Before	25.5	5	25.40	0.92	2.3	Motorcycle	small	77	21.39	momentum calculation	11	48
85	H021	20.5	-7	20.35	After	38	-2	37.98	0.44	1	Sedan/wagon/small utility	small	65	18.06	witness	12	75
85	H022	2.4	65	1.01	Before	62	0	62.00	0.63	2.3	Motorcycle	small	100	27.78	momentum calculation	12	48
85	H023	30.8	3	30.76	After	54	4	53.87	0.26	1	Motorcycle	small	60	16.67	driver	12	12
85	H025	2	-4	2.00	After	2	0	2.00	1.77	1	Sedan/wagon/small utility	large	30	8.33	driver	11	83
85	H028	9.4	16	9.04	Before	no info	no info	no info	no info	3.1	Sedan/wagon/small utility	med	39	10.83	projection distance	12	32
85	H032	13	7	12.90	After	25	-2	24.98	0.25	1	Sedan/wagon/small utility	large	40	11.11	driver	11	6
85	H038	27	-3	26.96	Before	50	13	48.72	0.78	2.3	Motorcycle	small	98	27.22	momentum calculation	1	55
85	H045	10.3	0	10.30	Before	18.5	8	18.32	1.08	2.3	Motorcycle	small	71	19.72	momentum calculation	12	80
85	H061	4	-11	3.93	no action	no info	no info	no info	no info	1	Sedan/wagon/small utility	large	50	13.89	driver	11	90
85	H070	17.3	10	17.04	After	18	0	18.00	0.64	3.1	Sedan/wagon/small utility	med	54	15.00	projection distance	11	14
85	H073	71	4	70.83	no action	no info	no info	no info	no info	1	Sedan/wagon/small utility	large	100	27.78	witness	1	27
86	H006	22	-7	21.84	no action	no info	no info	no info	no info	1	Sports coupe	small	70	19.44	driver	11	80
86	H016	11.8	-14	11.45	After	no info	no info	no info	no info	1	Sedan/wagon/small utility	Small	70	19.44	driver	11	7
86	H021	23	-4	22.94	no action	no info	no info	no info	no info	1	Sedan/wagon/small utility	large	55	15.28	driver	12	87
86	H023	17.5	-17	16.74	other avoiding actior	18.5	-11	18.16	0.78	1	Motorcycle	small	60	16.67	driver	12	85
86	H025	9	27	8.02	other avoiding actior	no info	no info	no info	no info	3.1	Motorcycle	small	37	10.28	projection distance	1	73
86	H027	71.1	-8	70.41	After	no info	no info	no info	no info	4.1	Sedan/wagon/small utility	med	90	25.00	projection distance	12	36
86	H030	20	0	20.00	no action	no info	no info	no info	no info	1	Sports coupe	small	60	16.67	driver	1	29
86	H032	19	-5	18.93	no action	no info	no info	no info	no info	1	Sedan/wagon/small utility	med	55	15.28	driver	11	81
86	H037	50	0	50.00	Before	no info	no info	no info	no info	1	Sedan/wagon/small utility	large	80	22.22	driver	11	14
86	H041	4	-48	2.68	After	no info	no info	no info	no info	3.1	Sedan/wagon/small utility	large	25	6.94	projection distance	11	33
86	H047	17	-16	16.34	no action	67	-4	66.84	0.18	1	Sedan/wagon/small utility	small	55	15.28	driver	1	68
86	H054	56	7	55.58	After	no info	no info	no info	no info	1	Sedan/wagon/small utility	med	80	22.22	driver	1	21
86	H057	18.6	0	18.60	After	no info	no info	no info	no info	3.1	Sedan/wagon/small utility	med	55	15.28	projection distance	11	24
86	H062	28	8	27.73	Before	29	-9	28.64	0.65	2.1	Sedan/wagon/small utility	med	69	19.17	Skid marks	1	14
86	H064	6	-3	5.99	After	no info	no info	no info	no info	3.1	SUV/4wd/large utility/van	large	32	8.89	projection distance	1	58
86	H068	15	-2	14.99	Before	8	-5	7.97	0.26	2.1	Sedan/wagon/small utility	large	23	6.39	Skid marks	12	6
86	H069	66	0	66.00	After	no info	no info	no info	no info	1	Sedan/wagon/small utility	med	80	22.22	driver	1	19

Table A(II).1: Pedestrian Throw Distances from Case Data for 'Vehicle Travel Speeds and the Incidence of Fatal Pedestrian Collisions' by McLean et al (1994)

Case Number		Throw distance (m)	Angle for pedestrian between impact and rest point, relative to vehicle travel direction at impact (-ve for left hand angle, +ve for right, degrees)	Actual throw distance (dped x cos(theta)) (m)	Braking (before or after impact, no braking)	Vehicle stopping distance (m)	Angle between vehicle travel at time of impact and rest point, relative to vehicle travel direction at impact (-ve for left hand angle, +ve for right, degrees)	Actual stopping distance (dveh x cos(theta)) (m)	Deceleration rate (G's)	Calculation type	Vehicle type (Sedan/wagon/small utility, Motorcycle, SUV/4wd/large utility/van, Truck/Bus, Sports coupe)	Vehicle size (small, med, large)	Impact speed (km/hr)	Impact speed (m/s)	Impact speed source (Driver, Skid mark, Projection Distance)	Impact point (11, 12, 1 etc o'clock)	Pedestrian age
Year	Case															
86	H073	17.5	0	17.50	unknown	9.5	0	9.50	0.66	2.1	Sedan/wagon/small utility	large	40	11.11	Skid marks	11	75
86	H076	5.5	-20	5.17	no action	no info	no info	no info	no info	1	Sedan/wagon/small utility	large	60	16.67	driver	10	53
86	H086	28	0	28.00	After	no info	no info	no info	no info	3.1	SUV/4wd/large utility/van	large	67	18.61	projection distance	12	26
86	H090	28.3	1	28.30	no action	no info	no info	no info	no info	3.1	Sedan/wagon/small utility	large	60	16.67	projection distance	12	3
86	H091	11	2	10.99	After	29.2	0	29.20	0.48	1	Sedan/wagon/small utility	large	60	16.67	driver	11	89
87	H008	15	0	15.00	Before	9	0	9.00	0.48	2.1	Sedan/wagon/small utility	med	33	9.17	Skid marks	11	81
87	H009	9	6	8.95	Before	no info	no info	no info	no info	3.1	Sedan/wagon/small utility	large	39	10.83	projection distance	12	8
87	H012	48	0	48.00	Before	43	0	43.00	0.69	2.1	Sedan/wagon/small utility	large	87	24.17	Skid marks	12	20
87	H025	13	-6	12.93	Before	8.5	0	8.50	0.98	3.1	Sedan/wagon/small utility	small	46	12.78	projection distance	1	38
87	H037	21	-6	20.88	After	no info	no info	no info	no info	3.1	Sedan/wagon/small utility	med	55	15.28	projection distance	11	64
87	H038	10	0	10.00	Before	10	10	9.85	0.64	3.1	Sedan/wagon/small utility	med	40	11.11	projection distance	11	90
87	H046	11.6	0	11.60	swerve	18	-3	17.98	0.90	2.3	Motorcycle	small	64	17.78	momentum calculation	?	80
87	H051	35	3	34.95	Before	28.5	2	28.48	0.50	2.1	Sedan/wagon/small utility	med	60	16.67	Skid marks	12	17
87	H053	41.6	0	41.60	After	33	0	33.00	0.43	2.1	Sedan/wagon/small utility	large	60	16.67	Skid marks	12	54
88	H003	39.5	1	39.49	Before	no info	no info	no info	no info	4.1	Sedan/wagon/small utility	med	60	16.67	projection distance	1	17
88	H007	24.1	0	24.10	Before	no info	no info	no info	no info	2.2	Sedan/wagon/small utility	small	46	12.78	Skid marks	1	65
88	H010	14.7	-10	14.48	Before	16	11.5	15.68	0.96	2.3	Motorcycle	small	62	17.22	momentum calculation	1	61
88	H012	47.8	-6	47.54	After	no info	no info	no info	no info	4.1	Sedan/wagon/small utility	large	80	22.22	projection distance	11	23
88	H015	53	-2	52.97	no action	61	-1	60.99	0.55	1	SUV/4wd/large utility/van	large	92	25.56	projection distance	11	12
88	H016	27.5	0	27.50	no action	27.5	16	26.43	0.54	1	Motorcycle	small	60	16.67	driver	11	64
88	H020	41.2	2	41.17	Before	37.6	0	37.60	0.72	2.1	Sedan/wagon/small utility	large	83	23.06	Skid marks	1	75
88	H025	10	-26	8.99	After	no info	no info	no info	no info	1	Sedan/wagon/small utility	med	60	16.67	driver	11	15
88	H035	28	4	27.93	no action	no info	no info	no info	no info	1	Sedan/wagon/small utility	med	100	27.78	witness	1	17
88	H038	3.5	-22	3.25	Before	no info	no info	no info	no info	3.1	Sedan/wagon/small utility	small	23	6.39	projection distance	12	72
88	H040	40.5	-2	40.48	After	42	0	42.00	0.60	1	Sedan/wagon/small utility	med	80	22.22	driver	1	53
88	H048	35	5	34.87	other avoiding actior	no info	no info	no info	no info	1	SUV/4wd/large utility/van	large	65	18.06	driver	11	17
89	H001	11.4	-9	11.26	Before	33.1	-6	32.92	0.22	3.1	Sedan/wagon/small utility	large	43	11.94	projection distance	1	77
89	H002	11.8	-4	11.77	Before	8.1	0	8.10	0.70	2.1	Sedan/wagon/small utility	large	38	10.56	Skid marks	11	5
89	H005	40.5	-2	40.48	Before	43	2	42.97	0.32	2.1	SUV/4wd/large utility/van	large	59	16.39	Skid marks	11	53
89	H014	5	8	4.95	Before	1	0	1.00	0.88	2.1	Sedan/wagon/small utility	small	15	4.17	Skid marks	12	73
89	H026	53	2	52.97	After	50	0	50.00	0.30	1	Sedan/wagon/small utility	large	62	17.22	Skid marks	12	22
89	H029	31	-5	30.88	After	no info	no info	no info	no info	1	Sedan/wagon/small utility	med	60	16.67	driver	12	87
89	H033	26.5	0	26.50	After	no info	no info	no info	no info	1	Sedan/wagon/small utility	med	65	18.06	driver	1	42
89	H031	35.7	-12	34.92	After	33.5	-12	32.77	0.30	1	Sedan/wagon/small utility	med	50	13.89	driver	12	28
89	H032	2.9	0	2.90	Before	no info	no info	no info	no info	2.2	Sedan/wagon/small utility	large	21	5.83	Skid marks	2	80
89	H034	33	0	33.00	After	no info	no info	no info	no info	3.1	Sedan/wagon/small utility	small	72	20.00	projection distance	12	36
89	H035	15.8	3	15.78	After	no info	no info	no info	no info	1	SUV/4wd/large utility/van	large	50	13.89	driver	11	22
89	H041	11.2	-12	10.96	After	8.6	0	8.60	0.85	3.1	Sedan/wagon/small utility	med	43	11.94	projection distance	11	50
90	H014	21	5	20.92	After	no info	no info	no info	no info	3.1	Sedan/wagon/small utility	small	58	16.11	projection distance	12	9
90	H015	24.1	1	24.10	no action	no info	no info	no info	no info	1	Sedan/wagon/small utility	med	62	17.22	projection distance	1	27
90	H016	8.5	15	8.21	Before	3	0	3.00	0.58	2.2	Sedan/wagon/small utility	large	21	5.83	Skid marks	1	26
90	H024	13	-14	12.61	no action	no info	no info	no info	no info	1	Sedan/wagon/small utility	med	40	11.11	driver	12	57
90	H028	25	0	25.00	no action	39	-5	38.85	0.58	1	Sedan/wagon/small utility	med	76	21.11	projection distance	1	29
90	H037	20	-7	19.85	Before	14	0	14.00	1.01	1	Sedan/wagon/small utility	small	60	16.67	driver	12	35
91	H012	4.2	0	4.20	Before	no info	no info	no info	no info	3.1	Sedan/wagon/small utility	small	26	7.22	projection distance	1	79
91	H016	18	-10	17.73	Before	13.1	-3	13.08	0.64	2.1	Sedan/wagon/small utility	small	46	12.78	Skid marks	12	27
91	H021	5.1	0	5.10	Before	12.5	22	11.59	0.29	3.1	SUV/4wd/large utility/van	med	29	8.06	projection distance	11	71

Table A(II).1 continued

Case Number		Throw distance (m)	Angle for pedestrian between impact and rest point, relative to vehicle travel direction at impact (-ve for left hand angle, +ve for right, degrees)	Actual throw distance (dped x cos(theta)) (m)	Braking (before or after impact, no braking)	Vehicle stopping distance (m)	Angle between vehicle travel at time of impact and rest point, relative to vehicle travel direction at impact (-ve for left hand angle, +ve for right, degrees)	Actual stopping distance (dveh x cos(theta)) (m)	Deceleration rate (G's)	Calculation type	Vehicle type (Sedan/wagon/small utility, Motorcycle, SUV/4wd/large utility/van, Truck/Bus, Sports coupe)	Vehicle size (small, med, large)	Impact speed (km/hr)	Impact speed (m/s)	Impact speed source (Driver, Skid mark, Projection Distance)	Impact point (11, 12, 1 etc o'clock)	Pedestrian age
Year	Case															
89	H022	34.6	7	34.34	Before	no info	no info	no info	no info	1	Sedan/wagon/small utility	large	80	22.22	driver	1	35
85	H065	11	31	9.43	Before	28	0	28.00	0.75	2.1	Sedan/wagon/small utility	large	73	20.28	Skid marks	12	39
89	H009	16	5	15.94	no action	no info	no info	no info	no info	1	Sedan/wagon/small utility	med	60	16.67	driver	12	38
84	H044-1	11.5	-21	10.74	After	31.5	-2	31.48	0.67	1	Sedan/wagon/small utility	med	73	20.28	Skid marks	12	76
84	H044-2	16.4	-12	16.04	After	31.5	-2	31.48	0.67	1	Sedan/wagon/small utility	med	73	20.28	Skid marks	12	60
84	H044-3	18.1	-5	18.03	After	31.5	-2	31.48	0.67	1	Sedan/wagon/small utility	med	73	20.28	Skid marks	12	81
86	H024	32	-15	30.91	no action	40	-11	39.27	no info	?	?	?	?	no info	?	12	57
87	H016-1	16.5	15	15.94	no action	38	15	36.71	no info	?	?	?	?	no info	?	12	39
87	H016-2	36.9	15	35.64	no action	38	15	36.71	no info	?	?	?	?	no info	?	12	unknown
87	H030	23.9	-3	23.87	Before	21.1	0	21.10	no info	?	?	?	?	no info	?	1	75
87	H048	15.5	0	15.50	Before	34.8	0	34.80	no info	?	Truck/Bus	large	?	no info	?	11	85
87	H054	40.4	0	40.40	After	51.2	0	51.20	no info	?	Truck/Bus	large	?	no info	?	12	7
89	H018-1	17.3	-8	17.13	Before	34.5	-4	34.42	no info	?	SUV/4wd/large utility/van	large	?	no info	?	11	79
89	H018-2	23	-7	22.83	Before	34.5	-4	34.42	no info	?	SUV/4wd/large utility/van	large	?	no info	?	11	unknown

Table A(II).1 continued

Appendix III: Case Study Background Material

A(III).1: Case Study 1 - Lyttelton

Summary of Witness Statements (provided by Professor John Raine):

1. The vehicle took off fairly suddenly according to [redacted], and [redacted] stated that he "saw an arm flung in the air as the front of the vehicle made contact with someone".
2. [redacted] thought that the vehicle moved forward about one car length, slowed, then moved off again. Black diesel smoke observed from the exhaust at this point is consistent with witness statements that the car accelerated away briskly from the scene.
3. [redacted] believed the vehicle lifted 12-18 inches off the ground as it rode over [redacted]'s body.
4. [redacted] stated, "[redacted] travelled about 10-15 ft on the vehicle before she fell off and under the vehicle." He noted that both front and rear wheels went over the body of xxx. In his opinion the driver had time to stop between when the vehicle first took off and when [redacted] fell off the bonnet.
5. [redacted] stated, "As soon as the vehicle struck xxx I saw her arch forward slightly onto the bonnet and then she fell straight back onto the ground with the line of her body about a 45º angle to the vehicle. I saw the front passenger's wheel run over [redacted]'s leg and as it did so [redacted]'s body jolted and moved forward. I then saw the rear wheel run over her pelvic area."
6. [redacted], coach driver, whose vehicle was following the Landcruiser of [redacted], thought that the vehicle accelerated away quickly.

Calculated Landcruiser Speeds and Elapsed Times		
Maximum Acceleration: Approx. 2.87 m/s^2		
Distance from rest (metres)	Speed (km/h)	Time (seconds)
1	8.6	0.83
2	12.2	1.18
3	14.9	1.45
4	17.3	1.67
5	19.3	1.86
6	21.1	2.04
Moderate acceleration 2 m/s^2		
Distance from rest (metres)	Speed (km/h)	Time (seconds)
1	7.2	1.0
2	10.18	1.41
3	12.47	1.73
4	14.4	2.0
5	16.1	2.24
6	17.63	2.45

Table A(III).1 Vehicle Acceleration Data Determined from Manufacturer Specifications (Source: Professor J. K. Raine)

Figure A(III).1 Vehicle Shortly Prior to Moving and Colliding with Pedestrian (Source: TV3)

Figure A(III).2 Vehicle in Storage Following Accident – Damage to Windscreen did not Result from Accident (source: NZ Police)

A(III).2: Case Study 2 - Lamar

Modelling Notes for Lamar:

In regard to the multibody pedestrian model the following should be noted:

- The model used has arbitrary muscle and joint stiffnesses. These can be modified, but there is usually insufficient information available when simulating a real-life incident to be able to 'program' the muscular responses adequately, e.g. the model will not brace itself before an impact as a real person would.

- Many of the necessary contact stiffnesses and damping coefficients are not well understood for many parts of the human anatomy, in particular the head damping coefficient. When evaluating the contact between two objects the contact stiffness of the stiffest object is usually used to determine the contact forces. For vehicle-pedestrian contacts, the stiffness of the vehicle is used to determine the contact forces. Likewise, for pedestrian-environment (e.g. the road) contacts the road stiffness is used. However, for other surfaces (e.g. grass) the head stiffness would be the determining factor and is hard to simulate.

In regard to the finite-element vehicle model, the following should be noted:

- The vehicle model was derived using a mechanical coordinate measuring device and as such is not expected to be perfectly accurate. Furthermore, a fairly coarse finite-element mesh was used to speed computation time and this again reduces accuracy. However, for the purposes of this series of simulations, the final level of model accuracy is considered adequate.

- Only the vehicle components thought to directly influence the vehicle-pedestrian interaction were modelled. This greatly speeds computation time. For this series of simulations the bumper, front grille, headlights, bonnet, windscreen and the filler panels and grille directly below the windscreen were modelled.

- Components were simplified – for example the outer skin and reinforcing structure of the bonnet were modelled by substituting a thicker and stiffer outer skin. This provides a considerably reduction in model complexity and again, computation time is reduced. As the bonnet was not noticeably deformed in the scenario being modelled, any reduction in accuracy would be negligible.

Figure A(III).3 Front View of Vehicle Prior to Measurement – Note Rails for Coordinate Measuring System to Left of Vehicle. Headlight has been lifted for Inspection

Figure A(III).4 Side View of Vehicle Prior to Measurement – Note Rails for Coordinate Measuring System at Bottom of Photo. Damage to Vehicle Caused After and not related to Pedestrian Impact

Figure A(III).5 Damage to Grille at Base of Windscreen from Pedestrian Head Impact

Figure A(III).6 Hair from Pedestrian Trapped in Plastic at Base of Windscreen

Figure A(III).7 Manoeuvring Tests of Exemplar Vehicle on Site

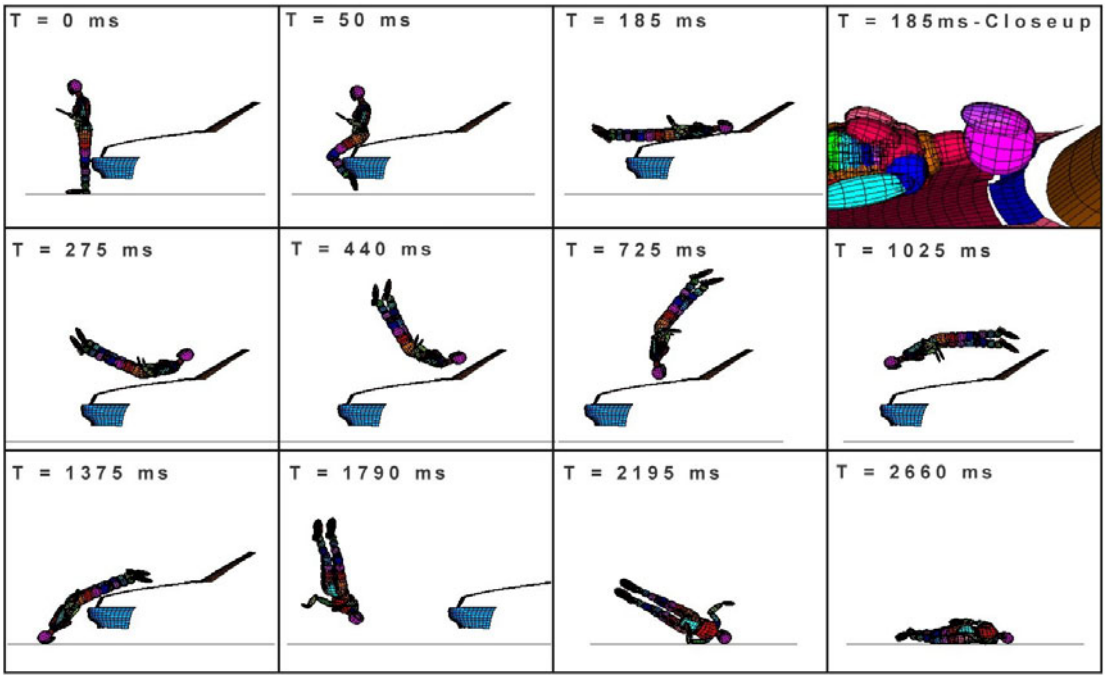

Figure A(III).8: Illustration for impact sequence with pedestrian facing away from vehicle, vehicle speed 25 km/h and decelerating moderately

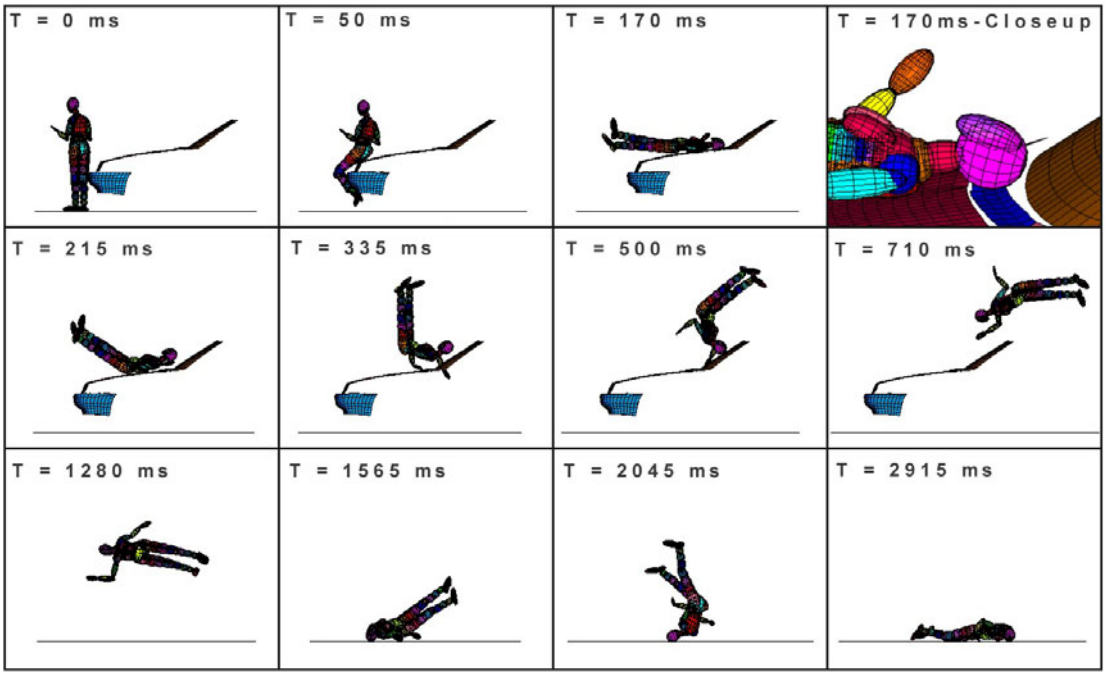

Figure A(III).9: Illustration for impact sequence with pedestrian facing away at 45° from vehicle, speed constant at 30 km/h

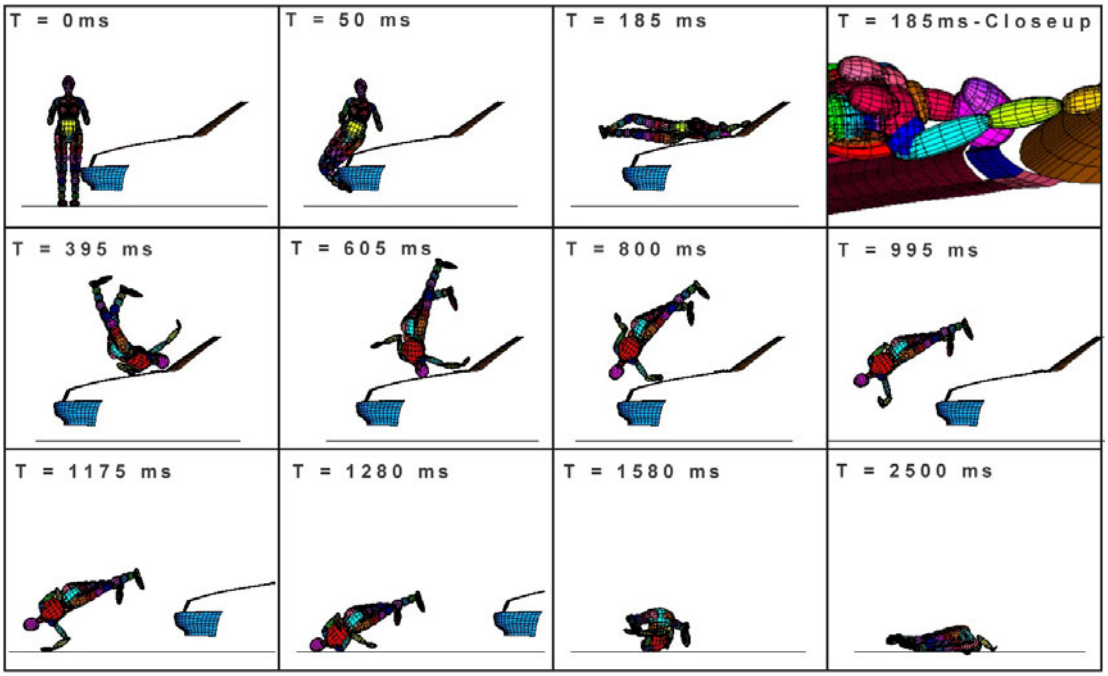

Figure A(III).10: Illustration for impact sequence with pedestrian side-on to vehicle, vehicle speed 30 km/h and decelerating heavily

Results for first simulation series for Operation Lamar

	Vehicle velocity (km/h)			
	20	25	30	35
Filename	prelude4g	prelude4h	prelude4i	prelude4j
Simulation duration (secs)	2.5	2.5	2.5	2.5
HIC	1050	1973	4345	8480
HIC source	Vehicle contact	Vehicle contact	Vehicle contact	Vehicle contact
Series 1: Pedestrian facing away from vehicle, vehicle speed constant	Head hits near trailing edge of bonnet, ped rolls end over end on bonnet	Head hits near trailing edge of bonnet, ped does a slow somersault onto windscreen	Head hits near trailing edge of bonnet, ped somersaults onto roof	Head hits near trailing edge of bonnet, ped somersaults onto roof
Filename	prelude2t	prelude2u	prelude2v	prelude2w
Simulation duration (secs)	2.5	2.5	2.5	2.5
HIC	9.6	113	255	2390
HIC source	Vehicle contact	Vehicle contact	Vehicle contact	Vehicle contact
Series 2: Pedestrian side-on to vehicle, vehicle speed constant	Head hits near trailing edge of bonnet, ped rolls up onto windscreen	Head cushioned by arm near trailing edge of bonnet, ped rolls up onto windscreen	Head hits near trailing edge of bonnet, ped rolls over car	Head hits across trailing edge of bonnet and grille, ped rolls over car
Filename	prelude6a	prelude6b	prelude6c	prelude6d
Simulation duration (secs)	1.5	1.5	1.7	1.7
HIC	938	1701	1588	2823
HIC source	Vehicle contact	Vehicle contact	Vehicle contact	Vehicle contact
Series 3: Pedestrian facing away from vehicle at 45deg, vehicle speed constant	Head hits near trailing edge of bonnet, pedestrian rolls onto windscreen	Head hits across trailing edge of bonnet and grille, pedestrian rolls over car	Head hits grill, pedestrian rolls over car	Head hits grill, pedestrian somersaults over car

Filename	prelude5d	prelude5e	prelude5b	prelude5f
Simulation duration (secs)	2.5	2.5	2.5	2.5
HIC	1437	2333	4314	7008
HIC source	Vehicle contact	Vehicle contact	Vehicle contact	Vehicle contact
Series 4: Pedestrian facing away from vehicle, vehicle deccelerating heavily	Head hits on rear 1/4 of bonnet, pedestrian projected forwards	Heat hits grille below windscreen, ped projected forwards, somersaults and lands face down on ground	Heat hits grille below windscreen, ped projected forwards, somersaults and lands face down on ground	Heat hits grille, ped projected forwards doing a backwards somersault and lands on head
Filename	prelude5i	prelude5j	prelude5k	prelude5l
Simulation duration (secs)	2.5	2.5	2.5	2.5
HIC	138	280	173	1210
HIC source				
Series 5: Pedestrian side-on to vehicle, vehicle deccelerating heavily	Head hits on rear 1/3 of bonnet, pedestrian projected forwards	Heat hits grille below windscreen, ped projected forwards, somersaults and lands face down on ground	Heat hits grille below windscreen, ped projected forwards, somersaults and lands face down on ground	Heat hits grille below windscreen, ped projected forwards, somersaults and lands face down on ground
Filename	prelude6m	prelude6n	prelude6o	prelude6p
Simulation duration (secs)	1.5	1.5	1.7	1.7
HIC	1204	2392	1954	3018
HIC source	Vehicle contact	Vehicle contact	Vehicle contact	Vehicle contact
Series 6: Pedestrian facing away from vehicle at 45deg, vehicle deccelerating heavily	Head hits on rear 1/4 of bonnet, pedestrian projected forwards	Head hits across trailing edge of windscreen and grille, pedestrian projected forwards, does a slow, tumbling somersault	Head hits across trailing edge of windscreen and grille, pedestrian projected forwards, does a slow, tumbling somersault	Head hits grille, pedestrian does a tumbling somersault and lands on back

Filename	prelude5u	prelude5v	prelude5w	prelude5x
Simulation duration (secs)	1.5	1.5	1.7	1.7
HIC	943	1469	4673	10146
HIC source	Vehicle contact	Vehicle contact	Vehicle contact	Vehicle contact
Series 7: Pedestrian facing away from vehicle, vehicle deccelerating moderately	Heat hits on rear 1/4 of bonnet, ped projected forwards, somersaults and lands on head	Head hits across trailing edge of bonnet and grille, pedestrian projected forwards, somersaults	Head hits across trailing edge of bonnet and grille, pedestrian somersaults, lands on bonnet, slides onto ground	Head hits across trailing edge of bonnet and grille, pedestrian somersaults, lands on bonnet, slides onto ground
Filename	prelude5o	prelude5p	prelude5q	prelude5r
Simulation duration (secs)				
HIC	18	124	569	2482
HIC source	Vehicle contact	Vehicle contact	Vehicle contact	Vehicle contact
Series 8: Pedestrian side-on to vehicle, vehicle deccelerating moderately	Head hits on rear 1/4 of bonnet, pedestrian projected forwards	Heat hits on rear 1/4 of bonnet, ped projected forwards, somersaults and lands on head	Heat hits on rear 1/4 of bonnet, ped projected forwards, somersaults	Heat hits on rear 1/4 of bonnet, ped projected forwards, somersaults
Filename	prelude6s	prelude6t	prelude6u	prelude6v
Simulation duration (secs)				
HIC	1197	1972	3579	6303
HIC source	Vehicle contact	Vehicle contact	Vehicle contact	Vehicle contact
Series 9: Pedestrian facing away from vehicle at 45deg, vehicle deccelerating moderately	Heat hits on rear 1/4 of bonnet, ped projected forwards, somersaults and lands on head	Heat hits on rear 1/4 of bonnet, ped projected forwards, somersaults and lands on ground	Head hits across trailing edge of bonnet and grille, pedestrian somersaults, lands on bonnet /windscreen, slides onto ground	Head hits across trailing edge of bonnet and grille, pedestrian somersaults, lands on bonnet /windscreen, slides onto ground

Table A(III).2 Results Summary on Preceding 3 Pages for On-road Simulation Sequences

Series 1: Pedestrian facing away from vehicle, vehicle speed constant

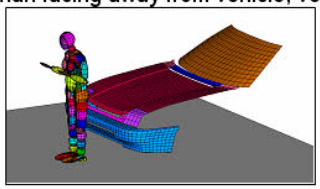

Vehicle speed - 20 km/hr

Filename	prelude4g
Simulation duration (secs)	2.5
HIC	1050
Results	Head hits near trailing edge of bonnet, ped rolls end over end on bonnet
Comments	

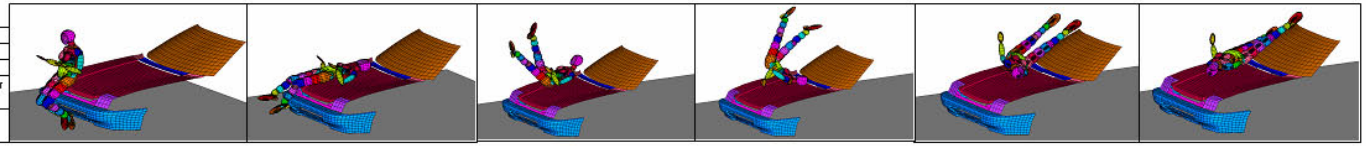

Vehicle speed - 25 km/hr

Filename	prelude4h
Simulation duration (secs)	2.5
HIC	1973
Results	Head hits near trailing edge of bonnet, ped does a slow somersault onto windscreen
Comments	

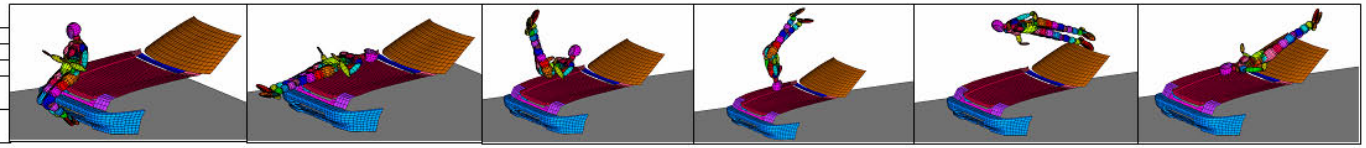

Vehicle speed - 30 km/hr

Filename	prelude4i
Simulation duration (secs)	2.5
HIC	4345
Results	Head hits near trailing edge of bonnet, ped somersaults onto roof
Comments	

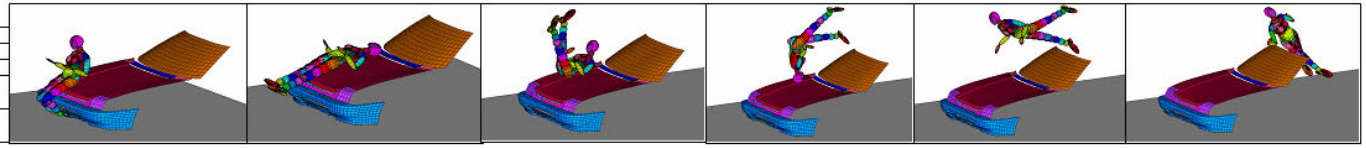

Vehicle speed - 35 km/hr

Filename	prelude4j
Simulation duration (secs)	2.5
HIC	8480
Results	Head hits near trailing edge of bonnet, ped somersaults onto roof
Comments	

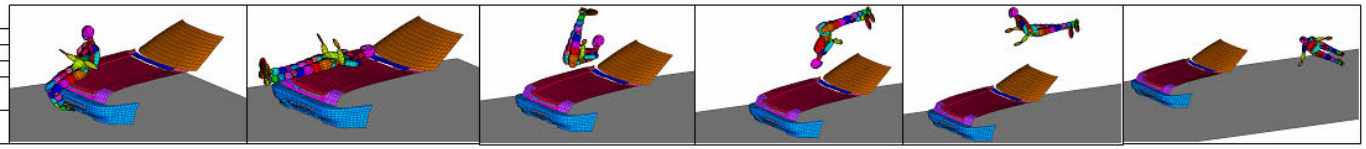

Figure A(III).11 Graphical Results From Series 1: Pedestrian Facing Away from Vehicle, Vehicle Speed Constant

Series 2: Pedestrian side-on to vehicle, vehicle speed constant

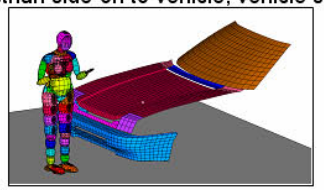

Vehicle speed - 20 km/hr

Filename	prelude2t
Simulation duration (secs)	2.5
HIC	9.6
Results	Head hits near trailing edge of bonnet, ped rolls up onto windscreen
Comments	

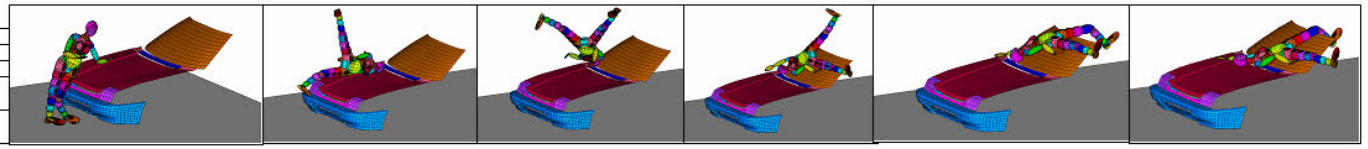

Vehicle speed - 25 km/hr

Filename	prelude2u
Simulation duration (secs)	2.5
HIC	113
Results	Head cushioned by arm near trailing edge of bonnet, ped rolls up onto windscreen
Comments	

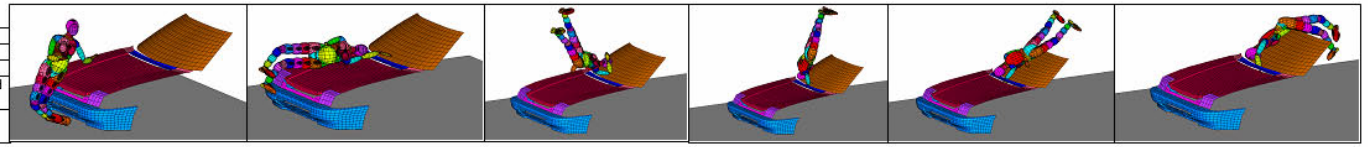

Vehicle speed - 30 km/hr

Filename	prelude2v
Simulation duration (secs)	2.5
HIC	255
Results	Head hits near trailing edge of bonnet, ped rolls over car
Comments	

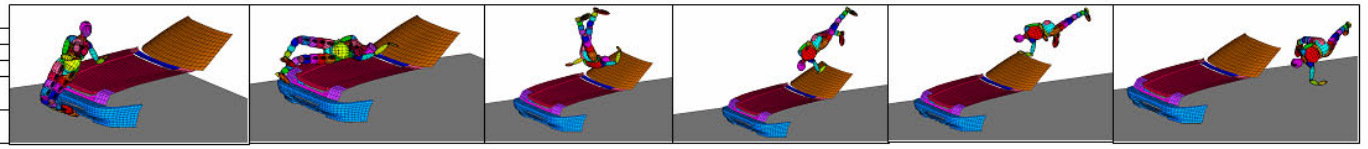

Vehicle speed - 35 km/hr

Filename	prelude2w
Simulation duration (secs)	2.5
HIC	2390
Results	Head hits across trailing edge of bonnet and grille, ped rolls over car
Comments	

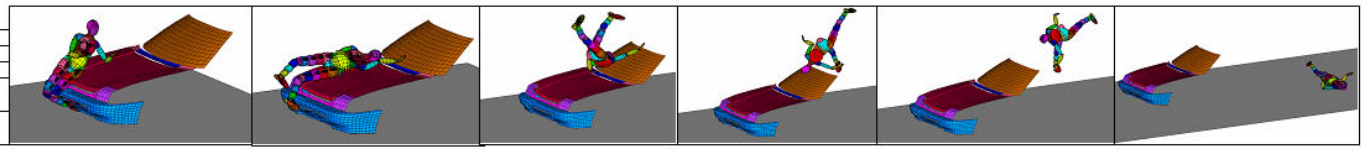

Figure A(III).12 Graphical Results From Series 2: Pedestrian Side on to Vehicle, Vehicle Speed Constant

Series 3: Pedestrian facing away from vehicle at 45deg, vehicle speed constant

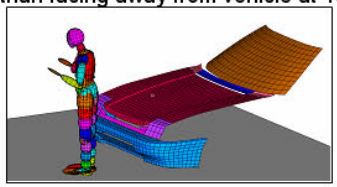

Vehicle speed - 20 km/hr

Filename	prelude6a
Simulation duration (secs)	1.5
HIC	938
Results	Head hits near trailing edge of bonnet, pedestrian rolls onto windscreen
Comments	

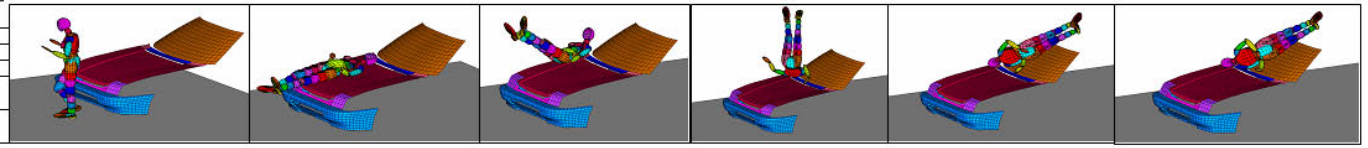

Vehicle speed - 25 km/hr

Filename	prelude6b
Simulation duration (secs)	1.5
HIC	1701
Results	Head hits across trailing edge of bonnet and grille, pedestrian rolls over car
Comments	

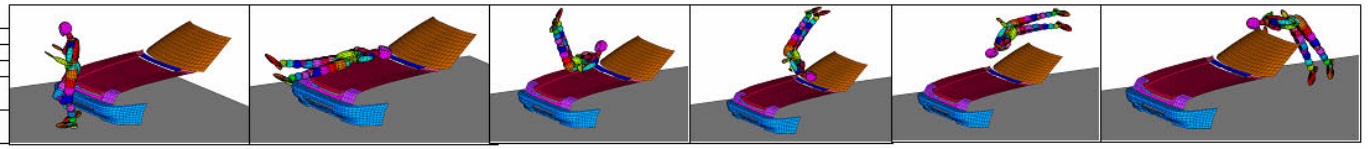

Vehicle speed - 30 km/hr

Filename	prelude6c
Simulation duration (secs)	1.7
HIC	1588
Results	Head hits grill, pedestrian rolls over car
Comments	

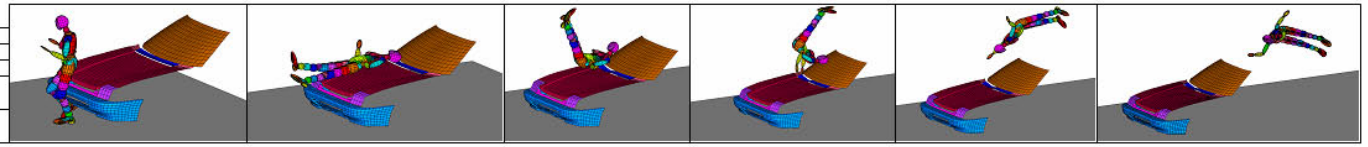

Vehicle speed - 35 km/hr

Filename	prelude6d
Simulation duration (secs)	1.7
HIC	2823
Results	Head hits grill, pedestrian somersaults over car
Comments	

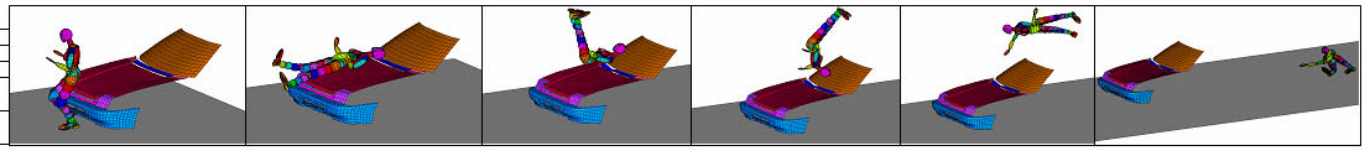

Figure A(III).13 Graphical Results From Series 1: Pedestrian Facing Away from Vehicle at 45 degrees, Vehicle Speed Constant

Series 4: Pedestrian facing away from vehicle, vehicle deccelerating heavily

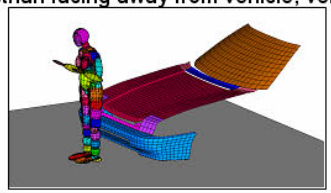

Vehicle speed - 20 km/hr

Filename	prelude5d
Simulation duration (secs)	2.5
HIC	1437
Results	Head hits on rear 1/4 of bonnet, pedestrian projected forwards
Comments	

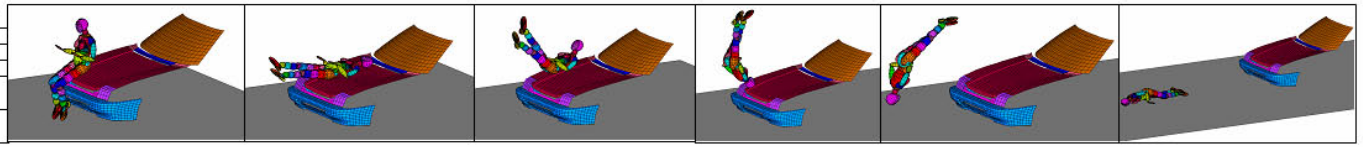

Vehicle speed - 25 km/hr

Filename	prelude5e
Simulation duration (secs)	2.5
HIC	2333
Results	Heat hits grille below windscreen, ped projected forwards, somersaults and lands face down on ground
Comments	

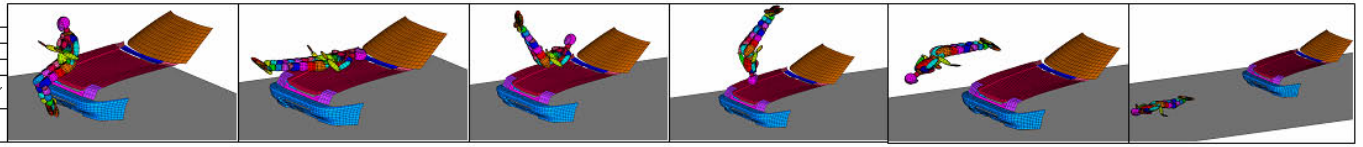

Vehicle speed - 30 km/hr

Filename	prelude5b
Simulation duration (secs)	2.5
HIC	4314
Results	Heat hits grille below windscreen, ped projected forwards, somersaults and lands face down on ground
Comments	

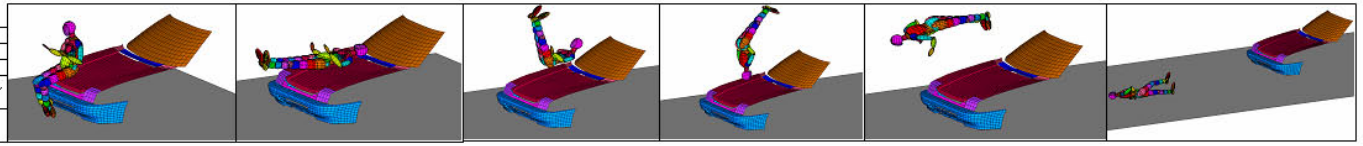

Vehicle speed - 35 km/hr

Filename	prelude5f
Simulation duration (secs)	2.5
HIC	7008
Results	Heat hits grille, ped projected forwards doing a backwards somersault and lands on head
Comments	

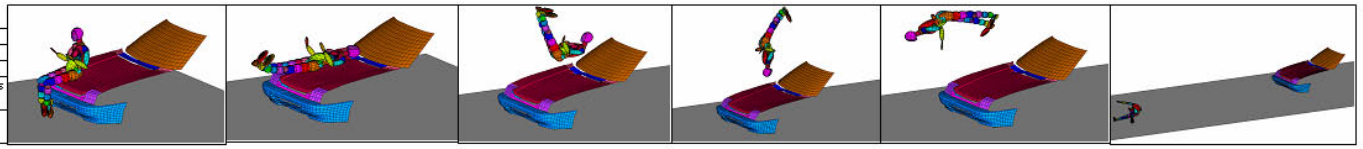

Figure A(III).14 Graphical Results From Series 1: Pedestrian Facing Away from Vehicle, Vehicle Decelerating Heavily

Series 5: Pedestrian side-on to vehicle, vehicle deccelerating heavily

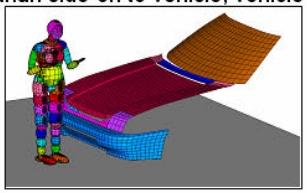

Vehicle speed - 20 km/hr

Filename	prelude5i
Simulation duration (secs)	2.5
HIC	138
Results	Head hits on rear 1/3 of bonnet, pedestrian projected forwards
Comments	

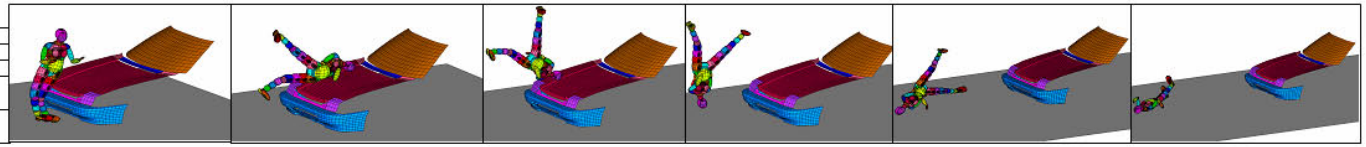

Vehicle speed - 25 km/hr

Filename	prelude5j
Simulation duration (secs)	2.5
HIC	280
Results	Heat hits grille below windscreen, ped projected forwards, somersaults and lands face down on ground
Comments	

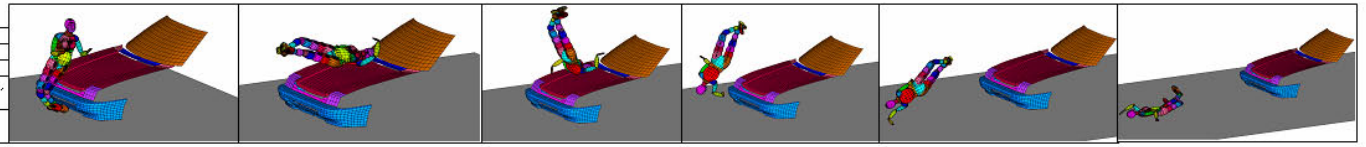

Vehicle speed - 30 km/hr

Filename	prelude5k
Simulation duration (secs)	2.5
HIC	173
Results	Heat hits grille below windscreen, ped projected forwards, somersaults and lands face down on ground
Comments	

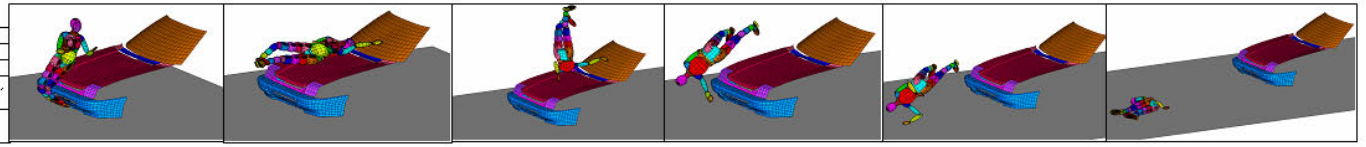

Vehicle speed - 35 km/hr

Filename	prelude5l
Simulation duration (secs)	2.5
HIC	1210
Results	Heat hits grille below windscreen, ped projected forwards, somersaults and lands face down on ground
Comments	

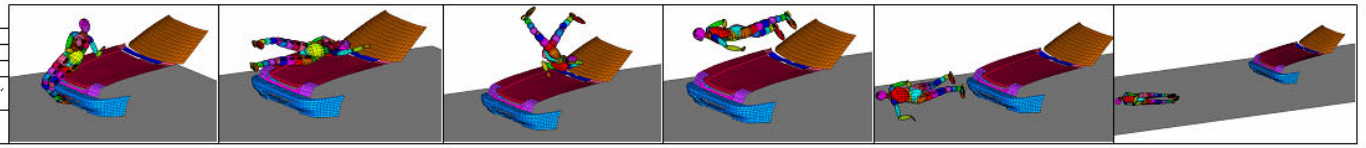

Figure A(III).15 Graphical Results From Series 1: Pedestrian Side on to Vehicle, Vehicle Decelerating Heavily

Series 6: Pedestrian facing away from vehicle at 45deg, vehicle deccelerating heavily

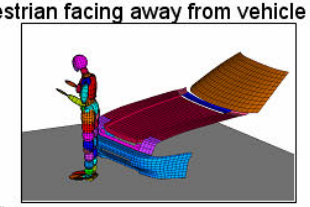

Vehicle speed - 20 km/hr

Filename	prelude6m
Simulation duration (secs)	1.5
HIC	1204
Results	Head hits on rear 1/4 of bonnet, pedestrian projected forwards
Comments	

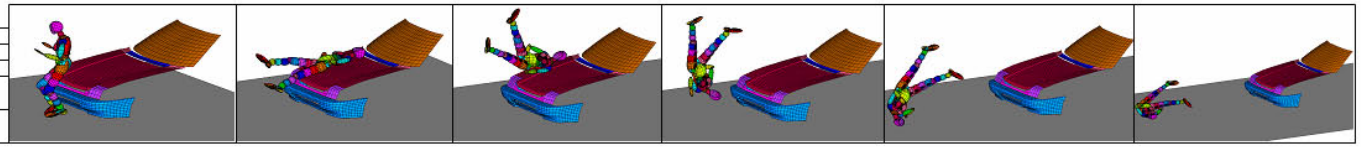

Vehicle speed - 25 km/hr

Filename	prelude6n
Simulation duration (secs)	1.5
HIC	2392
Results	Head hits across trailing edge of windscreen and grille, pedestrian projected forwards, does a slow, tumbling
Comments	

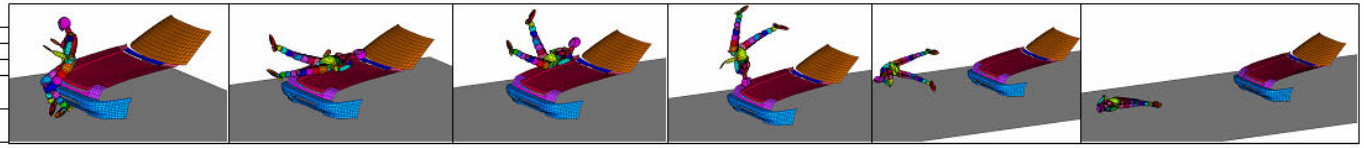

Vehicle speed - 30 km/hr

Filename	prelude6o
Simulation duration (secs)	1.7
HIC	1954
Results	Head hits across trailing edge of windscreen and grille, pedestrian projected forwards, does a slow, tumbling
Comments	

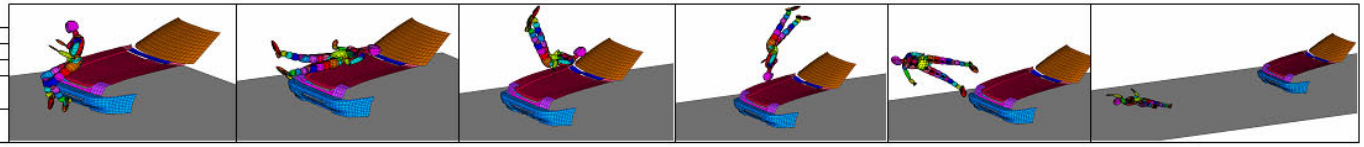

Vehicle speed - 35 km/hr

Filename	prelude6p
Simulation duration (secs)	1.7
HIC	3018
Results	Head hits grille, pedestrian does a tumbling somersault and lands on back
Comments	

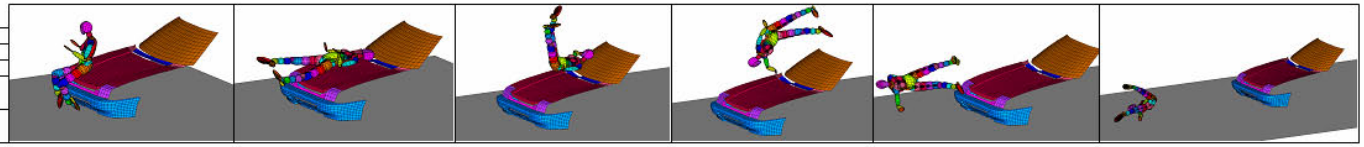

Figure A(III).16 Graphical Results From Series 1: Pedestrian Facing Away from Vehicle at 45 degrees, Vehicle Decelerating Heavily

Series 7: Pedestrian facing away from vehicle, vehicle deccelerating moderately

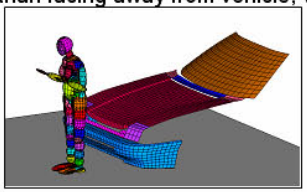

Vehicle speed - 20 km/hr

Filename	prelude5u
Simulation duration (secs)	1.5
HIC	943
Results	Heat hits on rear 1/4 of bonnet, ped projected forwards, somersaults and lands on head
Comments	

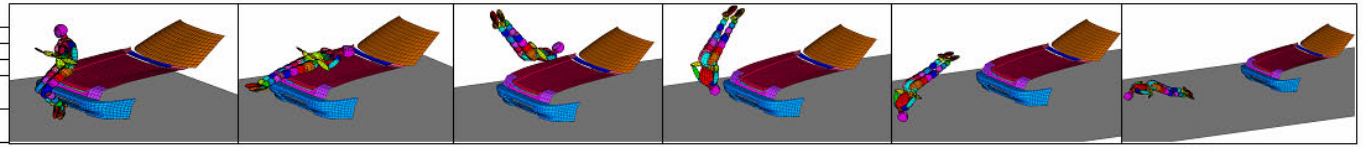

Vehicle speed - 25 km/hr

Filename	prelude5v
Simulation duration (secs)	1.5
HIC	1469
Results	Head hits across trailing edge of bonnet and grille, pedestrian projected forwards, somersaults
Comments	

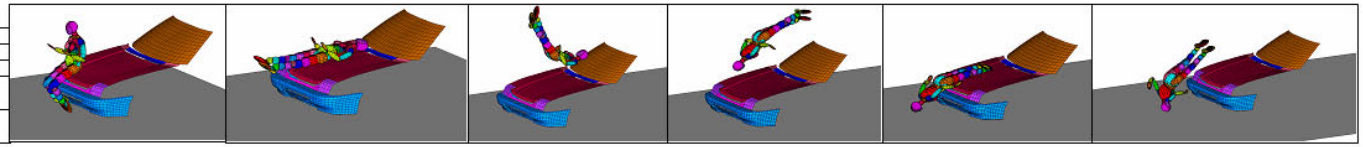

Vehicle speed - 30 km/hr

Filename	prelude5w
Simulation duration (secs)	1.7
HIC	4673
Results	Head hits across trailing edge of bonnet and grille, pedestrian somersaults, lands on bonnet, slides onto
Comments	

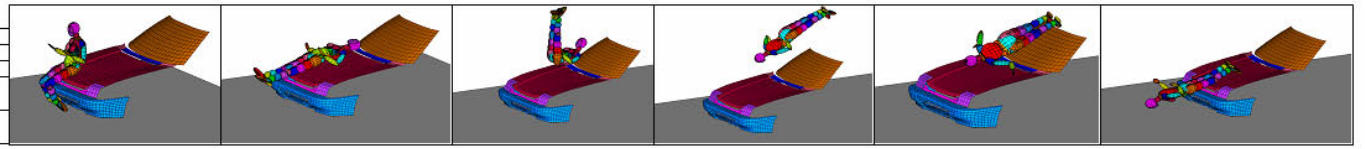

Vehicle speed - 35 km/hr

Filename	prelude5x
Simulation duration (secs)	1.7
HIC	10146
Results	Head hits across trailing edge of bonnet and grille, pedestrian somersaults, lands on bonnet, slides onto
Comments	

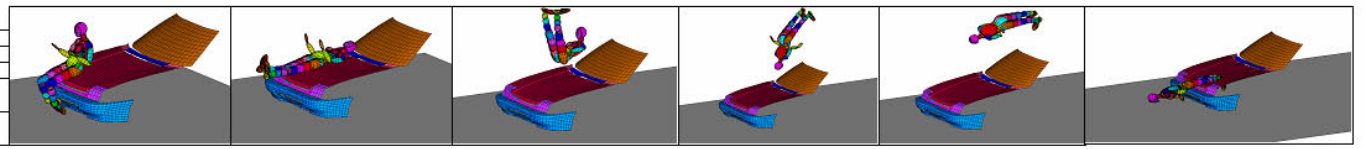

Figure A(III).17 Graphical Results From Series 1: Pedestrian Facing Away from Vehicle, Vehicle Decelerating Moderately

Series 8: Pedestrian side-on to vehicle, vehicle deccelerating moderately

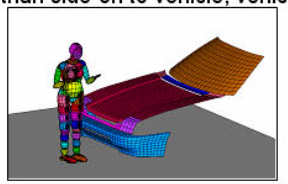

Vehicle speed - 20 km/hr

Filename	prelude5o
Simulation duration (secs)	1.5
HIC	18
Results	Head hits on rear 1/4 of bonnet, pedestrian projected forwards
Comments	

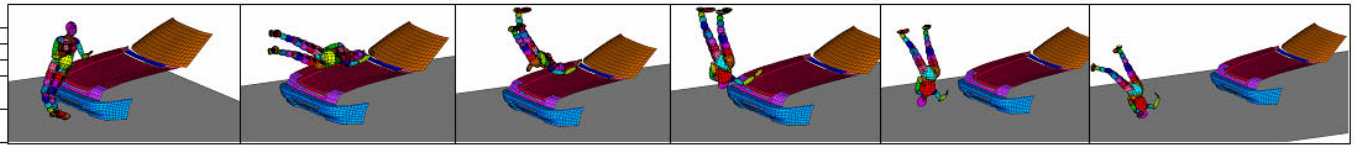

Vehicle speed - 25 km/hr

Filename	prelude5p
Simulation duration (secs)	1.5
HIC	124
Results	Heat hits on rear 1/4 of bonnet, ped projected forwards, somersaults and lands on head
Comments	

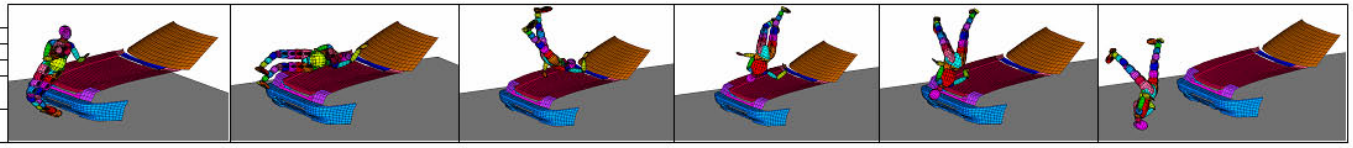

Vehicle speed - 30 km/hr

Filename	prelude5q
Simulation duration (secs)	1.7
HIC	569
Results	Heat hits on rear 1/4 of bonnet, ped projected forwards, somersaults
Comments	

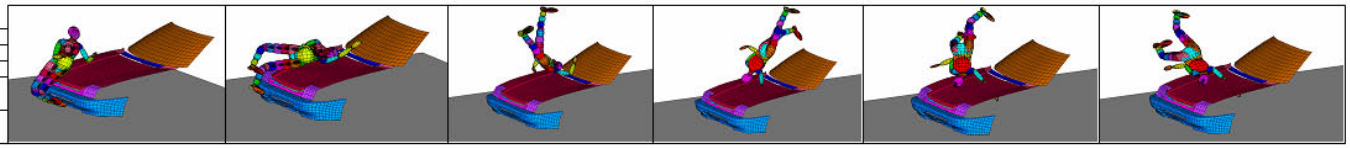

Vehicle speed - 35 km/hr

Filename	prelude5r
Simulation duration (secs)	1.7
HIC	2482
Results	Heat hits on rear 1/4 of bonnet, ped projected forwards, somersaults
Comments	

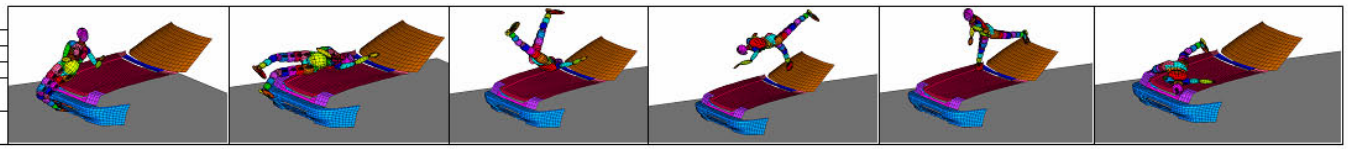

Figure A(III).18 Graphical Results From Series 1: Pedestrian Side on to Vehicle, Vehicle Decelerating Moderately

Series 9: Pedestrian facing away from vehicle at 45deg, vehicle deccelerating moderately

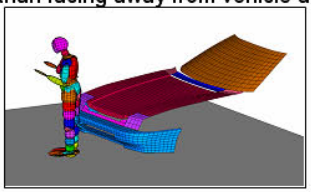

Vehicle speed - 20 km/hr

Filename	prelude6s
Simulation duration (secs)	1.5
HIC	1197
Results	Heat hits on rear 1/4 of bonnet, ped projected forwards, somersaults and lands on head
Comments	

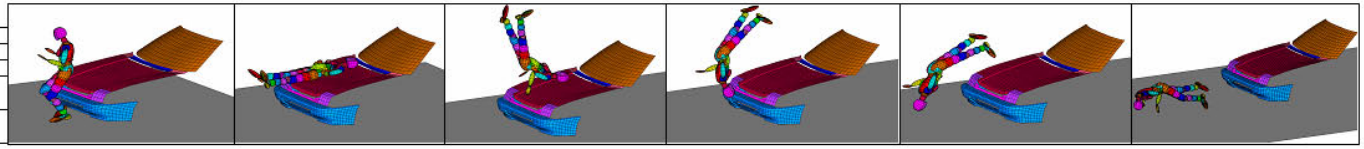

Vehicle speed - 25 km/hr

Filename	prelude6t
Simulation duration (secs)	1.5
HIC	1972
Results	Heat hits on rear 1/4 of bonnet, ped projected forwards, somersaults and lands on ground
Comments	

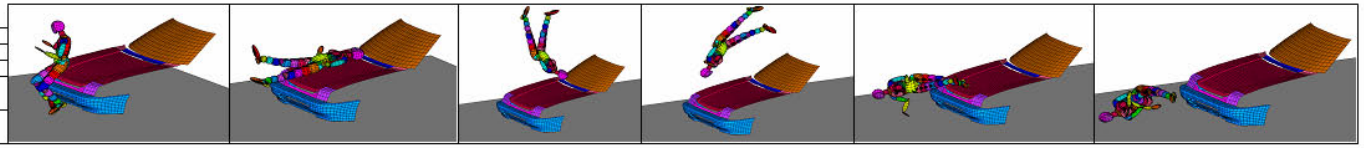

Vehicle speed - 30 km/hr

Filename	prelude6u
Simulation duration (secs)	1.7
HIC	3579
Results	Head hits across trailing edge of bonnet and grille, pedestrian somersaults, lands on bonnet /windscreen,
Comments	

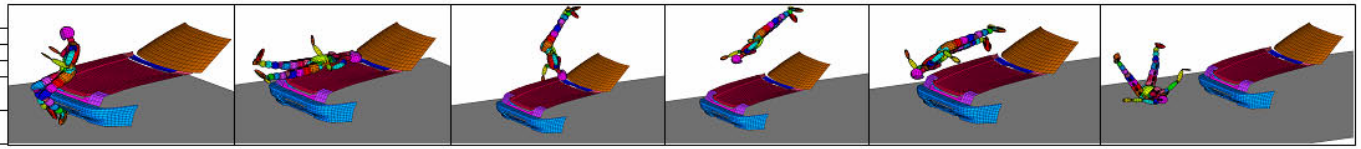

Vehicle speed - 35 km/hr

Filename	prelude6v
Simulation duration (secs)	1.7
HIC	6303
Results	Head hits across trailing edge of bonnet and grille, pedestrian somersaults, lands on bonnet /windscreen,
Comments	

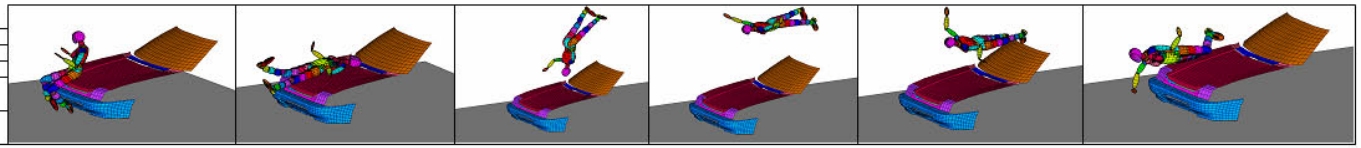

Figure A(III).19 Graphical Results From Series 1: Pedestrian Facing Away from Vehicle at 45 degrees, Vehicle Decelerating Moderately

Results for second simulation series for Operation Lamar					
	Target velocity				
	1	1.5	2.5	3.5	4.5
Filename	lamar20a	lamar20b3	lamar20c2	lamar20d2	lamar20e/lamar20e2
Sim duration (secs)	9	7	5	4	3
Initial velocity (m/s)	0	1.8	2.5	0	0
Initial acceleration (m/s^2)	0.39	0	0	2.4	3.9
Acceleration duration (secs)	4.7	0	0	1.6	1.25
Velocity at top of bank (m/s)	0.69	1.4	2.2	3.4	4.5
Pedestrian standing on top of bank, facing vehicle	Vehicle doesn't get over bank, ped falls over before vehicle gets there	Pedestrian falls onto car bonnet, slides off and down slope, vehicle catches-up pushes pedestrian through fence.	Ped projected forwards, slides face-down down bank, vehicle pushes ped through fence.	Ped projected forwards, lands on car bonnet, slides forward over bumper as car passes through fence	Pedestrian is flipped by vehicle impact onto vehicle roof and is carried over the fence
Filename	lamar22a	lamar22b6 - now on new underbody	lamar22c7 - note: new underbody on vehicle	lamar22d3 (from 22b2)	lamar22e
Sim duration (secs)	9	6	4	3	3
Initial velocity (m/s)	0	1	1	1	0
Initial acceleration (m/s^2)	0.39	0.6	1.2	2.3	3.9
Acceleration duration (secs)	4.7	2.2	1.7	1.3	1.25
Velocity at top of bank (m/s)	0	1.3	2.3	3.5	4.3
Pedestrian standing immediately in front of vehicle, facing vehicle	Vehicle jams on top of ped and stops	Pedestrian pushed backwards over bank and down slope before going through fence, partially under car.	Pedestrian pushed over bank, slides down bank - vehicle catches up at fenceline.	Ped falls onto bonnet, then falls onto ground just above fenceline and gets runover	Ped projected backwards over bank, slides down slope, vehicle lands on top of ped near fence and pushes ped through fence

Filename	lamar24a	lamar24b3	lamar24c1 (from 24b1) - now on new underbody	lamar24d2	lamar24e1
Sim duration	9	6	4	3	3
Initial velocity (m/s)	0	1	1	1	1
Initial acceleration (m/s^2)	0.39	1.2	2.4	3.6	4.5
Acceleration duration (secs)	4.7	2	1.5	1.1	1
Velocity at top of bank (m/s)		0	2.5	3.2	3.9
Pedestrian lying on back on ground, feet towards vehicle		Vehicle's front wheels are lifted off the ground and stops without going over bank.	Ped pushed off verge and run over on slope	Ped pushed by vehicle - pelvic injury source?	Ped pushed off verge and run over on slope
Filename	lamar26a	lamar26b	lamar26c	lamar26d	lamar26e
Sim duration	9	7	5	4	3
Initial velocity (m/s)	0	0	0	0	0
Initial acceleration (m/s^2)	0.39	0.55	1.25	2.4	3.9
Acceleration duration (secs)	4.7	3.8	2.3	1.6	1.25
Velocity at top of bank (m/s)	0.95	1.4	2.4	3.4	4.4
Pedestrian lying face-down on bonnet, head towards windscreen	Ped slides off bonnet and ends up 3/4 down the slope, veh gets stuck on top of bank	Ped slides off bonnet and is pushed by vehicle into fenceline	Pedestrian slides off bonnet, is pushed sideways and starts to get run-over by the vehicle - program crash -smaller timestep needed	Ped slides down bonnet, ends up between bumper and fence	Ped projected forwards and pushed through fence by vehicle

Filename	lamar28a	lamar28b	lamar28c	lamar28d	lamar28e
Sim duration	9	7	5	4	3
Initial velocity (m/s)	0	0	0	0	0
Initial acceleration (m/s^2)	0.39	0.55	1.25	2.4	3.9
Acceleration duration (secs)	4.7	3.8	2.3	1.6	1.25
Velocity at top of bank (m/s)	0.96	1.4	2.4	3.4	4.4
Pedestrian lying on back on bonnet, head towards windscreen	Ped slides off bonnet and ends up almost at fenceline, veh gets stuck on top of bank	Ped slides off bonnet and down slope, car catches up and is partially on top of ped through fence.	Pedestrian slides off bonnet and down slope, car catches up and forward rolls ped through fence	Pedestrian slides off bonnet and down slope, car bounces onto pedestrian's head and torso before going through fence	Pedestrian does a backflip and ends up overhanging the bumper before getting pushed through the fence
Filename	lamar30a	lamar30b	lamar30c	lamar30d	lamar30e
Sim duration		7	5	4	4
Initial velocity (m/s)		1.7	2.6	3.6	4.5
Initial acceleration (m/s^2)		0	0	0	0
Acceleration duration (secs)		0	0	0	0
Velocity at top of bank (m/s)		1.3	2.3	3.4	4.5
Pedestrian lying on back on slope, feet towards vehicle	Vehicle gets stuck at top of bank	Pedestrian run over mid-slope	Pedestrian run over mid-slope	Pedestrian run over mid-slope, vehicle bounces whilst over pedestrian	Vehicle comes down hard on pedestrian, although major impact appears to be to legs

Table A(III).3: Results Summary on Preceding 3 Pages for Off-road Simulation Sequences

Pedestrian standing at top of bank, facing vehicle

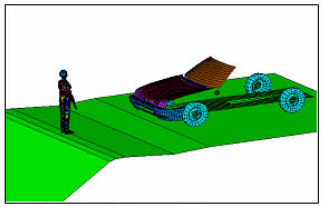

Minimum speed - automatic transmission creep

Filename	lamar20a
Velocity at top of bank (m/s)	0
Sim duration (secs)	9
Results	Vehicle doesn't get over bank.
Comments	Not a valid scenario.

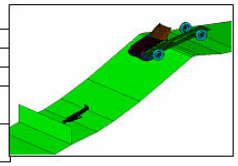

Low speed - approximately 5 km/hr

Filename	lamar20b3
Velocity at top of bank (m/s)	1.4
Sim duration (secs)	7
Results	Pedestrian falls onto car bonnet, slides off and down slope, vehicle catches-up pushes pedestrian through fence.
Comments	Depsite the blow to the pelvic region, other injury patterns are inconsistent with the actual event.

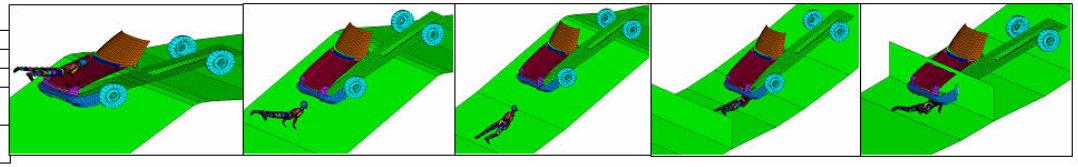

Medium speed - approximately 8 km/hr

Filename	lamar20c2
Velocity at top of bank (m/s)	2.2
Sim duration (secs)	5
Results	Pedestrian projected forwards, slides face-down down bank, vehicle pushes pedestrian through fence.
Comments	Pedestrian likely to sustain injuries from fence.

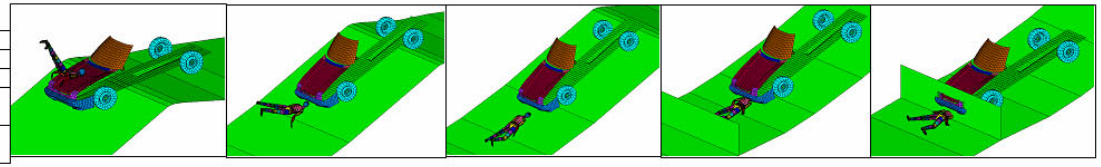

Moderate speed - approximately 13 km/hr

Filename	lamar20d2
Velocity at top of bank (m/s)	3.4
Sim duration (secs)	4
Results	Pedestrian projected forwards, lands on car bonnet, slides forward over bumper as car passes through fence
Comments	Pedestrian likely to sustain injuries from fence.

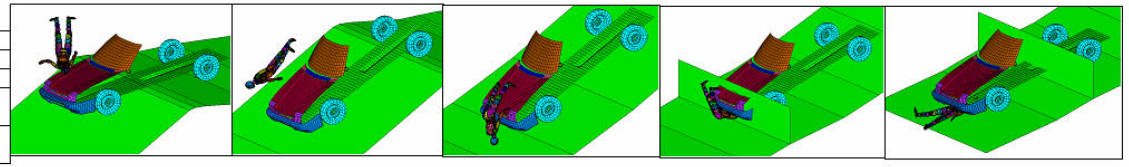

Maximum speed - approximately 16 km/hr

Filename	lamar20e/lamar20e2 (same result)
Velocity at top of bank (m/s)	4.5
Sim duration (secs)	3
Results	Pedestrian is flipped by vehicle impact onto vehicle roof and is carried over the fence
Comments	Not a valid scenario.

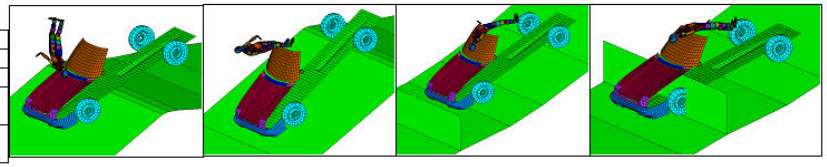

Figure A(III).20 Graphical Results From Series 2: Pedestrian Standing At Top of Bank, Facing Vehicle

Pedestrian standing in front of vehicle, facing vehicle

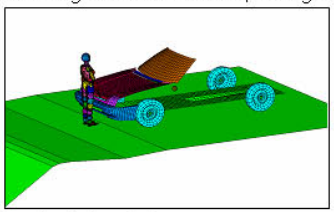

Minimum speed - automatic transmission creep

Filename	lamar22a
Velocity at top of bank (m/s)	0
Sim duration (secs)	9
Results	Vehicle jams on top of pedestrian's lower legs and stops
Comments	Not a valid scenario.

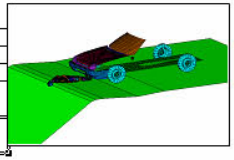

Low speed - approximately 5 km/hr

Filename	lamar22b6
Velocity at top of bank (m/s)	1.3
Sim duration (secs)	6
Results	Pedestrian pushed backwards over bank and down slope before going through fence.
Comments	Depsite the blow to the pelvic region, other injury patterns are inconsistent with the actual event.

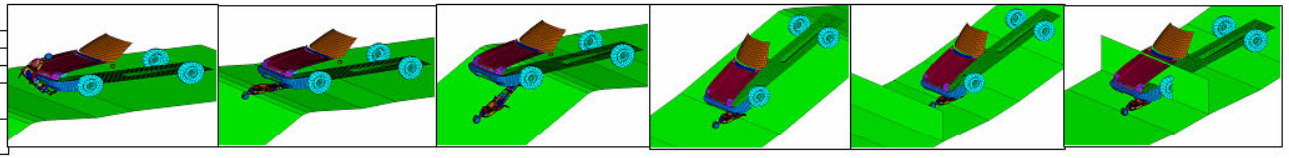

Medium speed - approximately 8 km/hr

Filename	lamar22c7
Velocity at top of bank (m/s)	2.3
Sim duration (secs)	4
Results	Pedestrian projected forwards, slides face-down down bank, vehicle pushes pedestrian through fence.
Comments	Pedestrian likely to sustain injuries from fence.

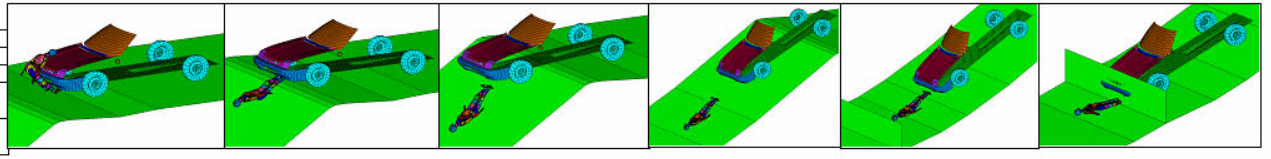

Moderate speed - approximately 13 km/hr

Filename	lamar22d3
Velocity at top of bank (m/s)	3.5
Sim duration (secs)	4
Results	Pedestrian projected forwards, lands on car bonnet, slides forward over bumper as car passes through fence
Comments	Pedestrian likely to sustain injuries from fence.

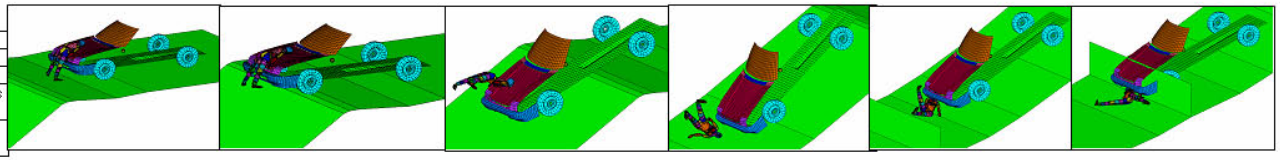

Maximum speed - approximately 16 km/hr

Filename	lamar22e
Velocity at top of bank (m/s)	4.4
Sim duration (secs)	3
Results	Ped projected backwards over bank, slides down slope, vehicle lands on top of ped near fence and pushes ped
Comments	Pedestrian run-over head-first and likely to sustain injuries from the fence, neither of which matches injury pattern.

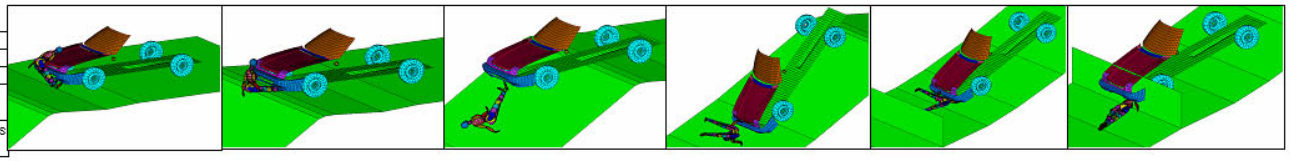

Figure A(III).21 Graphical Results From Series 2: Pedestrian Standing In Front of Vehicle, Facing Vehicle

Pedestrian lying on back, feet towards vehicle

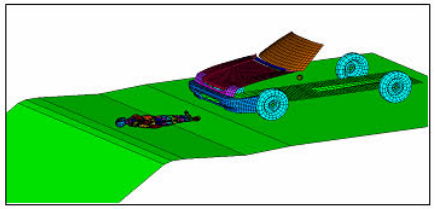

Minimum speed - automatic transmission creep

Filename	lamar24a
Velocity at top of bank (m/s)	0
Sim duration (secs)	9
Results	Vehicle speed too low - insufficient to push pedestrian or go over bank.
Comments	Not a valid scenario.

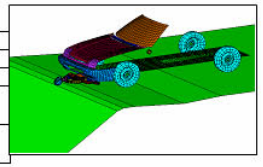

Low speed - approximately 5 km/hr

Filename	lamar24b
Velocity at top of bank (m/s)	0
Sim duration (secs)	7
Results	Vehicle's front wheels are lifted off the ground and stops without going over
Comments	Depsite the blow to the pelvic region, other injury patterns are inconsistent with the

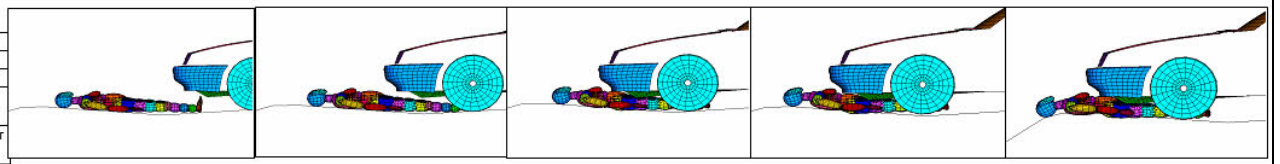

Medium speed - approximately 9 km/hr

Filename	lamar24c1
Velocity at top of bank (m/s)	2.5
Sim duration (secs)	5
Results	Pedestrian projected forwards, slides face-down down bank, vehicle pushes
Comments	Pedestrian likely to sustain injuries from fence.

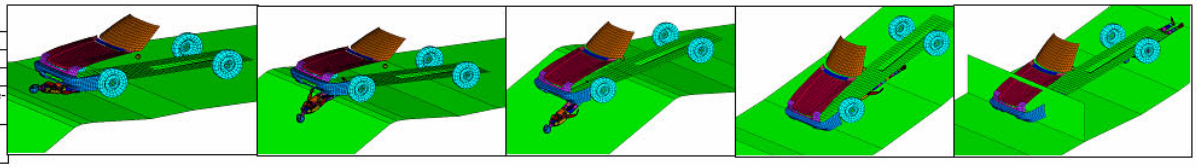

Moderate speed - approximately 12 km/hr

Filename	lamar24d2
Velocity at top of bank (m/s)	3.2
Sim duration (secs)	3
Results	Pedestrian projected forwards, lands on car bonnet, slides forward over bumper as
Comments	Pedestrian likely to sustain injuries from fence.

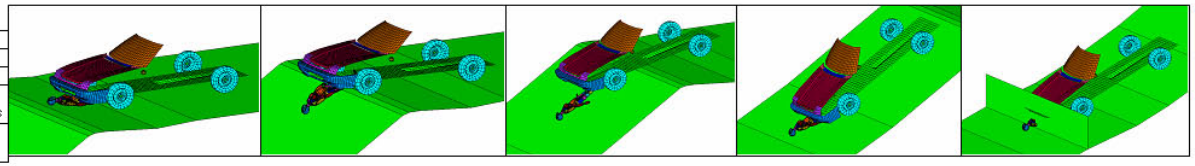

Maximum speed - approximately 14 km/hr

Filename	lamar24e1
Velocity at top of bank (m/s)	3.9
Sim duration (secs)	3
Results	Ped pushed off verge and run over on slope with a possible pelvic crushing
Comments	Possible but no marks on verge to support.

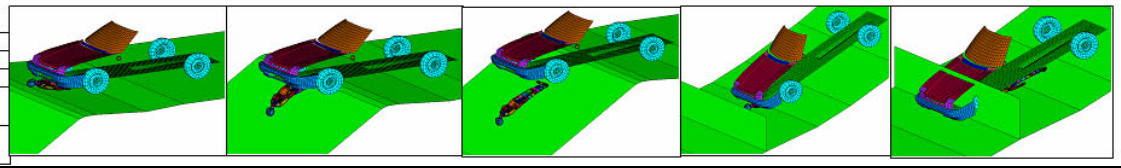

Figure A(III).22 Graphical Results From Series 2: Pedestrian Lying on Back, Feet Towards Vehicle

Pedestrian lying face-down on bonnet, head towards windscreen

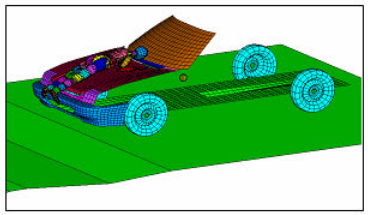

Minimum speed - automatic transmission creep

Filename	lamar26a
Velocity at top of bank (m/s)	0
Sim duration (secs)	9
Results	Pedestrian slides off bonnet and slides down to fenceline, vehicle gets stuck on top of bank
Comments	Not a valid scenario.

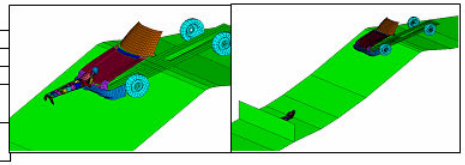

Low speed - approximately 5 km/hr

Filename	lamar26b
Velocity at top of bank (m/s)	1.4
Sim duration (secs)	7
Results	Pedestrian slides off bonnet and is pushed by vehicle into fenceline
Comments	Depsite the blow to the pelvic region, other injury patterns are inconsistent with the actual event.

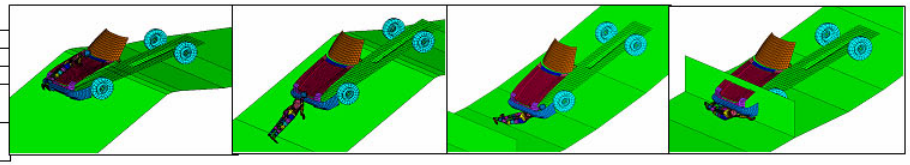

Medium speed - approximately 9 km/hr

Filename	lamar26c
Velocity at top of bank (m/s)	2.4
Sim duration (secs)	5
Results	Pedestrian projected forwards, slides face-down down bank, vehicle pushes pedestrian through
Comments	Pedestrian likely to sustain injuries from fence.

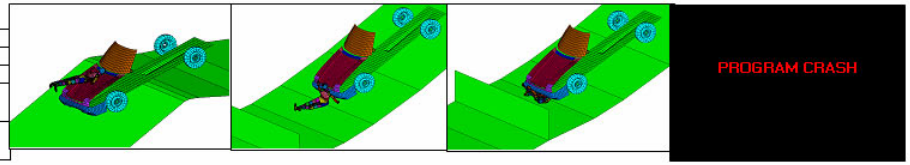

Moderate speed - approximately 12 km/hr

Filename	lamar26d
Velocity at top of bank (m/s)	3.4
Sim duration (secs)	4
Results	Pedestrian projected forwards, lands on car bonnet, slides forward over bumper as car passes through
Comments	Pedestrian likely to sustain injuries from fence.

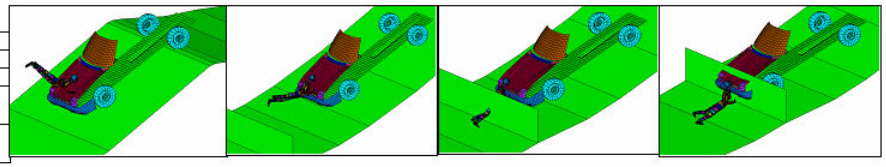

Maximum speed - approximately 16 km/hr

Filename	lamar26e
Velocity at top of bank (m/s)	4.4
Sim duration (secs)	3
Results	Ped projected forwards and pushed through fence by vehicle
Comments	Pedestrian likely to be injured by fence

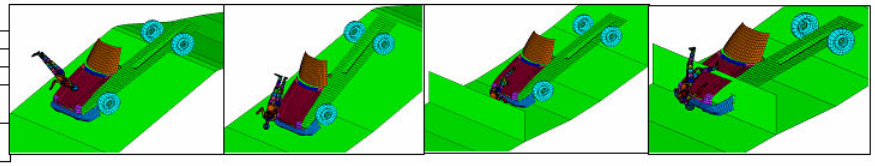

Figure A(III).23 Graphical Results From Series 2: Pedestrian Lying Face Down on Bonnet, Head Towards Windscreen

Pedestrian lying on back on bonnet, head towards windscreen

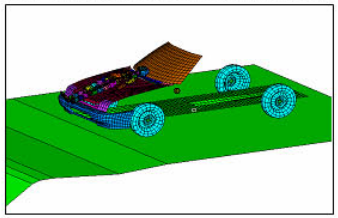

Minimum speed - automatic transmission creep

Filename	lamar28a
Velocity at top of bank (m/s)	0
Sim duration (secs)	9
Results	Pedestrian slides off bonnet and down slope almost to fenceline, meanwhile vehicle gets stuck on top of bank
Comments	Not a valid scenario.

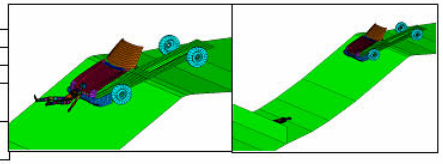

Low speed - approximately 5 km/hr

Filename	lamar28b
Velocity at top of bank (m/s)	1.4
Sim duration (secs)	7
Results	Pedestrian slides off bonnet and down slope, car catches up and is partially on top of pedestrian through fence.
Comments	Depsite the blow to the pelvic region, other injury patterns are inconsistent with the actual event.

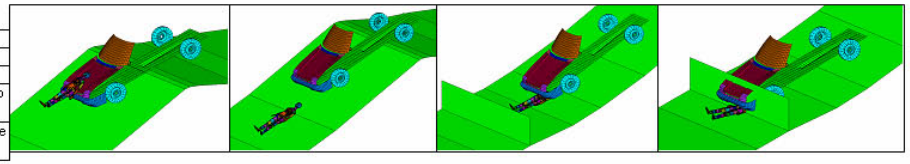

Medium speed - approximately 9 km/hr

Filename	lamar28c
Velocity at top of bank (m/s)	2.4
Sim duration (secs)	5
Results	Pedestrian projected forwards, slides face-down down bank, vehicle pushes pedestrian through fence.
Comments	Pedestrian likely to sustain injuries from fence.

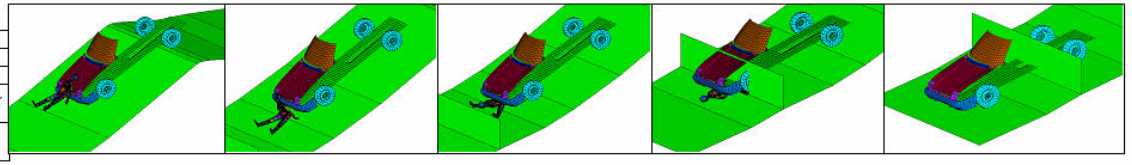

Moderate speed - approximately 13 km/hr

Filename	lamar28d
Velocity at top of bank (m/s)	3.4
Sim duration (secs)	4
Results	Pedestrian projected forwards, lands on car bonnet, slides forward over bumper as car passes through fence
Comments	Pedestrian likely to sustain injuries from fence.

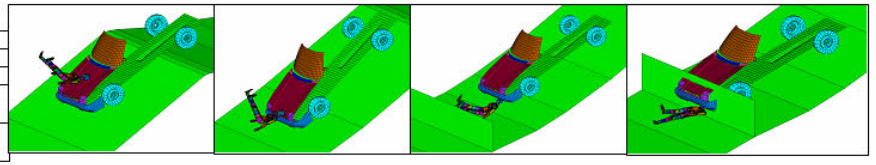

Maximum speed - approximately 16 km/hr

Filename	lamar28e
Velocity at top of bank (m/s)	4.4
Sim duration (secs)	3
Results	Pedestrian does a backflip and ends up overhanging the bumper before getting pushed through the fence
Comments	Pedestrian likely to be injured by fence

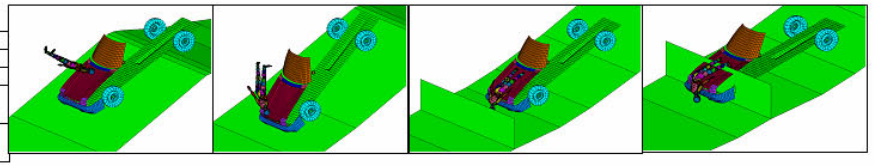

Figure A(III).24 Graphical Results From Series 2: Pedestrian Lying on Back on Bonnet, Head Towards Windscreen

Pedestrian lying on back, feet towards vehicle, on top of slope

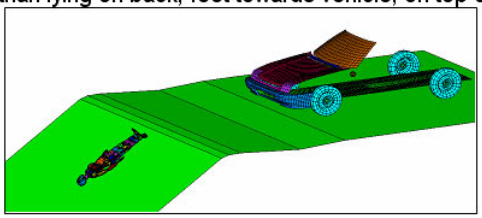

Minimum speed - automatic transmission creep

Filename	lamar30a
Velocity at top of bank (m/s)	0
Sim duration (secs)	9
Results	Insufficient velocity for vehicle to negotiate top of bank.
Comments	Not a valid scenario.

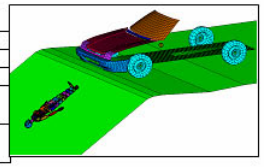

Low speed - approximately 5 km/hr

Filename	lamar30b
Velocity at top of bank (m/s)	1.3
Sim duration (secs)	7
Results	Pedestrian run over mid-slope
Comments	Depsite the blow to the pelvic region, other injury patterns are inconsistent with the actual event.

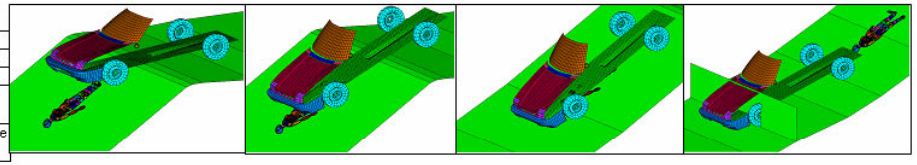

Medium speed - approximately 8 km/hr

Filename	lamar30c
Velocity at top of bank (m/s)	2.3
Sim duration (secs)	5
Results	Pedestrian projected forwards, slides face-down down bank, vehicle pushes pedestrian through fence.
Comments	Possible scenario

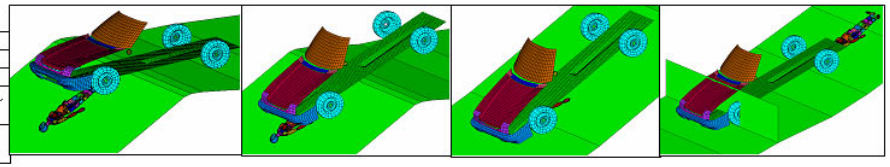

Moderate speed - approximately 12 km/hr

Filename	lamar30d
Velocity at top of bank (m/s)	3.4
Sim duration (secs)	4
Results	Pedestrian projected forwards, lands on car bonnet, slides forward over bumper as car passes through fence
Comments	Possible scenario

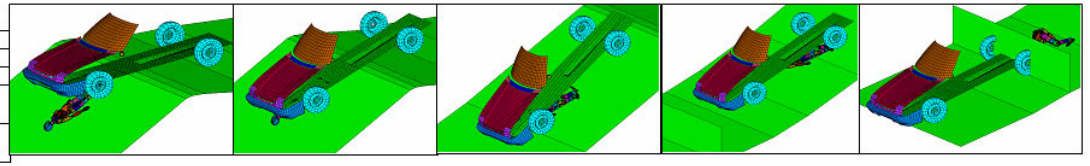

Maximum speed - approximately 16 km/hr

Filename	lamar30e
Velocity at top of bank (m/s)	4.5
Sim duration (secs)	4
Results	Vehicle comes down hard on pedestrian, although major impact appears to be to legs
Comments	Possible scenario

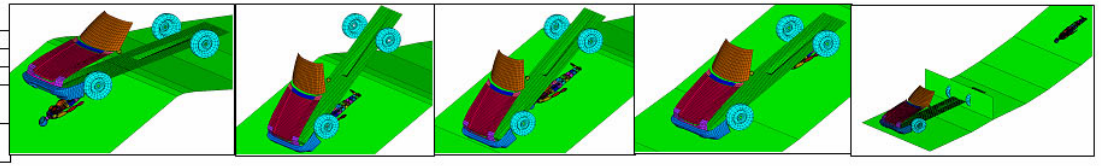

Figure A(III).25 Graphical Results From Series 2: Pedestrian Lying on Back, Feet Towards Vehicle, at Top of Slope

Appendix IV: Anecdotal Examples of Body-Armour Providing Protection in Vehicle and Vehicle Pedestrian Accidents

Body Armor Protects Illinois Officer in Vehicle Crash

Officer Mark D. Terveer of the Collinsville, Illinois, Police Department was making a nonemergency response to a reported motor vehicle crash when he was advised that an officer needed assistance with an unruly subject resisting arrest. Terveer diverted to help the officer and upgraded to an emergency response using his lights and siren.

As Terveer approached an intersection, a motorist who did not see or hear the approaching police vehicle pulled into the intersection and stopped. Terveer avoided hitting the civilian motorist's vehicle but lost control of his patrol unit and left the roadway, slamming into a tree and fence on the driver's side. A piece of the fence entered the patrol car and struck Terveer in the left lower shoulder blade. Since he was wearing personal body armor, the wood was unable to penetrate the vest. Terveer was trapped in the heavily damaged patrol car for more than an hour as fire personnel worked to extricate him. He was transported to an area hospital where he remained for one week receiving treatment for extensive injuries received in the crash. He sustained a severe bruise from where the piece of wood hit his vest but did not suffer a puncture wound.

According to Major Ed Delmore of the Collinsville Police Department, vests like those worn by Terveer "have become more wearable and the chances of officers being involved in an incident where the vest would potentially save them is a real possibility." Delmore noted that in Collinsville, its mandatory for police officers to wear vests while on duty and in uniform.

From The Police Chief, vol. 70, no. 11, November 2003. Copyright held by the International Association of Chiefs of Police, 515 North Washington Street, Alexandria, VA 22314 USA.

Body Armor Saves Colorado Officer during Assault with Motor Vehicle

Early on a spring morning, Officer Michael E. Kippes of the Lafayette, Colorado, Police Department was assisting fellow officers attempting to make a motor vehicle stop of a suspected drunk driver who was fleeing police. As Kippes sought a position on the road ahead where he could deploy a tire deflation device designed to slow the suspect's vehicle, the suspected drunk driver veered into the officer's lane of travel and collided head-on with the marked patrol car at approximately 70 miles an hour. There were no skid marks from either vehicle and both vehicles were destroyed in the collision.

Kippes was able to walk away from the accident but suffered a broken hand, a damaged knee, and contusions to the head. When he was taken to a nearby hospital for treatment, physicians reported that the body armor the officer was wearing probably spared him from severe internal injuries.

Officer Kippes was released from the hospital four hours after the incident and was out of work for three months. He has returned to full duty. The suspect, who was severely injured in the collision and required extrication from the vehicle, was later charged with multiple offences.

From The Police Chief, vol. 70, no. 9, September 2003. Copyright held by the International Association of Chiefs of Police, 515 North Washington Street, Alexandria, VA 22314 USA

All Examples from this Point Sourced From::
IACP/DuPont Kevlar Survivors' Club
http://www.dupont.com/kevlar/lifeprotection/survivors/stories_frame.html
Contact: Kelly Carson
804-383-3885
Kelly.h.Carson@usa.dupont.com

Wilks, Wilbert C, II, Trooper, North Charleston, SC, State Police/Highway Patrol

Incident classification: Struck by vehicle while working traffic stop, roadblock, etc.

Saturday, May 05, 2001 at 1236 hours — Trooper Wilbert C. Wilks, II, was critically injured when he was struck by a motor vehicle while working at a crash scene on I-26 in North Charleston. Trooper Wilks was in the process of clearing the wrecked vehicles from the roadway and had traffic stopped. A rapidly approaching tractor-trailer rig swerved into the median to avoid rear-ending stopped cars. The truck impacted the median divider cables one of which snapped, wrapped around an axle of the truck and was pulled from the ground. The cable was whipping back and forth as the truck driver attempted to pull back onto the roadway. Trooper Wilks reports that he felt the heat from the radiator of the truck tractor that was bearing down on him before it hit him a glancing blow and tossed him into the air. The cable attached to the truck wrapped around his legs, breaking them, and flinging him atop his patrol car and then onto the pavement before his body was freed from the cable.

Although critically injured, Trooper Wilks was able to crawl to his patrol vehicle to call for assistance. Bystanders came to his aid and he was transported to the Medical University of South Carolina Level 1 trauma center. Fortunately he was “dressed for survival” as his body armor protected much of his torso from the trauma of being smashed into the patrol car and to the ground. Equally important was the availability of first tier medical services. Trooper Wilks was placed in a medically induced coma for three weeks and with the aid of many he was able to recover. After six months he was able to return to modified duty for rehabilitation, and is now working his regular assignments. The truck driver was found guilty of traffic related violations that resulted in Trooper Wilks' brush with death.

Williams, Billy Joe, Officer, Miner, MO, Police Department

Incident classification: Struck by vehicle while working traffic stop, roadblock, etc.

Tuesday, December 30, 2003 at 1624 hours — Officer Billy Joe Williams was struck by a vehicle while working a traffic stop. Officer Williams completed the initial violator contact and was returning to his patrol vehicle with the violator. He was standing near the left front fender of his vehicle, guiding the violator to the right front seat of the patrol vehicle. An 81-year-old male driver failed to move over for the stopped police vehicle, and a portion of his vehicle struck Officer Williams in the back, causing severe bruising. Officer Williams was protected from more serious physical injury by his ballistic body armor. He was able to return to full duty for his next regularly scheduled watch.

Puckett, Bart , D. , Officer, Conway, AR, Police Department

Incident classification: Struck by vehicle while working traffic stop, roadblock, etc.

Sunday, April 18, 1999 at 2025 hours — Officer Bart D. Puckett was dispatched to the scene of motor vehicle crash involving a deer. He was walking along the edge of the roadway attempting to locate the injured animal to determine the proper course of action. An 18-year-old male motorist operating a pickup truck was passing the accident scene. Officer Puckett was struck by the right side mirror of the pickup truck. The impact was on his right rear upper torso. The force of the impact knocked Officer Puckett to the ground.
Officer Puckett recovered from the blow and summoned assistance using his portable radio. He was transported to an area hospital for emergency care. The attending physician determined that Officer Puckett's body armor absorbed the force of the impact and he suffered no significant injury and was treated and released.
Investigators determined that alcohol was not a factor in this incident. The driver of the truck was not issued a citation. Officer Puckett returned to duty.

Houlberg, John B., Trooper, Richmond, VA, State Police/Highway Patrol

Incident classification: Struck by vehicle while working traffic stop, roadblock, etc.

Thursday, November 22, 2001 at 0008 hours — Trooper Houlberg was struck by a vehicle during a traffic stop on I-95 in Petersburg. He was standing near the left driver's door of the stopped Chevrolet Suburban speaking with the operator. A second motorist headed in the same direction veered off the roadway striking Trooper Houlberg. The motorist failed to stop to render aid and fled the scene.
Trooper Houlberg was struck on the right side of his body by the right front of the moving vehicle, impacting the windshield. The force of the impact flung Trooper Houlberg onto the hood of the Suburban. He came to rest in front of the Suburban. The operator of the Suburban called 911 to report the incident and requested emergency aid for Trooper Houlberg. He was air evacuated to a regional trauma center where it was determined that he had suffered severe injuries to his right arm and legs. The only injury to his torso was backface signature bruising with his vital organs protected by his ballistic vest.
Trooper Houlberg was hospitalized for eight days and underwent extended care for more than ten months during his rehabilitation period. He was able to resume his police duties. State police investigators charged the twenty-four year old female hit-and-run motorist and she was convicted.

Vena, Jr., Joseph A., Officer, Sewell, NJ, Police Department

Incident classification: Struck by vehicle while working traffic stop, roadblock, etc.

Wednesday, August 7, 2002 at 1332 hours — Officer Joseph Vena stopped a motorist for an observed traffic violation alongside State Highway 42. The emergency warning lights were left activated on his patrol vehicle that was stopped one car length to the rear of the violator's vehicle with the left fender angled slightly to the left to provide a safe zone for the officer. Officer Vena followed all of the safety procedures, yet a motorist sideswiped his patrol vehicle and then sandwiched him against the left side of the stopped violator's vehicle. Officer Vena received serious injuries to his shoulders, elbows, hips, knees, and ankles. Marks on the vehicles tell a story about Officer Vena being protected by his leather belt and holsters. The only injuries to his torso were massive severe bruising. His rib cage was not fractured, and his vital organs were protected from damage by his protective body armor. The motorist was cited for reckless driving. Ths incident is being used by the New Jersey General Assembly to enact a statewide move over, slow down law to protect police officers and other public safety workers as they work on streets and highways.

Fee, James T., Sergeant, Madison County, KY, Sheriffs Department

Incident classification: Struck by vehicle while directing traffic, assisting motorist, etc.

Wednesday, January 22, 2003 at 0000 hours — Sergeant Fee was working a traffic crash when an approaching motorist lost control on the ice-covered roadway. The skidding vehicle rammed into the vehicles stopped at the crash scene, striking Sergeant Fee as he stood next to the vehicles. Sergeant Fee was knocked across the hood of one of the vehicles and landed in a wooded area off the roadway. He suffered contusions to his torso, but no broken bones. The driver was not cited.

Conte, Debra, Officer, Summitt, NJ, Police Department

Incident classification: Struck by vehicle while directing traffic, assisting motorist, etc.

Friday, January 28, 2000 at 0745 hours — Officer Conte was working a fixed traffic post when she was struck by a motor vehicle. She received serious injuries to her head and legs. Officer Conte was evacuated by helicopter to a trauma center for medical care. The attending physician noted the protection afforded to her torso by the personal body armor she was wearing had prevented more serious injuries to her vital organs. Officer Conte survived because of her decision to wear a protective ballistic vest.
Carlson,C.,Keith , Trooper, Gladstone, MI, Police Department

Incident classification: Struck by vehicle while directing traffic, assisting motorist, etc.

Tuesday, March 16, 2004 at 2105 hours — Trooper Keith C. Carlson stopped to aid a stranded motorist that had run off the roadway due to ice and snow conditions. Trooper Carlson parked his unit and was walking toward the stranded vehicle to offer assistance. The sound of a collision caused Trooper Carlson to turn and look back toward his parked unit. His first observation was an airborne debris burst of glass and metal from the side of his vehicle. He then saw a vehicle coming at him and he was unable to escape from the path.
Trooper Carlson was struck by the left side of the out of control vehicle with his body impacting between the front fender and driver's door. His body was hurled into the air and he landed on a fence. Trooper Carlson was transported to a hospital in Toledo, Ohio where he remained overnight. Attending doctors determined that he had suffered extensive bruising on his left arm, hip and leg but suffered no injuries to his vital organs or factures. Trooper Carlson credits his body armor for saving him from more serious physical injuries. He has returned to duty.
The operator of the vehicle that struck Trooper Carlson was a seventeen year old female with no prior criminal history. She was charged with failing to show care when passing a stationary emergency vehicle. The driver was found to be guilty.

Anonymous, Trooper, Waukesha, WI, State Police/Highway Patrol

Incident classification: Struck by vehicle while directing traffic, assisting motorist, etc.

Thursday, September 1, 2005 at 0230 hours — A state trooper, who prefers to remain anonymous, was performing solo highway patrol duties when he located a stopped vehicle alongside the highway. The vehicle was on fire. The trooper notified his dispatcher about the incident and requested that fire service be dispatched. The trooper was standing with the operator of the burning vehicle awaiting arrival of fire apparatus.
A police officer from another agency responded to the fire scene. As the responding police officer arrived on scene, he misjudged speed and distance, and rammed into the rear of the parked state highway patrol vehicle. The trooper, who was standing next to his patrol vehicle, was struck by the wreckage, hurled several feet and landed face down in the roadway. The police officer's vehicle continued across the median and burst into flames. The officer was able to extricate himself from the wreckage and crawl to safety. The officer was treated and released from a local hospital.
The trooper was battered by the impact of the wreckage hitting his body and the secondary impact when he landed in the roadway. The trooper reported that his body armor protected his vital organs preventing him from suffering more serious physical injuries or death. The trooper was hospitalized for a day and one-half for injuries to his head, arms and hands, back and shoulders. He suffered no internal injuries. The trooper has returned to duty.

Meeker, Brian, A. , Trooper, Ottumwa, IA, State Police/Highway Patrol

Incident classification: Struck by vehicle while directing traffic, assisting motorist, etc.

Tuesday, December 23, 1997 at 2241 hours — Trooper Brian A. Meeker responded to the scene of a traffic crash involving a suspected drunk driver. Trooper Meeker was operating an unmarked police vehicle. When he arrived he found that the crash had occurred in a sharp curve. He established a traffic control point at the east end of the approach to the turn and a second trooper was working the other end. They were coordinating traffic flow through the crash zone.
Trooper Meeker donned his patrol parka as it was a chilling evening. The parka was fitted with reflective material to increase his visibility to approaching motorist. He placed a portable revolving emergency light atop his patrol vehicle and activated all available warning lights. Trooper Meeker placed a road flare as another means to alert motorist to the danger ahead.
Trooper Meeker has no recollection of being struck by a ¾ ton truck that was operated by a drunk driver. The driver was arrested and charged with causing serious physical injury by vehicle while under the influence. Investigators learned that the driver had a prior criminal history and was on probation for a previous drunk driving charge at the time he drove his truck into Trooper Meeker. The driver entered a plea of guilty as charged and was sentenced to three years.
The first memory Trooper Meeker had after being run down occurred when he awoke in a bed at University of Iowa Hospital. He was critically injured suffering from fractures to the skull, collar bone and pelvis. His left foot and ankle were crushed. Trooper Meeker's attending physician publicly stated that his survival was attributable to his age, excellent physical condition and body armor. It was reported, "The vest absorbed tremendous force and likely spared his heart, lungs and other vital organs. Amazingly, Meeker didn't suffer a single broken rib."

Rivera, Briana M., Officer, Shreveport, LA, Police Department

Incident classification: Struck by vehicle while directing traffic, assisting motorist, etc.

Thursday, October 17, 2002 at 1520 hours — Officer Rivera was assisting other police officers when it became necessary for her to cross a four-lane roadway. As she walked across the street, the operator of a large SUV came to a stop on the inside opposite flow lane. Officer Rivera believing that her path was clear began to jog to rapidly clear the traffic lanes. Unexpectedly a second driver operating under the posted speed limit in the outside opposite lane passed the stopped SUV and struck Officer Rivera.
Crash investigators determined that the speed of the vehicle that struck Officer Rivera was in the low twenty miles per hour range at the moment of impact. Officer Rivera was hit with the left front bumper of the vehicle and slid across the hood with her body and police equipment denting the metal. She impacted just left of center on the windshield shattering the glass and leaving an impression of the back of her torso. The windshield was pushed in where Officer Rivera body impacted but the glass held preventing her from entering the passenger compartment.
Officer Rivera was transported for emergency medical care. After examination it was determined that she suffered muscular injuries to her right leg. Attending physicians reported, "…thankfully she was wearing a bullet proof vest that took the blunt from her chest…." Officer Rivera clearly avoided serious physical injury or death due to the fact she was wearing a ballistic vest when struck. Officer Rivera returned to full duty. The crash investigator determined that the driver of the vehicle was operating with reasonable care and no enforcement action resulted.

Metcalf, Kevin J., Officer, Lexington, KY, Police Department

Incident classification: Other: falls, drowning, fire, etc.

Friday, February 13, 2004 at 1700 hours — Officer Kevin Metcalf fell from a moving vehicle while he and other members of the emergency response team (ERT) were responding to an active shooting incident. The team was riding in the back of an armored truck. The truck, escorted by marked police units, was moving at an estimated 35 miles per hour when a motorist cut in front of one of the escort vehicles, forcing the driver of the truck to brake suddenly. Officer Metcalf's body was thrown forward, striking the right door. The door popped open, and he was ejected from the vehicle, landing on his back and right side. His feet became entangled in the vehicle causing him to be dragged along the roadway. He broke free and his left foot was run over by the truck's rear wheels. He then tumbled for a considerable distance before coming to rest in the median of the four-lane highway.
Team members rushed to assist Officer Metcalf. He was able to stand without assistance. After a quick medical assessment, the team proceeded to the scene of the shooting, while Officer Metcalf was taken to a regional hospital for examination. It was determined that the only obvious injuries were a severe sprain with swelling and bruising to the ligaments on his left foot. While at the hospital, his personal ERT gear was inspected. His Kevlar® helmet had two large gashes where it impacted with the roadway. The fall and skid along the pavement marked his outer gear, including his tactical vest. Officer Metcalf reported that, were it not for his ballistic helmet and tactical vest, he would have certainly suffered disabling or fatal injuries.
The shooter was arrested and charged. He remains incarcerated pending final court action. Officer Metcalf resumed his assigned duties with the Lexington Division of Police.

Kang, James , Officer, Los Angeles, CA, Police Department

Incident classification: Other: falls, drowning, fire, etc.

Wednesday, March 11, 1998 at 1500 hours — Officer James Kang was assigned to bicycle patrol and was working with a partner. As he traversed an intersection a motorist ran a stop sign. Officer Kang was unable to avoid a collision and hit the violator's passenger car head on. Officer Kang was knocked off his bicycle and suffered extensive damage to his neck, shoulder area, back and legs. Officer Kang was subsequently transported to an area hospital for medical evaluation and treatment.
The attending physician informed Officer Kang that the body armor he was wearing at the time of the incident protected him from far more serious spinal cord injuries. Officer Kang underwent three years of physical therapy and was able to return to full duty with the LAPD. Information on disposition of the crash investigation and possible enforcement action against the violator is not available.

Flores, Jon R., Officer, Shreveport, LA, Police Department

Incident classification: Automobile accident

Tuesday, August 5, 2003 at 0345 hours — An accident had closed I-20 to eastbound traffic. A marked temporary detour route had been established by a Department of Transportation crew with a barricade truck, and Officer Jon R. Flores was positioned in his patrol vehicle to ensure compliance with the temporary traffic restrictions.
Officer Flores was seated in his vehicle checking his computer screen when a tractor-trailer rig rammed his vehicle. The impact was on the passenger side. The rig ran over the patrol vehicle and sent it spinning causing extensive damage. Parts of the vehicle and installed police equipment were scattered across a wide area. Officer Flores was quoted, "I stayed in my seat and went along for the ride." The tractor-trailer rig then impacted the unoccupied barricade truck knocking it a reported 600 feet down the roadway. Investigators were unable to locate the right front wheel of the patrol vehicle, the battery was located 200 yards from the point of impact, and the right side of the vehicle body was sheared off by the rig as it passed over the patrol vehicle.
Officer Flores was transported to an area hospital for medical evaluation. His physician found that he was in remarkably good shape and credited the lack of internal injuries to the protection provided by the officer's body armor. Officer Flores reported that his undershirt was ripped by the impact but his vest and outer shirt remained intact. Officer Flores was able to return to full duty.

Hall, Christopher J., Deputy, Orlando, FL, Sheriffs Department

Incident classification: Automobile accident

Friday, April 2, 2004 at 1236 hours — A motorist operating a pickup truck pulling a boat merged onto the highway from an entrance ramp. The driver of the truck cut across the right and middle lanes. Deputy Hall was forced to take evasive maneuvers to avoid a collision with the truck.
Deputy Hall's recollections of the incident are sketchy, and he remembers little about the incident after taking evasive action. A motorist who witnessed the crash reported that the truck pulled directly into the path of Deputy Hall and that he swerved his patrol unit to avoid hitting the truck. The patrol vehicle went out of control, leaving the right edge of the roadway before impacting with a cement bridge pillar. The left front of the patrol vehicle impacted the pillar head-on. Deputy Hall was trapped in the wreckage. Fire rescue responded and extricated him from the wreckage. He was airlifted to a regional hospital, where he was treated for non-life-threatening injuries to his head and arms.
A combination of lap belt, airbag, and protective body armor protected Deputy Hall from injuries to his torso. Deputy Hall was released after a nine-hour hospital stay and continues rehabilitation for an injured hand. Deputy Hall and his wife celebrated the birth of their child just days after this horrific traffic crash. The driver of the pickup truck fled the scene without providing information or rendering aid. Witnesses were unable to provide sufficient details to permit a suspect to be developed.

Guck, Justin H., Officer, Lawrenceville, GA, Police Department

Incident classification: Automobile accident

Sunday, September 14, 2003 at 0350 hours — Officer Guck was monitoring traffic on I-85 when he detected a motorist running 86 mph in a 65 mph zone. Officer Guck made a traffic stop, using care to position his patrol vehicle to maximize his safe zone, and activated all emergency warning lights. Officer Guck walked around the rear of the patrol vehicle, noted that all warning lights were operational and approached the violator on the passenger side. He spoke briefly with the driver and passenger, obtained necessary information, and returned to his patrol vehicle to prepare a speeding citation. Officer Guck was not strapped in as he prepared the citation. The intoxicated driver of a full-size pickup truck operating at 65 mph smashed into the rear of Officer Guck's stopped patrol car, pushing it forward into the rear of the violator's vehicle. Officer Guck has no memory of the impact that literally smashed the back half of the patrol vehicle completely into the rear passenger seat area. His first recollection after the crash was the realization that the patrol car was facing the median concrete barrier, the wind was knocked from his body, and he was trapped in the wreckage. Officer Guck used his portable radio to summon help. The violator that Officer Guck had stopped came to his aid along with another motorist. Officer Guck instructed the citizens to not move him and wait for EMS arrival. Officer Guck suffered a variety of injuries as he bounced about the inside his vehicle, and he was transported to an area hospital for examination. He was treated for lacerations and other relatively minor injuries. Officer Guck reports that his protective body armor prevented injuries to his chest. Officer Guck has returned to duty. The driver of the vehicle that struck him was arrested and charged with driving while under the influence.

Boisclair, Paul A., Officer, Narragansett, RI, Police Department

Incident classification: Automobile accident

Saturday, January 11, 2003 at 0451 hours — Officers Paul A. Boisclair and Robert H. Grieco, Jr. were struck by a vehicle while working a traffic stop on Saturday, January 11, 2003 at 0451 hours. The officers stopped a motorist suspected of driving while under the influence of alcohol. The officers made a determination to arrest. The suspect resisted arrest, and the officers took him to the ground for handcuffing.

Another officer responding to assist the officers encountered reduced visibility from road dust. He spotted the two officers and the suspect in the roadway, but was unable to stop before he overran their position.

All three individuals were pinned under the police vehicle until responding officers was able to lift the car enough so the officers and suspect were freed.
All three were transported for medical attention with the suspect being treated, released, and jailed for DUI and resisting arrest. Officers Boisclair and Grieco suffered cuts and abrasion. Officer Boisclair was hospitalized the longest, being discharged after 24 hours of care and observation. Attending physicians reported that body armor worn by the officers protected them from more serious injuries or death. The officers recovered and have returned to full duty.

Anonymous, Corporal, Lincoln, IL, Police Department

Incident classification: Automobile accident

Saturday, April 28, 2001 at 0100 hours — An officer was assisting fire crews at the scene of a fuel spill at the interchange of Rt. 10 and n I-55, when radio assigned him to a domestic disturbance in progress. The officer, maneuvering his vehicle to enter traffic flow, had his view of oncoming traffic obstructed by parked fire apparatus. He was slowly moving into the active traffic lane, when an ambulance responding to another emergency struck the officer's driver's door. It was determined that the ambulance was traveling at a speed of 64 mph through the temporary work zone, which was marked by emergency warning lights on fire and police vehicles. The officer was trapped in the wreckage, which required considerable time for fire personnel to extricate him. He was transported for medical treatment. The officer suffered broken bones and internal injuries. The attending physician credited the officer's protective vest from his suffering more serious physical injuries or death. The officer recovered from his injuries and returned to full duty.

Greico, Donn A., Officer, Utica, NY, Police Department

Incident classification: Automobile accident

Wednesday, December 10, 2003 at 2300 hours — Officer Greico was making an emergency response to a report of a domestic disturbance in progress. His last memory prior to impact was a set of headlights approaching on the passenger side of his patrol vehicle. Crash investigators determined that a motorist impacted the passenger side of Officer Greico's marked patrol unit, sending it spinning into a utility pole that then severed at the base. The police vehicle continued, striking two parked vehicles before coming to a complete rest.
Officer Greico's next memory was the presence of fire personnel, working to extricate him from the heavily damaged patrol vehicle. Officer Greico was transported to a local hospital, where he was admitted to the intensive care unit for five days of treatment. His injuries included four broken rips, two broken vertebrae, and a bruised lung. The attending physician informed Officer Greico that his body armor absorbed most of the impact, protecting him from more serious physical injuries or death.
The driver of the other vehicle was not injured, and no charges were filed. Officer Greico returned to modified duty for rehabilitation.

Chavez, Gilbert O., Lieutenant, Carlsbad, NM, Sheriffs Department

Incident classification: Automobile accident

Thursday, February 14, 2002 at 1050 hours — Lieutenant Gilbert Chavez was involved in a motor vehicle crash as he responded to assist a deputy on a home intrusion alarm. Lieutenant Chavez did not observe a railroad train approaching as he started to cross an unprotected grade crossing. Skid marks indicated that he attempted to avoid the collision, but the right of his patrol vehicle impacted with the train. The patrol vehicle spun 180 degrees, and the driver's side impacted with the train several times. Lieutenant Chavez was trapped in the wreckage, and it took 30 minutes to extricate him. He suffered extensive injuries that included a severe head injury to the left front and side of his face, open wounds of the left arm, shoulder, elbow and leg, fractured spine, and five broken ribs, one of which punctured his left lung. His protective body armor prevented any other damage to his torso or other vital organs. Lieutenant Chavez was evacuated by helicopter to University Medical Center in Lubbock, Texas, where he remained for 16 days. His recovery and rehabilitation required two additional hospital visits for surgery. Lieutenant Chavez has returned to full duty.

Hernandez, Frank J., Deputy, Bell County, TX, Sheriffs Department

Incident classification: Automobile accident

Tuesday, September 11, 2001 at 0705 hours — Deputy Hernandez made a life-saving decision on September 9, 2001, when he inserted a metal armadillo plate into his protective body armor. On Tuesday, Septemeber 11, 2001, Hernandez had just completed his midnight patrol watch and was driving home. It was 705 am when for reasons unknown, Hernandez impacted with a manufactured home that was being towed. A 4' x 2" x 6" wood beam used in the construction of the manufactured home penetrated the front of the patrol car and was deflected to the left side of Hernandez's torso, passing through his body. Hernandez's patrol car was then involved in a secondary impact with a passenger vehicle that was following the manufactured home and went off the roadway over a hill into a creek bed, where it was hidden from view by the foliage. He was pinned in his demolished patrol car by the beam that was protruding from his front and back. For an extended period, it was believed that the patrol vehicle had been driven from the accident scene, until it was found in the creek bed with Hernandez pinned inside. It was nearly three hours later before he was extricated from the vehicle and taken to a trauma center with the beam sill in him. Attending physicians noted that the only reason that Hernandez survived was because of the protective body armor and metal trauma plate that diverted the beam away from vital organs. Deputy Hernandez has returned to modified duty for rehabilitation and plans to return to full duty. He has promised himself that he will always wear body armor with a metal trauma plate.